International
Progress Report

IPR-02-38

Äspö Hard Rock Laboratory

Hydrogeological and hydrochemical impact of the tunnel and shaft construction in the Äspö site

Phase 2, Task 5. Concentration prediction and optimisation using concentration data

J. Wendling

ANTEA, France

September 2000

Svensk Kärnbränslehantering AB
Swedish Nuclear Fuel
and Waste Management Co
Box 5864
SE-102 40 Stockholm Sweden
Tel +46 8 459 84 00
Fax +46 8 661 57 19

Äspö Hard Rock
Laboratory

Report no.	No.
IPR-02-38	F65K
Author	Date
Wendling	00-09-01
Checked by	Date
Y. Barthelmy	00-09-01
Approved	Date
Christer Svemar	02-11-19

Äspö Hard Rock Laboratory

Hydrogeological and hydrochemical impact of the tunnel and shaft construction in the Äspö site

Phase 2, Task 5. Concentration prediction and optimisation using concentration data

J. Wendling

ANTEA, France

September 2000

Keywords: Groundwater flow, Solute transport, Coupled Hydrogeochemistry, Äspö, Task 5

Fiche signalétique

Rapport

Titre : *Hydrogeological and hydrochemical impact of the tunnel and shaft construction in the ÄSPÖ site. Phase 2 : concentration prediction and optimisation using concentration data.*
Numéro : *A 20699 - D RP 0ANT 00-043/A*
Date d'envoi : *Septembre 2000*
Statut du rapport : *provisoire*
Nombre de pages : 28
Nombre d'annexes dans le texte : 0
Nombre d'annexes en volume séparé : 1
Diffusion (nombre et destinataires) : 3
2 ex. clients
1 ex. DOC/STO

Client
Coordonnées complètes : *A.N.D.R.A./DS/HG*
Parc de la Croix Blanche - 1-7, rue Jean Monnet
92298 CHATENAY-MALABRY Cedex
Interlocuteur : H. BENABDERRHAMANE

ANTEA
Unité réalisatrice : *STO*
Nom des intervenants et fonction remplie dans le projet :
J. WENDLING, auteur
P. SIEGEL (BRGM), expert éléments finis
Y. BARTHÉLEMY, chef de projet

Qualité :
Approbateur ANTEA : *Y. BARTHELEMY*
Visa A. Q. : *M. VANDENBEUSCH*
Approbateur ANDRA : *H. BENABDERRHAMANE*
N° du projet : *AND 99/789 - STOP990789*
Références et date de la commande : lettre de commande 011182 du 18/06/99

Mots-clés **:** *Modélisation hydrodynamique - 3D – éléments finis – ÄSPÖ – galerie – transport - ANDRA*

ABSTRACT

In May 1999 ANDRA invited ANTEA to join the Task 5 of the ÄSPÖ HRL, more than a year after the beginning of this task.

The objective of this study is to simulate the hydrogeological and hydrochemical impact of the tunnel and shaft construction on the groundwater in the Äspö site and to compare the simulation results with measured data. The main results in this final report are dealing with sensitivity analysis and a general method to improve evaluation of the impact linked to the use of chemical data.

Earlier work in Task 1 of the Äspö HRL concerned model construction and first prediction of impact using only hydrological data to calibrate heads. The model developed for the purpose of Task 5 is a Mixte Hybrid Finite Element (MHFE) double porosity model taking into account the fracture network and the surrounding rock matrix. The fractures are explicitly modelled in 3D, each of them having their own parameter values. The rock matrix is considered as a porous media; a "high" permeability zone (SRD 4) is separated from the "mean rock matrix".

The extension of the model reproduces the volume on which all types of data are available (hydrogeological and hydrochemical); this is the volume used in the M3 (Multivariate, Mixing and Mass balance) calculations.

A quick sensitivity analysis was made to adjust the deep recharge and permeability of each fracture and rock matrix zone.

For transient modelling we have chosen to commence calculations following the stop at tunnel front at 2600 m (December 1993) and to end the exercise at the beginning of May 1995.

After an encouraging first result, a complete sensitivity analysis was made over the main parameters defining as well the general hydraulic and transport conditions.

Analysis of the general conditions has given important information about mathematical conceptualisation and data treatment :

- The rock matrix can account for 5 to 10% of the calculated concentrations.
- Due to a fine geometric discretisation and a high dispersivity value, time step duration is not a real issue.
- The way initial data are interpolated can modify significantly the results.
- The uncertainty on M3 concentration is not implying significant bias in the concentration results.

Analysing the hydraulic and transport parameters has resulted in:

- Calculated concentrations are very sensitive to fracture permeability changes.
- Even though the model is quite large, the boundary conditions in heads have a very sensitive effect on the results.
- Kinematic porosity, specific storage and dispersivity have a sensitive effect on calculated concentrations, but in a less important manner.

To "calibrate" the model in terms of concentration, we have used the results of the sensitivity analysis and added all the changes leading to major improvements (i.e. use 0 MASL as a constant head boundary, multiply dispersivity by 2, multiply kinematic porosity and specific storage of NE-2, NE-4 and NNW-7 by 10). The optimised model based on the 4 end-member concentrations shows a 0.11 mean error, that compares very well with an uncertainty of ±0.1 in the M3 data.

SAMMANFATTNING

I maj 1999 bjöd ANDRA in ANTEA till att gå med i Task 5 hos ÄSPÖ HRL, mer än ett år efter det att Task 5 startat.

Syftet med denna studie är att simulera den hydrogeologiska och hydrokemiska påverkan från tunnlar och schakt på grundvattensituationen i Äspö HRL, och att jämföra resultaten med uppmätta värden. De viktigaste resultaten i denna slutrapport behandlar känslighetsanalys och en allmän metod för att förbättra utvärderingen av den påverkan som är kopplad till användandet av kemiska data.

Tidigare arbete i Äspös Task 1 rörde modellkonstruktion och en första prediktion av påverkan baserat på kalibrering av grundvattennivåer med endast hydrauliska data. Modellen som utvecklats för Task 5 är en Mixad Hybrid Finit Element-modell (MHFE) för dubbel porositet, som beaktar nätverket av sprickor liksom den omgivande bergmatrisen. Sprickzonerna modelleras uttryckligen i 3D, var och en med egna parametervärden. Bergmatrisen behandlas som ett poröst medium; en högpermeabel domän (SRD 4) separeras från den ”genomsnittliga bergmatrisen”.

Den utökade modellen reproducerar den volym för vilken alla data är tillgängliga (hydrogeologiska och hydrokemiska). Denna volym används in M3-beräkningarna (Multivariate, Mixing och Mass balance).

En snabb känslighetsanalys gjordes för att justera den djupa geundvattenbildningen och permeabiliteten i varje sprickzon och bergmatrisdomän på djupet.

För transient modellering har vi valt att påbörja beräkningarna från tiden efter stoppet vid 2600 m ramplängd (december 1993) och att avsluta övningen i början av maj 1995.

Efter ett uppmuntrande första resultat gjordes en komplett känslighetsanalys för de viktigaste parametrarna med definition av även de allmänna hydrauliska och transportmässiga förhållandena.

Analys av de allmänna förhållandena har givit betydelsefull information om matematisk konceptualisering och datahantering:

- Bergmatrisen kan svara för 5-10% av de beräknade koncentrationerna.
- Till följd av fin geometrisk diskretisering och ett högt värde för dispersion utgör tids-diskretiseringen inte något reellt problem.
- Sättet att interpolera ursprungliga data kan påverka resultatet betydligt.
- Osäkerheten i M3-koncentrationen betyder inte att betydelsefulla avvikelser finns i koncentrationsresultaten.

Analys av hydrauliska och transportmässiga parametrar har resulterat i:

- Beräknade koncentrationer är mycket känsliga för ändringar i sprickzonspermeabiliteten.
- Även om modellen är relativt stor har randvillkoren för grundvattennivåerna stor påverkan på resultaten.
- Kinematisk porositet, specifik magasinskoefficient and dispersivitet påverkar beräknade koncentrationer, men på ett mindre betydelsefullt sätt.

Vi har vid ”kalibrering” av modellen med avseende på koncentrationer använt resultaten från känslighetsanalysen och lagt till alla ändringar som lett till betydelsefulla förbättringar (t ex användning av 0 möh som en konstant grundvattennivå, multiplicering av dispersivitet med 2, multiplicering av kinematisk porositet och specifik magasinskoefficient hos NE-2, NE-4 och NNW-7 med 10). Den optimerade modellen, baserad på de 4 ursprungvattnens koncentrationer, ger ett medelvärdesfel på 0,11, vilket väl stämmer överens med en osäkerhet på ± 0,1 i M3-data.

CONTENTS

LIST OF FIGURES (APPENDIX)

LIST OF TABLES

1 INTRODUCTION

The Äspö Hard Rock Laboratory (HRL) is an underground site for the development and testing of methods for detailed characterisation of the rock volume from excavated tunnels. Furthermore the Äspö HRL is a full scale laboratory for testing construction and handling techniques and for the demonstration of important parts of a repository system. It also provides a multitude of data for developing our knowledge of important processes in deep crystalline bedrock and for testing of models for groundwater composition, groundwater flow and radionuclide migration.

After participating in Task 1 (1994), ANDRA invited ANTEA to join Task 5 which aims to evaluate the hydrogeological and hydrochemical impact of tunnel and shaft construction on the Äspö groundwater. The main emphasis is to integrate hydrodynamic and hydrochemical modelling.

During Task 1 three models were already completed by ANTEA: one using a Finite Difference scheme (SKB ICR 94-14), one representing only the fractures field using 1D Finite Elements in a 3D discrete network (SKB ICR 94-16), and one Finite Element double porosity model representing explicitly the rock matrix and the fracture field (SKB ICR 94-15). Unfortunately all these models were elaborated using a conceptual model not compatible with the work to be done in Task 5. For example, in 1994 the assumed local fracture field was different from the one now available for Task 5 and, furthermore, the total volume modelled in 1994 is to small for the aim of Task 5 (see § 2.4 and § 2.5).

This explains why the work done by ANTEA consisted initially in constructing a double porosity hydrogeological model taking into account the actual geometry of the fracture field and the excavation of the tunnels and shafts. In a second phase this model was used to simulate, and predict, the hydrogeological and hydrochemical impact of construction on the Äspö groundwater chemistry.

In the Äspö context (i.e. fractured granite) we have considered it important to represent fractures and rock matrix with the same accuracy. Flow is occurring mainly in the fractures but most of the water is contained in the “micro-fractured” rock matrix and this tank effect may be important for transient calculations, especially when transport of concentration is concerned. Since the flow differs considerably between fracture zones and rock matrix zones, it is also very important for the local mass balance to be as exact as possible. This is why we have chosen to use a Mixte Hybrid Finite Element (MHFE) double porosity model instead of a “Galerkine” type finite element scheme.

To represent our results (i.e. head fields, concentration evolution with time, …), and to be as explicit and objective as possible, we have chosen to use as many figures as possible. For convenience these are compiled at the end of the report to maintain the flow of the text.

2 ANALYSIS OF DATA/CONSTRUCTION OF THE MODEL

By analysing the data and the work already done by other modelling teams we have constructed a conceptual model which is described below. Due to time constraints and computer linked considerations, the model presented is not exactly what should be done "in theory" but tries to include what we consider the most important features present in the data and to reflect initial results from other teams[1].

2.1 LOCAL HYDROCLIMATOLOGY

The island of Äspö is situated at the south-eastern coast of Sweden (Fig. 1). Its surface is more or less 1 km^2. It is surrounded by other land masses, either other islands or the Sweden coast, which are never further than 500 m away. The topographical highs of the surrounding land play an important role in the local flow pattern, especially as the background (rock matrix) hydrogeological parameters are not varying much with depth (only one or two orders of magnitude for permeability) so local surface conditions are penetrating deeply. The sea arms represent the bottom points of the local water heads.

In the model we are taking into account all the emerged land present on the model's surface.

The boundary condition imposed on the sea surface is a constant head corresponding to zero MASL (Metres Above Sea Level). On the land part of the model a constant recharge is imposed. This deep recharge is initially assumed to be 10 mm/year, this value being changed in the "calibration" process.

The total salinity is not very high (25 g/l for Äspö brine water, only 6 g/l for seawater, and a calculated "mean" of around 9 g/l, see SKB TR 97-06). Therefore, the head field calculated with or without taking into account this salinity will have the same general aspect. A salinity of around 25 g/l can affect locally the flow field significantly, but such a salinity represents a maximum and is concentrated at the bottom of the model and will only affect the flow field locally. Most of the modelled volume will be affected by a salinity less than 10 g/l and such a concentration has little effect on the flow field. The density is changed from about 1% creating variations in heads in the order of magnitude of a few metres. This is the order of magnitude of the discrepancies we will find between measured and calculated heads. From our point of view there is no need to complicate the calculation scheme (taking into account the effect of salinity on the density field) for something which only marginally modifies the head field. Would the

[1] A summary of the work presented in the 12th TASK 5 meeting, in may 1999, can be found in the ANDRA report D RP 0ANT 99-034/A. This report includes also a first description of the conceptual model as proposed by ANTEA.

concentration be of 100 g/l, then the change of effect on heads could reach several tens of metres and this effect could not be neglected, but this in not the case. For these reasons **we have chosen to neglect the effect of density on flow calculation.**

2.2 FRACTURES

At the Äspö site we can consider that the explicitly determined fractures can be divided into two types: regional fractures and the local fractures (Fig. 2). The differences between these two fracture sets lies not only in the characteristic dimensions, but also in the fact that the local fractures were investigated in much more detail than the regional ones.

Some hints (see 2.4) suggest that regional fractures can play an important role in the transport of concentration, so **the model is taking into account all the fractures** (i.e. regional and local) which was not the case for the models build in 1994 for Task 1.

As we want to use a double porosity model representing with the same accuracy fractures and rock matrix, and taking into account that computing time must stay reasonable, we will have to use some simplifications.

In order to simplify the way fractures are modelled, we have linearised them. This means that the geometry of the fractures was assimilated to planes (i.e. the trace on the surface becomes a line; this can be seen comparing Figs. 2 and 3). Furthermore, fractures assumed to play the same hydrogeological role (e.g. very close and/or parallel fractures) were merged (for example NE-4 and EW-7, EW-1N and EW-1S). We are trying to reproduce a "regional" pattern and not a very detailled local pattern, this is why we assume that fractures that are close and parallel will play a similar hydrological role and, subsequently, in order to simplify the mesh we merge them. Finally fractures with no significant effect were suppressed, i.e. NNW-3 because it is not related to any other fracture and its effect on the head field should therefore be of second order. As a result, we are left with the 19 fracture networks presented in Figure 3; this figure gives all the geometrical characteristics of the fractures (e.g. surface trace and dip). When two fractures intersect, to choose whether one or both of them existed after or before intersecting, we have used integrally all the data contained in SKB TR 97-06.

Another way to simplify the fracture network would have been to represent only the fractures connected with the tunnel, assuming that the others would have a second order effect on the head and concentration fields. We think the approach we have chosen is more realistic, i.e. fractures connected to model boundaries, themselves connected to fractures connected to the tunnel, can have a significant effect on heads and transport. With the computers we have, it is impossible for us to represent the fracture field in a double porosity model approach, without any simplifications. The simplifications we have assumed are certainly not the only ones, but we think they are representative of the scale and mechanisms we want to model.

An further assumption made to represent the fractures is that the hydraulic properties are the same over the whole fracture plane, exept at fracture intersections were they are supposed to be equal to the highest value found into the fracture field.

The fractures are modelled explicitly in 3D where each fracture is represented by 2 cells in its width, a certain number of cells in its length, and an unknown number of cells in its depth, **and are all arbitrarily 10 m wide**. We have assumed the same width for each fracture in order to simplify the mesh, but the real transmissivity of the fracture is conserved. This implies that the transmissivity of the fractures is 10 times the permeability used in the model (input data for defining hydraulic properties of a given material includes permeability and not transmissivity).

A table containing all the hydraulic parameters of the fractures (e.g. initial values, optimised values, comparison with values used in other modelling) is present in §3 "Parameter Values".

2.3 ROCK MATRIX

The background (i.e. rock matrix) is formed of "micro-fractured" granite. Since the dimensions of the problems tackled in the Task 5 are greater than the R.E.V. (Representative Elementary Volume), **the rock matrix can be considered as an homogeneous porous media**. Hydraulic properties of this rock matrix can vary spatially, and certain authors identify up to 5 permeability zones (SKB TR 97-06), although some have quite a similar character. This is why **we have decided to divide the rock matrix permeability field only into two zones corresponding to a "mean" rock matrix and the so-called SRD 4 zone** (i.e. most conductive zone, see SKB TR 97-06).

2.4 HYDROCHEMICAL CONCENTRATION

The available hydrochemical data measured before tunnel construction have shown that the chemical composition of the Äspö groundwater is mainly resulting from the mixing of 4 end members :

- present meteorological water (referred to as Meteo in this report)
- present Baltic sea water (referred to as Baltic in this report)
- old water from last glaciation (referred to as Glacial in this report)
- deep ancient saline water (referred to as Brine in this report)

For this reason **we have chosen to neglect all chemical reactions and to consider only mixing transport from these four end members**.

As we will only take into account mixing of the 4 end members, the data used are mainly the results of the M3 calculations[2]. These data cover a 3.7 km x 2.5 km x 1.5 km volume with 10 x 10 x 10 voxels of equal volume 3D cells. This 3D matrix is available for two different periods, before and after tunnel construction. Figure 4 shows the concentration at around –500 m for all four end members for these two periods and for the difference in concentration between them; in the right part of Figure 4 (representing the difference in concentration due to tunnel excavation) a negative concentration represents a decrease due to tunnel excavation. This figure is just an example to illustrate some valid comments for all depths between 0 and –1500 m:

- Under natural conditions the fractures do not appear to influence the concentrations; meteoric water is under the land and sea water under the sea. This can be explained by a low regional gradient and homogeneous permeability with depth creating local flow linked to local topography.
- The change in concentration seems to follow local or regional fractures (especially for Brine).
- The change in concentration cannot be neglected, even on the boundary of the M3 volume

The boundary conditions in concentration have to reflect the spatial (and temporal) variability of the M3 data. **But, in the first simulation, even if the calculation will be transient with respect to hydraulics and transport, we will only use spatial variability of the concentration to determine the boundary conditions in concentration (boundary conditions in concentration will be considered constant with type)**. An attempt to evaluate the role of temporal variability will be considered in a future sensitivity analysis phase.

2.5 HYDRAULIC HEADS

The main data used to specify the head boundary conditions are taken from Svensson's regional model results (SKB TR 97-09). One of the conclusions of this model is that the tunnel construction will have sensitive effects on heads more than 2 km away from the site in a horizontal direction and at depth greater than 1.5 km. To minimise the boundary effects the model should be larger than this. As we don't have concentration data on such a large volume **we have chosen the M3 calculation volume for our model dimensions, since this volume is the largest on which all types of data (hydrogeology and geochemistry) are available**.

Figure 5 represents the drawdown, as calculated by Svensson (SKB TR 97-09), due to tunnel excavation, on the extension chosen for our model (this is the M3 calculation volume) and for different depths. This shows that the drawdown is important even on the boundaries, and even as we have chosen a model extension much larger than the one proposed intially by Task 5 project. The hydraulic boundary conditions should therefore

[2] M3 (Multivariate Mixing and Mass balance calculation) is a new method to evaluate separately the effect of mixing and chemical reactions on the actual water concentration assuming the origin and the evolution of groundwater are known. See SKB TR 97-06 for more explanation.

be variable in space and time. However **in the first calculation we will only use space variability of hydraulic boundary conditions**; influence of temporal variability will be evaluated in a following sensitivity analysis. In the sensitivity analysis other ways of representing heads will be used, i.e. constant head at 0 MASL (Svensson calculated heads at different dates), to try to evaluate the impact of heads boundary conditions on the results.

2.6 TUNNEL CONSTRUCTION

The model we want to use is a double porosity model representing both fractures and rock matrix. To achieve this goal, the mesh is quite large and running this model for transient flow and concentration field is quite time consuming. This is why we have tried to reduce the modelled period to a minimum.

Tunnel and shaft construction lasted from October 1990 to November 1994. During this period work stopped several times, especially from June to November 1993 when the total flow entering the tunnel stabilised (SKB TR 97-06). **We have assumed that a pseudo-permanent hydraulic flow could be achieved in around 6 months. Therefore, our transient calculation starts at the end of this "no work" period (November 1993) and ends at the beginning of May 95 (6 months after completion of the tunnel when flow should have regained steady state).**

We understand that the transient state from the beginning of the tunnel construction to November 1993 could contain important information about fracture properties and connections with rock matrix (and/or between them), but it was impossible for us, for computing time reasons, to made the calculation over such a long period.

We have assumed that a pseudo-permanent hydraulic flow can be achieved in about 6 months, but will the concentration field be stationary after this same time interval? If the concentration is transported by pure convection it will be stationary because the flow will be so. As the 4 end members are considered as perfect flow tracers, the convection velocity is the same for flow and concentration field. If the "reservoir" of end-members is not emptying, the assumption of a stationary concentration field when flow field is stationary is, from our point of view, acceptable as a first approximation (dispersion will play a role, but of the second order). The "reservoir" of end-members is obviously not being depleted for Meteoric water and Baltic waters (because these types of water are regenerated) and Brine water (because the volume available is quite large). For Glacial water, however, this assumption is not so true, but we will live with it.

To initiate the flow pattern in November 1993 we calculated a permanent flow and concentration field using the 2600 m long tunnel. The internal boundary conditions specified along the completed part of tunnel is the measured flow. Distribution between rock matrix and fractures is made according to the distance from the entrance of the tunnel and the assumption that 90% of the flow is coming from the fractures. This assumption is derived from some results achieved by other modelling teams (D RP 0ANT 99-034/A). Influence of this assumption on the results will be considered in a following sensitivity analysis.

The external (limits of the model) boundary conditions for flow and concentration used to generate this "permanent initial state" are a linear approximation taking into account the natural condition state (tunnel at 0 m), the completed tunnel state (tunnel at 3800 m) and the assumed advance of the tunnel front (tunnel at 2600 m).

For transient calculation the internal boundary conditions are up-dated each time the tunnel crosses a fracture in the model (see table 1 for more details). The up-dating is made at the beginning of a given period.

Table 1	**Time period definition**			
Period number	**Name**	**Date at beginning**	**Date at end**	**Duration (d)***
1	Initialisation Tunnel at 2600 m Shaft at 220 m	06/06/93	21/12/94	204
2	Passing NNW-1	22/12/93	26/01/94	36
3	Passing NNW-2 and NE-2 Shaft at 330 m	27/01/94	10/02/94	15
4	Passing NNW-4	11/02/94	10/04/94	59
5	Passing NNW-4 Shaft at 450 m	11/04/94	11/07/94	92
6	Passing NNW-2	12/07/94	03/08/94	23
7	Passing NNW-1and NE-2	04/08/94	15/09/94	43
8	Passing EW-1(N&S)	16/09/94	01/04/95	196

* : these durations are not the same as the ones used as time steps for the model calculation. Each period is containing one or more time steps, depending on its duration.

Shafts (SHAFTH, SHAFTV and SHAFTW) are modelled as one structure. Updating of boundary conditions linked to simulated shaft construction is made each time this modelled shaft crosses the tunnel spiral and approximated at the beginning of a tunnel construction period (Table 1).

2.7 SUMMARY OF THE MAIN CHARACTERISTICS OF THE MODEL

- ***Mathematical method used***: MHFE (Mixte Hybrid Finite Element) method

- ***Volume modelled***: Volume of the M3 data (3.7 km x 2.5 km x 1.5 km). Horizontal extension can be found on figure 3.

- ***Duration of calculation*** : from November 1993 to Mai 1995.

- ***Type of model***: - Double porosity model (rock matrix and fractures are explicitly modelled). A model representing only fractures is treated as sensitivity analysis (§ 5.1.1)
  - Transient calculation for heads and concentrations.

- ***Fractures***: They are explicitly represented as 3D structures embedded in the rock matrix. The network of fracture was simplified. A representation of the network used is given Figure 2

- ***Rock matrix***: Explicitly represented by 3D elements around the fractures.

- ***Boundary conditions in concentration***: Constant in time, varying in space, interpolated from M3 data assuming chainage of the tunnel at 2875 m (see below, initial conditions for concentration). A sensitivity analysis on interpolation method and uncertainty of the data is presented in § 5.1.4 and 5.1.5

- ***Boundary conditions for flow***: - On the surface: Constant recharge on land (Äspö and other pieces of land) (value is calibrated in § 3), constant head (0 MASL) for sea .
  - On the other boundary: Heads are constant in time, varying in space according to Svensson regional model calculations (SKB TR 97-09). Sensitivity analysis on these boundary heads is presented in § 5.2.2.

- ***Initial conditions for heads***: Determined by linear interpolation between Svensson's regional calculated heads values for initial conditions (beginning of the tunnel construction) and completed tunnel, assuming tunnel at chainage 2875 m (November 1993).

- ***Initial conditions for concentrations***: Determined by linear interpolation between M3 calculated concentrations for initial conditions (beginning of the tunnel construction) and completed tunnel, assuming tunnel at chainage 2875 m (November 1993).

3 PARAMETER VALUES

All geometrical and boundary condition assumptions, and model evolution with time, are described above.

3.1 SENSITIVITY ANALYSIS IN THE PSEUDO-PERMANENT HYDRAULIC STATE

To find out the best permeability and deep recharge values to be used in the model a first sensitivity analysis has been performed in the pseudo-permanent hydraulic state. The aim of this first calibration is to reproduce the main features of the measured piezometric field for initial conditions (prior to tunnel construction) and for chainage 2875m (November 1993). For both states we have assumed a permanent flow field (as described in § 2.6 for November 1993)

Table 2 gives the results of this calibration in terms of transmissivity. As we have simplified the geometry of the real fracture network, some fractures represented in the model have characteristics not really present in the nature. This is true for dip and orientation (due to linearisation these values may have slightly changed from the measured data) but also for anisotropy on SFZ 07 / EW-1 N&S. We have merged EW-1N and EW-1S thus, geometrically, there is no more rock matrix zone between them. To take into account this simplification, we have introduced an anisotropy factor so that the permeability perpendicular to the modelled fracture plane is 10^{-7} m/s, which is more or less the value used by Svensson in his SRD2 zone (SKB TR 97-17).

The principal results obtained by this sensitivity analysis are as follows:

- Deep Recharge: Starting from a 10 mm/year value we have concluded a **5 mm/year deep recharge.** From the available rain and evaporation data (SKB TR 97-06), we can estimate an infiltration of around 100 mm/year. From our calculations it seems then that most of this water is flowing as subsurface hypodermic flow, and only a very limited volume is able to serve as deep recharge. **This value of 5 mm/year is used for natural and disturbed conditions, and will be used also for transient calculations**.
- Rock matrix permeability: We have tested several permeability values for the two rock matrix zones. The optimised values that will be used in the following transient simulation are **10^{-8} m/s for "mean rock matrix" and 10^{-7} m/s for SRD 4 (i.e. most of the hydraulically conductive rock matrix zone)**. The same order of magnitude for these values was used by Svensson in his local model (SKB TR 97-17). We can note that some fractures, NW-1 for example, have a calibrated permeability just one order of magnitude over the value of the "mean rock matrix", but some others are much more conductive (SFZ 05, NE-3, NE-4, NNW-4, NNW-7).

- Fracture transmissivity: All the optimised values can be found in Table 2 together with the value used at the beginning of the sensitivity analysis (i.e. "mean" of the measured values). Some transmisivities have not changed, some have changed drastically. **The largest change concerns NE-2 which is in the order of 10^3**. We needed this large permeability to achieve realistic flow rates in the shaft together with a more gentle drawdown in the surroundings. Table 2 also indicates the optimised values obtained at the end of the calibration process of Task 1 (Hydraulic impact of LPT2 long-term pumping test). One can see that the permeability values optimised for Task 5 are in agreement for all the features in common with the one calibrated for Task 1, even for NE-2 for which the optimised value is quite different from the measured one. Some fractures were discovered after the Task 1 exercise and thus no comparison is possible. This implies two comments. First, LPT2 seems to have generated a large enough perturbation to affect " significantly " all the "site scale " heads, so that the permeability deduced from the interpretation of this test are still in agreement with the latest values calculated. Second, the type of mathematical model (Finite Difference, Galerkine Finite Elements, MHFE, double porosity, discrete fracture modelling) used to calibrate the permeability seems not to affect significantly the optimised values.

Figure 6 shows on the same page the measured extrapolated water table in natural conditions and the results of our permanent flow calculation under similar conditions.

Figure 7 shows, one above the other, the measured extrapolated water table at chainage 2875 m and the results of our permanent flow calculation for the completed tunnel. Although the states are not exactly the same for the two parts of the figure, we think the drawdown at chainage 2875 m is representative of the final drawdown. Effectively, as the total flow entering the system is quite constant from chainage 2875 m to the completed tunnel (SKB TR 97-06), the drawdown should not change much.

We have done no calibration on point data because there is no measured head sequence during the modelled period. Some control points have measurements before November 1993, some after May 1995, but we found no available data between these two dates. Anyway, as the calculated water table global pattern for natural and disturbed conditions present no major discrepancy with the corresponding measured fields, the calculated heads should do the same (on a general basis, but not necessary for point values, and assuming boundary conditions are correct). So achievement in terms of heads is considered satisfactory, and we will not try to improve our results.

Table 2	Fracture transmisivities			
Fracture name	**Initial transmissivities (m^2/s)**	**Calibrated transmissivities (m^2/s)**	**Transmissivities form SKB ICR 94-16 (m^2/s)***	**Transmissivities from SKB ICR 94-15 (m^2/s)***
SFZ 05	10^{-4}	$2\ 10^{-4}$		
SFZ12 / NE-1	$3\ 10^{-4}$	$3\ 10^{-4}$	$2\ 10^{-5}$	$2\ 10^{-4}$
SFZ 11	$3\ 10^{-6}$	$3\ 10^{-6}$		
EW-3	$2\ 10^{-5}$	$2\ 10^{-5}$	$1\ 10^{-5}$	$3.3\ 10^{-5}$
SFZ-03	$3\ 10^{-6}$	$3\ 10^{-6}$		
SFZ-14	$3\ 10^{-6}$	$3\ 10^{-6}$		
SFZ-04	$3\ 10^{-6}$	$3\ 10^{-6}$		
SFZ-07 / EW-1N&S**	$2\ 10^{-5}$ / 10^{-7}	$2\ 10^{-5}$ / 10^{-7}	$2.2\ 10^{-5}$	$6\ 10^{-5}$
NW-1	$3\ 10^{-7}$	$3\ 10^{-7}$	$7\ 10^{-6}$	$7\ 10^{-4}$
NE-2	$3\ 10^{-7}$	10^{-4}	$4\ 10^{-5}$	$2\ 10^{-4}$
NNW-5	$3\ 10^{-6}$	$3\ 10^{-6}$	$5\ 10^{-5}$	$5\ 10^{-7}$
NNW-7	$6\ 10^{-6}$	10^{-4}		
NNW-1	10^{-5}	10^{-5}	$1.5\ 10^{-5}$	$1.5\ 10^{-7}$
NNW-2	$4\ 10^{-6}$	$4\ 10^{-5}$	$4\ 10^{-5}$	$4.8\ 10^{-5}$
NE-3	$3\ 10^{-4}$	$6\ 10^{-4}$	$3\ 10^{-5}$	10^{-4}
NNW-4	$9\ 10^{-5}$	$5\ 10^{-4}$	$4\ 10^{-4}$	$4\ 10^{-3}$
NNW-6	10^{-5}	10^{-5}	$5\ 10^{-5}$	$9\ 10^{-7}$
NNW-8	$9\ 10^{-6}$	$9\ 10^{-6}$		
NE-4	$3\ 10^{-5}$	$2\ 10^{-4}$	$3.2\ 10^{-4}$	$2\ 10^{-4}$
Fractures intersections	$3\ 10^{-4}$	$6\ 10^{-4}$		

* : for comparison. Values optimised on LPT2 long-term pumping test data during Task I. Modelling performed by ANTEA and BRGM using a finite difference software (MARTHE, SKB ICR 94-16) and a finite element model (ROCKFLOW, SKB ICR 94-15). A third model, based on discrete fracture modelling, was made with the CHANNET software (SKB ICR 94-14) but gave no additional interesting information about this topic.

** : anisotropy. First value is referring to fracture plan, second one to the perpendicular direction.

3.2 OTHER PARAMETERS

In the permanent flow sensitivity analysis we have found some permeability and recharge values; for other parameters we have used values extracted from the literature :

- Baltic bottom: Different studies (SKB ICR 94-15, SKB ICR 94-14) give some hints that the bottom of the Baltic sea could be formed by a less permeable marine sedimentary layer. We assume therefore that the **permeability** of the modelled elements directly in contact with the sea bottom is **divided by 1000**.

- Storage: We used **for the fractures the formula** found in SKB TR 97-06:

  $$\mathbf{S = 9.22\ 10^{-3}\ T^{0.785}}$$

  With: S : Storage (-)
  T : transmissivity (m^2/s)

  For the "mean" rock matrix we used 10^{-6} and for SRD 4 we have assumed 3 10^{-6} (SKB TR 97-06).

- Kinematic porosity: For all the different zones (fractures + rock matrix) we used the formula found in SKB TR 97-06 :

  $$\mathbf{n_e = 34.87\ K^{0.753}}$$

  With: n_e : Kinematic porosity (-)
  K : permeability (m/s)

- Dispersivity: There are no data about material dependent dispersivity at the Äspö site. So, we have used the **same dispersivity for fractures and rock matrix: 100 m for the longitudinal value, 10 m for the transversal value.**

4 TRANSIENT FLOW AND CONCENTRATION CALCULATION

Using the model described above we have calculated the transient flow and the transport of concentration for the four end members.

Figure 8 gives for the 22/12/93 our calculated concentration along the tunnel. This Figure also presents the M3 calculation results, with an uncertainty ±0.1, for September 1993, since there are more values for this date. The five M3 data values available for December 1993 are also plotted. One can see that the September M3 data are in good agreement with the December M3 data and that comparison between our results and the data (M3 results) is possible using the September M3 data.

Our model reproduces the general trend found in the data along the tunnel, but individual values are not in good agreement for all the four end members. For Brine water our results are always plotting within the area of uncertainty. For glacial water it is not so obvious, but the greatest number of results are in agreement with the data.

For this first run, the model is completely missing the relationship between Baltic and Meteo waters. Around 1000-2000 m there is too much Baltic water and not enough Meteo water; one explanation could be that the permeability decrease imposed on the bottom of the Baltic is large big enough. Another explanation could be that the deep recharge is too small. (See following sensitivity analysis to find out that the model can reproduce quite good results in these two end-members)

With respect to time-series data, SKB wanted us to take into account 15 measurement points representing 11 control points, but due to the numerical geometric discretisation some measurement points were merged. In our model, the only control point represented by more than one calculation point is CP3. Figures 9 to 20 represent the time varying concentration for the four end members at the 11 control points (represented by 12 calculation points).

For some control points there are no concentration data available in the modelled period, consequently nearby values have been used (CP3-SA1327A, CP6). For some other points there is only one or two measurements at the beginning or at the end of the modelled period (CP7, CP8, CP9, CP10). For all these control points it is difficult to estimate if the variation of concentration during the modelled period is realistic or not.

Nevertheless, for all the other points having adequate measured data, one can see that individual point calculated concentrations based only on a global head pattern calibration is not very representative of the data measured at the same individual point. This is true not only for values but also for variation trends.

Trying to improve our model, we have made a sensitivity analysis on different factors affecting the concentration results.

5 SENSITIVITY ANALYSIS

In the above, the optimisation we have performed was focused only on hydraulic heads. The sensitivity analysis described below is dealing with most of the parameters that can affect the calculated concentrations of the four end members at the control points.

These parameters can be classified as three types:

- General conditions: This group is dealing with the influence of factors as different as double porosity/discrete fracture modelling, mathematical resolution, duration of time steps, type of interpolation on original point data and influence of uncertainty on concentration data.
- Hydraulic parameters: This class includes permeability and external head boundary conditions.
- Transport parameters: Three parameters are analysed: kinematic porosity, storage coefficient and dispersivity.

We will present the results of this sensitivity analysis following the order described above. The sensitivity analysis used is a "parameter by parameter" analysis. As some parameters are interacting this analysis should be completed by a "multivariate" analysis. Anyway, the simple "parameter by parameter" approach will permit a quantitative determination of the most sensible parameters.

As there are 12 control points to consider, it is impossible to represent all of them for all the sensitivity analysis. We have chosen to represent only 2 to 4 results representative of the global behaviour linked to a given analysis.

Table 3 (in the appendix, after the figures) is reproducing, for all the control points, for the 4 end members, and at two different dates (22/12/93 and 01/05/95, "beginning" and end of the modelled period), the error made by each model. For some points there are no data available at those dates, which explains why some columns of the table are empty.

This error is calculated as follows. M3 concentrations are already presented as percentage values (between 0 and 100); our calculated concentrations are presented under the same form (on all the figures). The error is the absolute value of the difference between the M3 value and the calculated value. The far right part of Table 3 gives the mean error for each end-member, this is the sum of the errors calculated for all the control points were data were available, for the two dates (if available) divided by the number of summed values.

5.1 GENERAL CONDITIONS

5.1.1 Double Porosity/Discrete Fracture Modelling

To distribute the measured flow entering the tunnel between rock matrix and fracture we have assumed that 90% of this flow is coming from the fractures. This assumption has obviously some influence on calculated heads, but also on calculated concentrations. Trying to estimate the real influence of the rock matrix, in terms of calculated concentrations, we have "extruded" the fracture mesh from the rock matrix and made a new calculation with it. By "extruded" we mean that everything that represents the fractures is exactly the same as before (nodes, elements, external and internal boundary conditions, …). The only change is that the part of the fractures initially in contact with the rock matrix is now in contact with "nothing"; we have created a discrete fracture model.

In general the difference in calculated concentration is less then 5% (Figs. 21 and 22), but for some control points it can be more significant (Figs. 23 and 24). However, **on the average we can say that the role of the rock matrix is not predominant.** In other terms, two calculations made with and without the rock matrix will give globally the same results in terms of heads and concentration. This is why we will make all future calculations using the "fracture only" model. This model is much smaller than the "global" one, reducing considerably the memory needed and the calculation time. Without this substitution we would not have achieved a sensitivity analysis as complete as the one we did.

In the following sensitivity analysis, especially in the legend of the figures, the "reference" relates to the "fracture only" model we have constructed.

5.1.2 Type of Mathematical Resolution

The mathematical method used for the above calculations was the MHFE method. This method is quite demanding in terms of computer resources and we will try another mathematical scheme, less demanding, trying to reduce computer time and computer resources. The other method used is the Galerkine finite element method. This method can work on the linear hexaedric element mesh we already have and we only have to change the boundary conditions.

Trying to be synthetic, and to emphasise only the implications in terms of heads/velocity results, we can say that the principal difference between these two methods lies in the fact that, for Galerkine method, the flow velocity is not continuous at the local scale (boundaries between elements), which implies that the mass balance is not respected at this same scale (element scale).

The way boundary and initial conditions are applied depends of the type of mathematical scheme, e.g. on nodes for the Galerkine method and on faces for the MHFE method. We have tried to use boundary and initial conditions as close as possible for the two runs. For head and concentration conditions we have interpolated initial

data, either on nodes or on faces, using the same algorithm. For flow conditions (in the tunnel) we have distributed the face value used in the MHFE method uniformly on the 4 nodes defining this face (in our model, all the elements are hexahedric) using for each of them a ¼ of the global value.

Although the difference in terms of head field is not significant, Figures 25 and 26 show that the differences in concentration can be very significant for certain control points, and these can be attributed to two factors:

- Although we tried to reproduce as closely as possible the conditions (boundary and initial) used in the MHFE method, it is possible that the residual discrepancies can create significant changes in the results.
- The fact that the Galerkine method is less accurate in terms of local velocity field, local mass balance can generate errors, especially in zones where the elements are large and/or have distorted shapes. Maybe the numerical discretisation used is not sufficient near the boundaries (outer parts of the model) and this generate oscillations during concentration calculations that are more important for the Galerkine method than for the MHFE method.

Because differences in terms of calculated concentrations are significant, we will stick to MHFE method since, on the average, it should give better results in terms of concentration field.

5.1.3 Time Step Duration

As our initial model was quite large in terms of computer demands, we used quite large time steps to reduce as much as possible the calculation time. In order to estimate the influence of the time step duration on the results we have made a run with time steps not greater than 15 days. This means that some initial time steps were not changed, but some were divided by more than 3.

Figures 27 and 28 present the results for CP2 and CP11 respectively; there is no significant change and this is true for all the control points. **Due to a fine mesh, and a high dispersivity, the calculation time step is not really important** for the type of responses we want to analyse (month to year variations).

5.1.4 Type of Interpolation

To interpolate the data (heads and concentrations) over the mesh, we have used 3D linear interpolation. As the data are quite sparse, especially for concentration, the type of interpolation can have an importance. The difference in value due to different types of interpolation may not be significant for initial conditions as it vanishes with time. But it may be essential for boundary conditions as it will condition the long-term results.

We have tried two simple interpolation methods: “inverse of the distance” (“dist” on the figures) and “nearest neighbour” (“near” on the figures). As one can see from Figures 29 to 31 the differences in calculated concentrations can be very important, even the variation trend can change.

The “inverse of the distance” method gives results quite close to the initial “3D linear interpolation”. Even if 5% of difference can be found between these two interpolation methods, at least the type of variation during time remains the same. However, this is not the case for the “nearest neighbour” method. Discrepancies can be greater than 70% and the variation can be inverted, i.e. a decreasing concentration with time can become an increasing one.

“Nearest neighbour” is a crude interpolation method, but the M3 group providing us with the “extrapolated” concentration data were reluctant to define a coarser mesh since there are not enough measurements to extract more significant spatial variability, so we did not pursue this.

Nevertheless, looking at Figures 29 to 31 we can see that the results obtained by the “nearest neighbour” interpolation method can show a large divergence from the data, which is not the case for the results of the two other interpolation methods. Due to this fact, **we have chosen the “3D linear interpolation” method.**

5.1.5 Uncertainty of Concentration Data

The uncertainty associated with the M3 “measured” concentration data is about ±0.1. This can be equally important as the interpolation method, especially on boundary conditions. To evaluate the uncertainty of the results linked to the uncertainty of the initial data we have made two calculations introducing a “sort of white noise” of 0.1 in the M3 data.

What we did was to generate a random number drawn from a normal distribution with a standard deviation of 0.1, add such a number to each of the four end-members, and “adjust” the values so that the sum of the four is still equal to 1. Mathematically speaking, returning to a sum of 1 is reducing the uncertainty from 0.1 to about 0.09, which we assume is not significant. Following this approach, we assume that the uncertainty is not correlated in space (at the M3 voxels scale). This is not realistic, and the uncertainty should be smaller if we are not far from the points were measurements were made. So the representation we use is somehow overestimating the uncertainty. So this crude representation, using simple tools, will provide an estimation of the “maximum” impact of the uncertainty on the M3 data.

Figures 32 to 34 represent some of the results. The differences in calculated concentration are on average less than 0.05. This could be somewhat surprising since the “white noise” is 0.1 (0.09 in fact), but, because dispersivity is high and the control points are far from the outer limits of the model, the differences in boundary conditions are smoothed out along the travelling paths.

We can than say that **the relatively high uncertainty of the calculated M3 concentrations is causing no significant bias in the results.**

In the paragraph dealing with data analysis we said that it would be interesting to use time varying boundary conditions (§ 2.4). We have seen here that a random variation of boundary conditions can be smoothed out along the travelling path to the control point. Perhaps if the change is greater than 0.1 the smoothing process will no more be so efficient. Perhaps if the variation in boundary conditions is correlated in space over a scale greater than the M3 voxels, the smoothing process will no more be so efficient. But even like this, a change in concentration boundary conditions will not have an effect as large as if no smoothing effect could take place at all. The hypothesis made by considering constant boundary conditions with time is therefore more realistic than it seems initially.

5.2 HYDRAULIC AND TRANSPORT PARAMETERS

In all the above sensitivity analysis we have only dealt with general conditions. This was not done directly to improve the results, but to see if the way to interpret the data and to apply a mathematical scheme can have significant effects on the results. In the following part of this sensitivity analysis we will try to find better hydraulic/transport parameter values so as to improve the results.

Table 3 (in the appendix, after the figures) presents the error incurred by each model, for all the control points, for the four end members and at two different dates (22/12/93 and 01/05/95, "beginning" and "end" of the modelled period). For some control points there are no data available at those dates, and some colomns of the table are therefore empty.

5.2.1 Permeability

Whilst calibrating heads we have changed significantly some of the fracture permeability compared to the means of measured values (see Table 2 in § 3.1), especially true for NE-2, NE-4 and NNW-7. This calibration process was somehow crude, and anyway it is not certain that a "somehow" optimal value for head reconstitution is similarly optimal for the concentration calculation. This is why we have tried larger (*10) and smaller (/10) values for the 3 fractures listed above. This analysis will also permit is to estimate the influence of a permeability change in terms of calculated concentrations.

For those control points far from the 3 fractures with altered permeability, the calculated concentrations are not influenced (Fig. 35). The more the control point is near the influence field of one of the modified fractures, the more the calculated concentrations can be different (Figs. 36 and 37).

From this sensitivity analysis two different conclusions can be drawn:

- A punctual calculated concentration can be very sensitive to a change in permeability.
- On the average (over all the control points) the results of the model are not improved significantly by changing the permeability.

Conclusion : We will stay with the permeabilities estimated from the head calibration process.

5.2.2 Head Boundary Conditions

In paragraph 2.5 we have seen that, even if the model is quite large, the heads on its boundaries are normally varying with time due to tunnel excavation. So far we have assumed fixed boundary conditions in time. It would be too great a task to implement varying boundary conditions with time, but in any case different types of head boundary conditions will be used to estimate the influence of this hypothesis.

The head boundary conditions used untill now were a linear interpolation of the undisturbed and the disturbed conditions calculated by Svensson in his regional model (SKB TR 97-09), assuming the tunnel was at chainage 2875 m. Considering undisturbed natural conditions (as calculated by Svensson) ("H ini" in the figures), in addition to hydrostatic pressure at 0 MASL ("H 1000" in the figures), Figure 38 shows that for certain points the influence of this change is not significant. On the other hand Figures 39 and 40 show that a change in head boundary conditions can generate a large change in calculated concentration.

In terms of improving the model for concentration calculations, on the average, the hydrostatic pressure conditions are producing better results than boundary conditions extracted from the "realistic" head field calculated by Svensson, especially for trend estimation (Fig. 40).

This is a quite surprising result. One would expect that more realistic boundary conditions would help to recreate the variation in concentrations. Several explanations can be advanced:

- The model is not reproducing well the "real" flow mechanism and this has implications on the concentration calculation. To create the model we have made some assumptions on fracture geometry, but we have kept all the main characteristics, so we don't think this is the main explanation (although it could be an explanation of the second order).
- The Svensson regional model has: a) rectangular cells of quite large dimension, b) the fractures are not implemented directly into this mesh, c) the fractures are represented by an increase in integrated conductivity between two cells, and d) a "fracture" is relatively large, which is not the case in our model.
- The data available from Svensson's regional model are permanent head fields for undisturbed conditions and the completed tunnel. Maybe (especially for undisturbed conditions) the natural variation due to climate change gives a mean flow field which is better represented by homogeneous boundary conditions, at least at the scale we are looking at.
- We have linearised the fractures. Measured topographical traces for some of them were quite far from lines, and the point on which the modelled fracture and the equivalent "measured fracture" are intersecting the model boundary can be different. Therefore, it is possible that on certain points our model is taking into account boundary conditions that are not meant to be attributed to fractures but

to rock matrix (and vice versa). Having more smoothed boundary conditions, somehow representing the reality (0 MASL cannot be to far from reality on a coast line), may help to reproduce the concentration field.

Remark: If this last explanation is right, it could also affect the concentration boundary conditions. But the M3 voxels are much larger than the Svensson regional model elements, and therefore the influence for concentration boundary conditions is less important.

In order to improve the results of the model it would be better to use hydrostatic pressure at 0 MASL for boundary conditions in heads.

5.2.3 Kinematic Porosity

We have used a relationship between permeability and kinematic porosity to determine the values of this latter parameter (see § 3.2). This type of relationship is suitable to define a general tendency but is not very accurate. Two different models have been run changing certain kinematic porosities (*10, /10), but conserving all permeabilities at the values found during the calibration process (Table 2, § 3.1). The fractures where kinematic porosity were modified are the 3 fractures for which the permeabiliy has drastically changed during the calibration process (NE-2, NE-4, NNW-7).

For some control points the calculated concentration is not very sensitive to kinematic porosity changes (Figs. 41 and 42), but, on the average, **having a higher kinematic porosity in these three fractures improves the results** (example in Fig. 41).

5.2.4 Specific Storage

As for kinematic porosity the values of specific storage are also related to the permeability (§ 3.2). This relationship is not more accurate than the previous one, and we have tried the same type of sensitivity analysis by changing the specific storage of NE-2, NE-4 and NNW-7 by a factor 10 and 0.1.

The conclusions are the same as for kinematic porosity; for some control points there is no important change (Figs. 44 and 45) but, on the average, **a higher specific storage gives better results** (example in Fig. 46).

5.2.5 Dispersivity

The value of dispersivity used is essentially derived from the general hypothesis that the longitudinal value of this parameter is more or less 1/10 of the general pathway length (Appelo & Postma, 1994, page 363), the transversal value being 1/10 of the longitudinal value. The dimensions of the model are 2 or 3 kilometres in X and Y; the control points are more or less in the middle of this surface so the longitudinal dispersivity should be around 100 m and the transversal dispersivity around 10 m. There are no data available to distribute these values depending on the fractures and/or the rock matrix zone.

We have tried larger (α_L=200 m and α_T=20 m) and smaller (α_L=50m and α_T=5m) values. Results are presented in Figures 47 to 50; no significant changes in general can be observed (Figs. 47 and 48) but **some improvements occur with α_L=200 m and α_T=20 m** (Figs. 49 and 50).

5.3 OPTIMISED VALUES

We will not use the first part of this sensitivity analysis (general conditions) trying to improve the calibration on the concentration calculation. But the second part (sensitivity analysis on hydraulic/transport parameters) gives us some information on **how to achieve a better fit from the data :**

- **Use constant boundary head conditions at 0 MASL.**
- **Multiply kinematic porosity of NE-2, NE-4 and NNW-7 by 10 (compared to values given in § 3)**
- **Multiply specific storage of NE-2, NE-4 and NNW-7 by 10 (compared to values given in § 3)**
- **Multiply dispersivity by 2 (compared to values given in § 3) to have α_L=200 m and α_T=20 m**

We have not changed the initial values of the other parameters tested. This does not mean that the model is not sensitive to these parameter changes, but only that these parameters were already at an acceptable value (i.e. permeability, boundary values in concentration)

Based on these results we should carry on with a "multivariate" sensitivity analysis using only these 4 parameters, trying to find the optimal value for each of them. But, in a first attempt to improve calibration, we have introduced all these changes during a single run producing the results shown in Figures 51 to 62 for all the control points.

Table 3 (in the appendix, after the figures) is reproducing, for all the control points, for the 4 end members, and at two different dates (22/12/93 and 01/05/95, "beginning" and end of the modelled period), the error incurred by each model. For some points there are no data available at those dates, which explains why some columns of the table are empty.

This error is calculated as follows. M3 concentrations are already presented as percentages (values between 0 and 100). Our calculated concentrations are presented under the same form (on all the figures). The error is only the absolute value of the difference between the M3 value and the calculated value. The far right part of Table 3 gives the mean error for each end-member; this is the sum of the errors calculated for all the control points were data were available, for the two dates (if available) divided by the number of summed values.

From the figures we can see that **improvement is quite important for a large majority of the control points.** Looking at Table 3 (appendix, after the figures) we can quantify this improvement. On the average (all control points and the four end members) we pass from an error of around 0.17 to less than 0.11. **It is important at this point to remember that the accuracy in the M3 data is ±0.1 and, for this reason, an average divergence from these data of 0.11 is quite a good fit**. The largest improvement is for Brine where the average error was 0.18 and the residual error is now 0.05.

We have no complete explanation about this quite surprising improvement. What we can say is that the 4 parameters (head boundary value, kinematic porosity, specific storage and dispersivity) we have retained for optimisation are relatively independent. For example, there is no relation between head boundary value and kinematic porosity, or between specific storage and dispersivity. Even if a "conceptual" relationship can be found between kinematic porosity and specific storage, this relation is weak in practice. Due to this "orthogonality" of the parameters, the gain due to a change in one parameter is "independent" of the gain due to a change in an other parameter. Therefore, the global gain obtained by changing simultaneously the 4 parameters is somehow an "addition" of the 4 individual gains.

Another point is that the range of values used during "parameter by parameter" sensitivity analysis is related to the uncertainty of each parameter. Because of the thorough data base available for the Äspö site, the initial values tend to be quite correct and the uncertainty ranges are relatively small. Therefore, after "parameter by parameter" optimisation, even if we are not really at the optimum value, we cannot be too far from it.

Since this fit is satisfactory, we have not tried to achieve better optimisation using a "multivariate sensitivity analysis". Such an exercise would certainly improve the results by determining "the" optimum value for each parameter, but it would be time consuming for an improvement which perhaps is not significant since the residual error is already the same as the uncertainty in the M3 data.

6 CONCLUSIONS

The model presented in this report is taking into account all the deterministic fractures present at the Äspö site, and representing the rock matrix as a homogeneous porous media.

The model has a 3.7 km x 2.5 km x 1.5 km extension trying to avoid as much as possible the boundary condition effects. The boundary conditions are based on data for heads and concentrations on all sides except the surface side where a constant head is assumed for sea elements and constant infiltration for land elements.

In a first calibration only the permeabilities were fitted using a sensitivity analysis on permanent flow calculations; all other parameters were extracted from the literature and used without fitting.

Generally, we can say that this model is behaving correctly as far as heads are concerned, but less satisfactorly when it comes to concentration. In order to understand why the model gives such poor results and to improve the fit in concentration, we have carried out a sensitivity analysis on general conditions and hydraulic/transport parameters.

The analysis on general conditions has given important information about mathematical conceptualisation and data treatment:

- The rock matrix can account for 5 to 10% of the calculated concentrations.
- Due to a fine geometric discretisation and a large dispersivity value, time step duration is not a real issue.
- The way initial data are interpolated can modify significantly the results.
- The uncertainty of the M3 concentration is not causing significant bias in the concentration results.

Analysing the hydraulic and transport parameters we obtain the following:

- Calculated concentrations are very sensitive to fracture permeability changes.
- Even though the model is quite large, the boundary head conditions have a very sensitive effect on the results. Although of less importance, this is also true for the concentration boundary conditions.
- Kinematic porosity, specific storage and dispersivity have a sensitive, but less important effect on calculated concentrations.

To “calibrate” the model in terms of concentration, we have used the results of the sensitivity analysis and implemented all the changes leading to major improvements (e.g. using 0 MASL constant head boundary, multiply dispersivity by 2, multiply kinematic porosity and specific storage of NE-2, NE-4 and NNW-7 by 10). The optimised model of the four end-members concentrations shows a 0.11 mean error, that compares very favourably with the quoted uncertainty of ±0.1 in the M3 data.

What has been learned about Äspö from this exercise is the following:

- The drawdawn created by the tunnel construction has a significant effect on the flow and concentration fields much less than the volume generally used to represent the Äspö island in the hydrogeological modelling. Investigating a larger volume to find suitable boundary conditions for the models could be of some interest.
- The influence of the rock matrix in the flow and concentration fields (as far as only maxing fractions are concerned) is of second order importance compared to the influence of the fracture network.
- The estimated deep recharge is of some 5mm/year; this means that most of the rain is returned to the sea by run-off or hypodermic flow processes.
- There exists a "clay" layer on the bottom of Baltic sea reducing flow from the sea to the hydrogeological system represented by the bedrock fracture field.
- We have initially carried out a rough calibration on heads only, followed by a sensitivity analysis only on the concentration field. We have found that the fracture transmissivities used to calibrate heads are suitable values for fitting also the concentrations. In other words, once the calibration is done for the heads, there is no longer any need to fit the transmissivity if the ultimate aim is the concentration field.
- From our calculations we can say that even if the transmissivity is well calibrated, it is possible to miss completely the concentration field, even though the other parameters consist of "generic values" representing good orders of magnitude.
- According to our calibration the transmissivity of NE-2 is much greater than the measured value. This is in agreement with an earlier calibration conducted during Task 1.
- According to our calibration the transmissivity values of the fractures are spreading over more than 3 orders of magnitude. Maybe eliminating the less transmissive fractures from the modelling could help simplify the meshes without changing the results.

BIBLIOGRAPHY

Appelo, C.A.J. and Postma,D., 1994. A. A. Balkema (Ed.)., Geochemistry, groundwater and pollution. Rotterdam, Brookfield, 1994

Barthelemy, Y., Schwartz, J. and Sebti, K., 1994. Hydrodynamic modelling of the original steady state ans LPT2 experiments. MARTHE and SESAME codes. SKB Äspö HRL Int. Coop. Rep. (ICR 94-16), SKB, Stockholm, Sweden. (Äspö HRL – Simulation du pompage LPT2 à l'aide d'un modèle aux différences finis. Rapport final - 663 RP BRG 93-012)

Billaux, D., Guérin, F. and Wendling, J., 1994. Hydrodynamic modelling of the Äspö HRL. Discrete fracture modelling. SKB Äspö HRL Int. Coop. Rep. (ICR 94-14), SKB, Stockholm, Sweden. (Äspö HRL – Simulation du pompage LPT2 à l'aide d'un modèle discret. Rapport final - 663 RP BRG 93-018).

Noyer, M.L. and Fillion, E., 1994. Hydrodynamic modelling of the ÄSPÖ Hard Rock Laboratory. ROCKFLOW code. SKB Äapö HRL Int. Coop. Rep. (ICR 94-15), SKB, Stockholm, Sweden. (ÄSPÖ HRL – Simulation du pompage LPT2 à l'aide d'un modèle à double porosité. Rapport final - 663 RP BRG 93-016).

Rhén, I., Gustavson, G., Stanfors, R. and Wikberg, P., 1997. Äspö HRL – Geoscientific evaluation 1997/5. Models based on site characterization 1986-1995. SKB Tech. Rep. (TR 97-06), SKB, Stockholm, Sweden.

Svensson, U., 1990. The island of ÄSPÖ. Numerical calculations of natural and forced groundwater simulations. SKB Prog. Rep. (PR 25-90-03), SKB, Stockholm, Sweden.

Svensson, U., 1997. A regional scale analysis of groundwater flow and salinity distribution in the ÄSPÖ area. SKB Tech. Rep. (TR 97-09), SKB, Stockholm, Sweden.

Svensson, U., 1997. A site scale analysis of groundwater flow and salinity distribution in the ÄSPÖ area. SKB Tech. Rep. (TR 97-17), SKB, Stockholm, Sweden.

Wendling, J., 1999. Laboratoire souterrain d'ÄSPÖ TASK 5. Résultats intermédaires présentés à la 12ème réunion de la Task Force, et modélisation conceptuelle proposée par ANTEA. D RP 0ANT 99-034/A

APPENDIX 1, Figures

APPENDIX 1

LIST OF FIGURES

Figure 1 : Localisation of the ÄSPÖ site

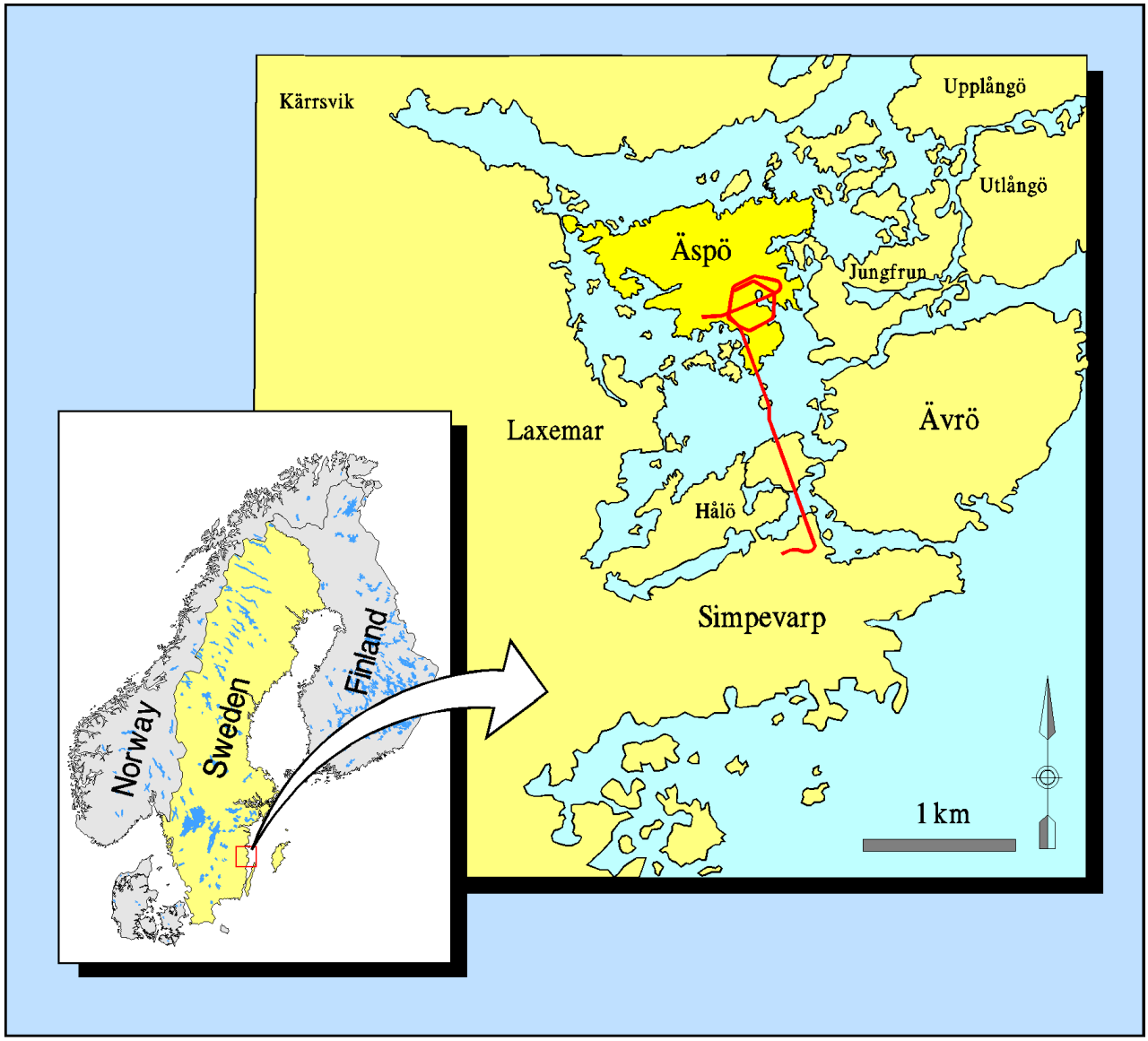

Figure 2 : Regional and local fractures

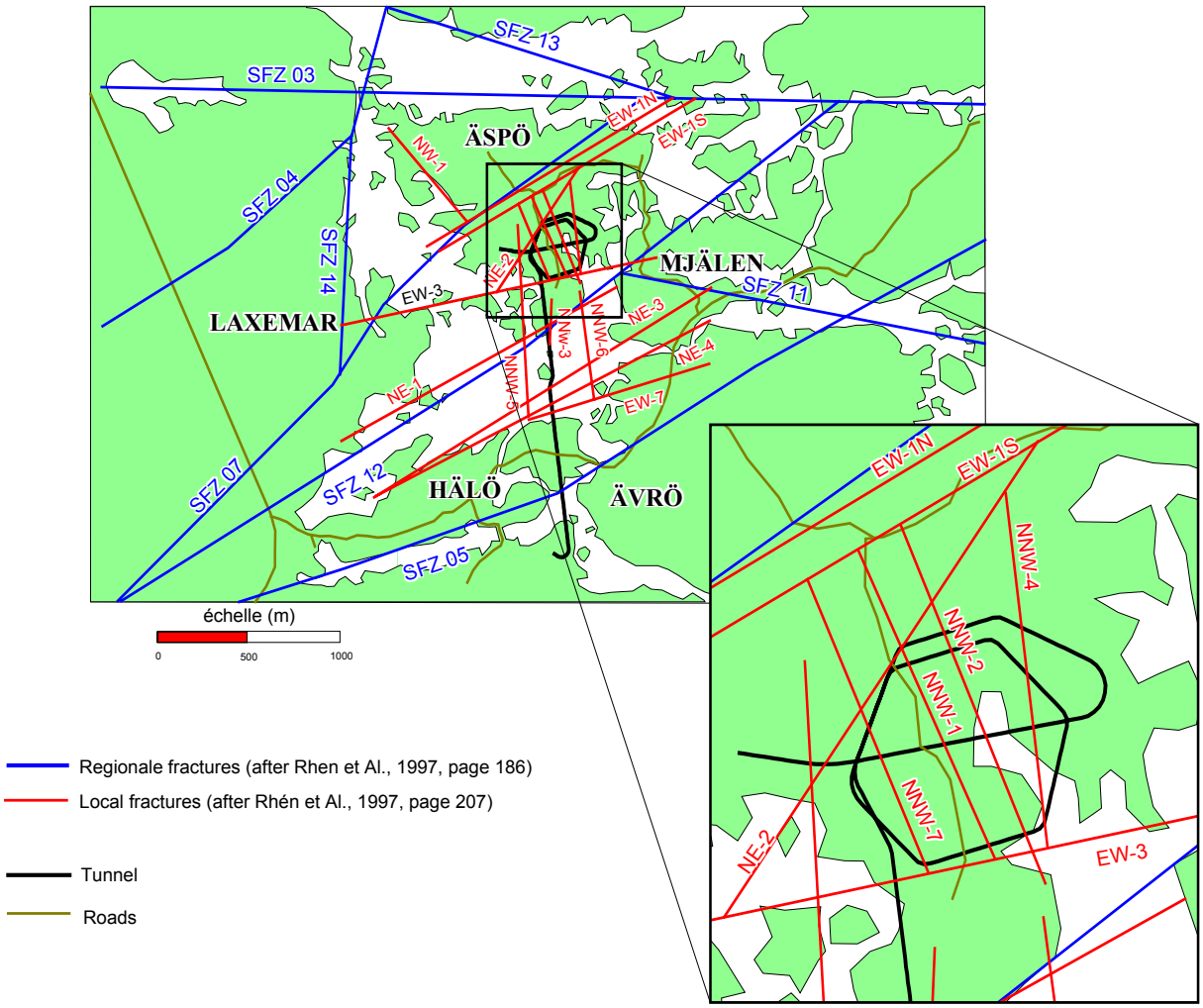

Figure 3 : Modelled fractures

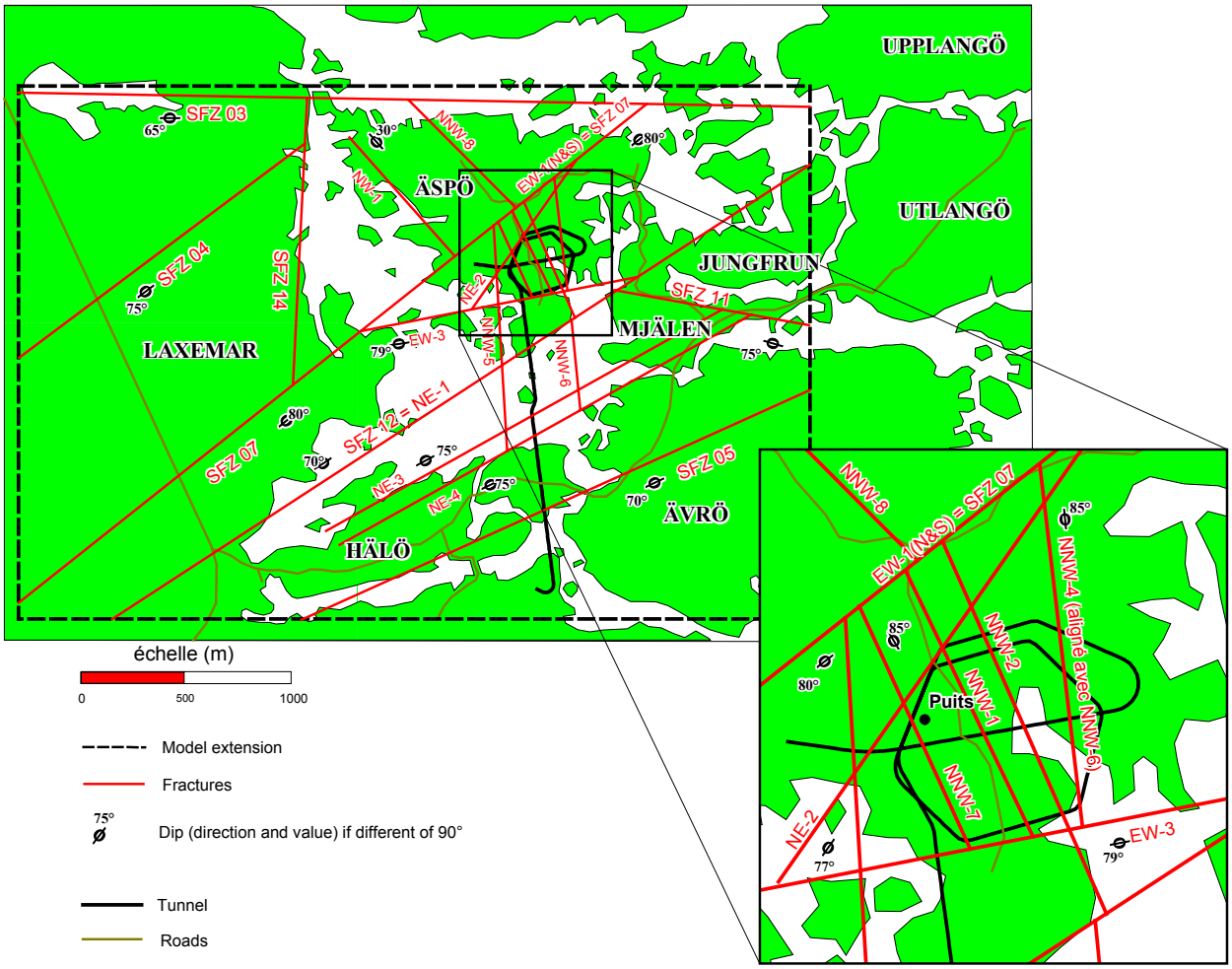

Figure 4 : M3 calculated concentrations at –500 m

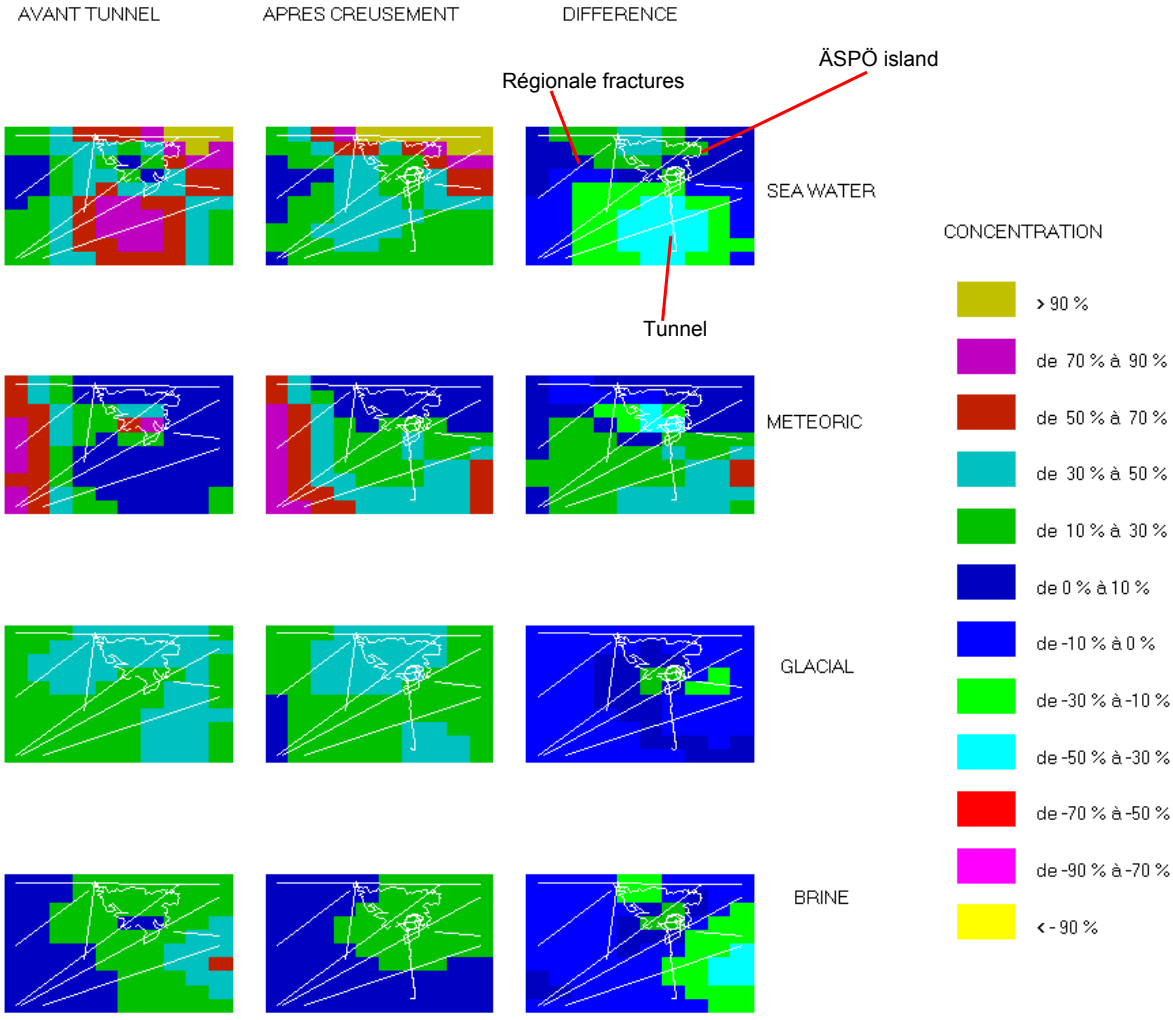

Figure 5 : Drawdown due to tunnel construction (after Svensson, 1997)

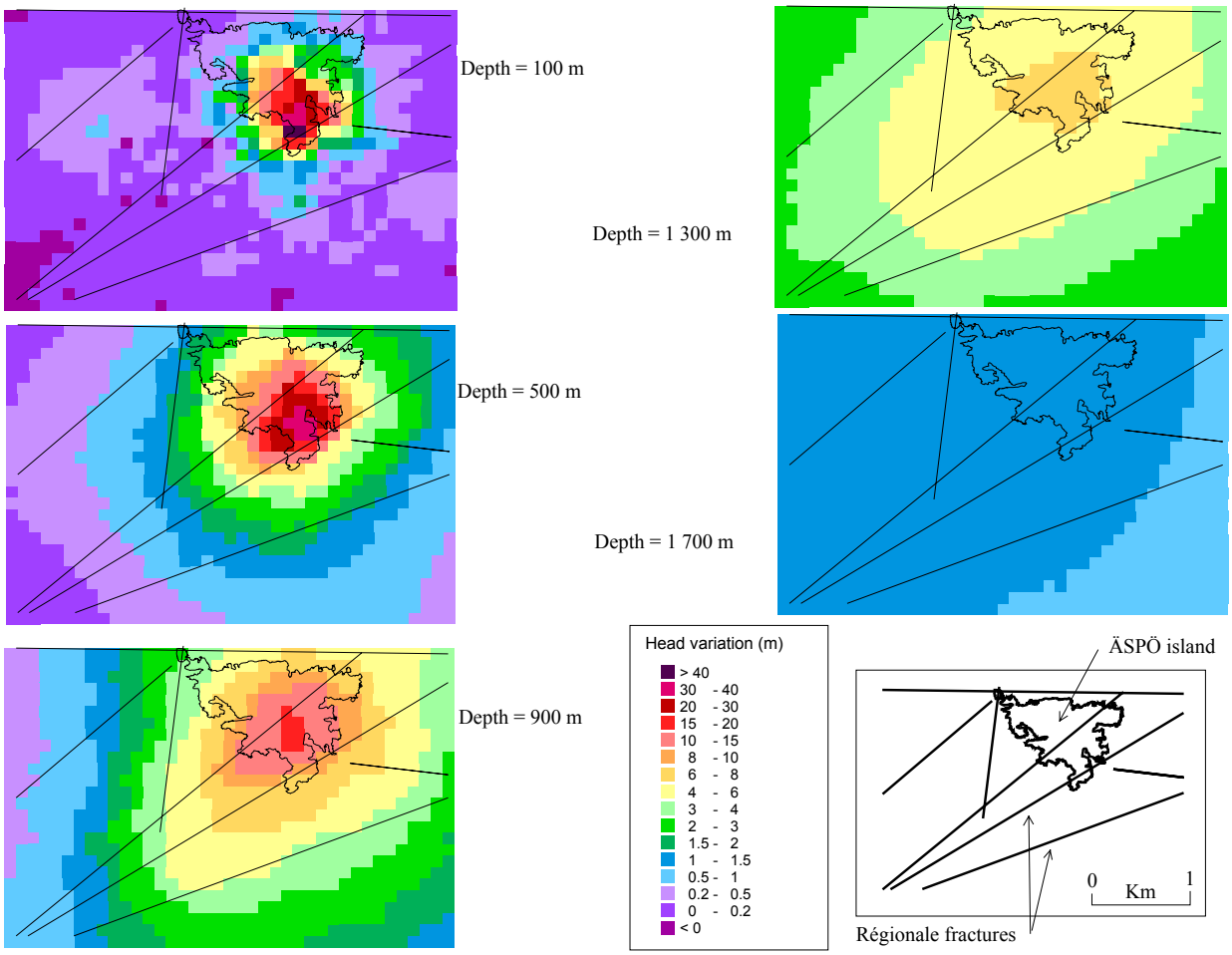

Figure 6 : Comparison between results and data for natural watertable

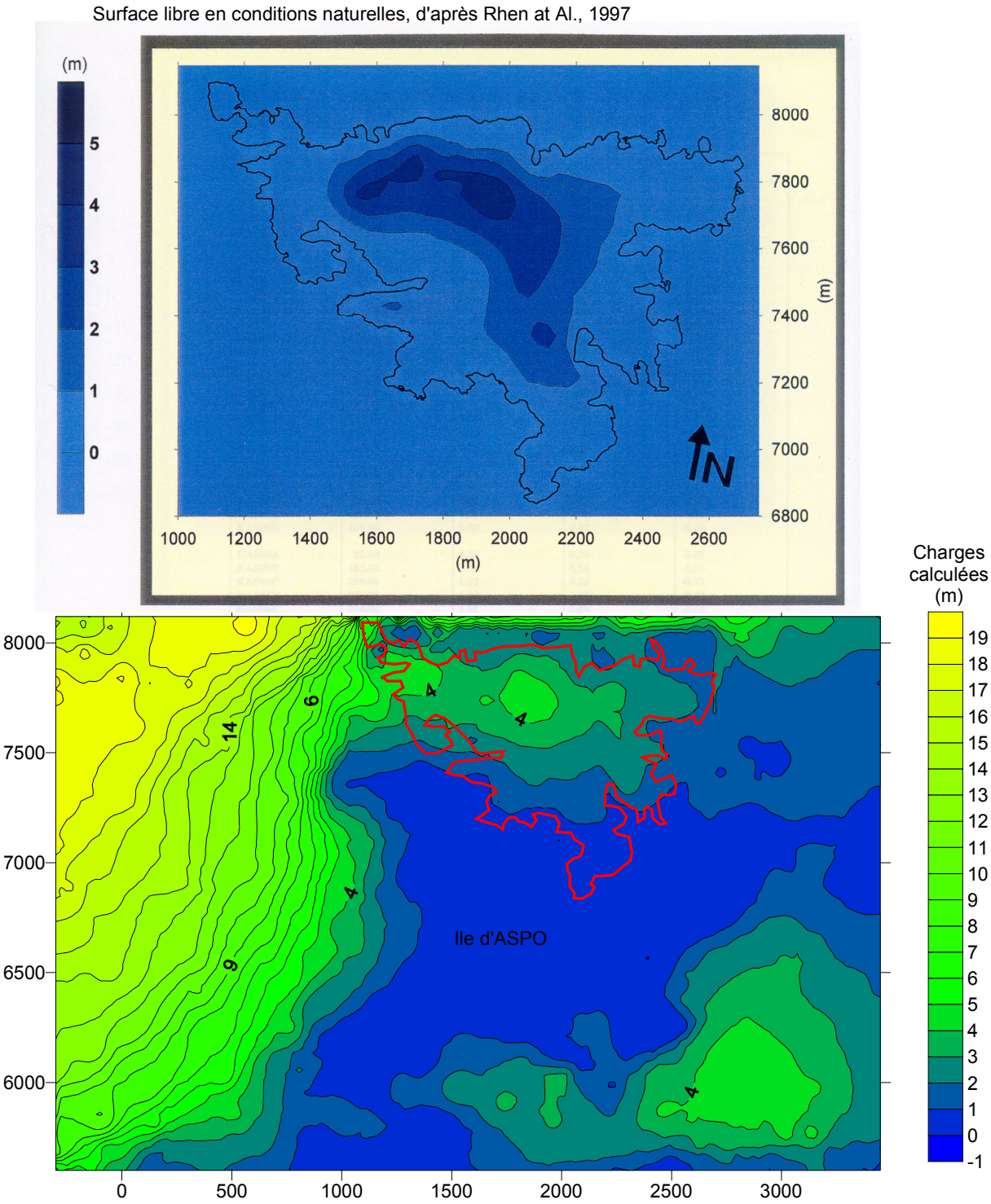

Figure 7 : Comparison between results and data for modified watertable

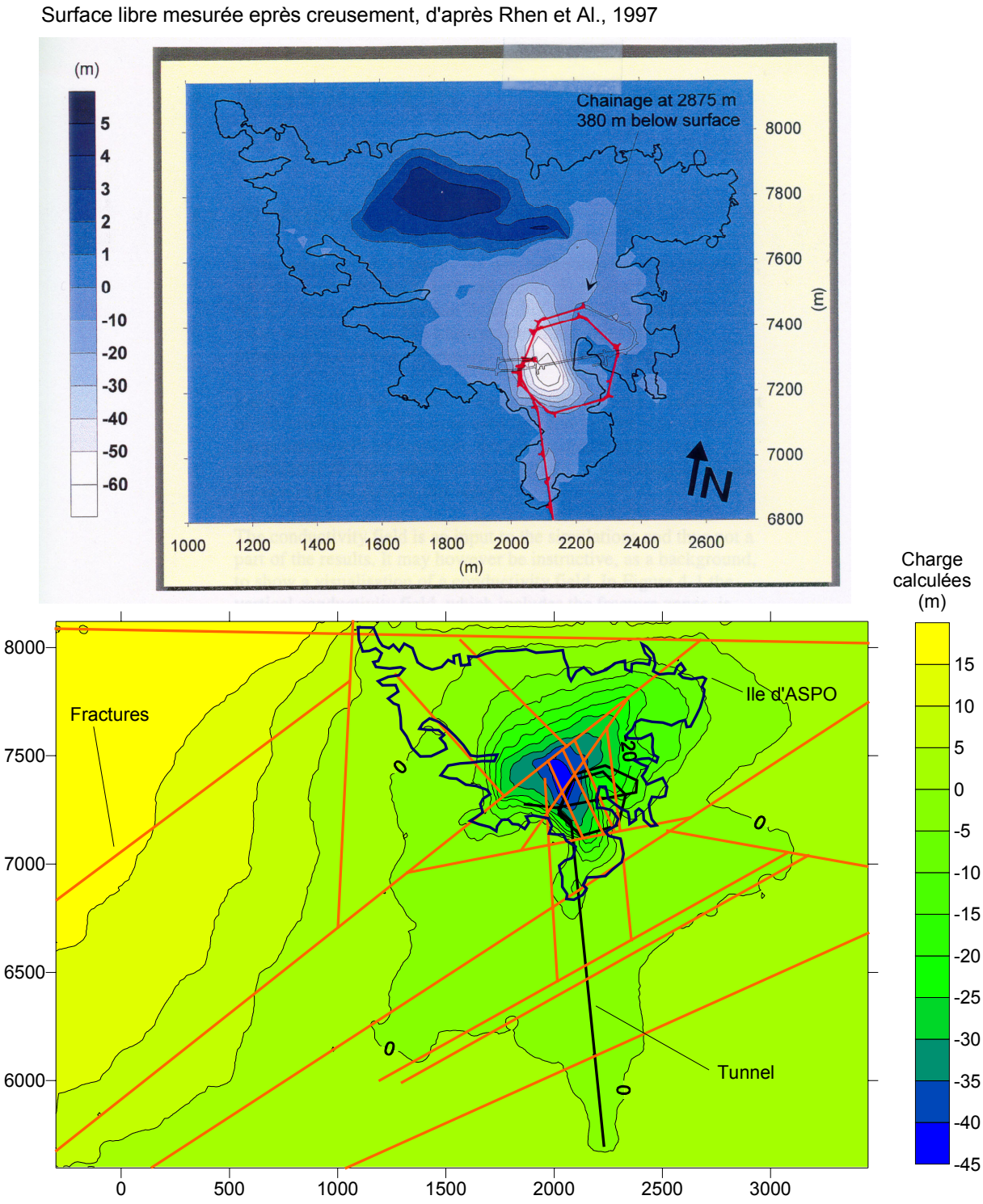

Figure 8 : Concentration along the tunnel for 22/12/93

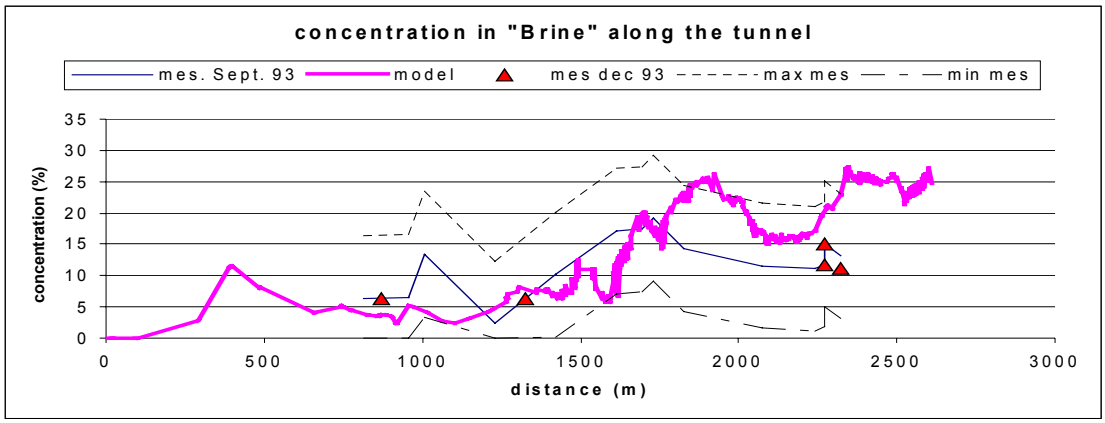

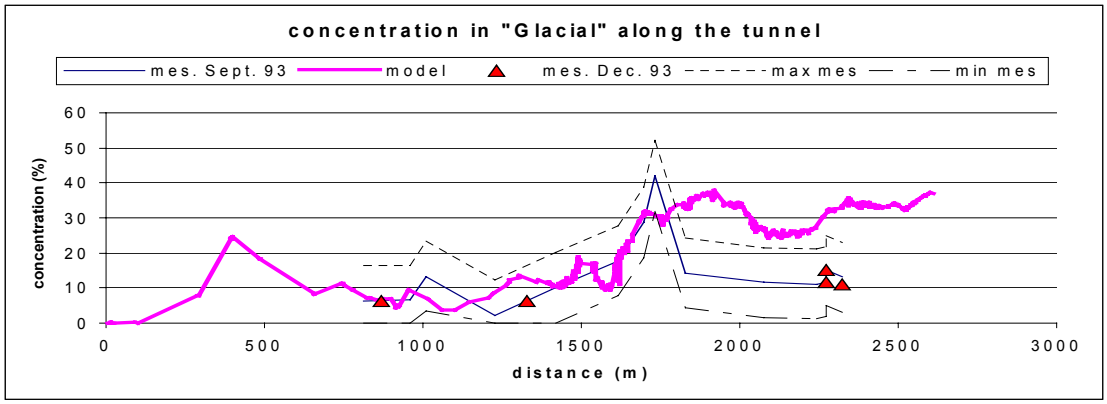

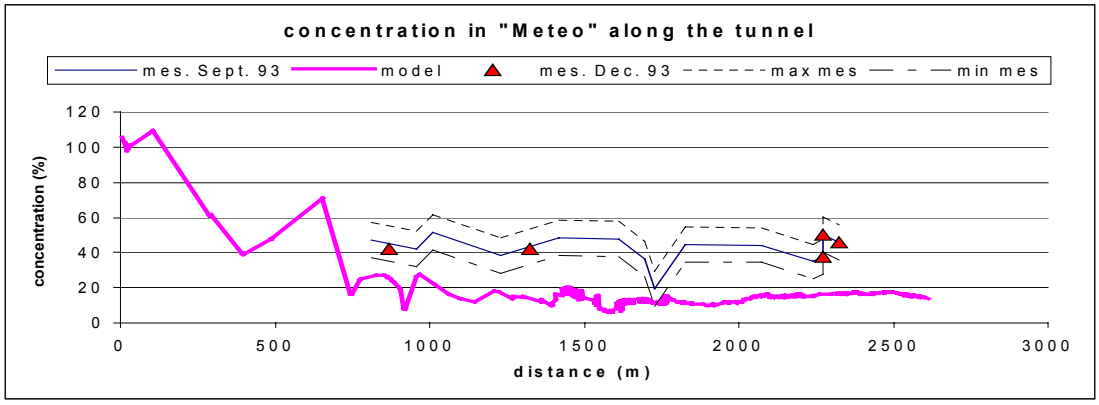

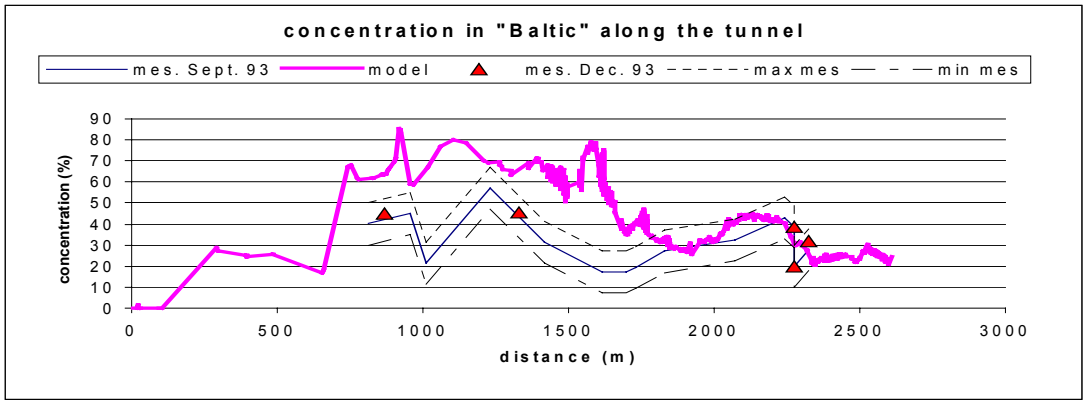

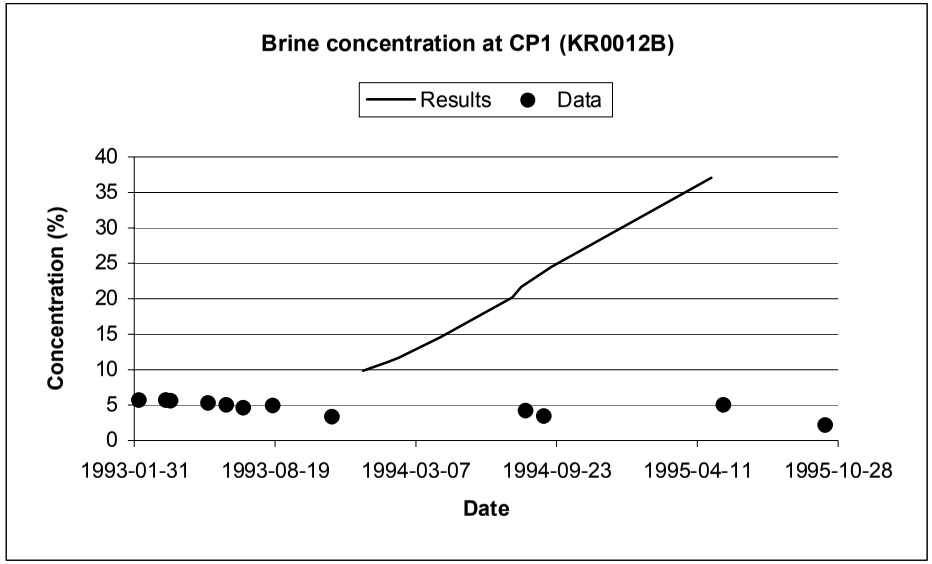

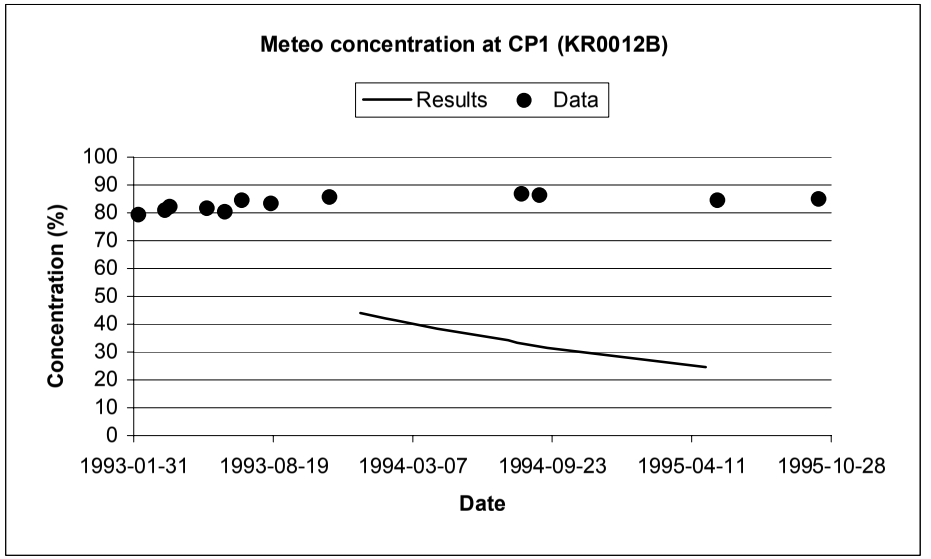

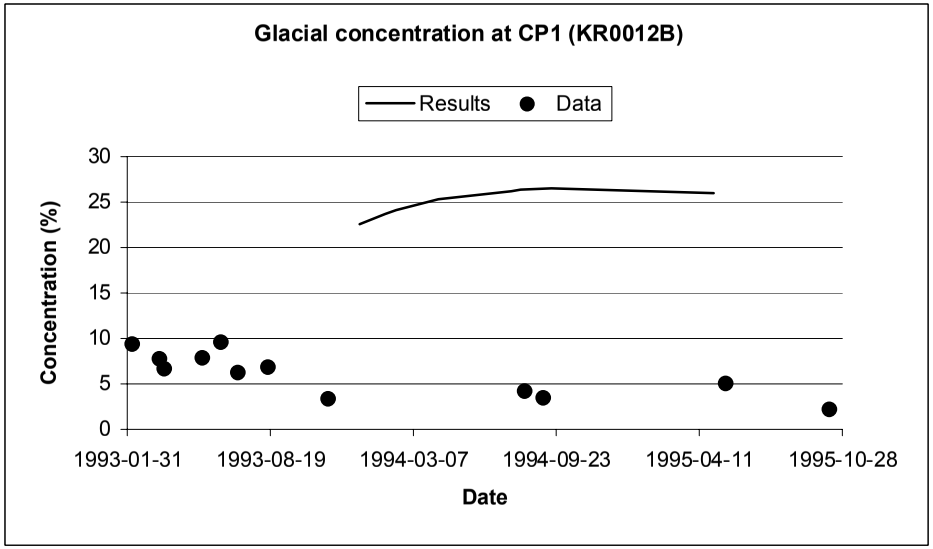

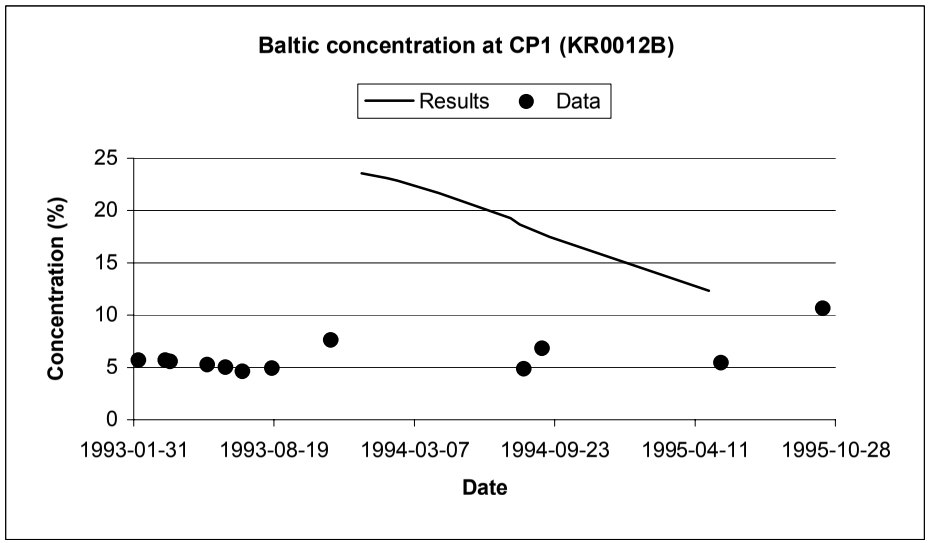

Figure 9 : first results at CP1

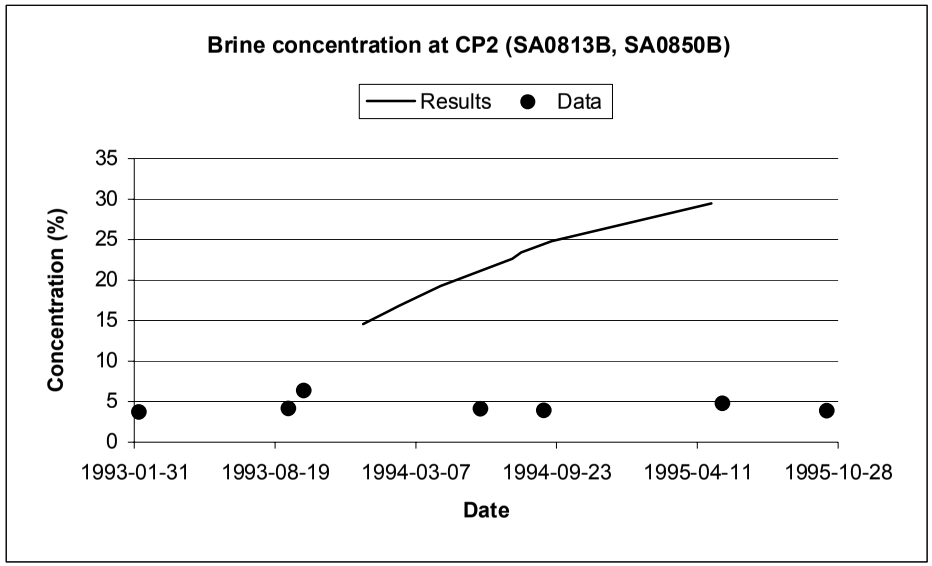

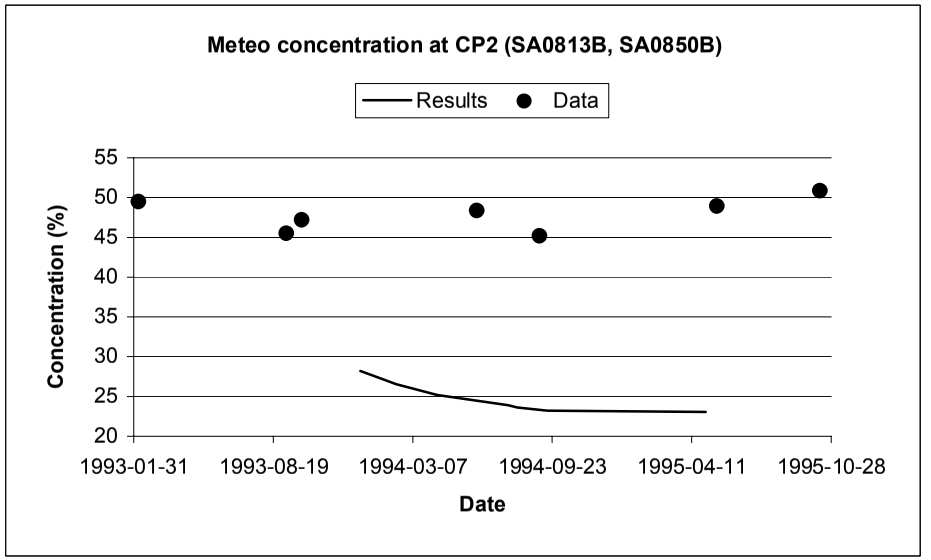

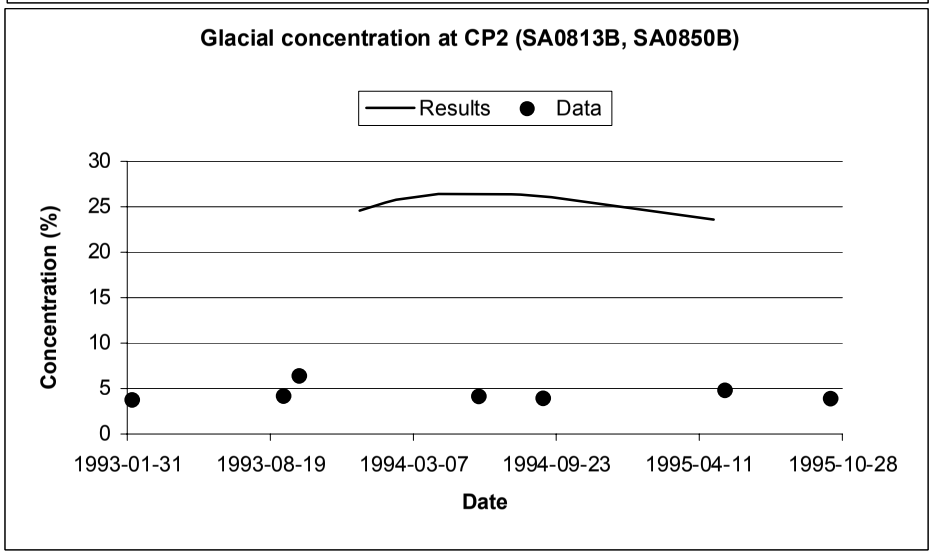

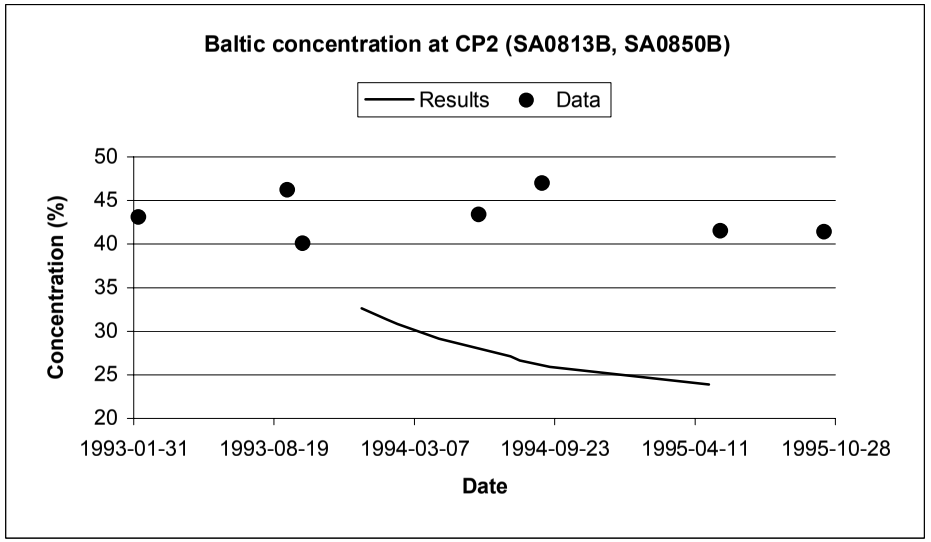

Figure 10 : first results at CP2

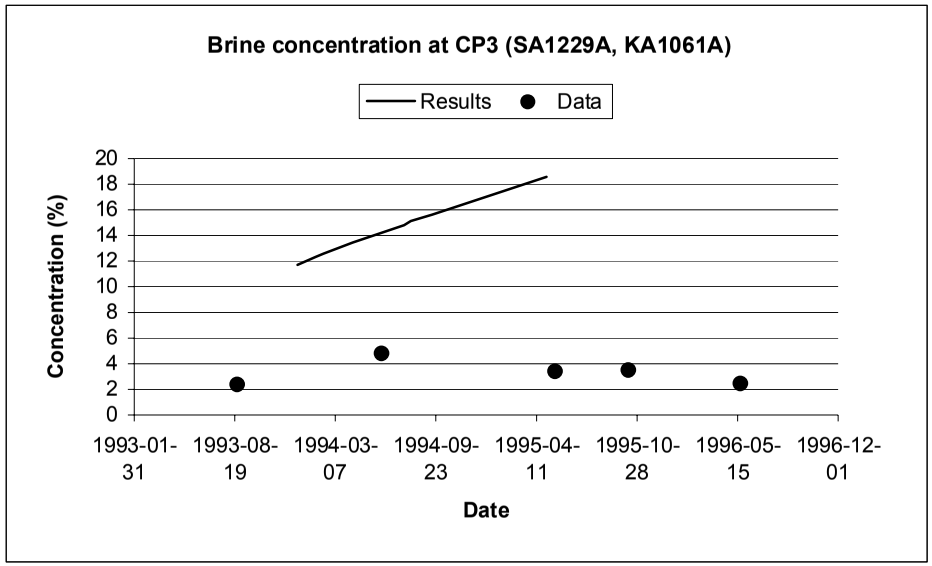

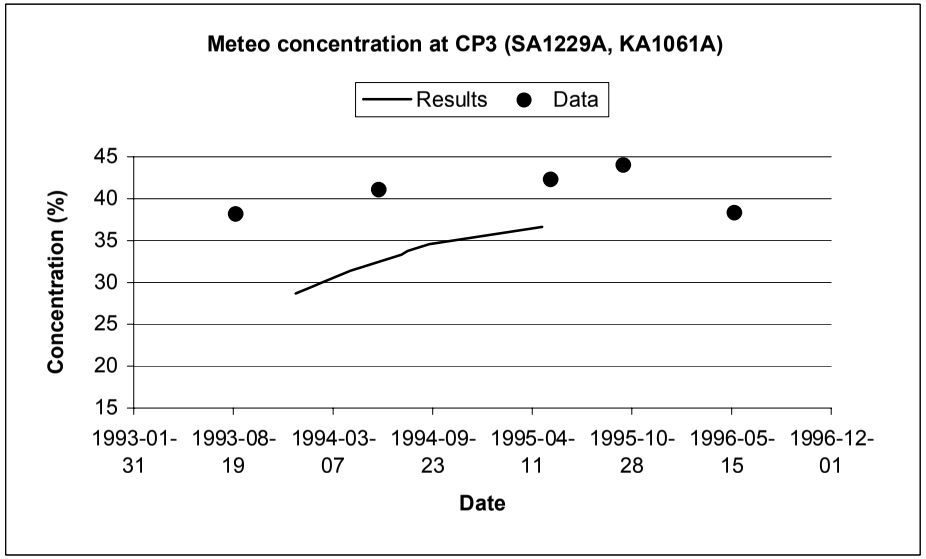

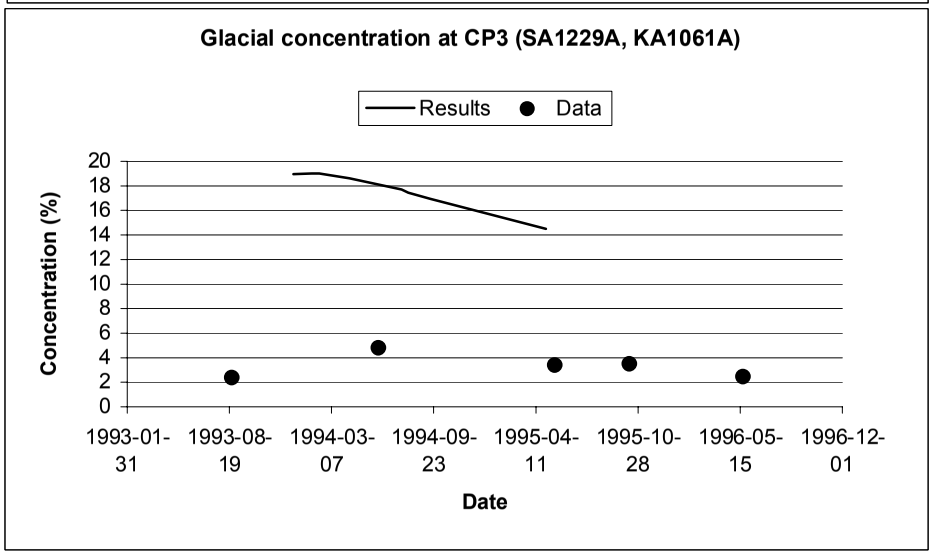

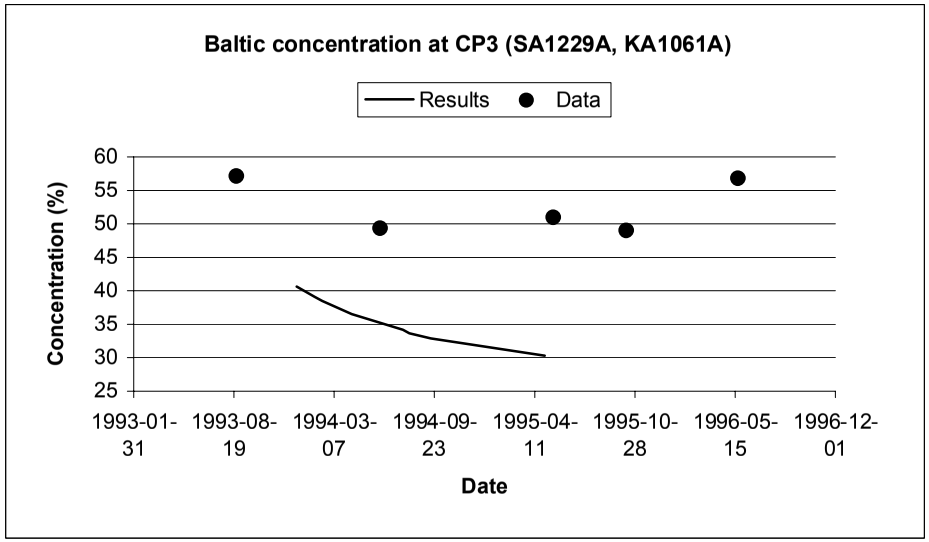

Figure 11 : first results at CP3-1

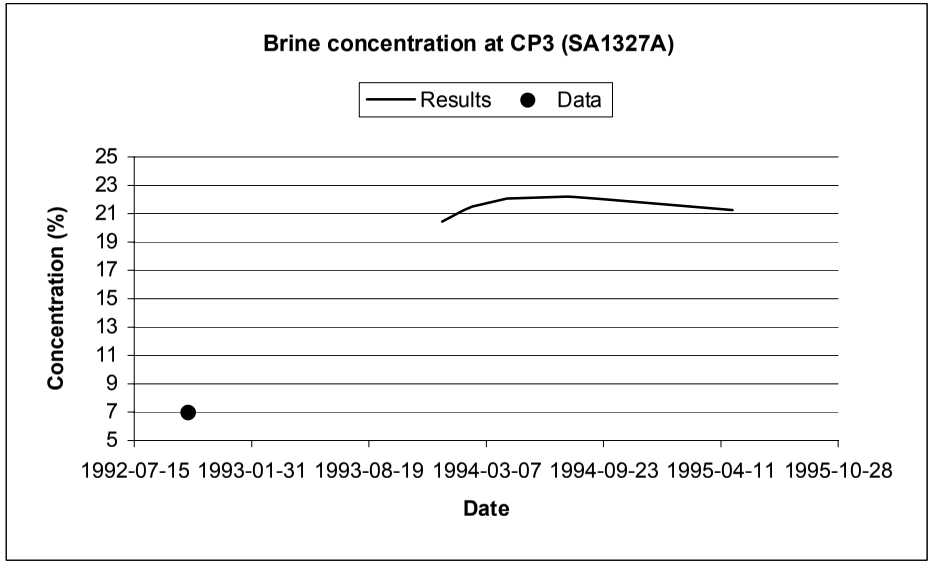

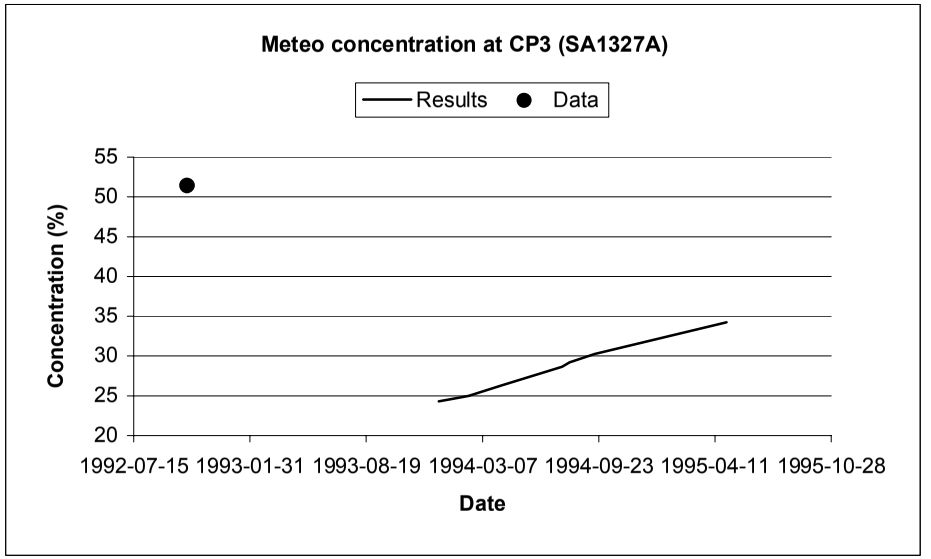

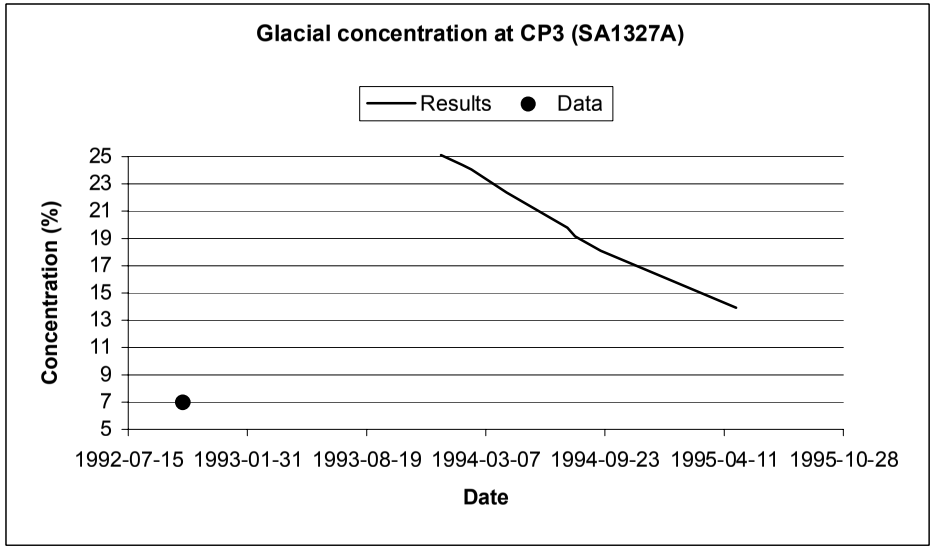

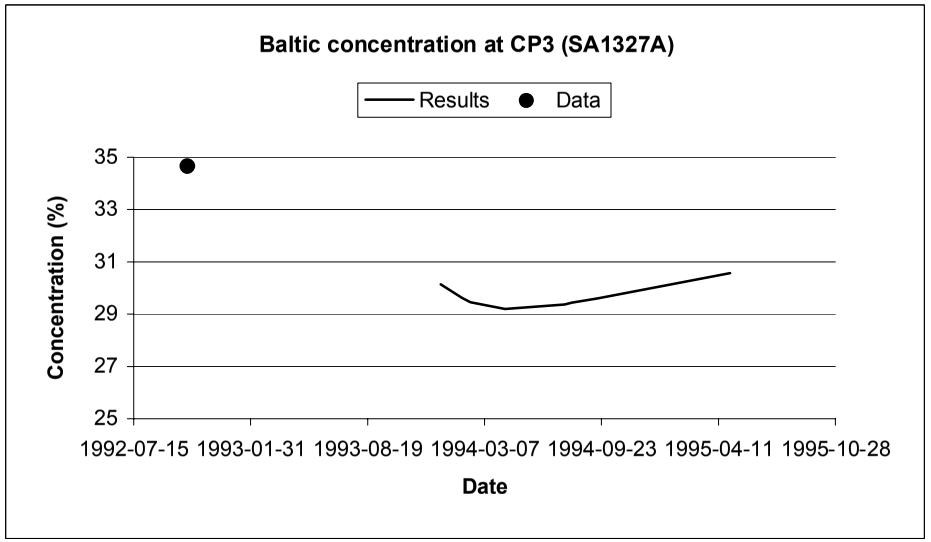

Figure 12 : first results at CP3-2

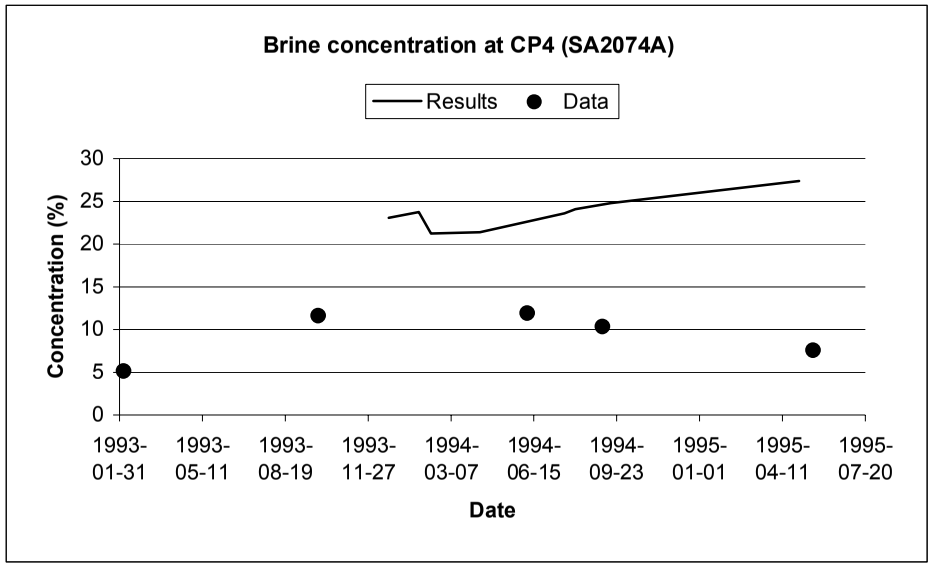

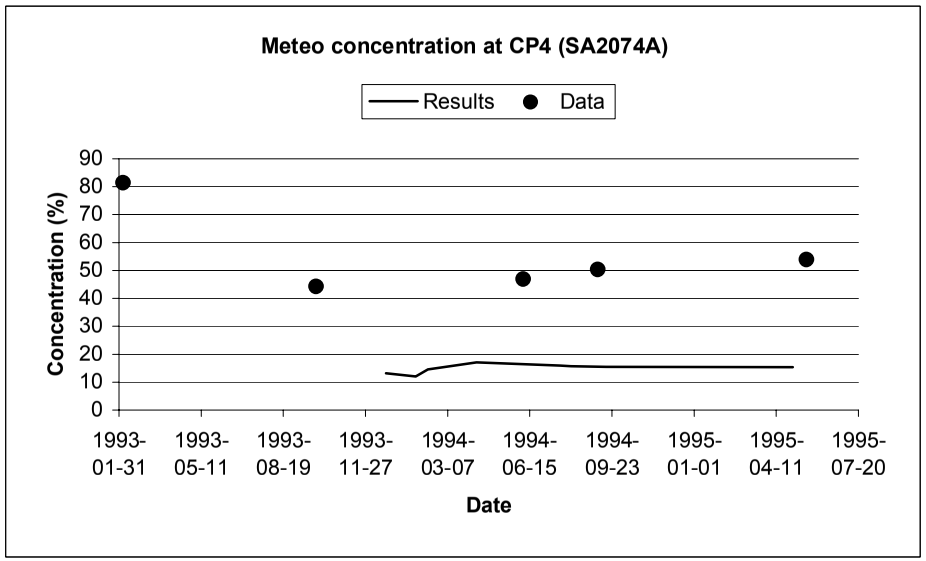

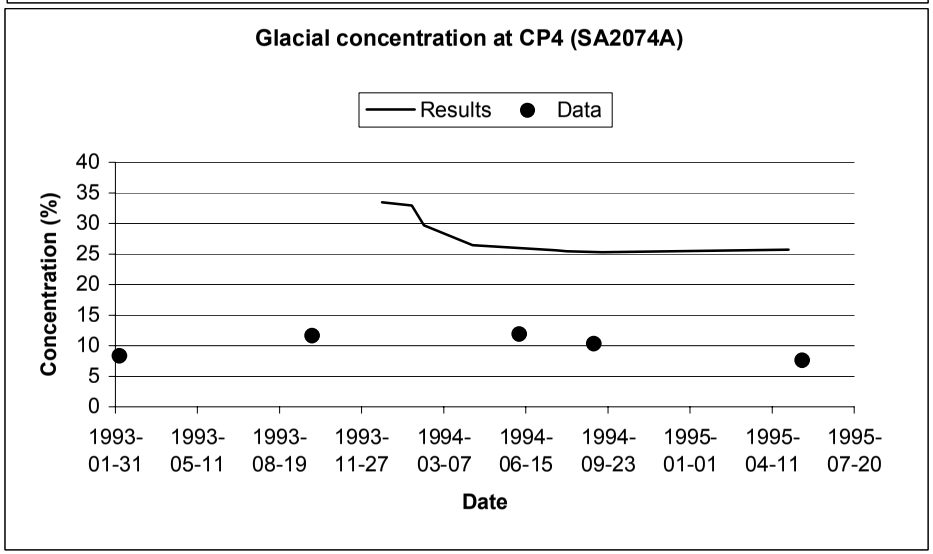

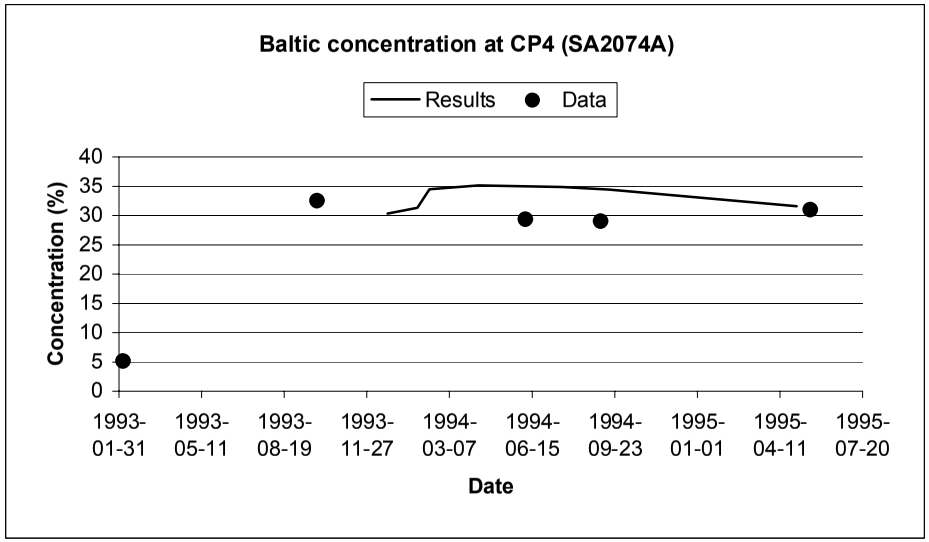

Figure 13 : first results at CP4

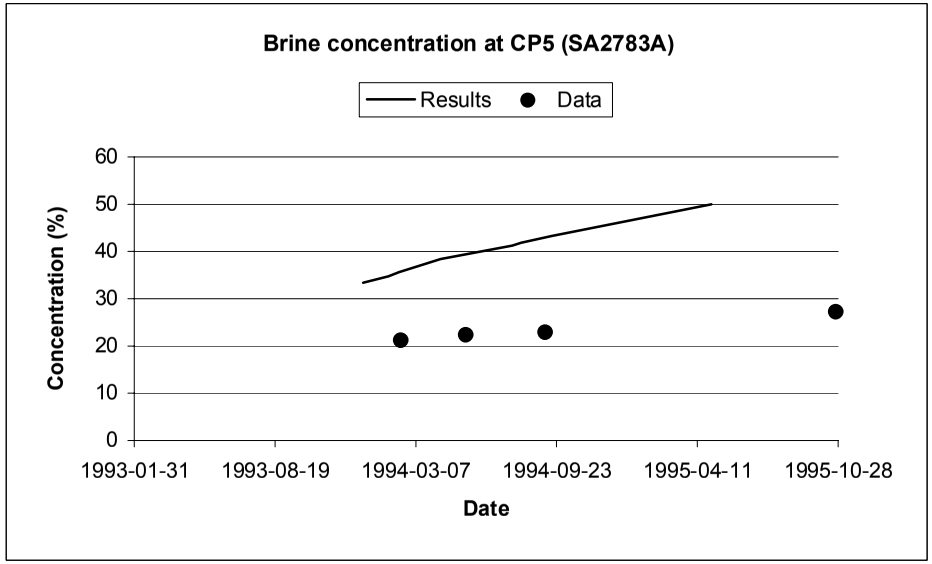

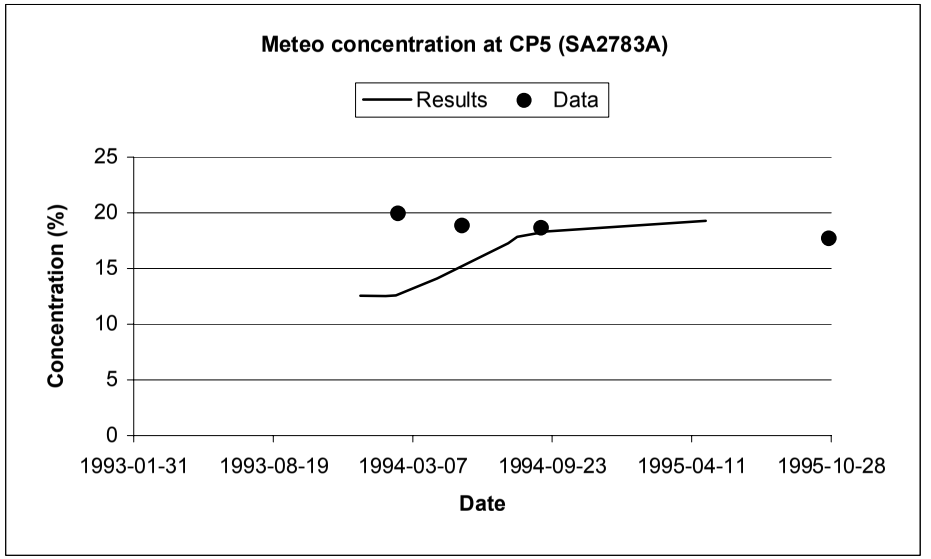

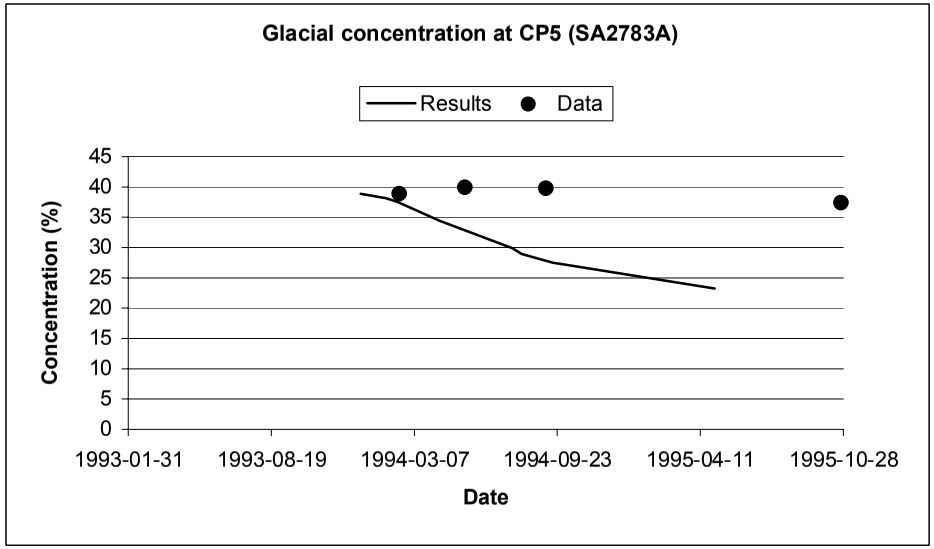

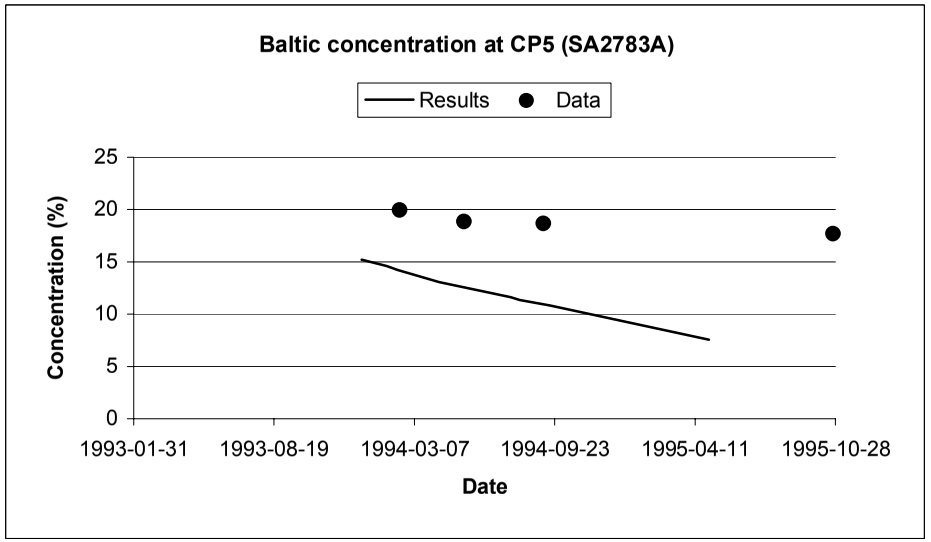

Figure 14 : first results at CP5

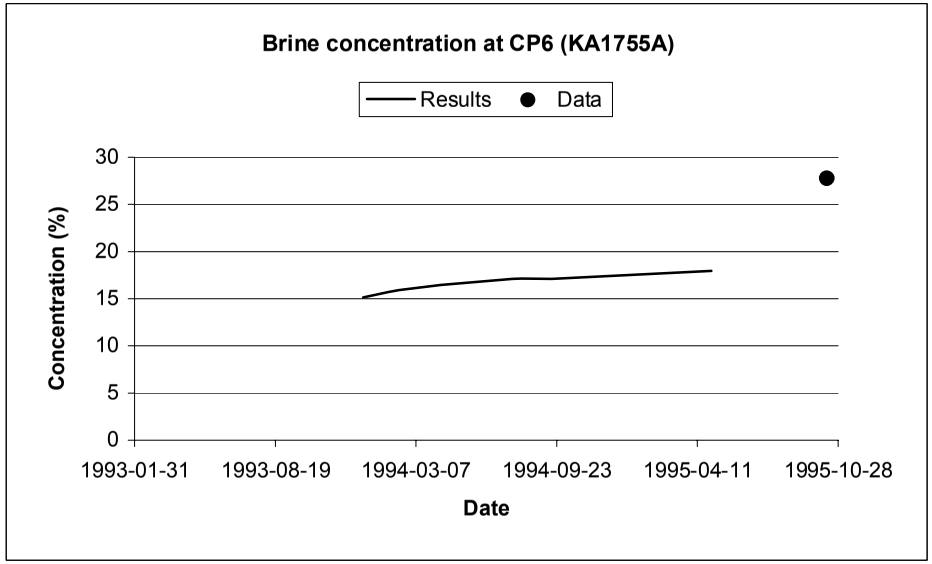

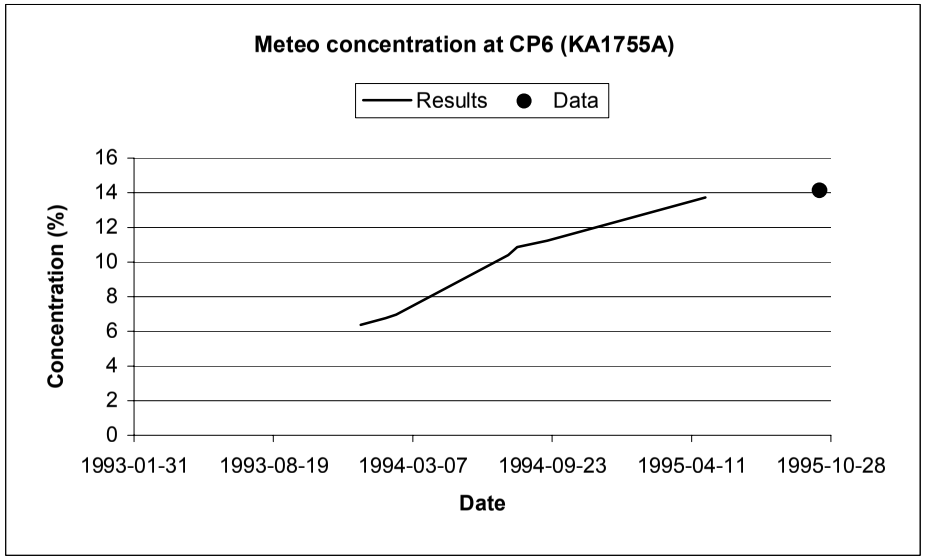

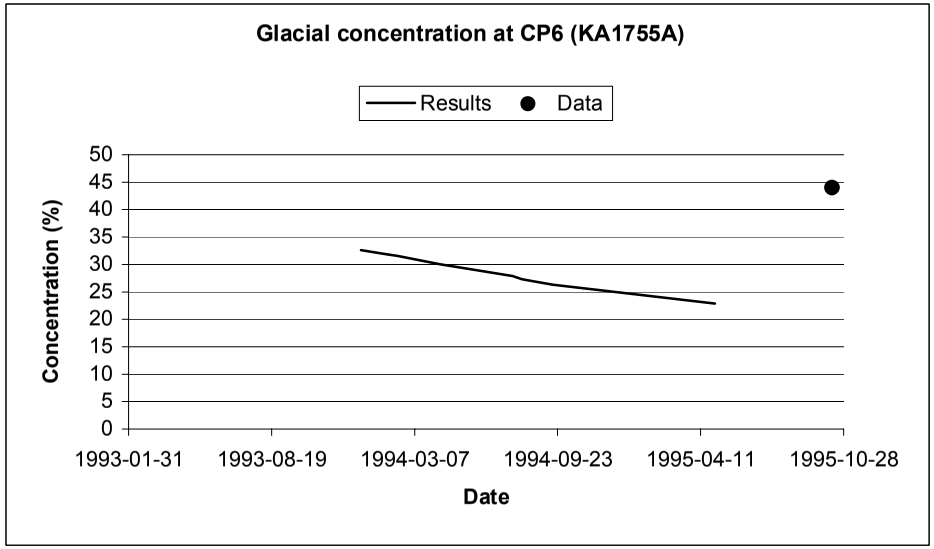

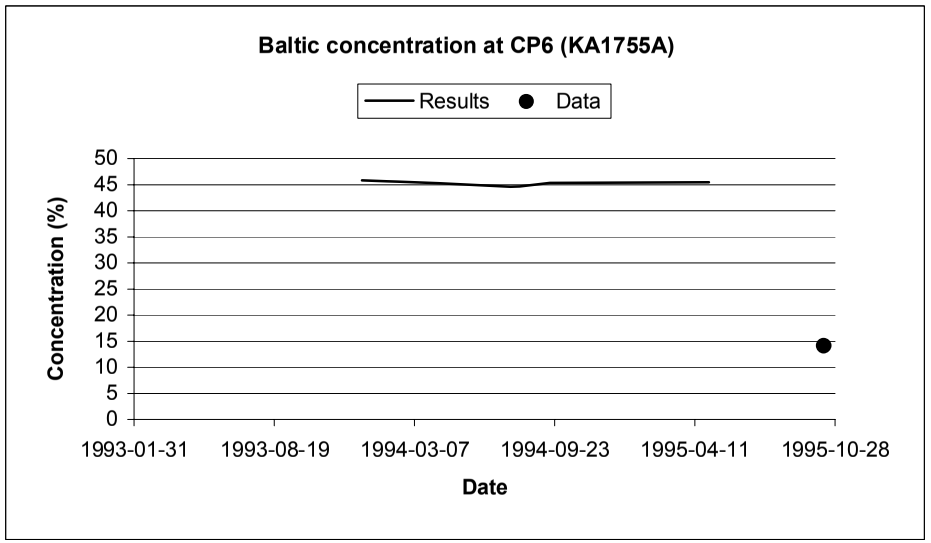

Figure 15 : first results at CP6

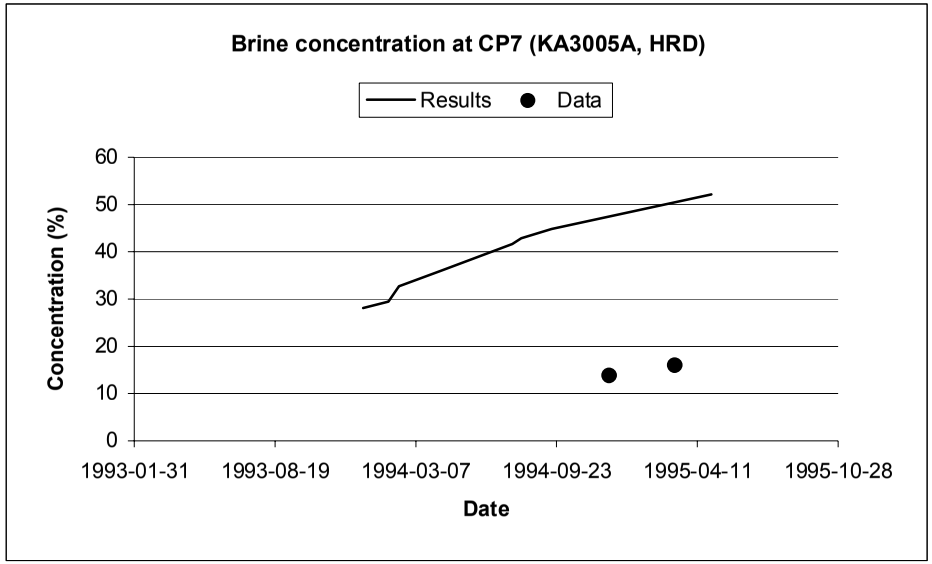

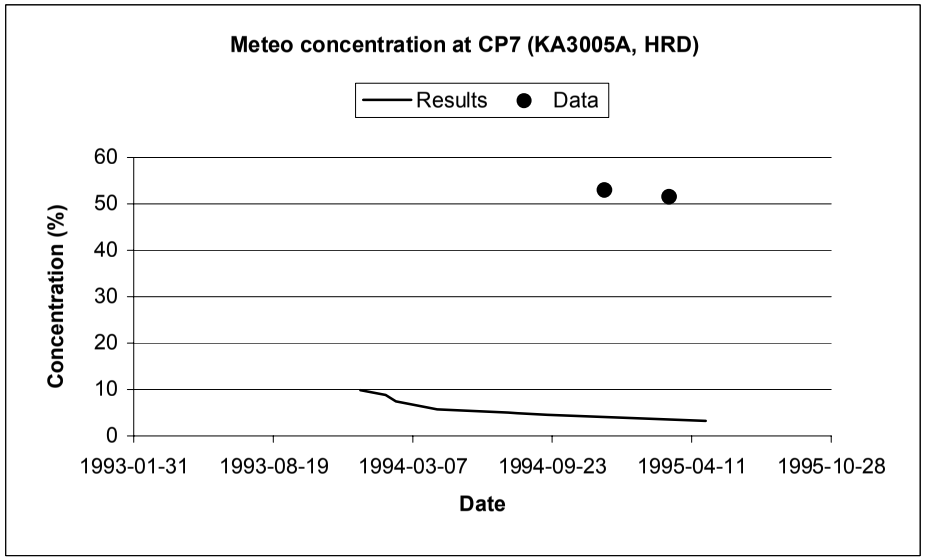

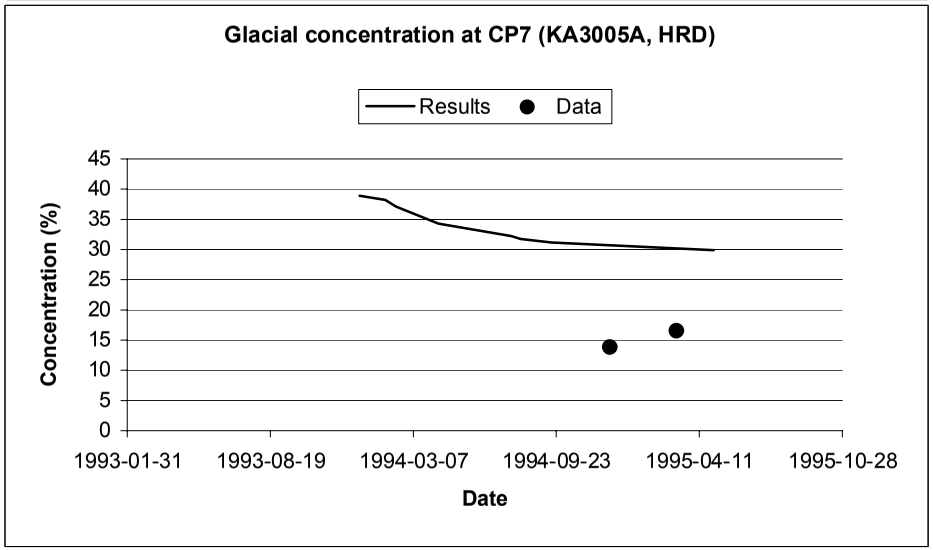

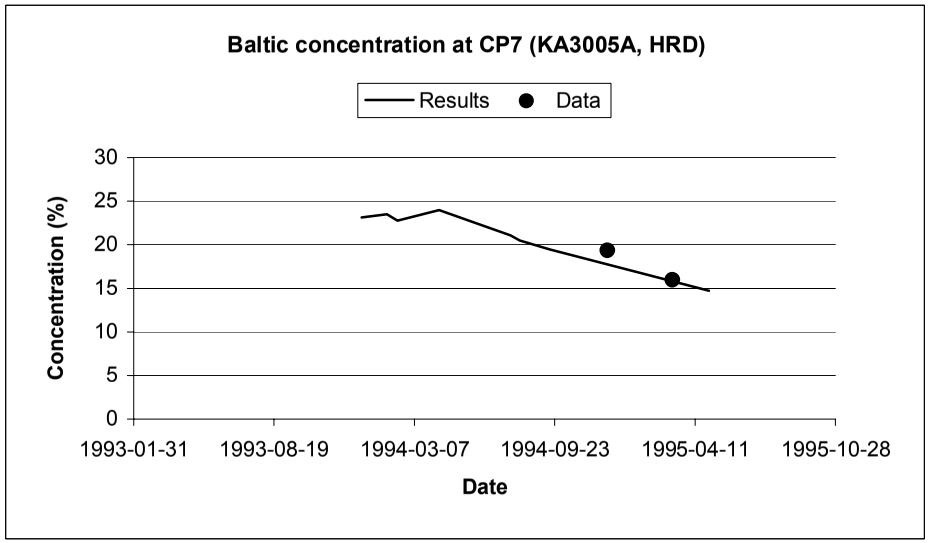

Figure 16 : first results at CP7

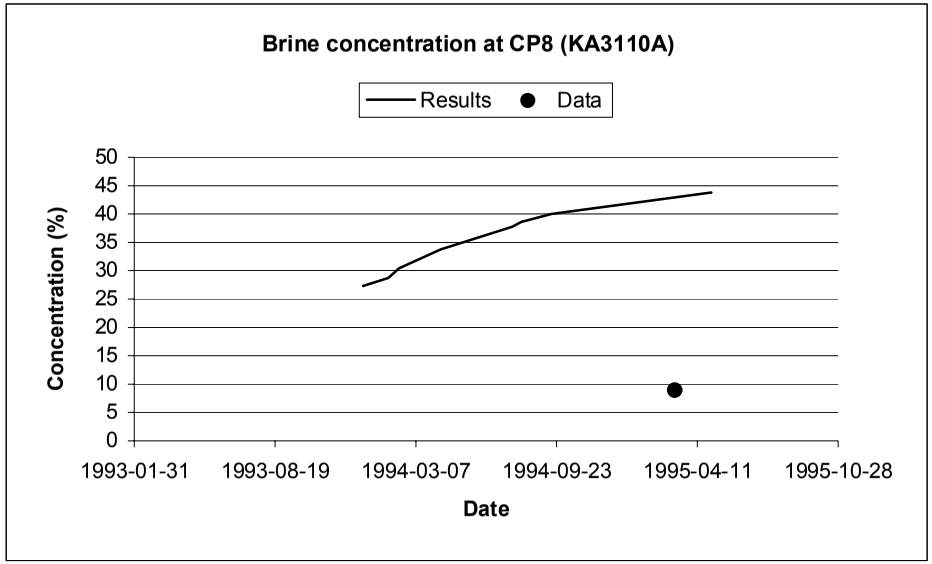

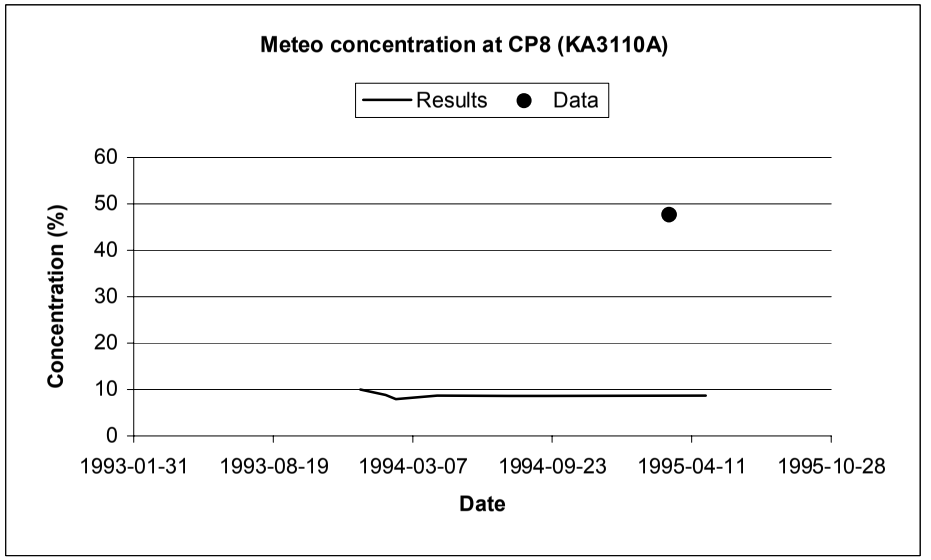

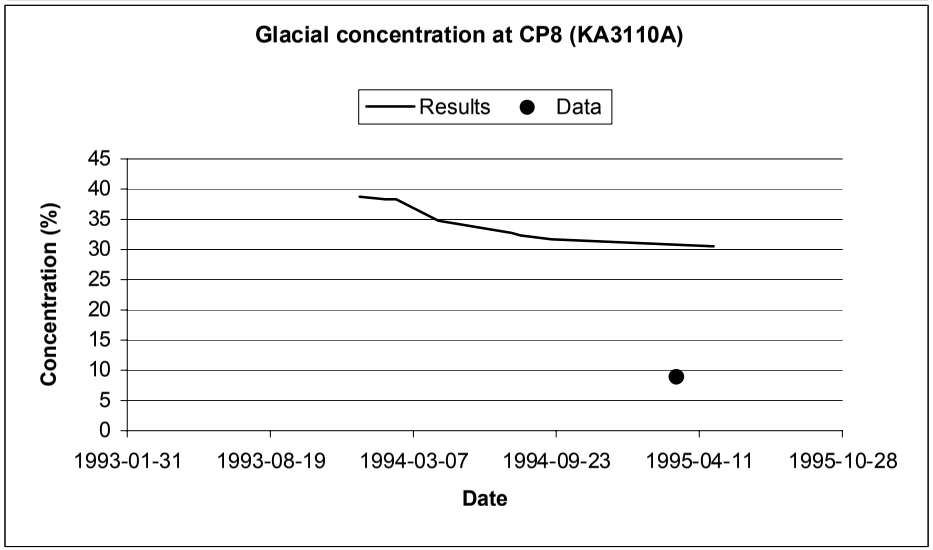

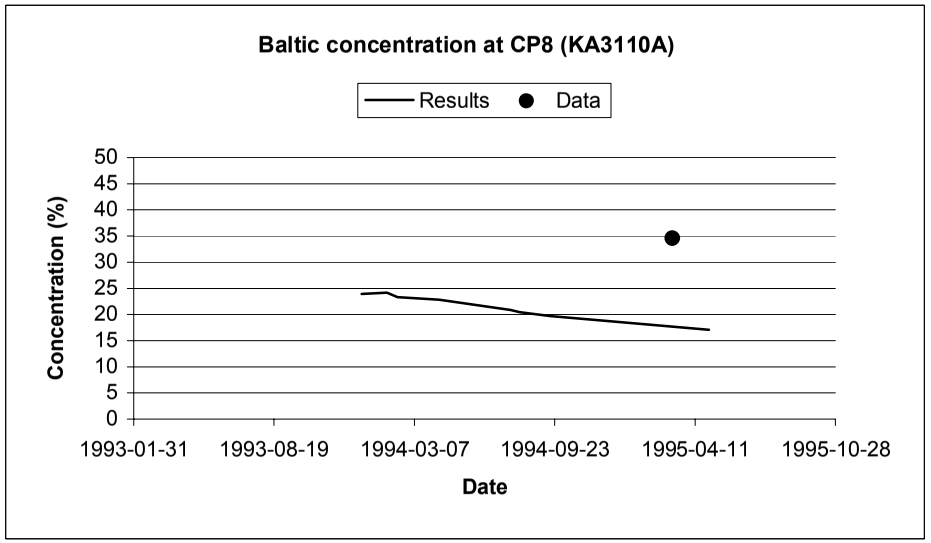

Figure 17 : first results at CP8

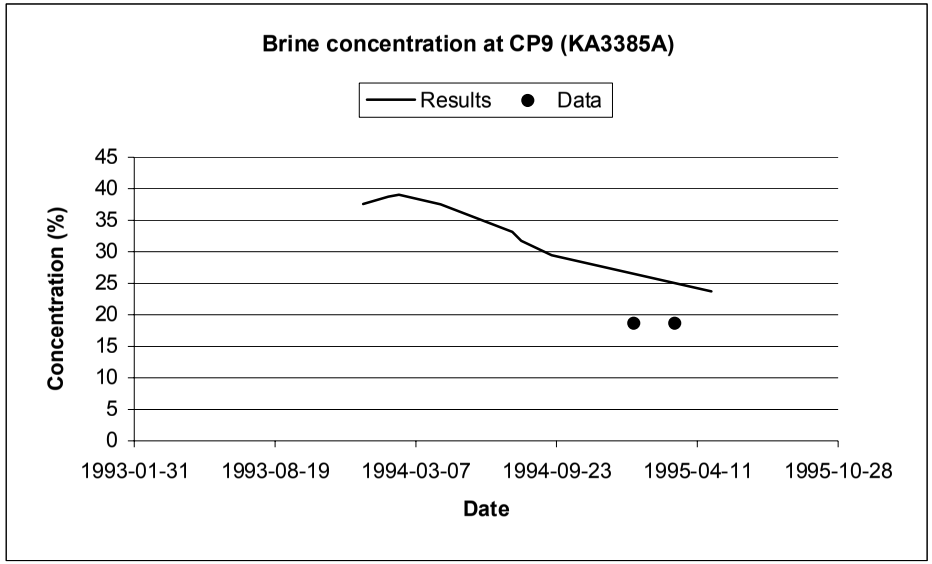

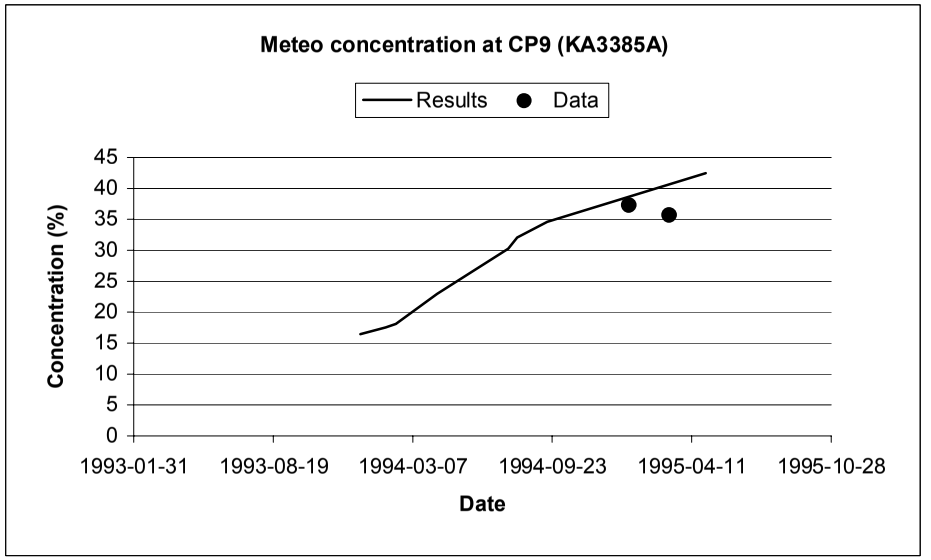

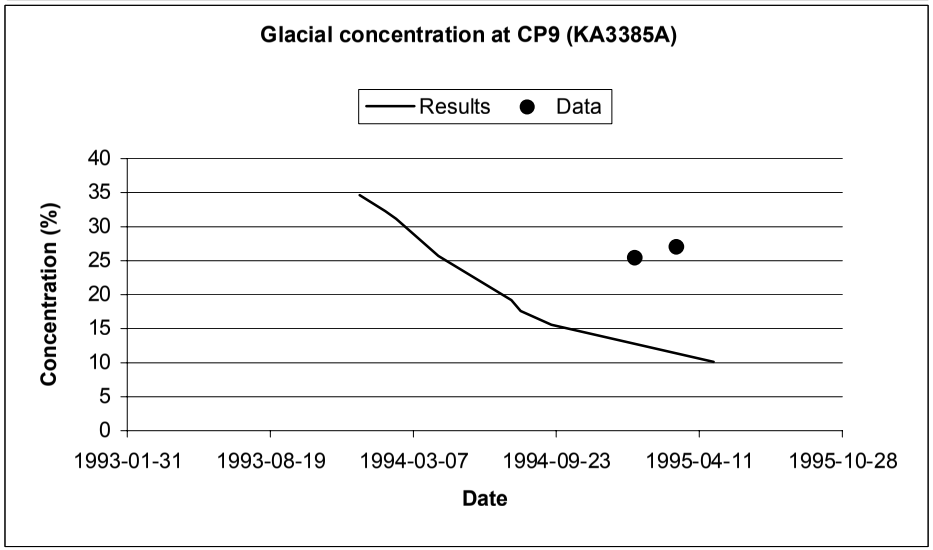

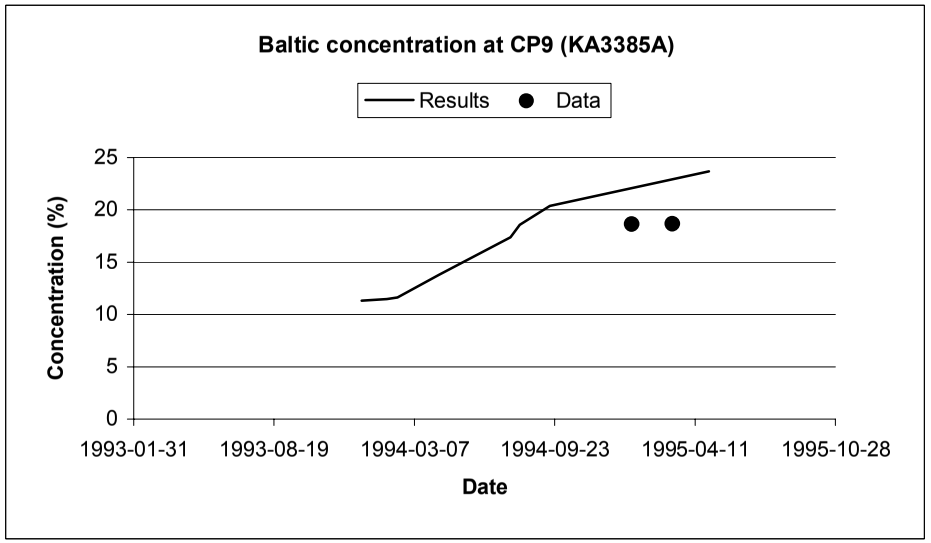

Figure 18 : first results at CP9

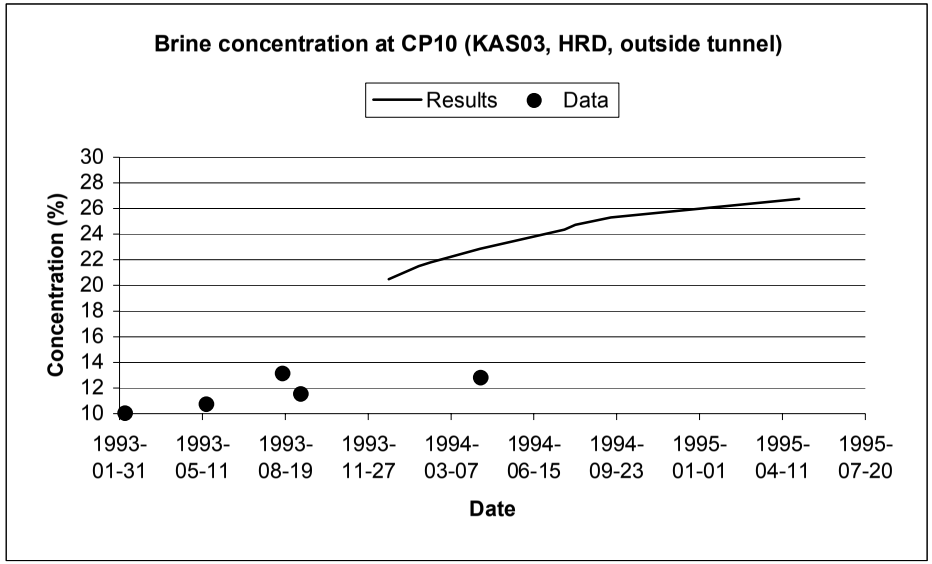

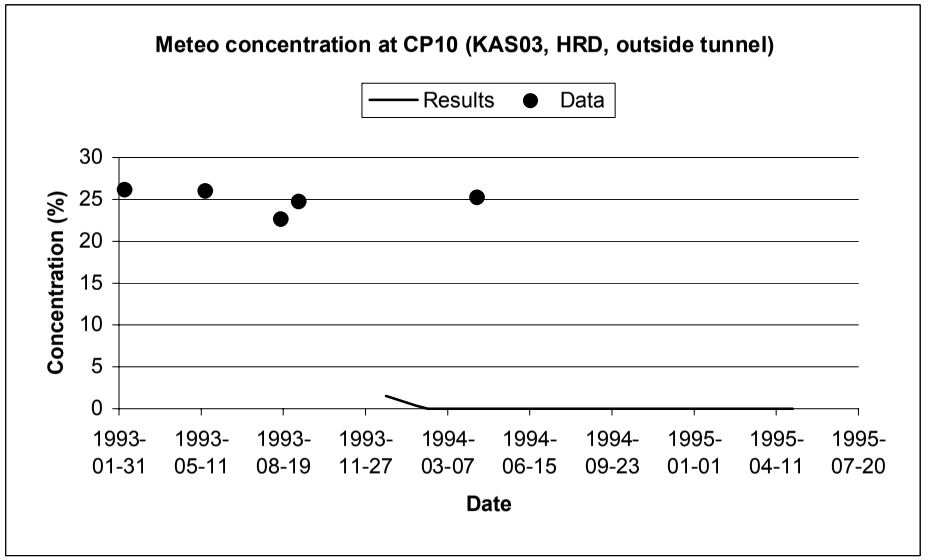

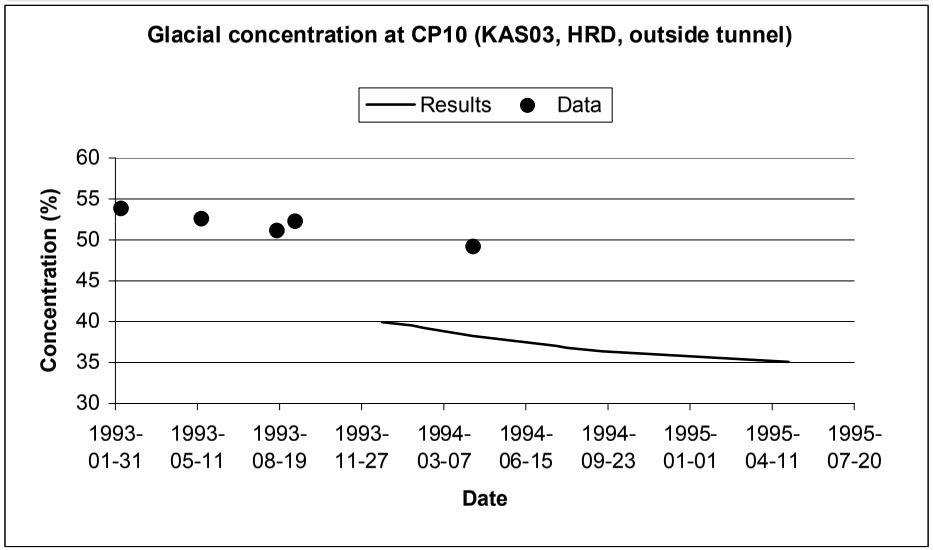

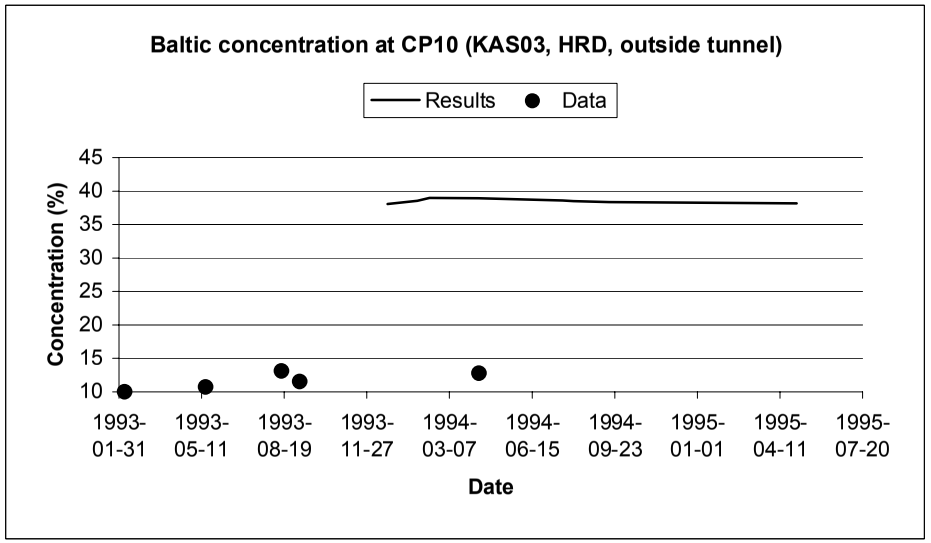

Figure 19 : first results at CP10

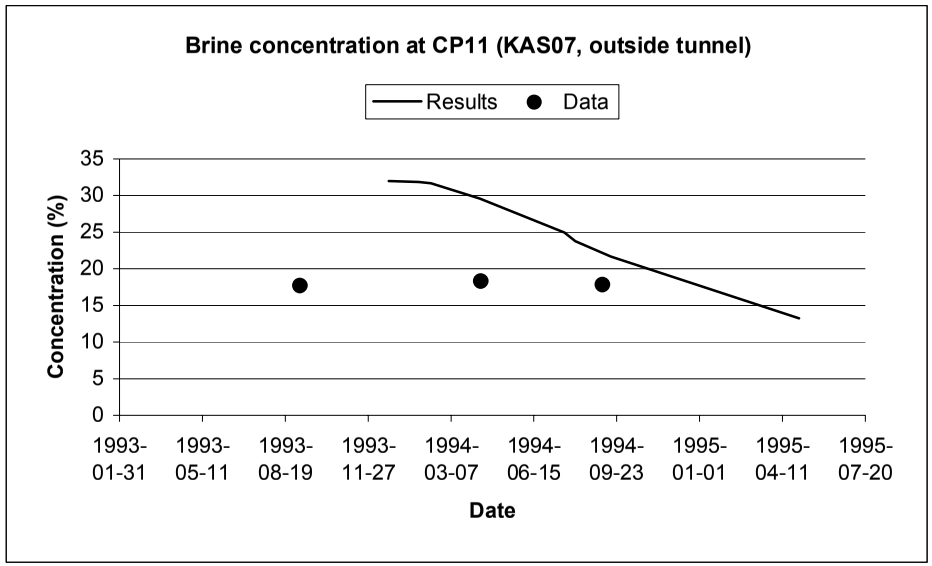

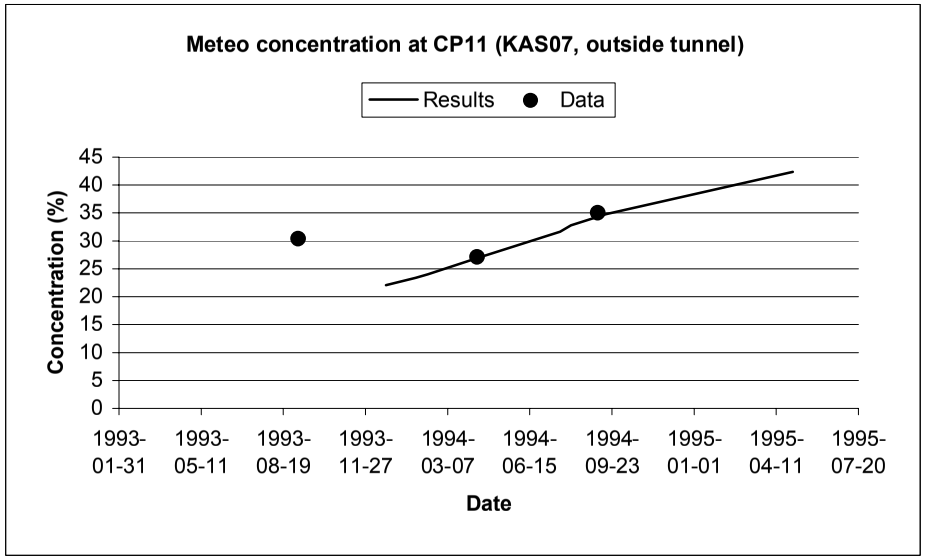

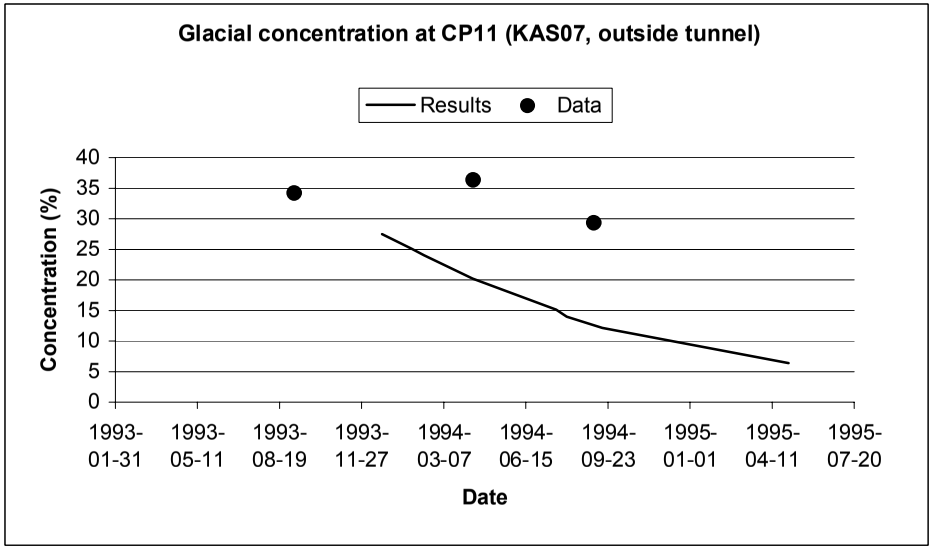

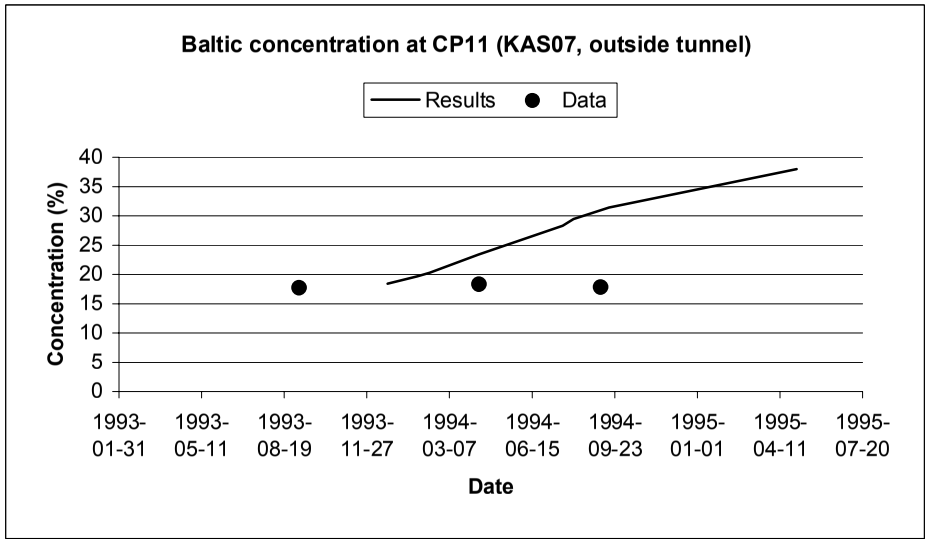

Figure 20 : first results at CP11

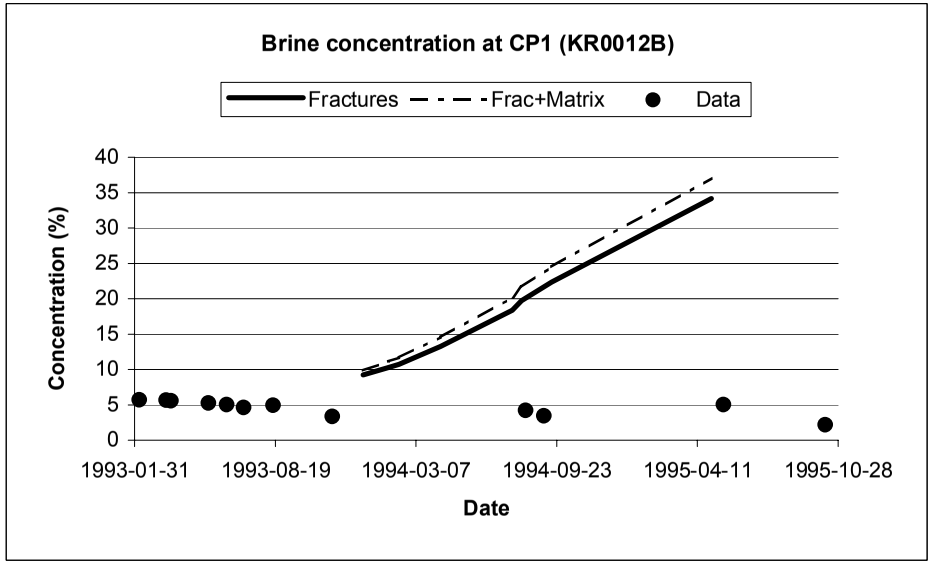

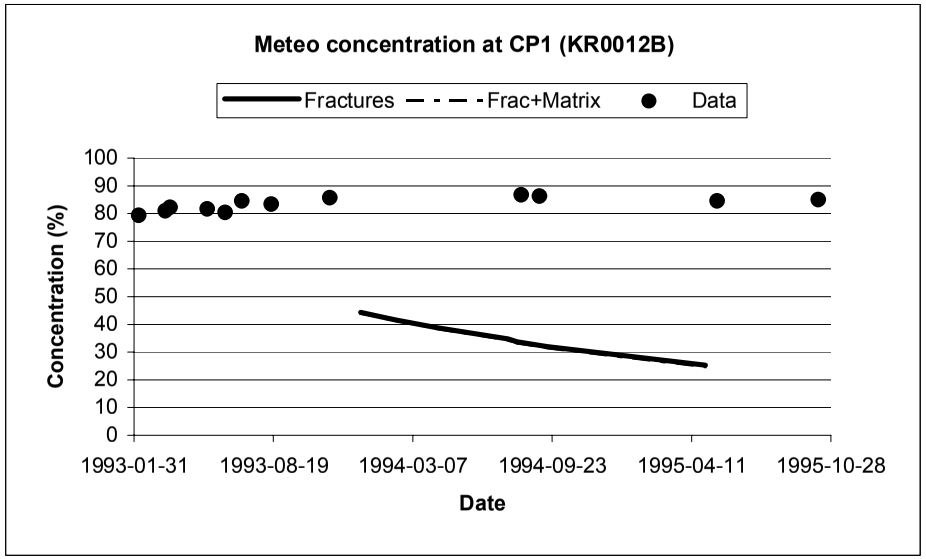

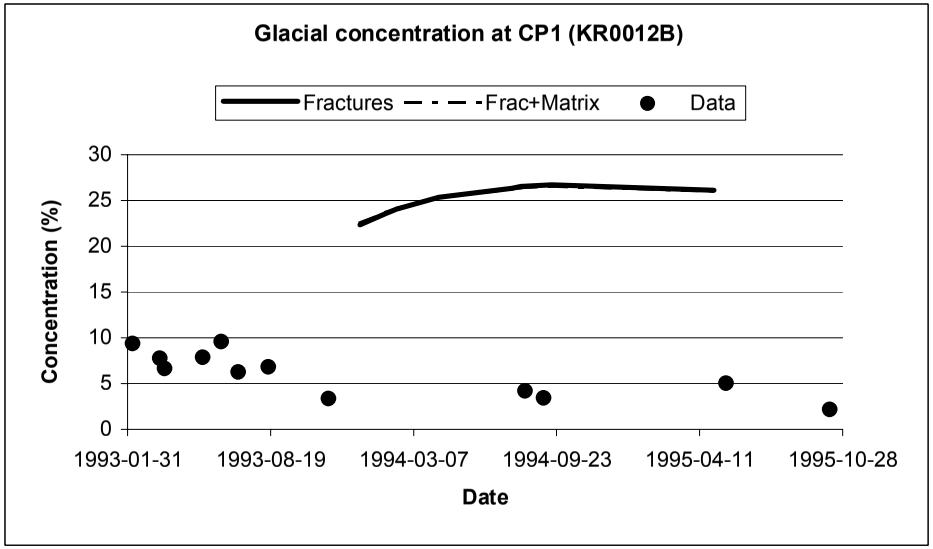

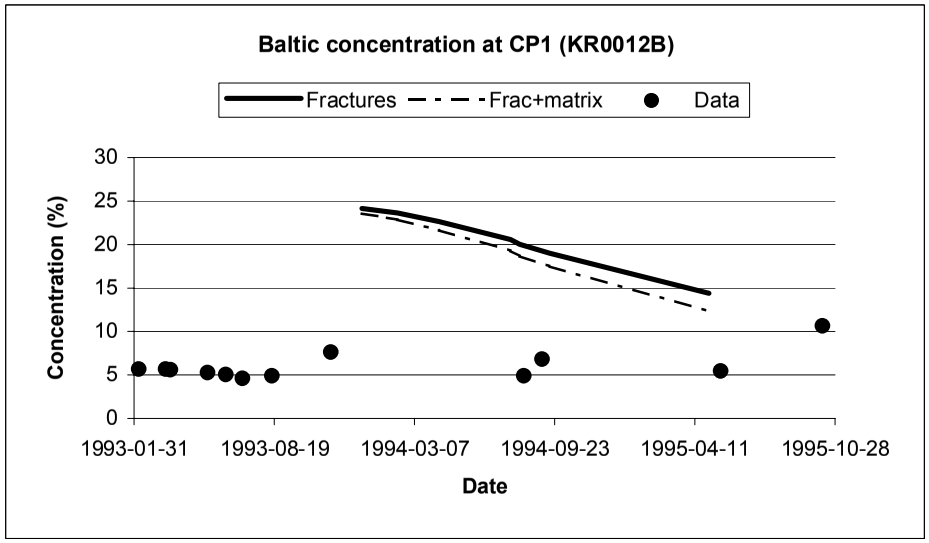

Figure 21 : role of the matrix at CP1

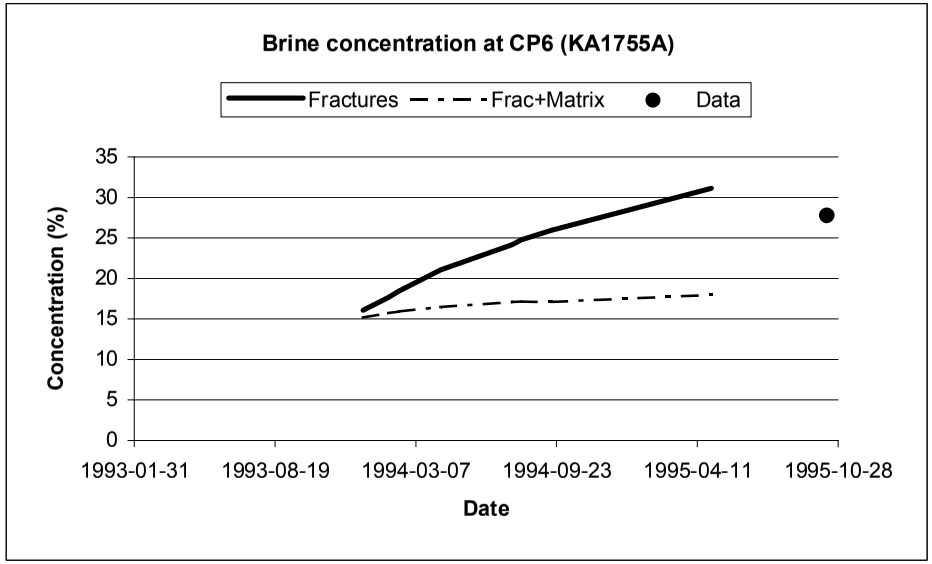

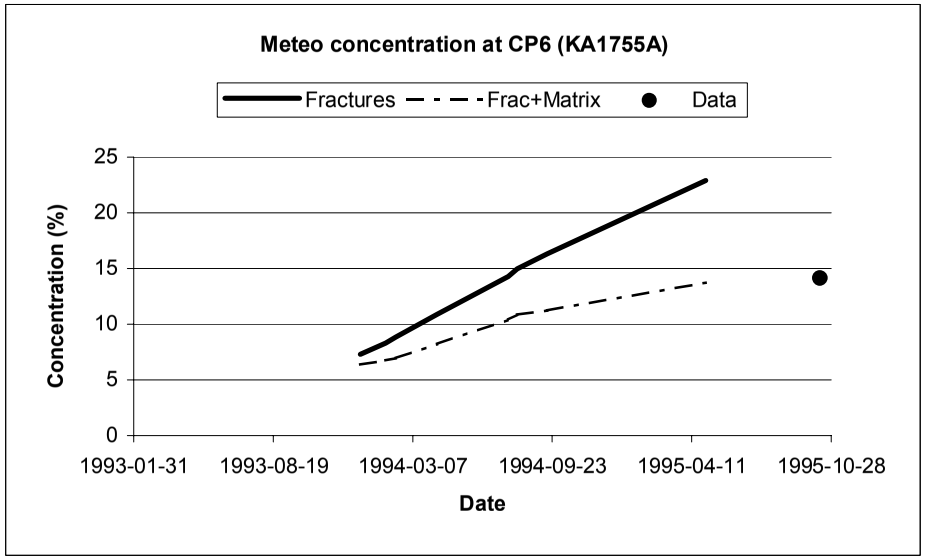

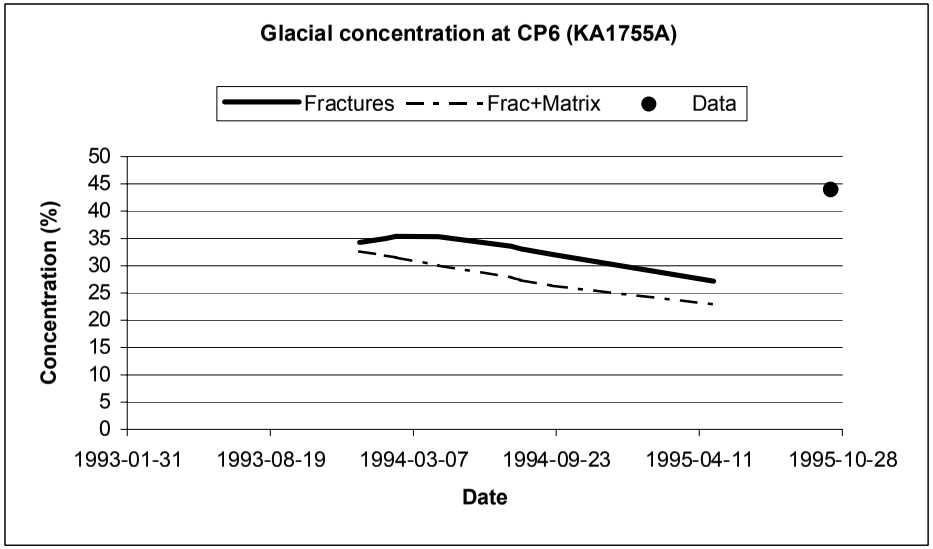

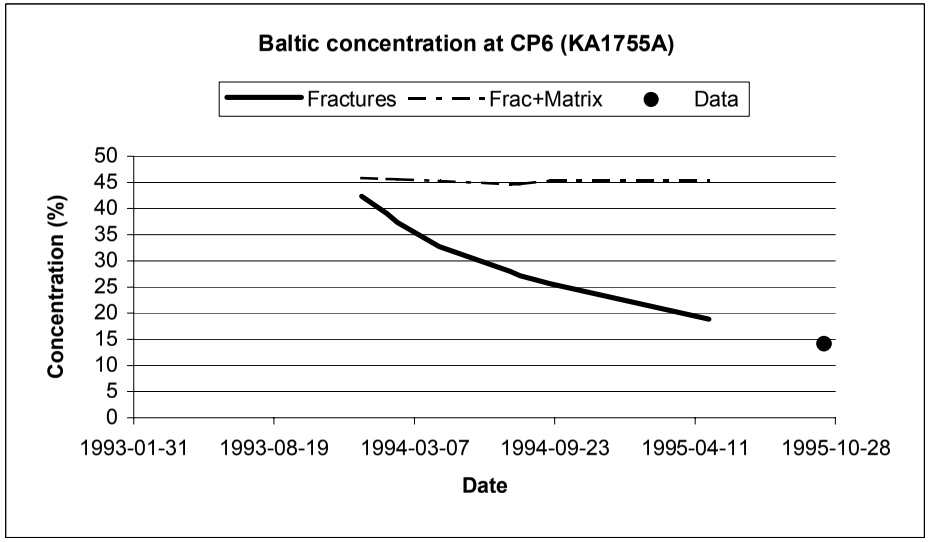

Figure 22 : role of the matrix at CP6

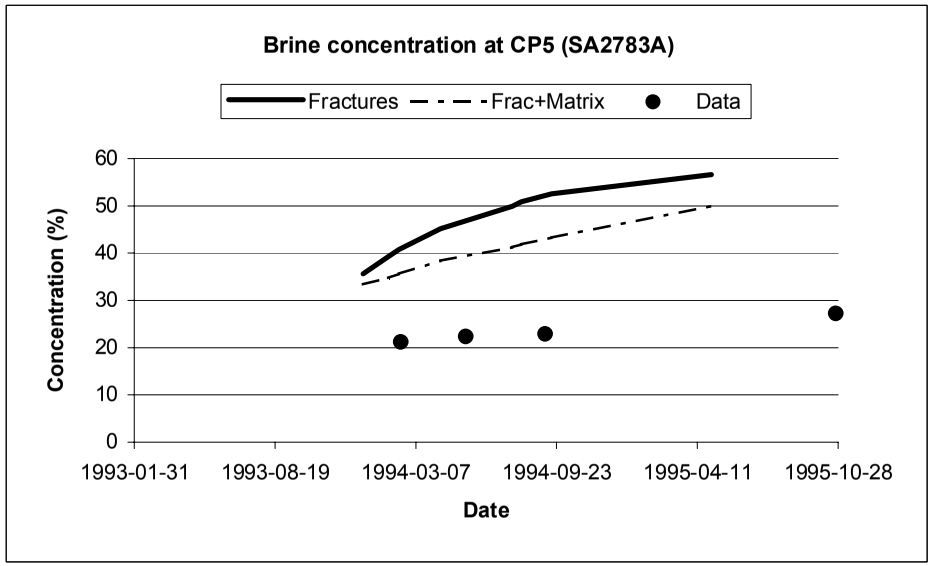

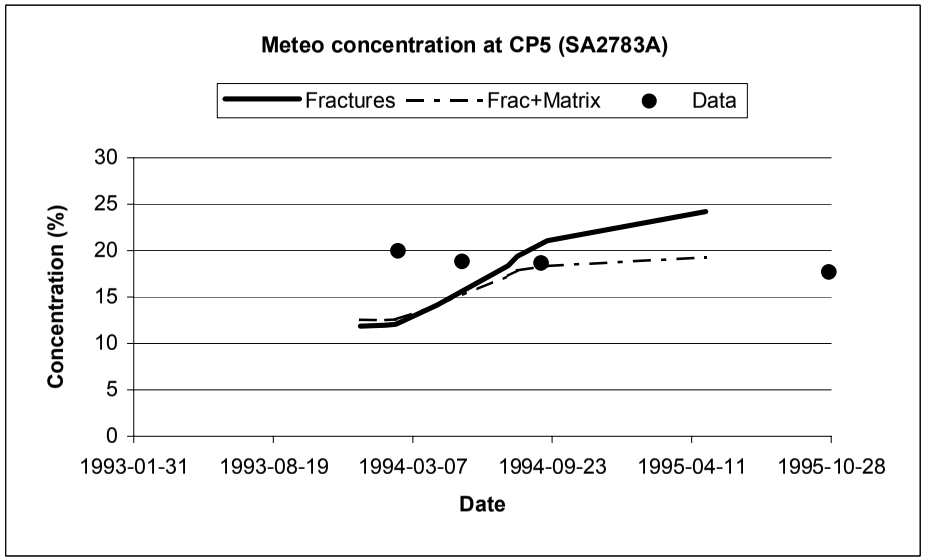

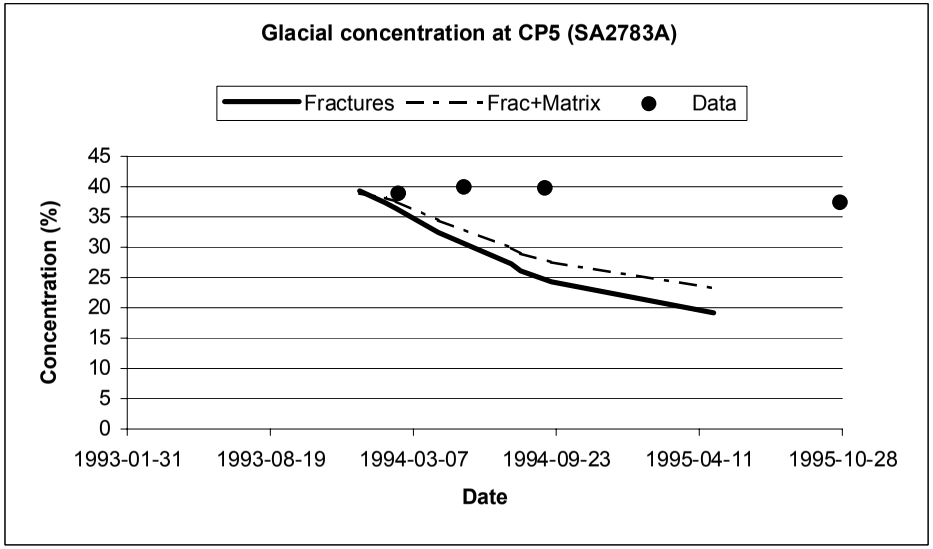

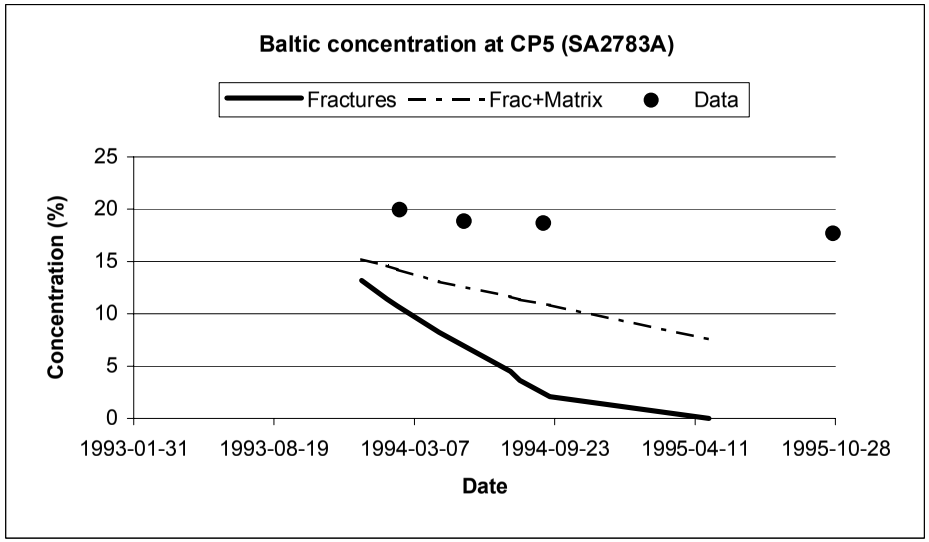

Figure 23 : role of the matrix at CP5

Role of the matrix

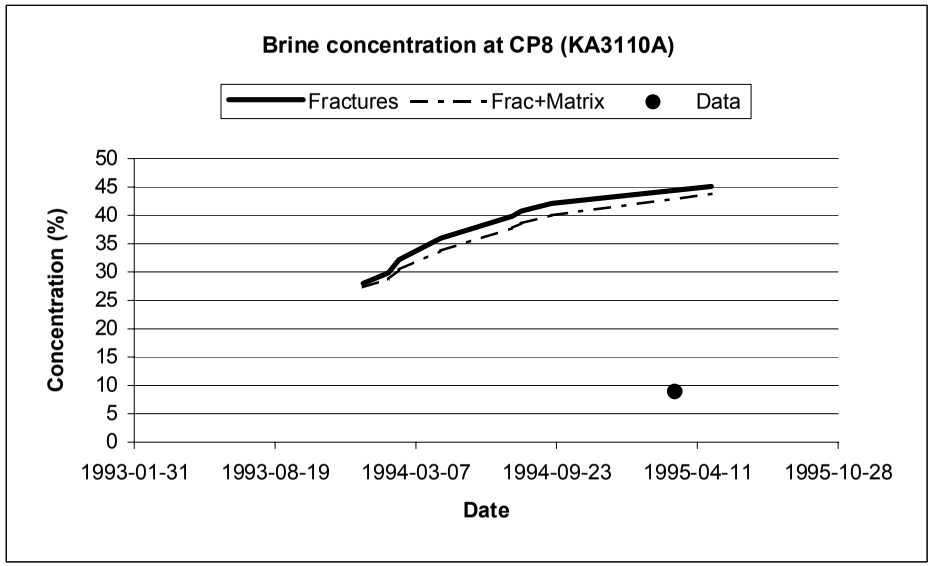

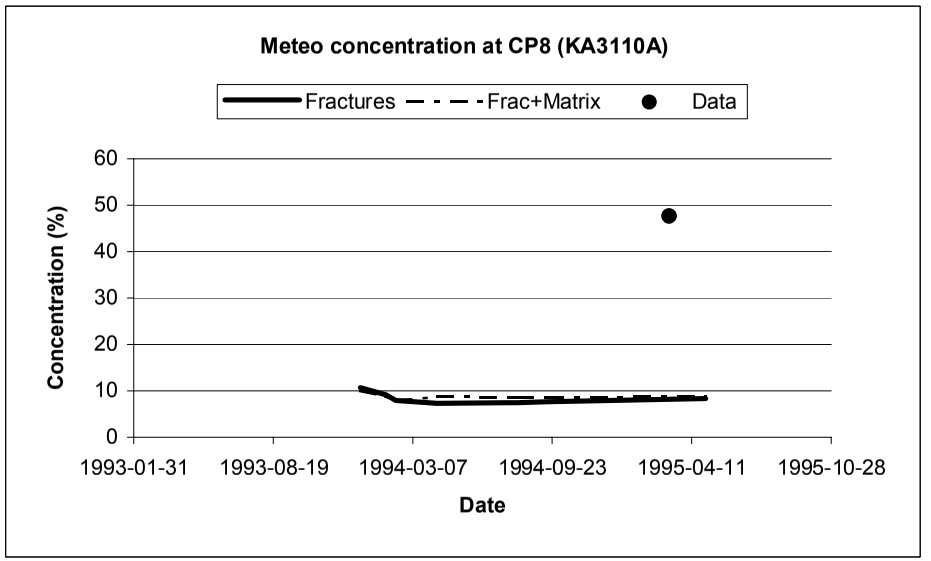

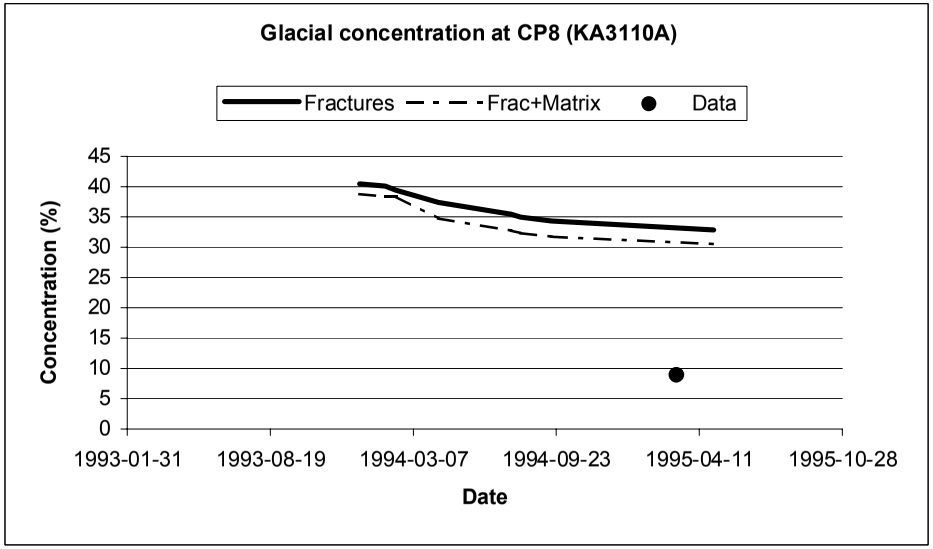

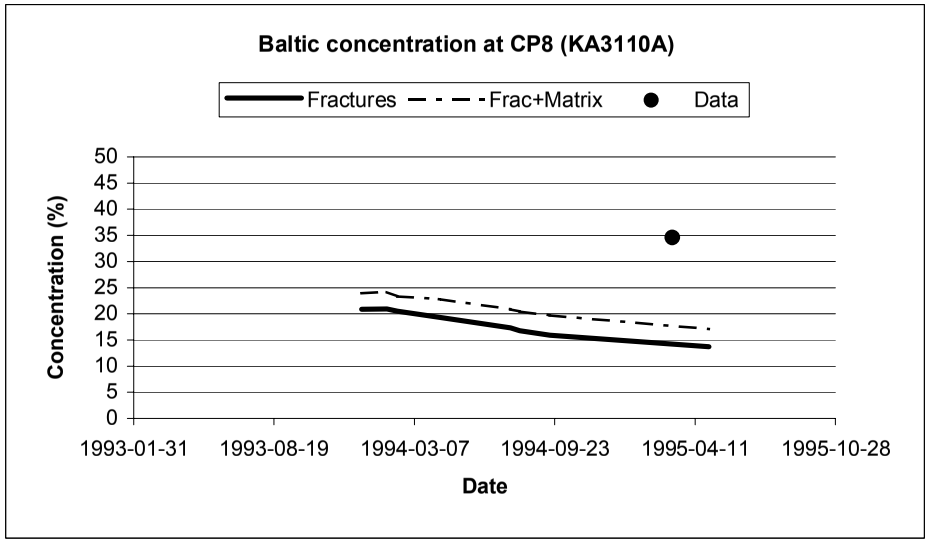

Figure 24 : role of the matrix at CP8

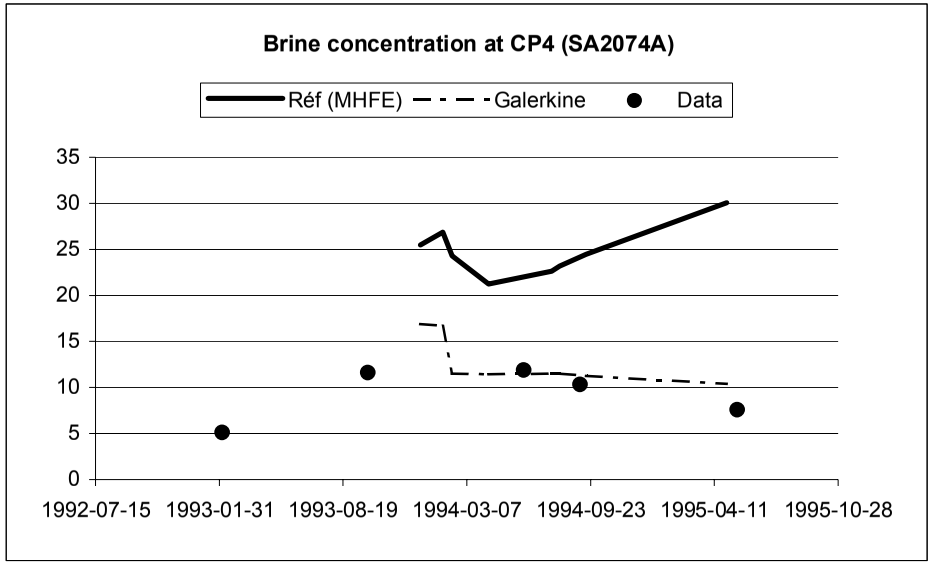

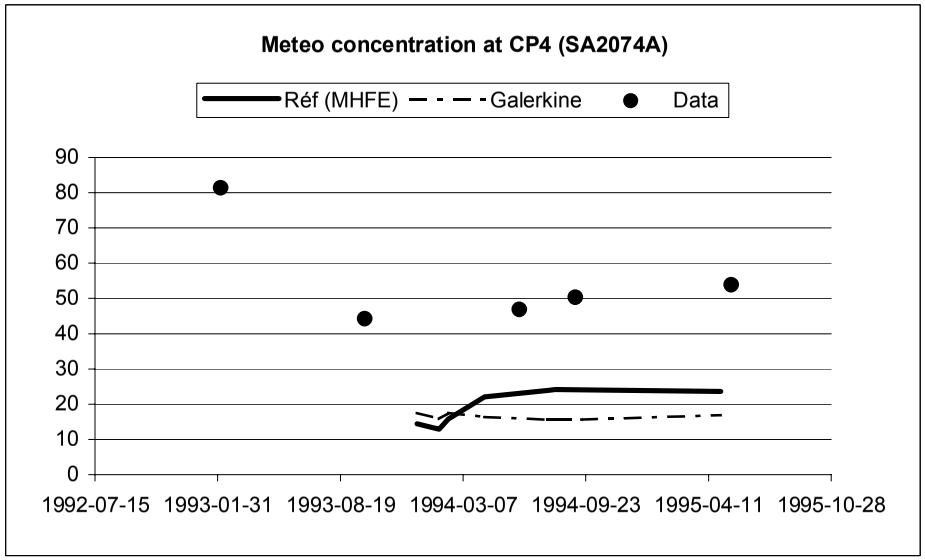

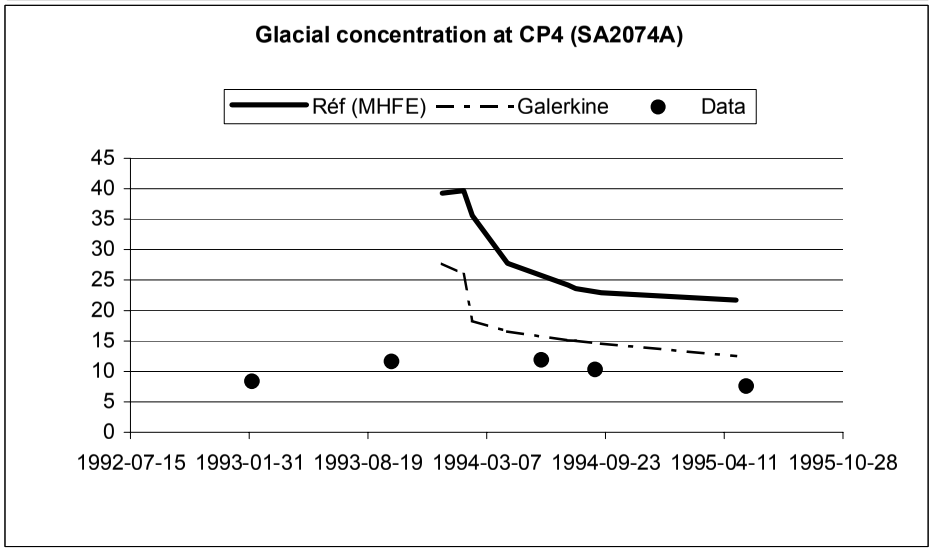

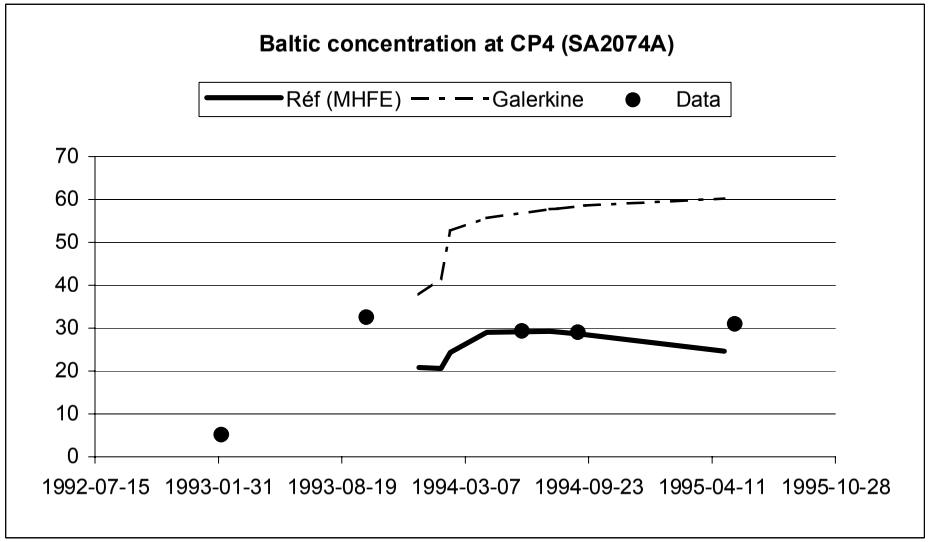

Figure 25 : influence of mathematical scheme at CP4

Sensitivity analysis on mathematical scheme

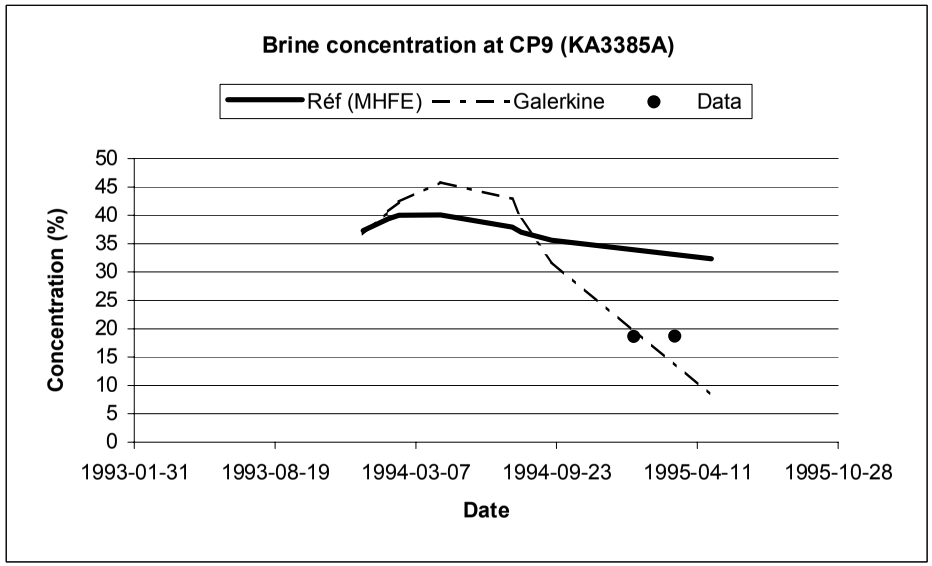

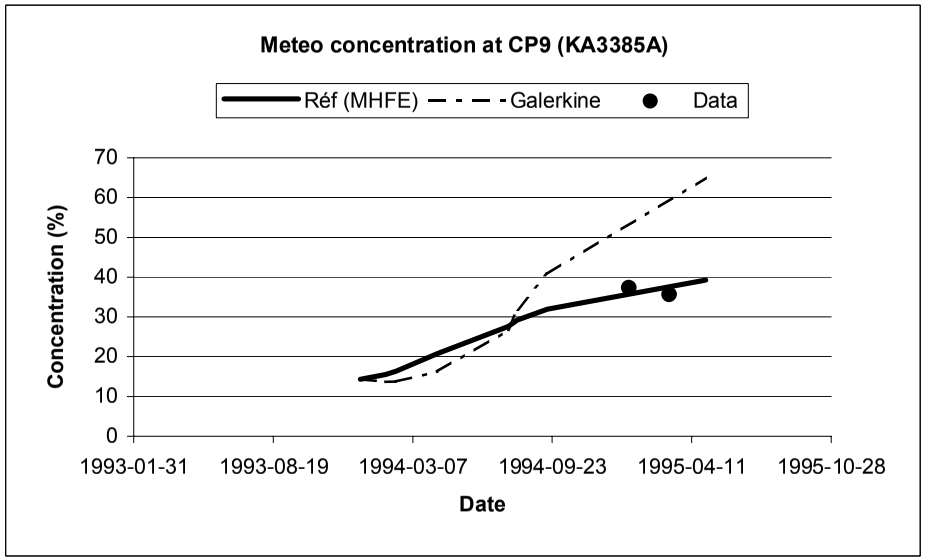

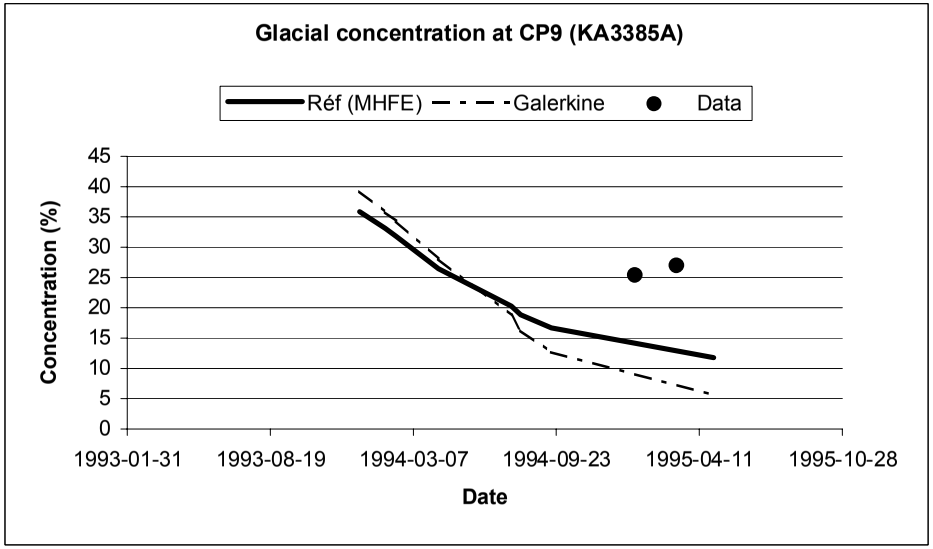

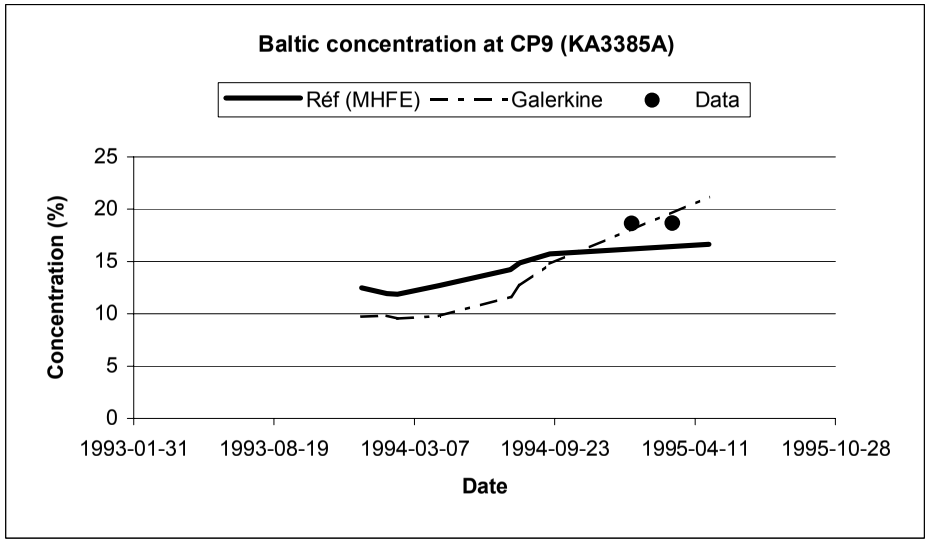

Figure 26 : influence of mathematical scheme at CP9

Sensitivity analysis on time step duration

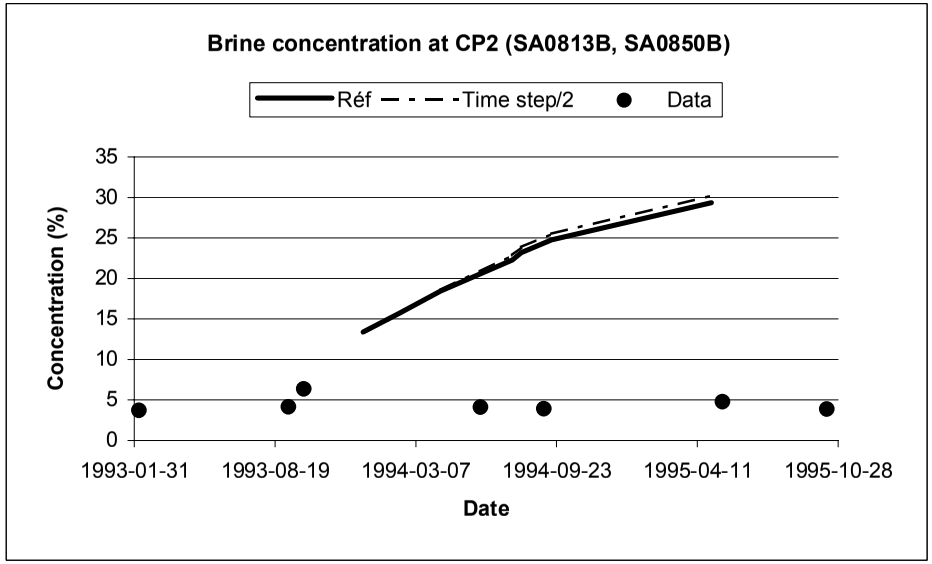

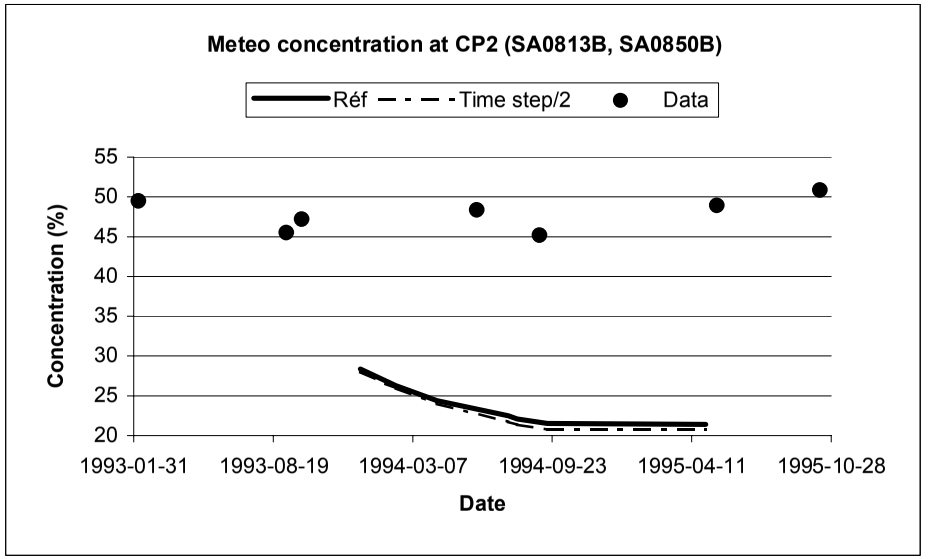

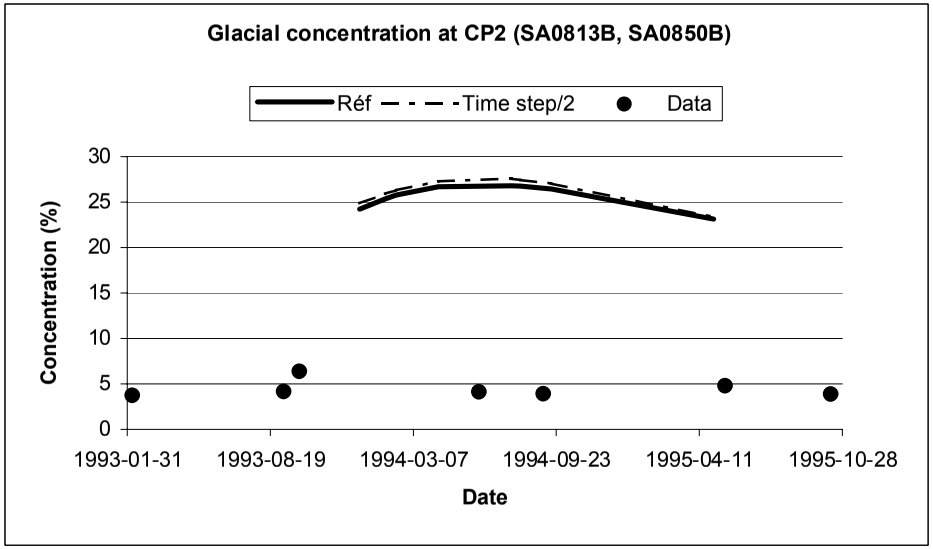

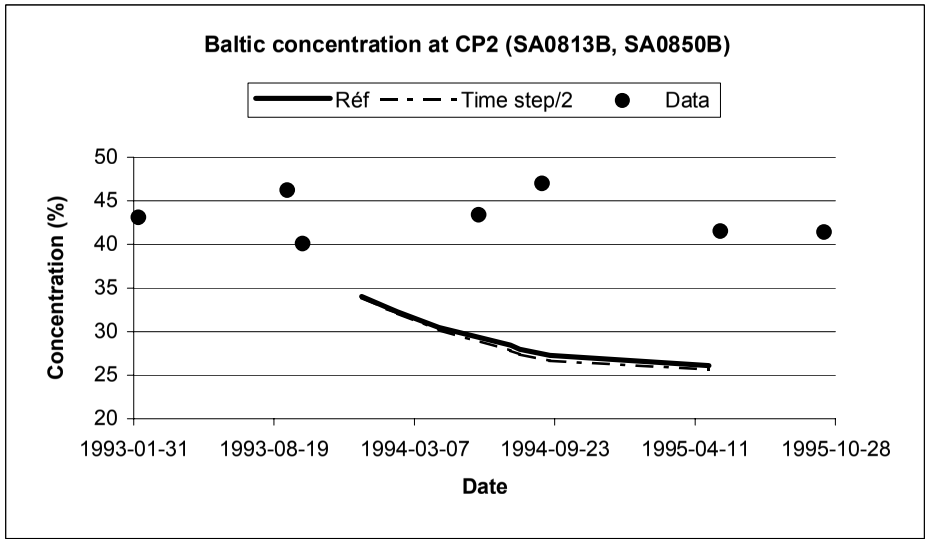

Figure 27 : role of time steps duration at CP2

Sensitivity analysis on time step duration

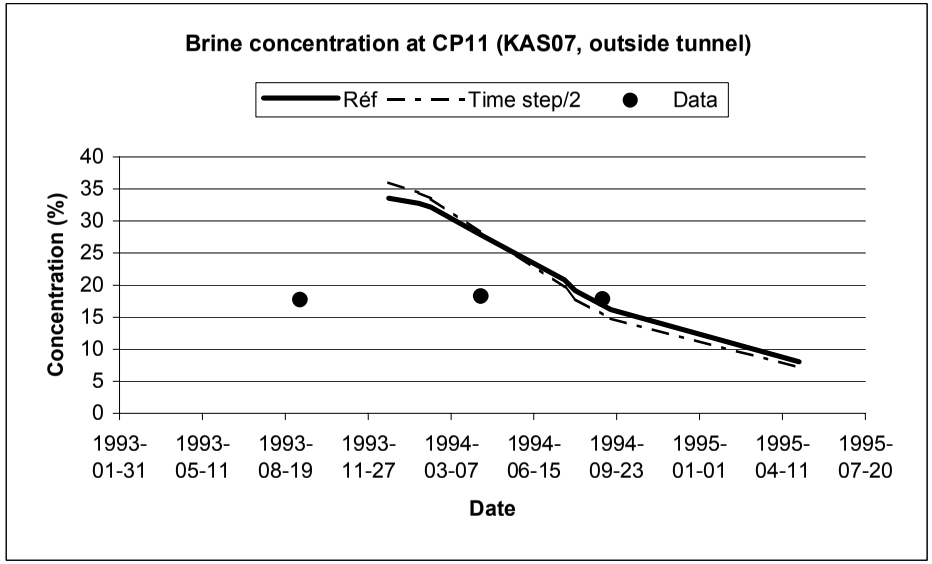

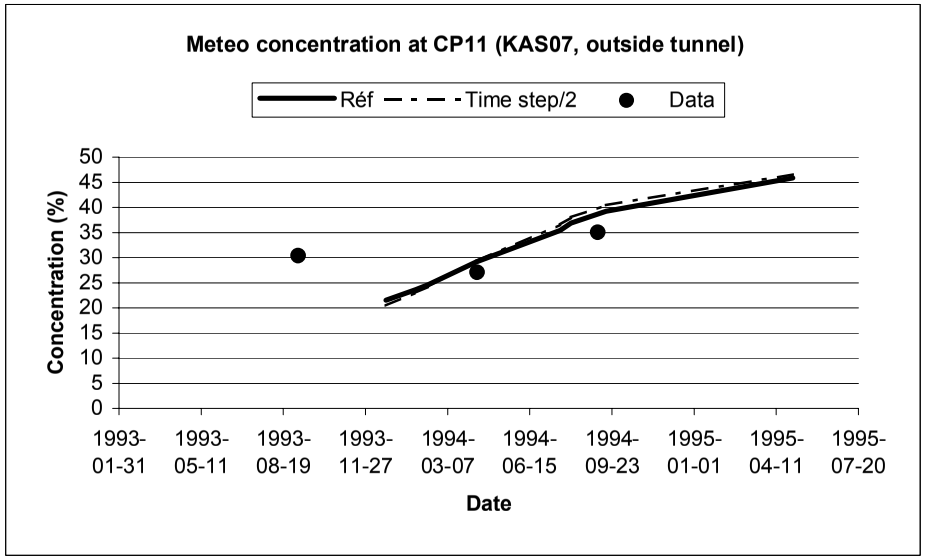

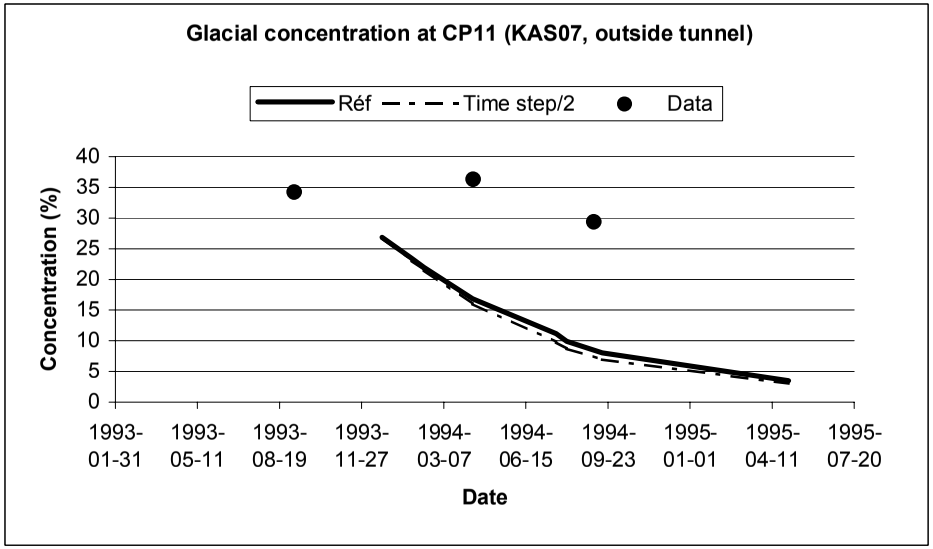

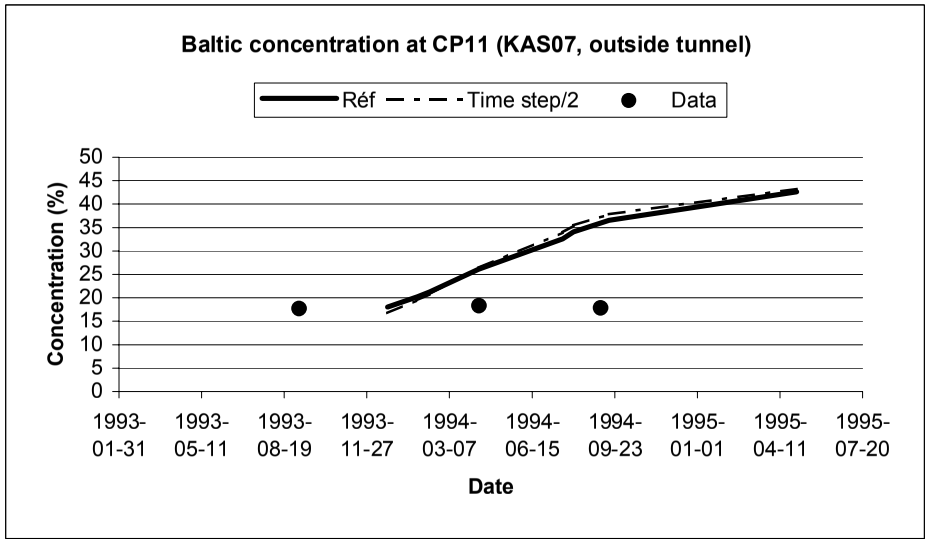

Figure 28 : role of time steps duration at CP11

Sensitivity analysis on interpolation method for M3 concentration data

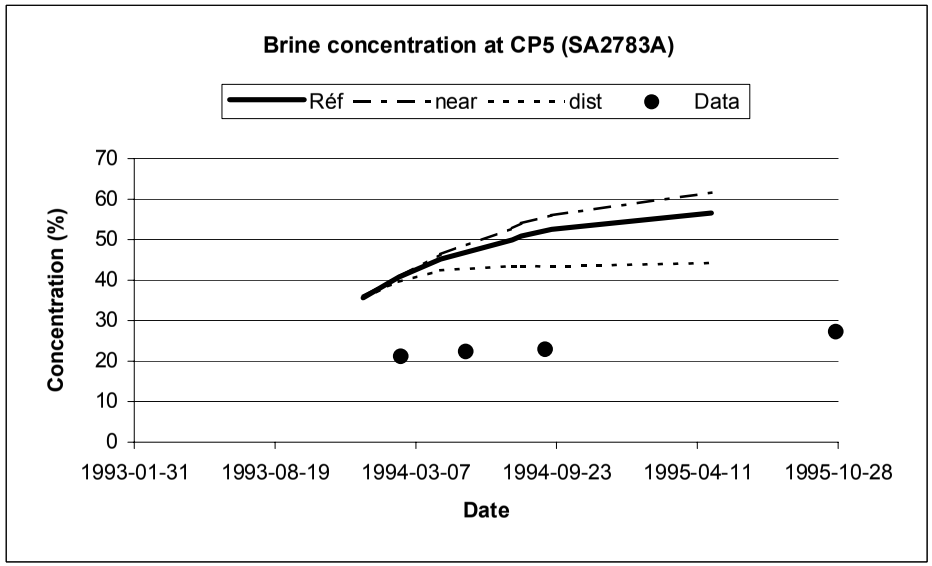

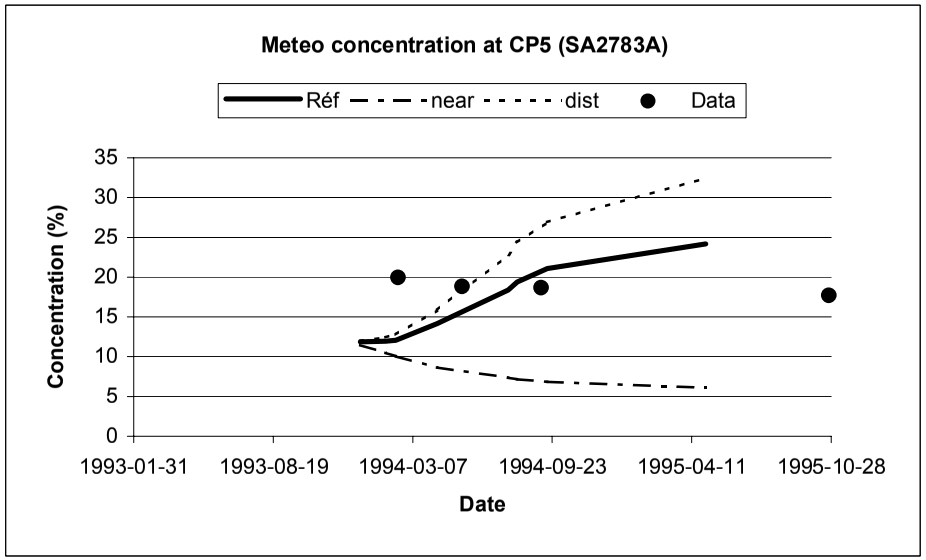

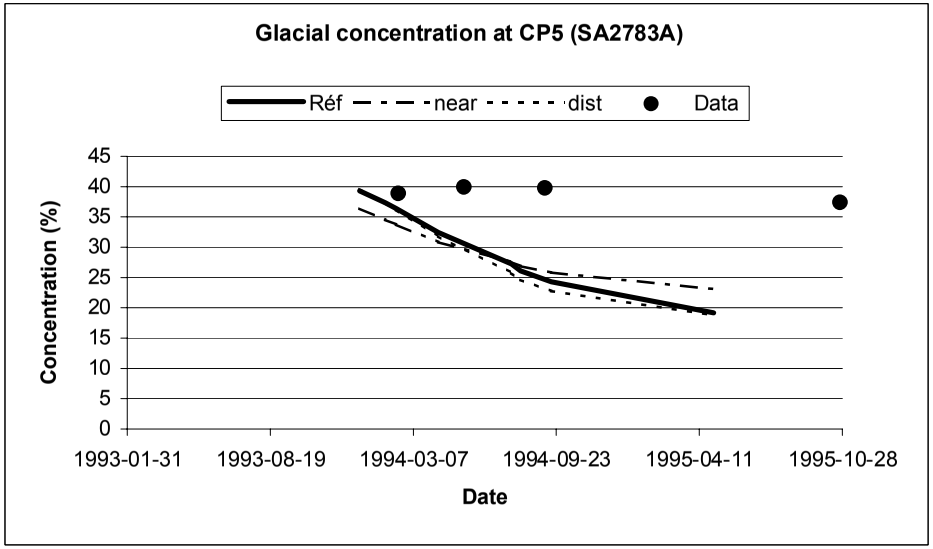

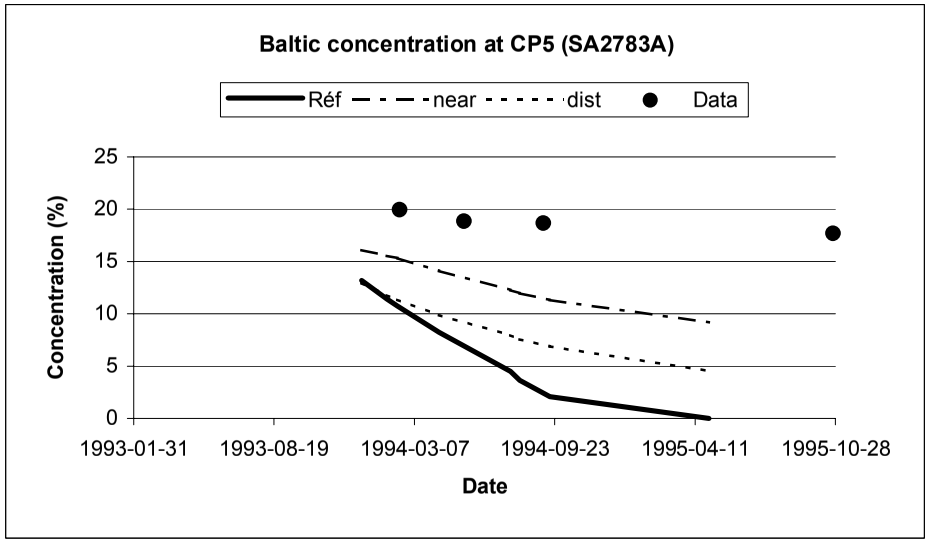

Figure 29 : role of interpolation method at CP5

Sensitivity analysis on interpolation method for M3 concentration data

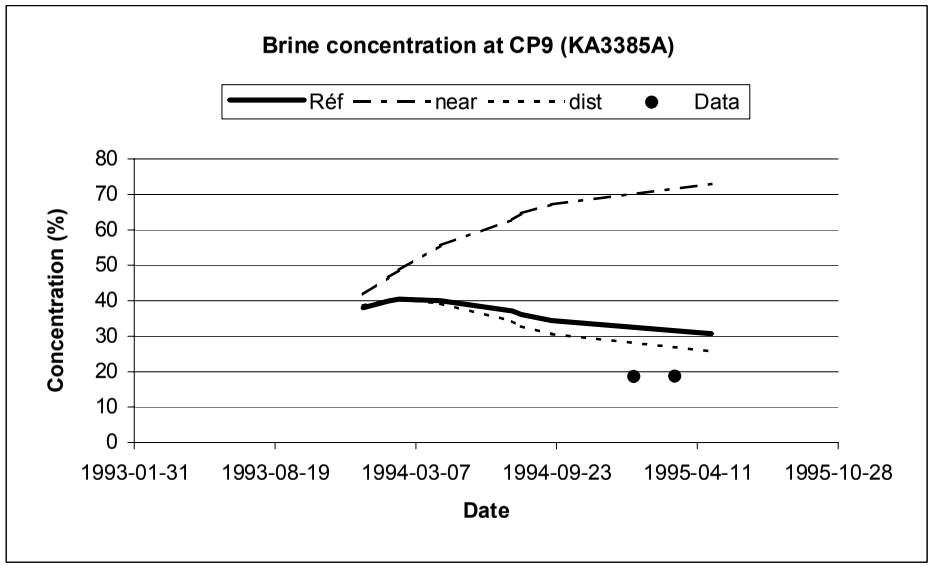

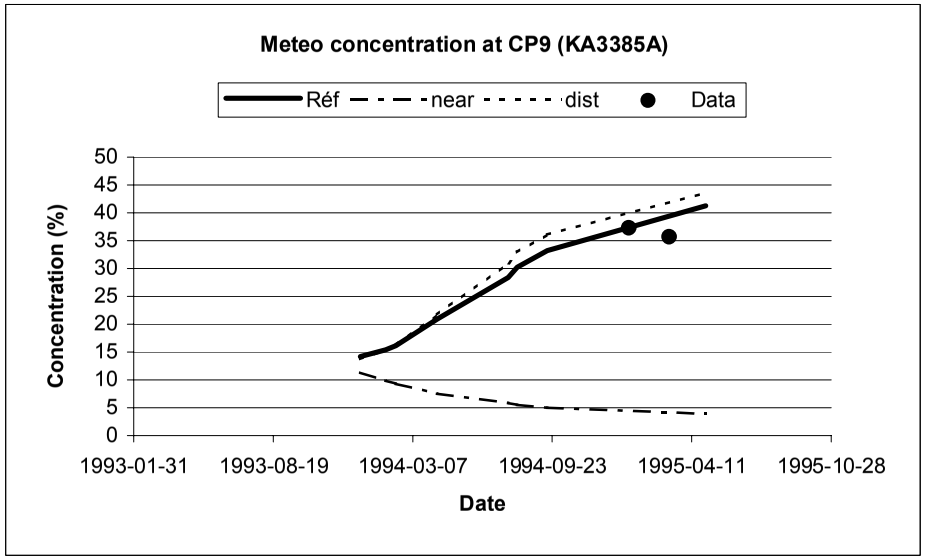

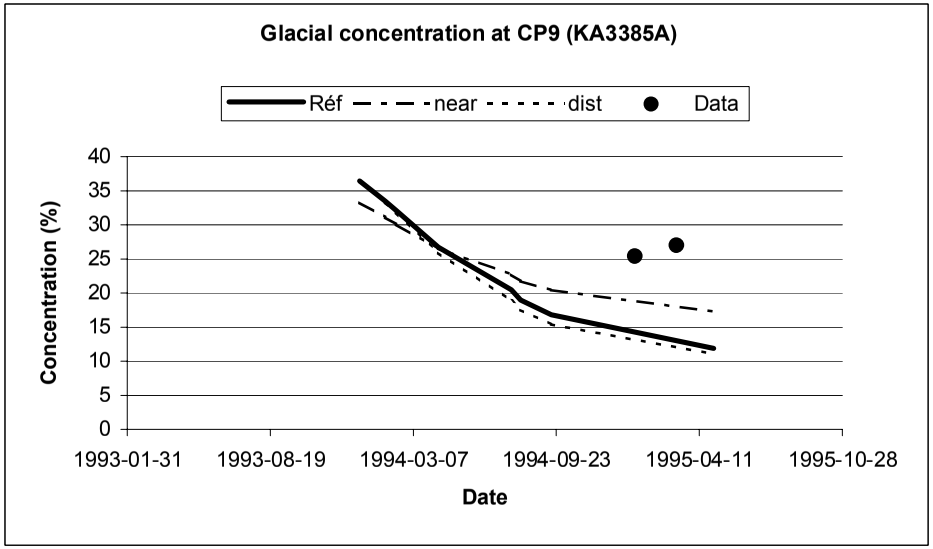

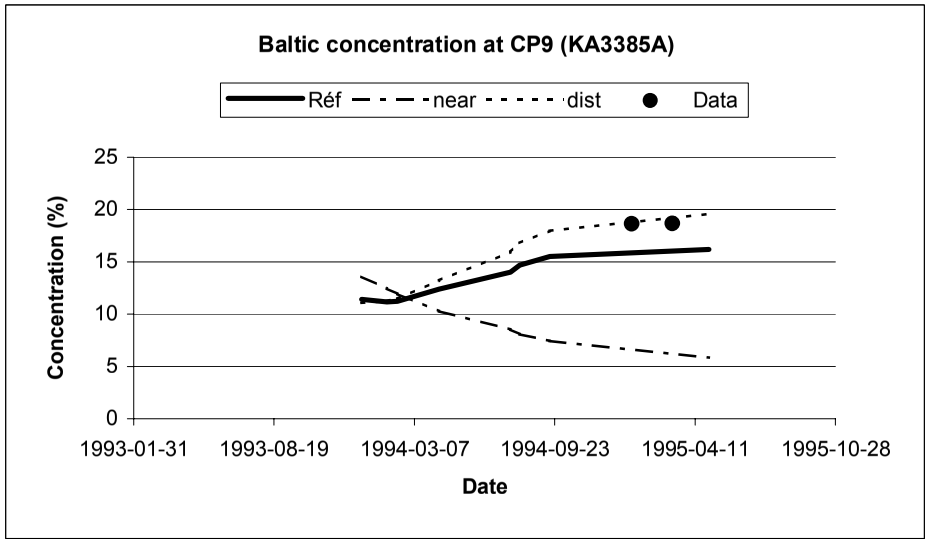

Figure 30 : role of interpolation method at CP9

Sensitivity analysis on interpolation method for M3 concentration data

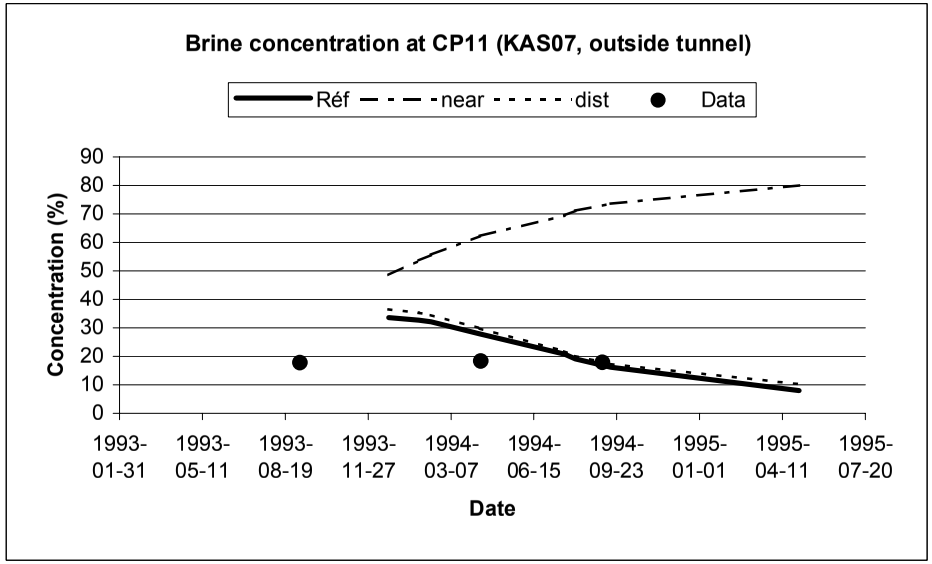

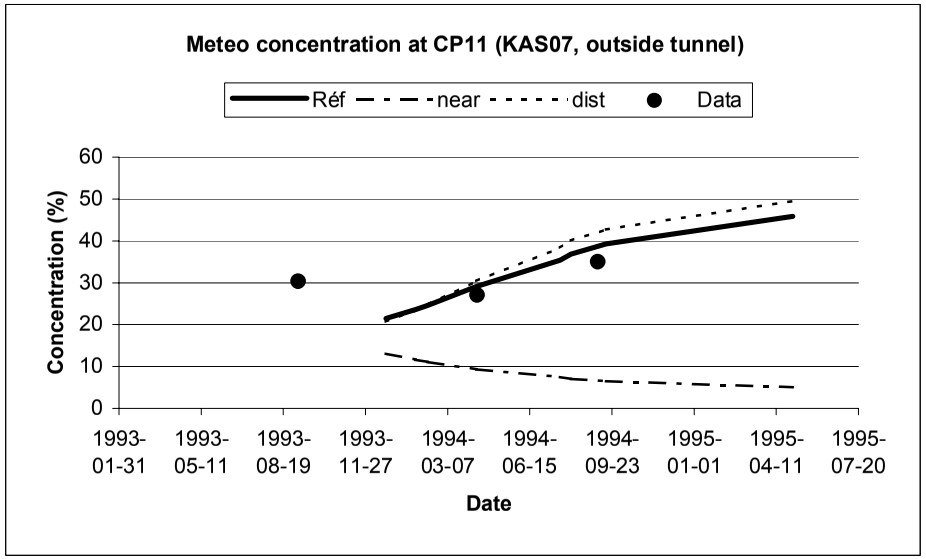

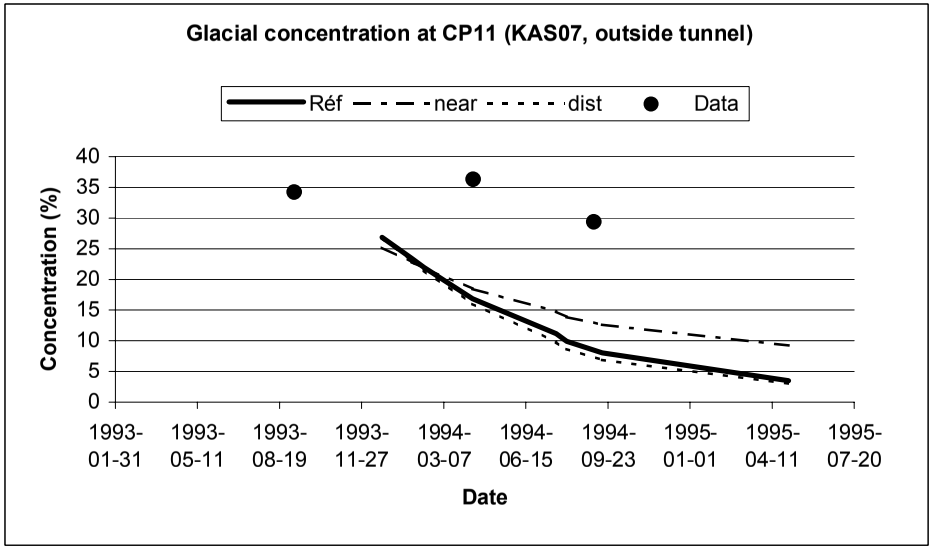

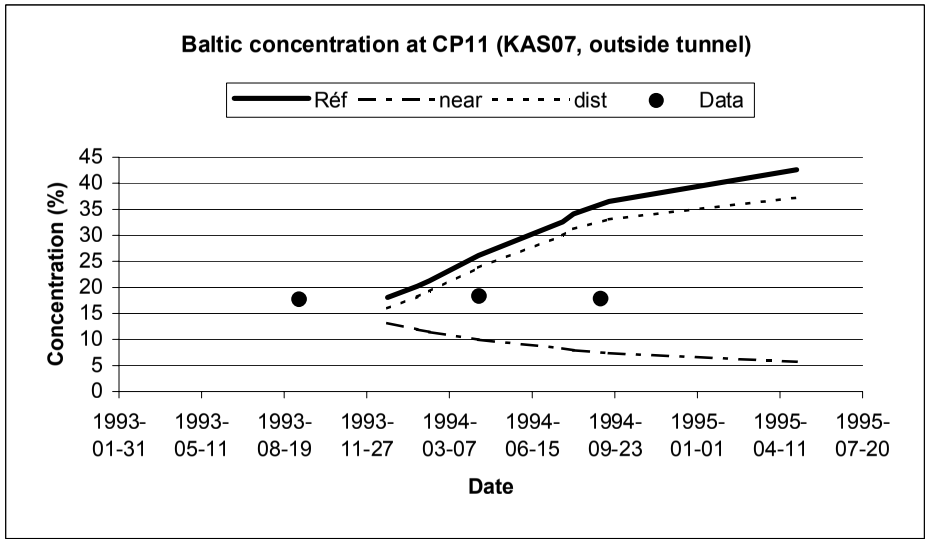

Figure 31 : role of interpolation method at CP11

Sensitivity analysis on M3 calculation for initial and boundary concentrations

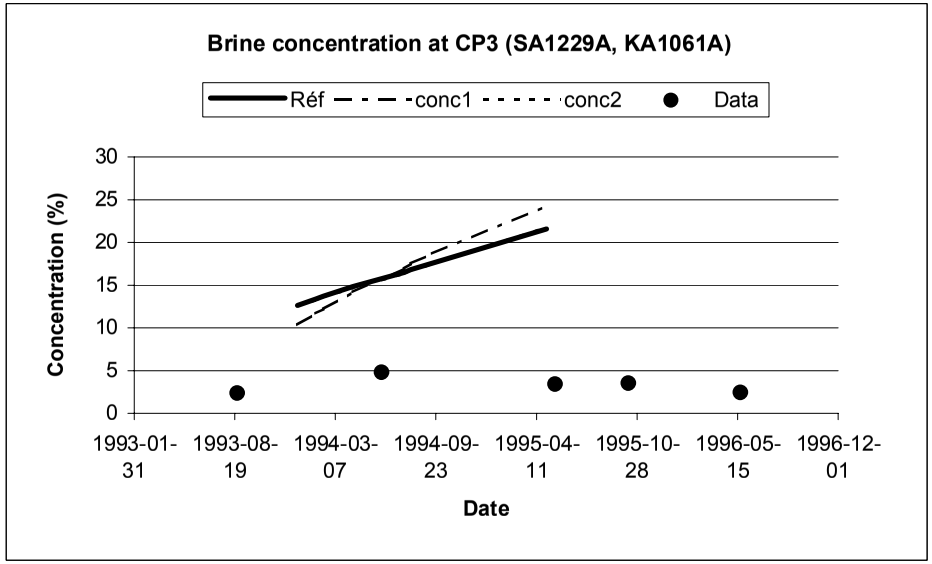

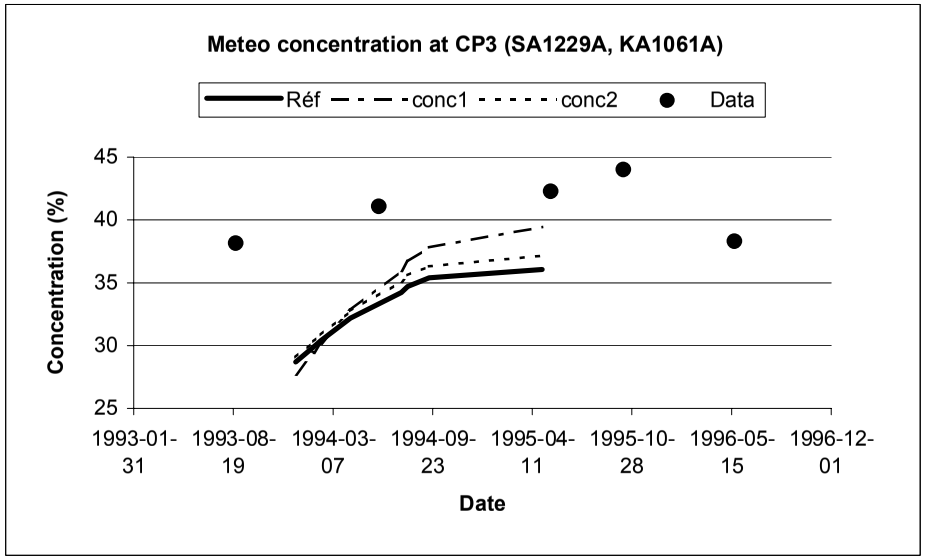

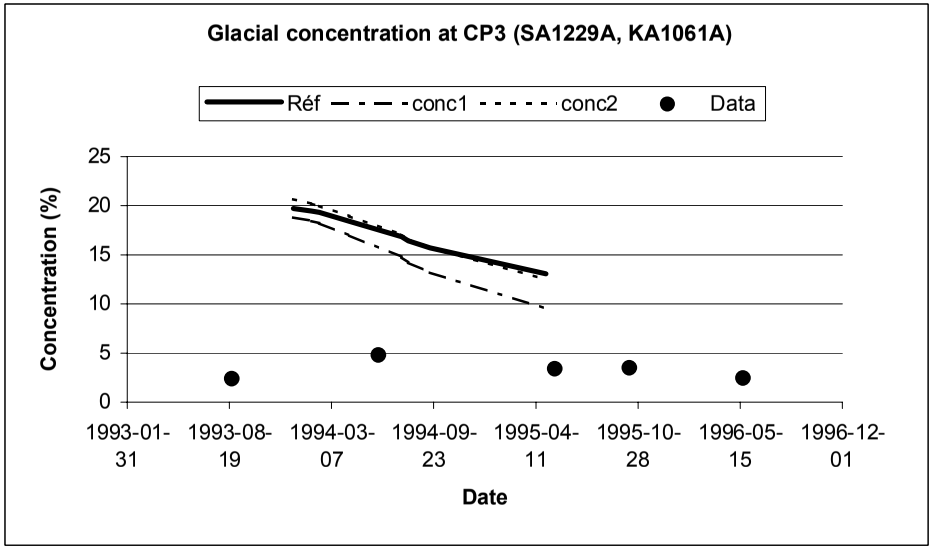

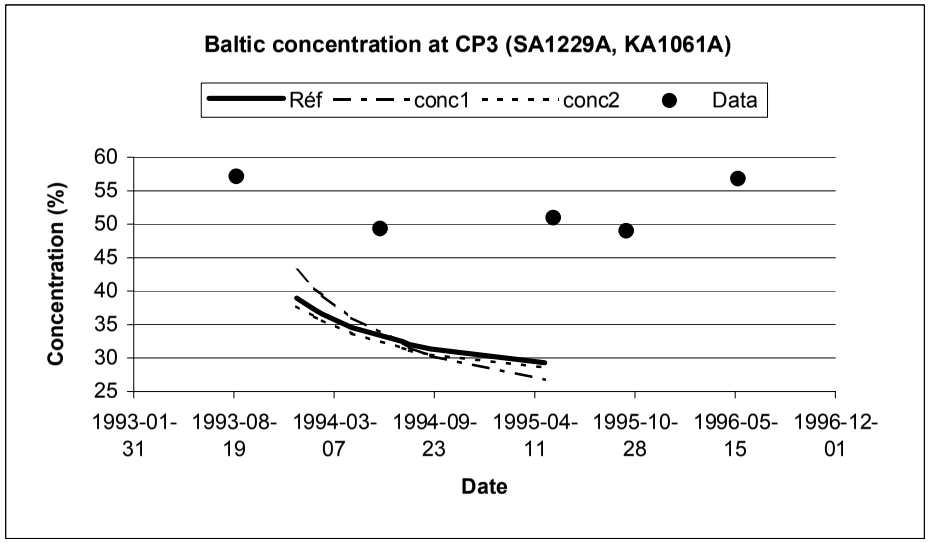

Figure 32 : role of M3 data values at CP3

Sensitivity analysis on M3 calculation for initial and boundary concentrations

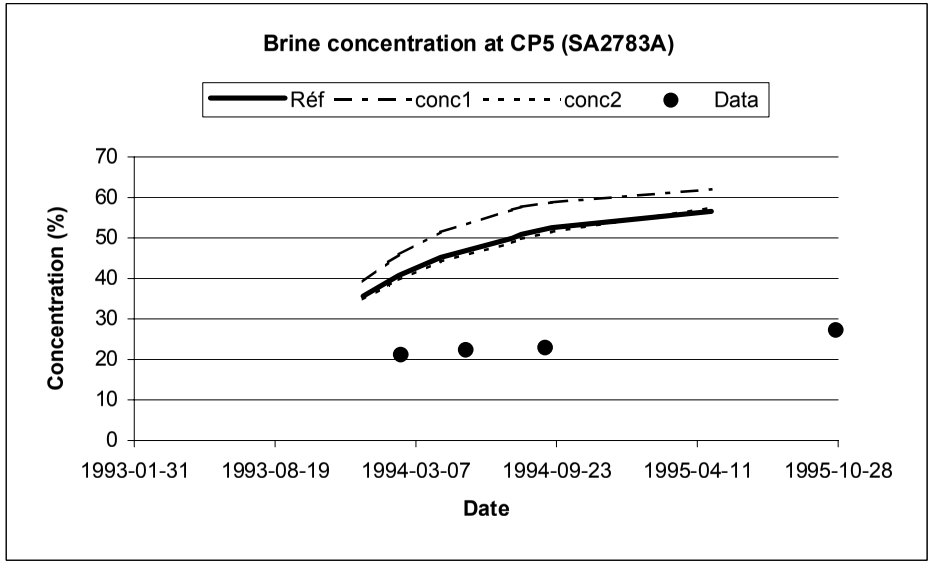

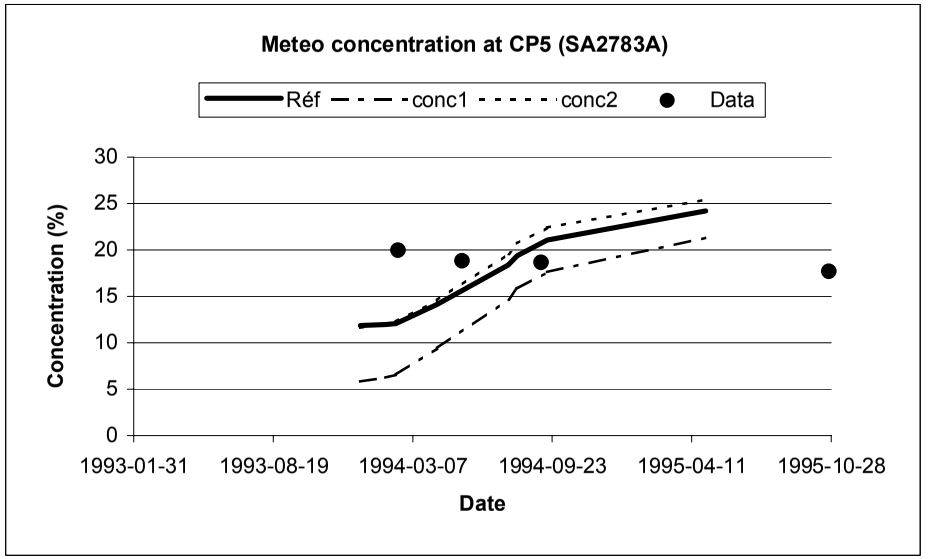

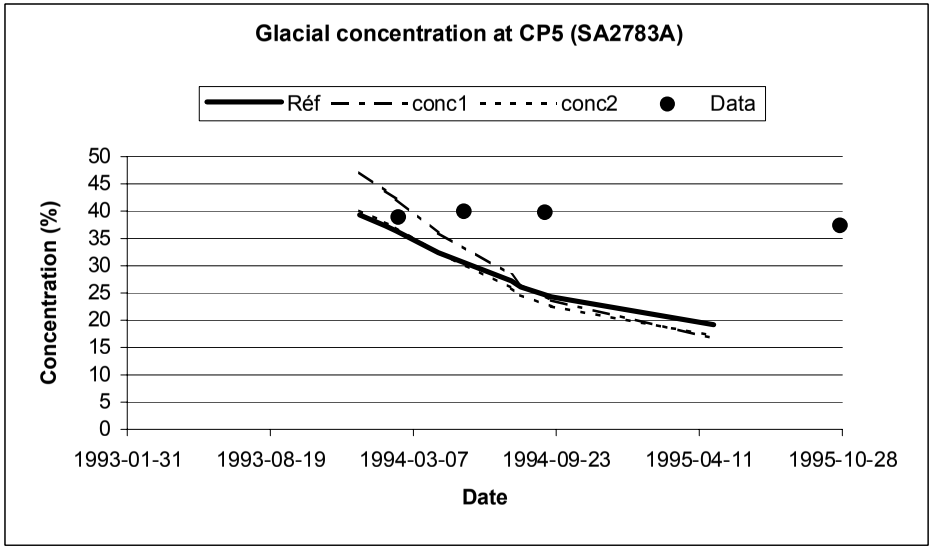

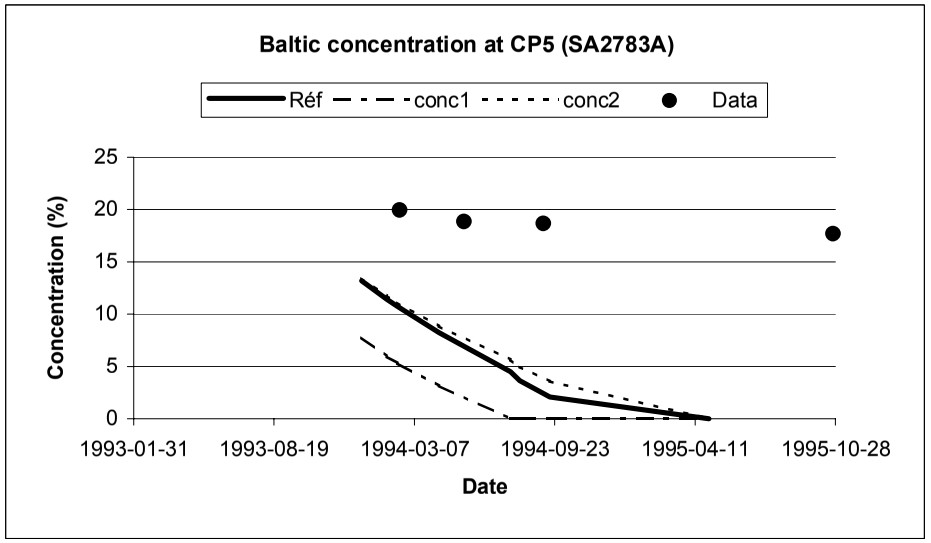

Figure 33 : role of M3 data values at CP5

Sensitivity analysis on M3 calculation for initial and boundary concentrations

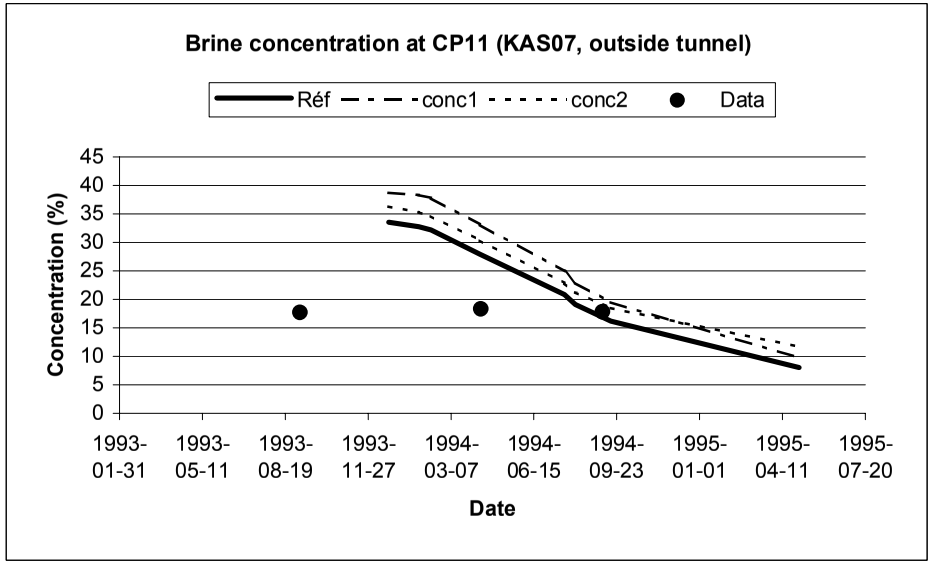

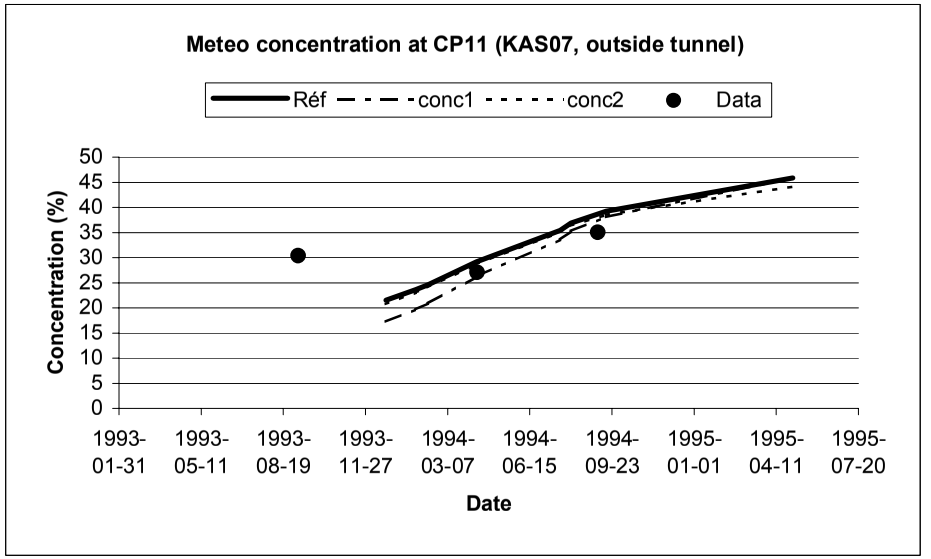

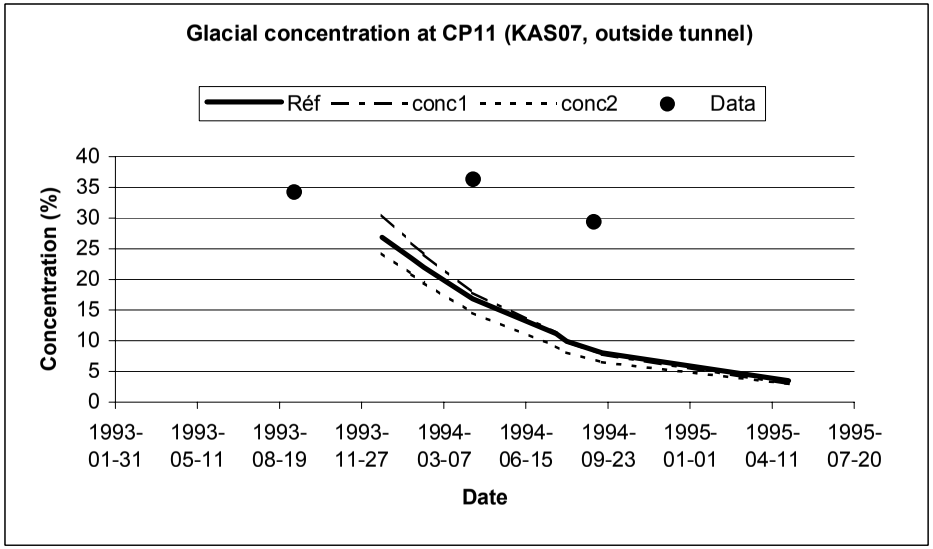

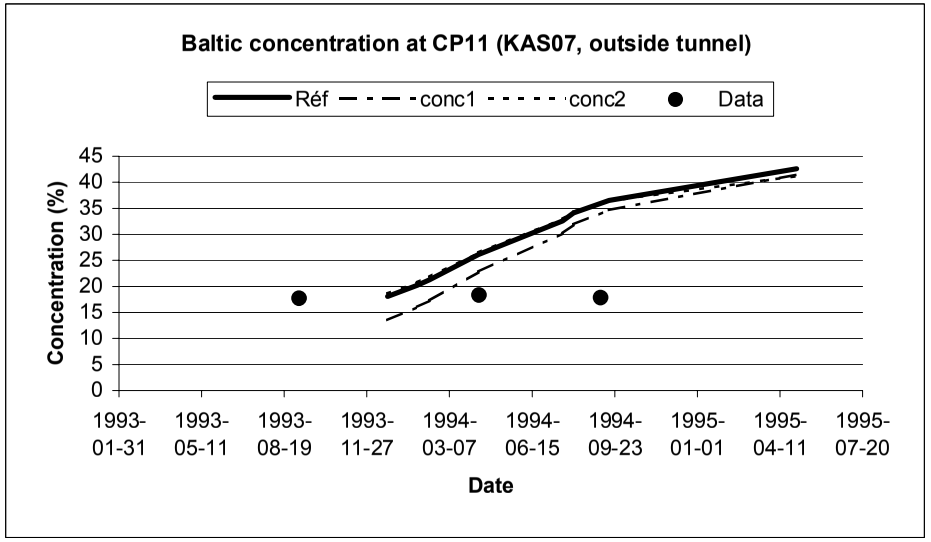

Figure 34 : role of M3 data values at CP11

Sensitivity analysis on K for NE-2, NNW-7 and NE-4

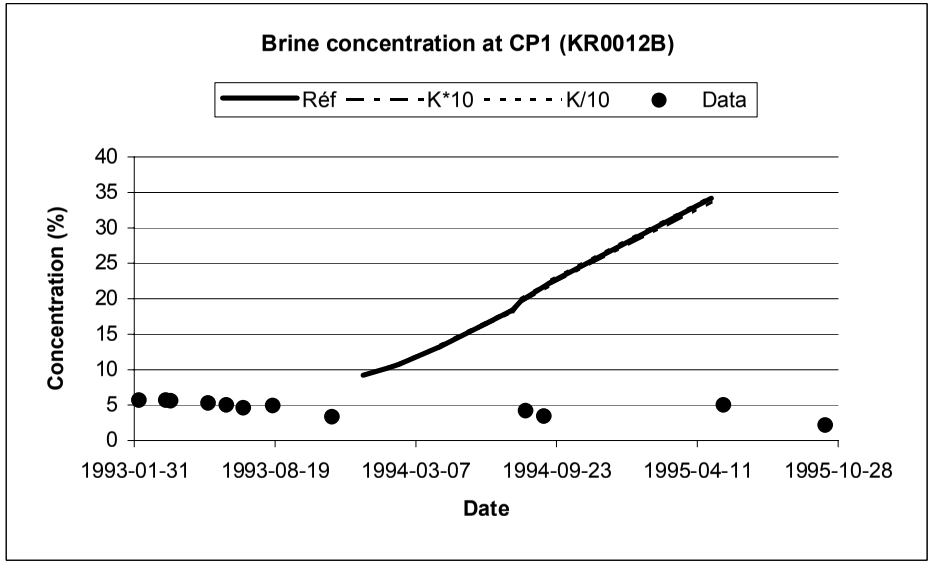

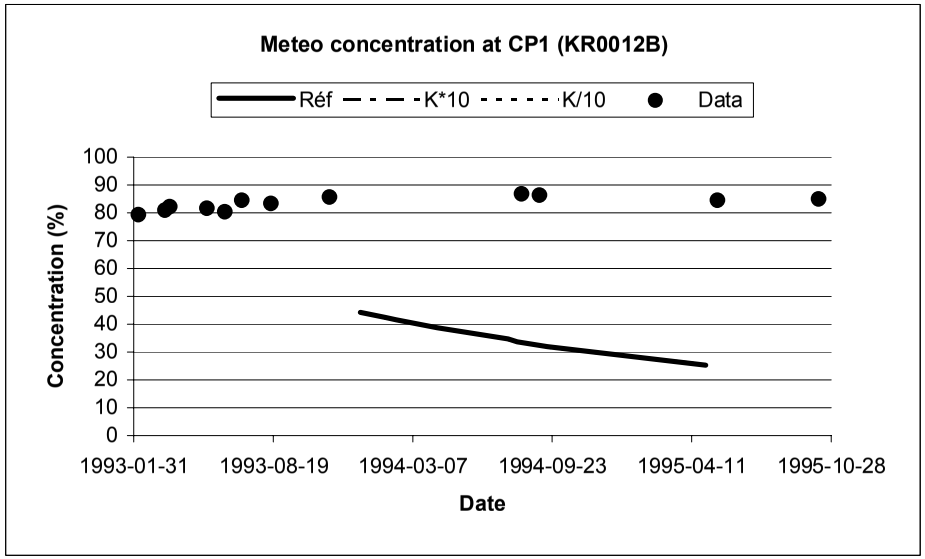

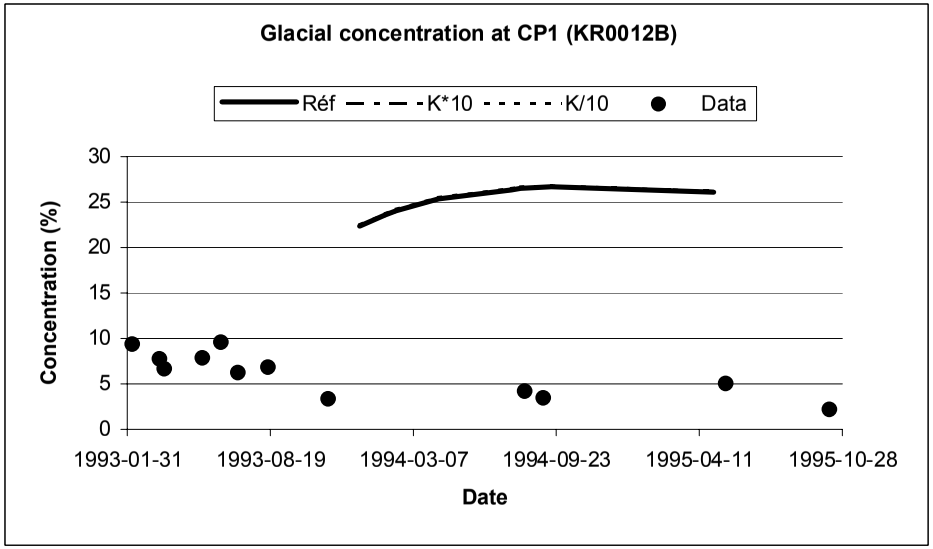

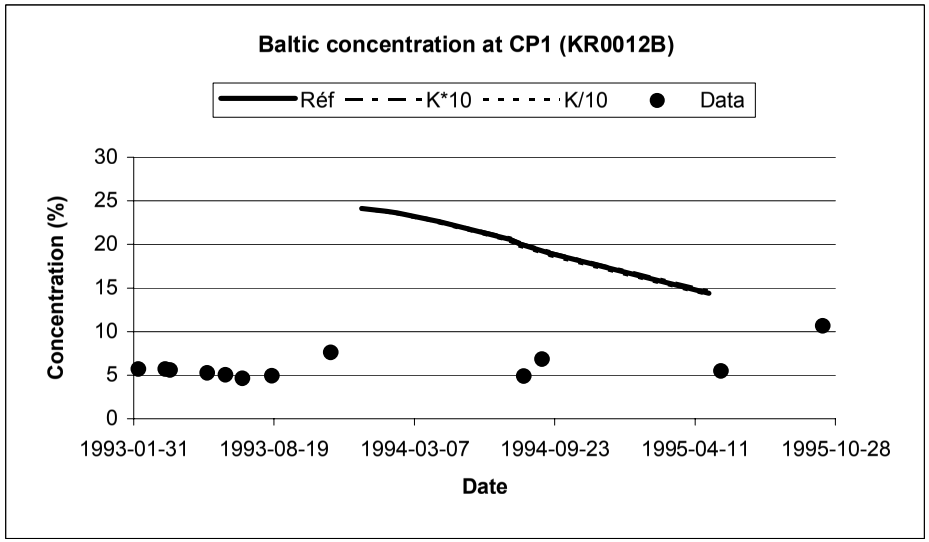

Figure 35 : role of permeability values at CP1

Sensitivity analysis on K for NE-2, NNW-7 and NE-4

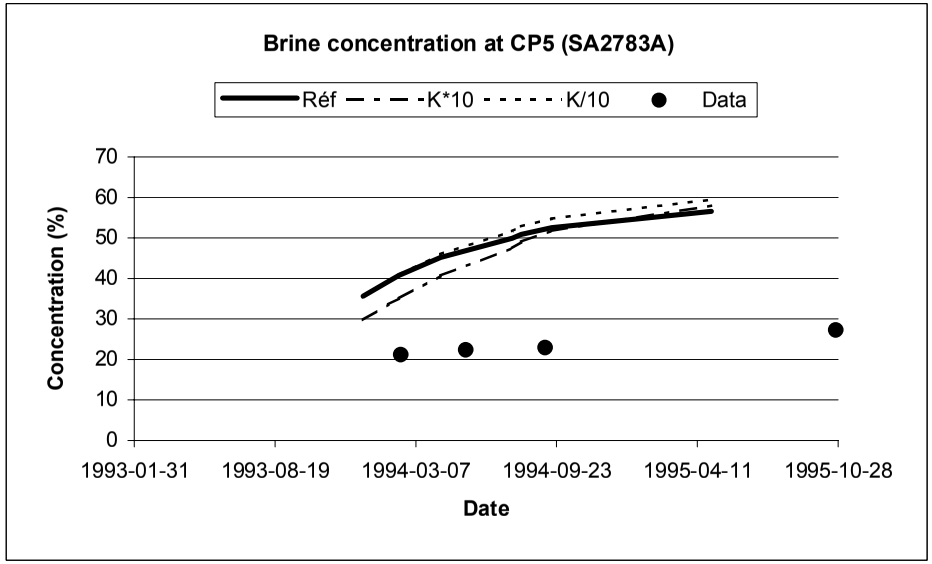

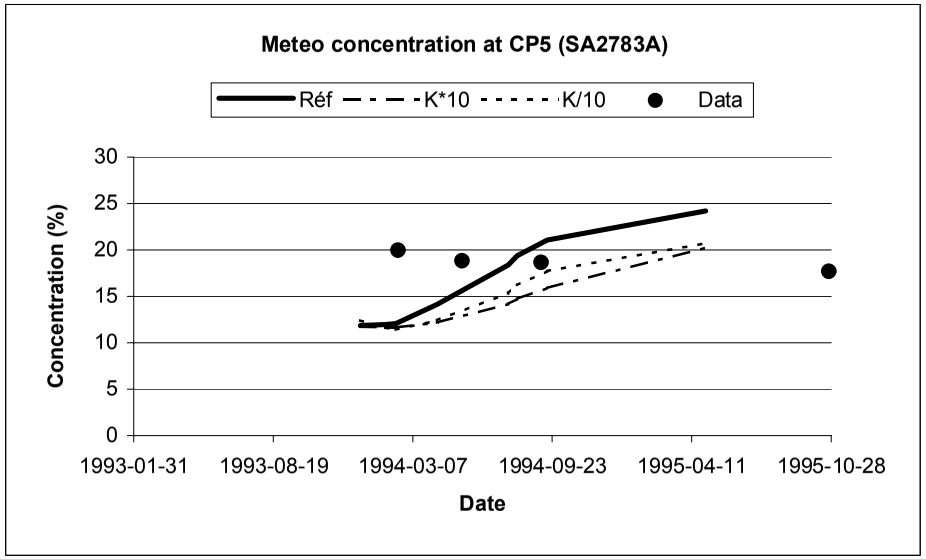

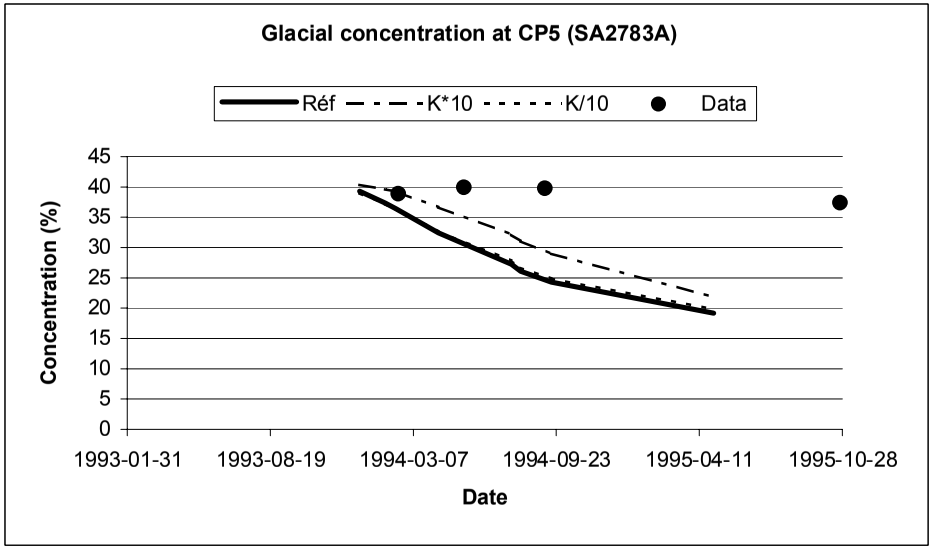

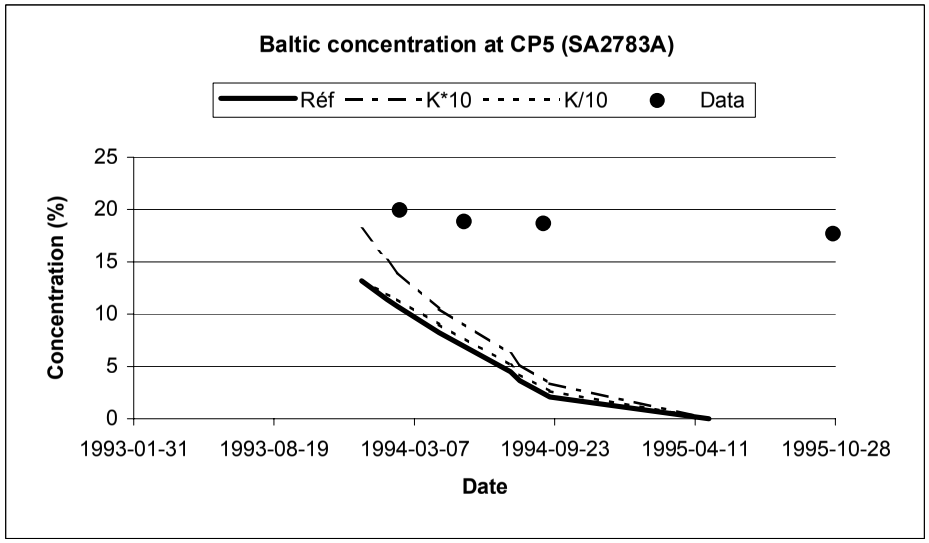

Figure 36 : role of permeability values at CP5

Sensitivity analysis on K for NE-2, NNW-7 and NE-4

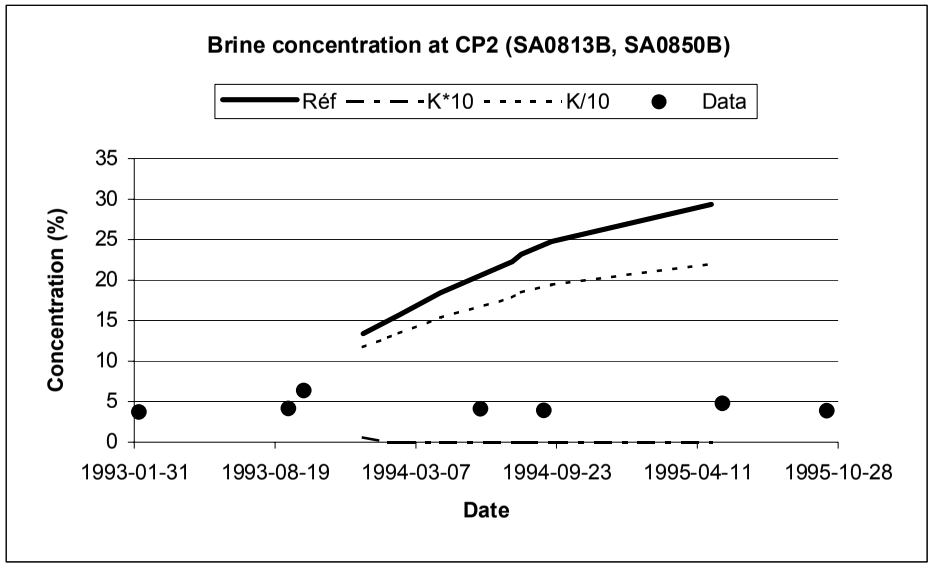

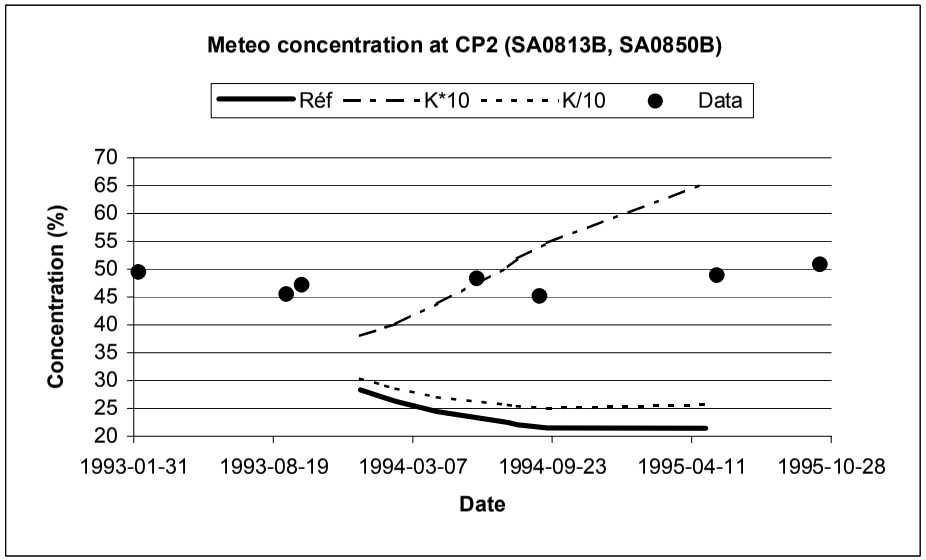

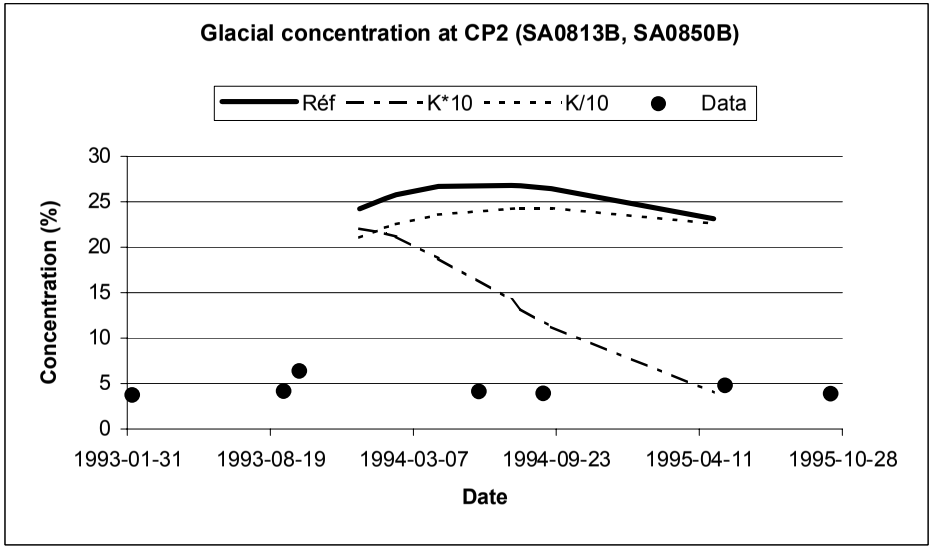

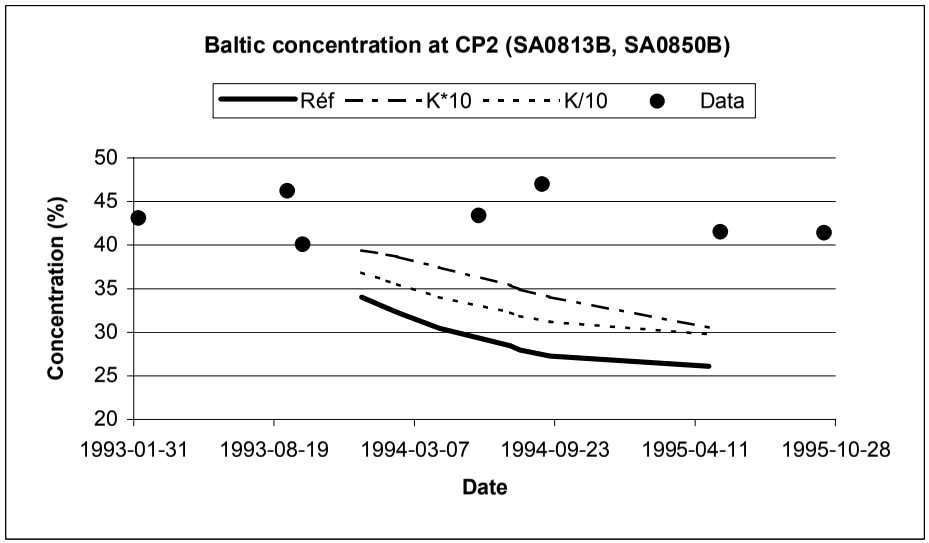

Figure 37 : role of permeability values at CP2

Sensitivity analysis on initial and boundaries conditions in Head

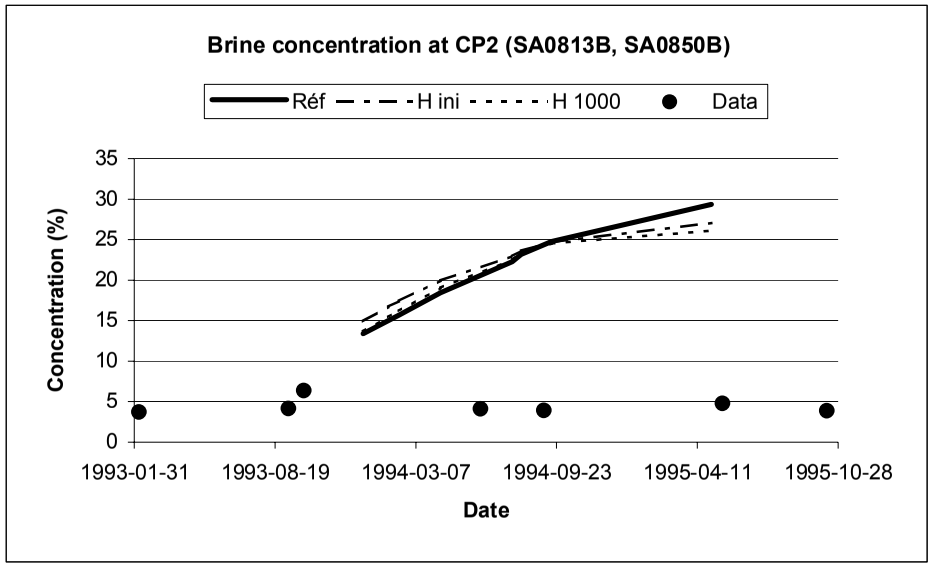

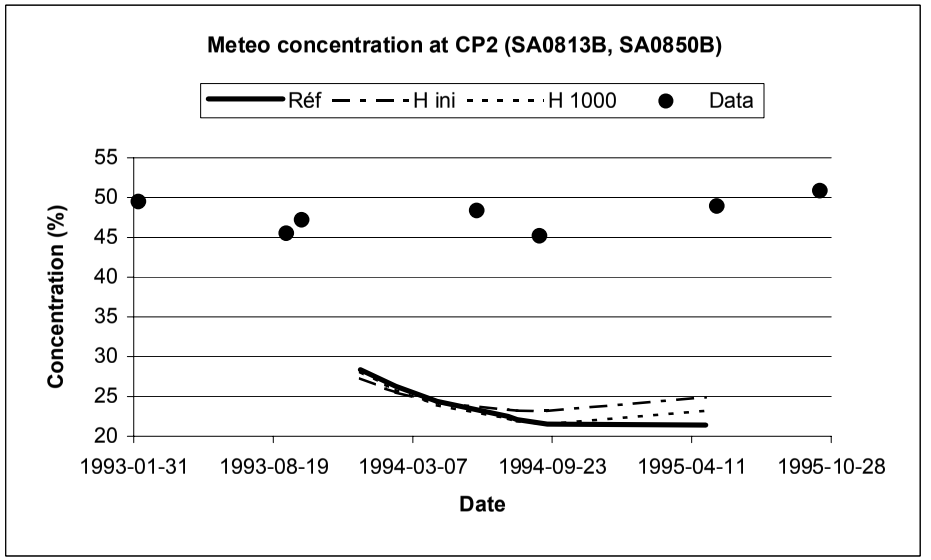

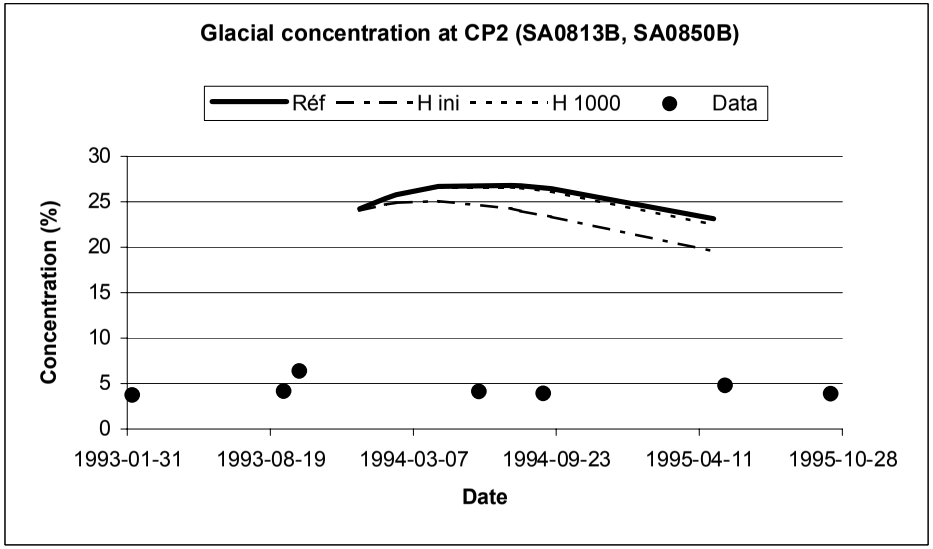

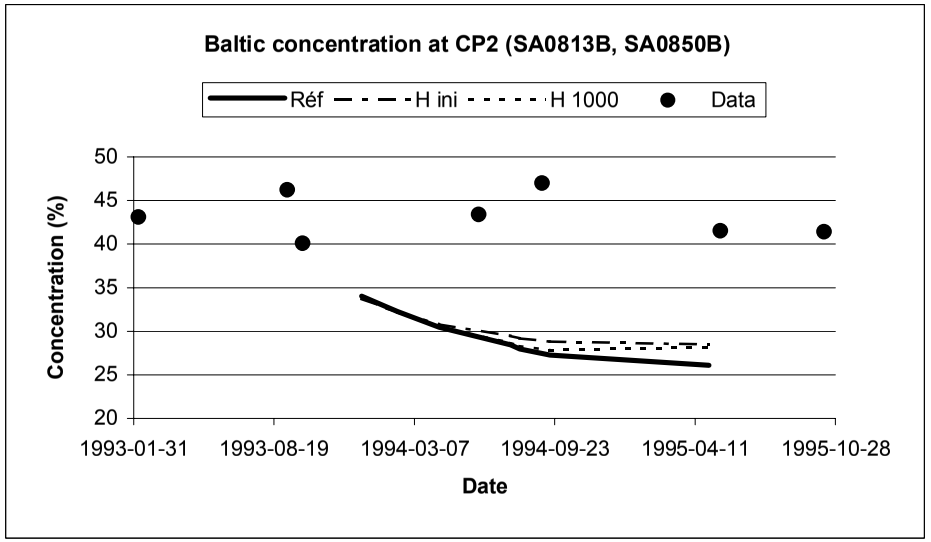

Figure 38 : role of boundaries heads values at CP2

Sensitivity analysis on initial and boundaries conditions in Head

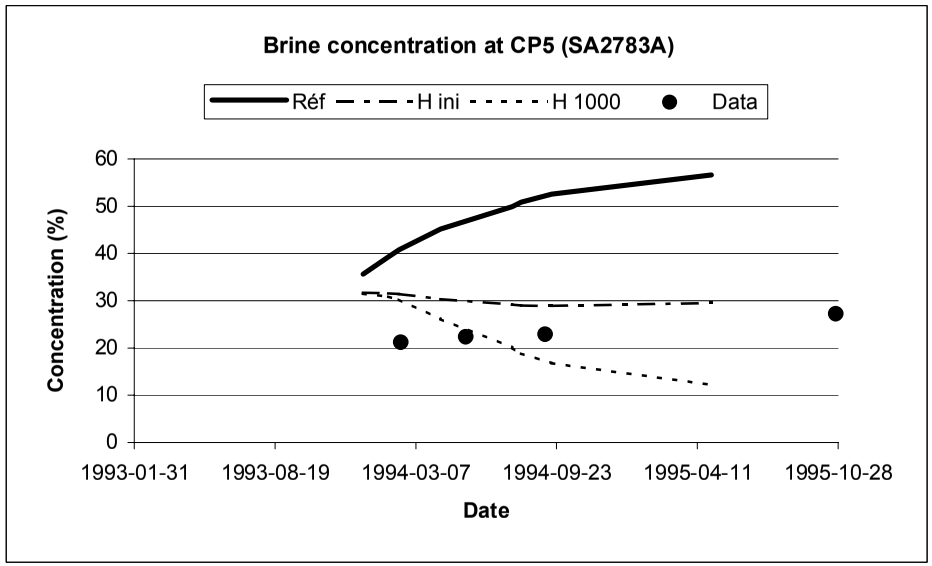

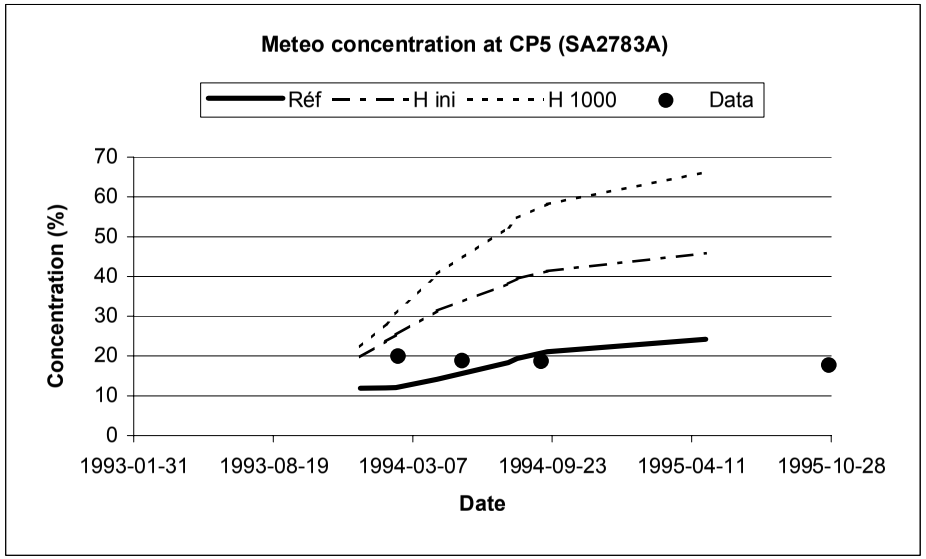

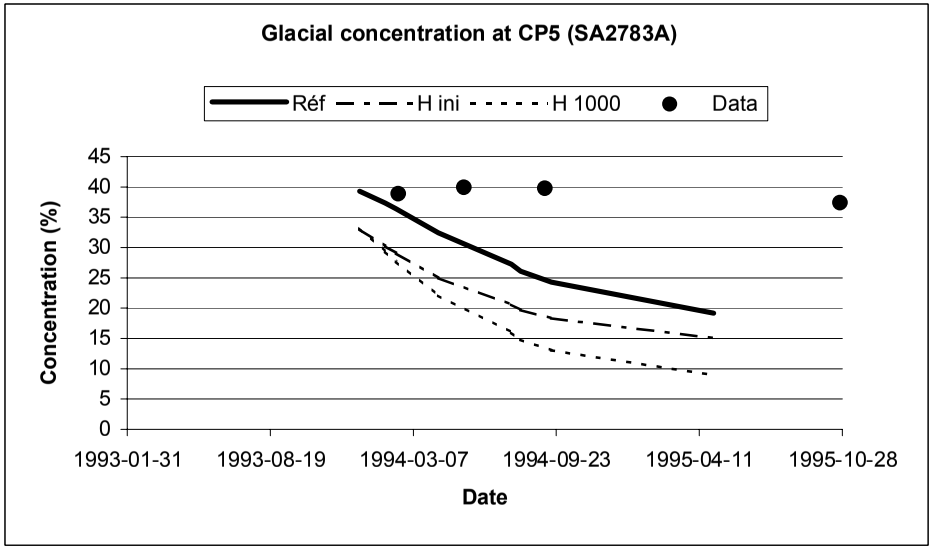

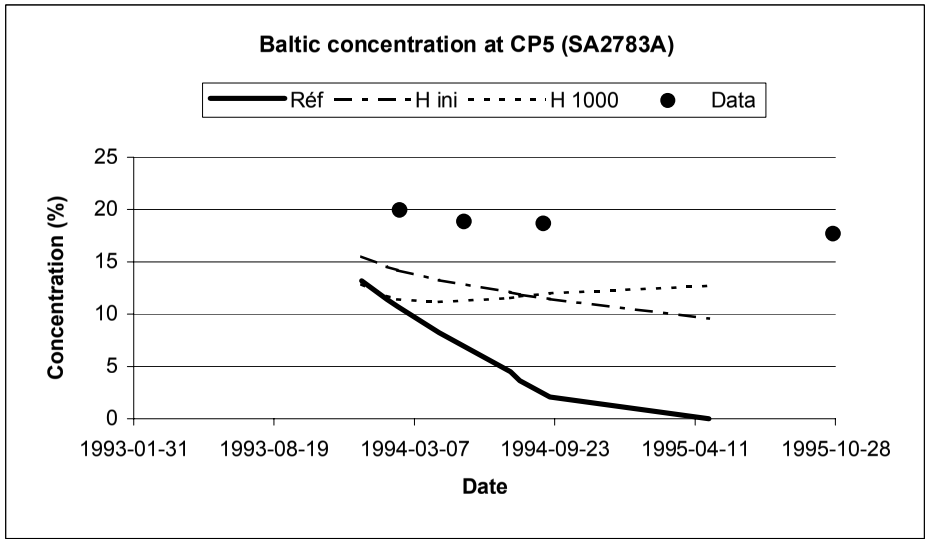

Figure 39 : role of boundaries heads values at CP5

Sensitivity analysis on initial and boundaries conditions in Head

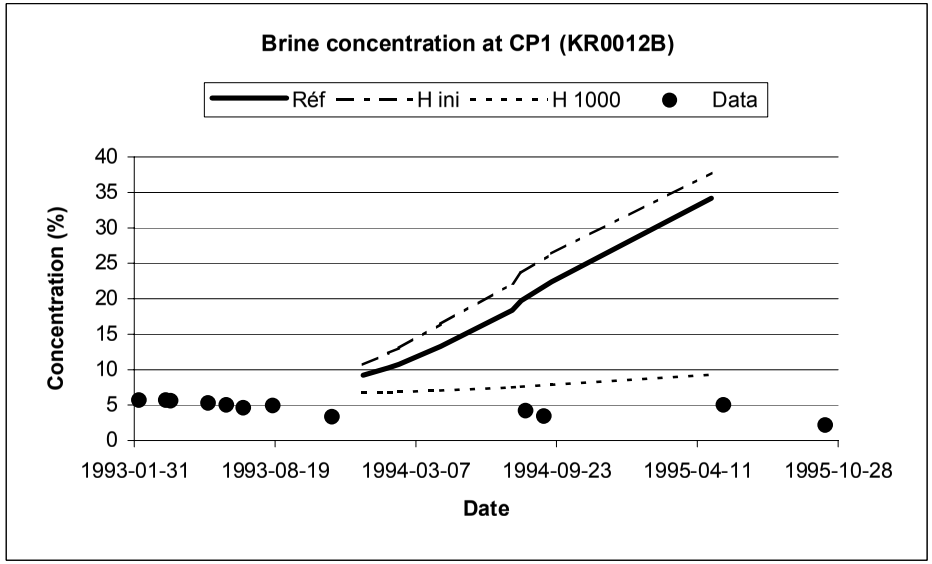

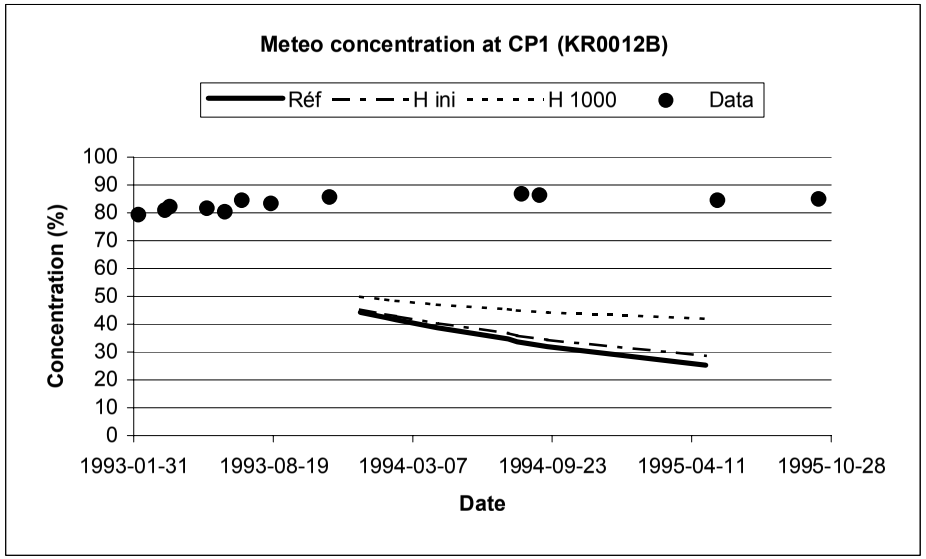

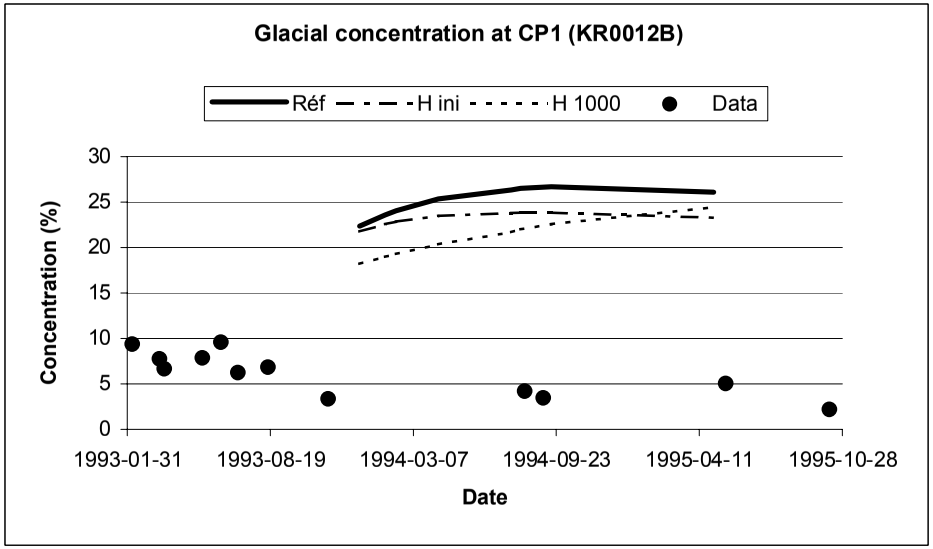

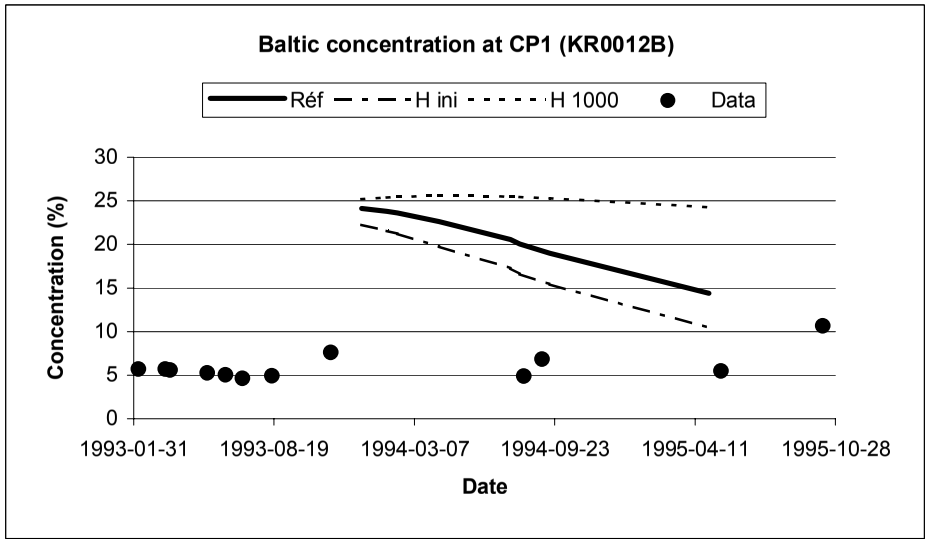

Figure 40 : role of boundaries heads values at CP1

Sensitivity analysis on Pc for NE-2, NNW-7 and NE-4

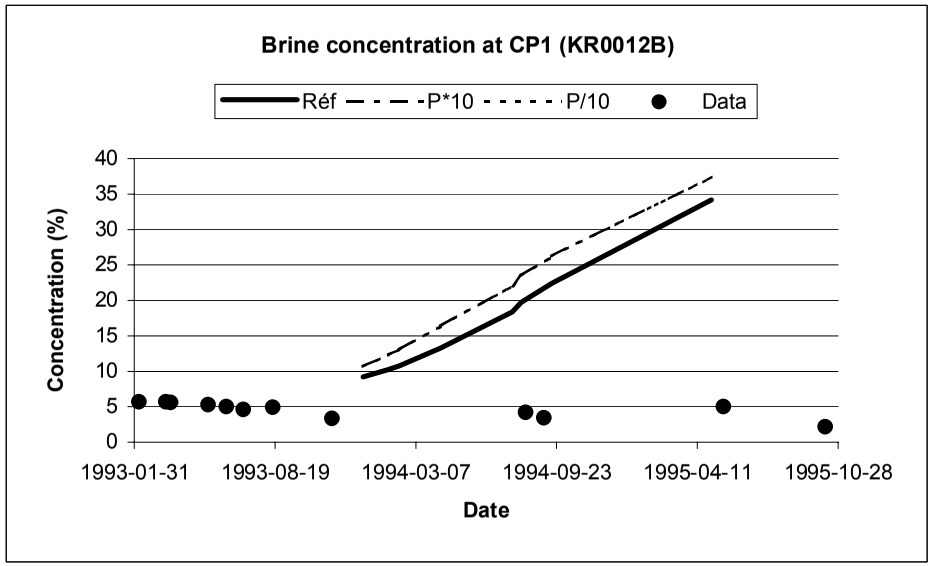

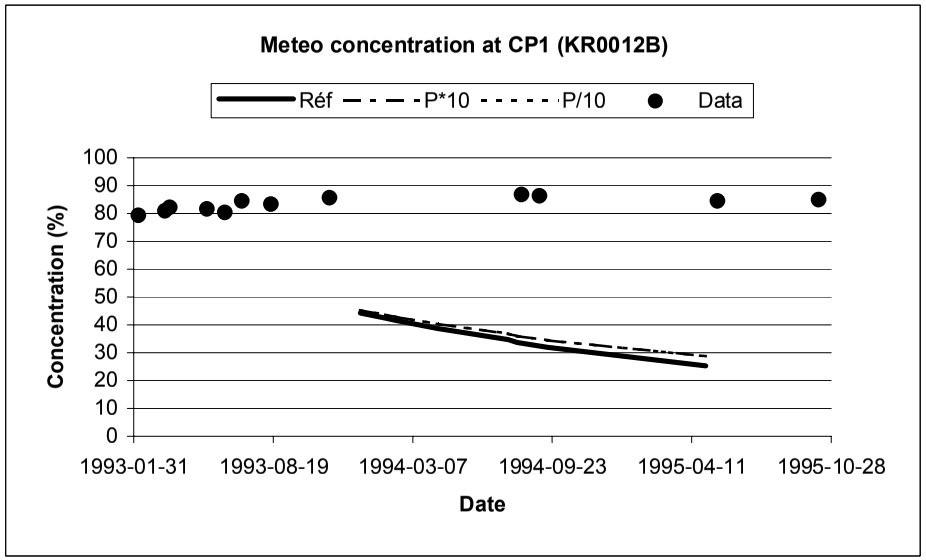

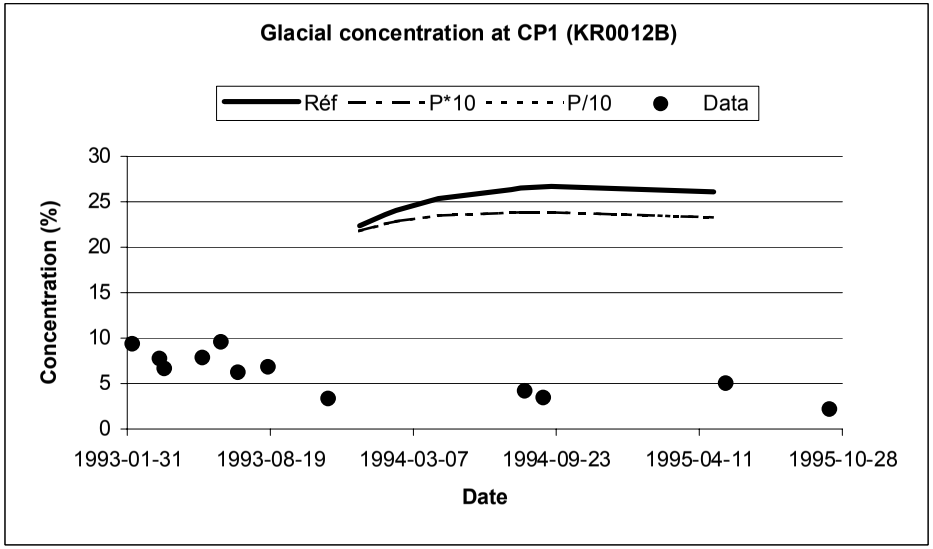

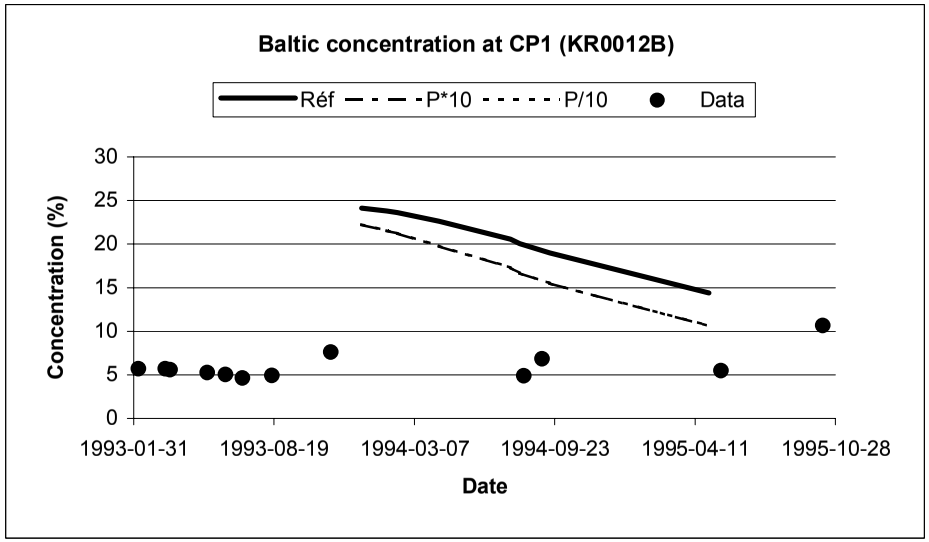

Figure 41 : role of kinematic porosity at CP1

Sensitivity analysis on Pc for NE-2, NNW-7 and NE-4

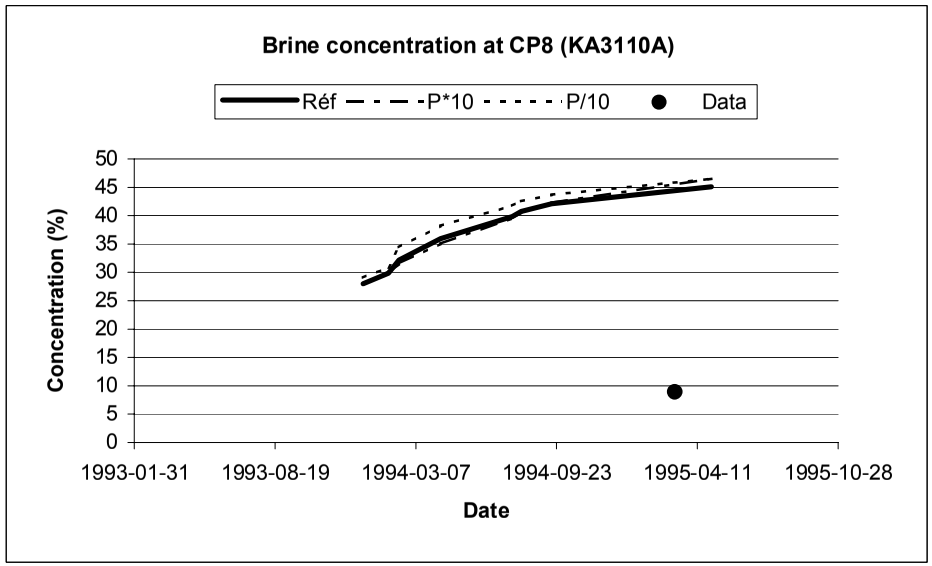

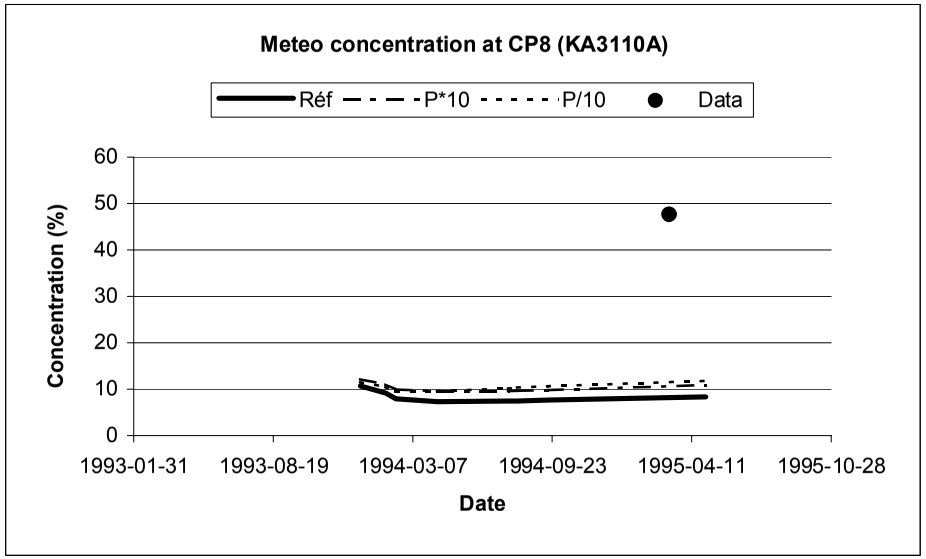

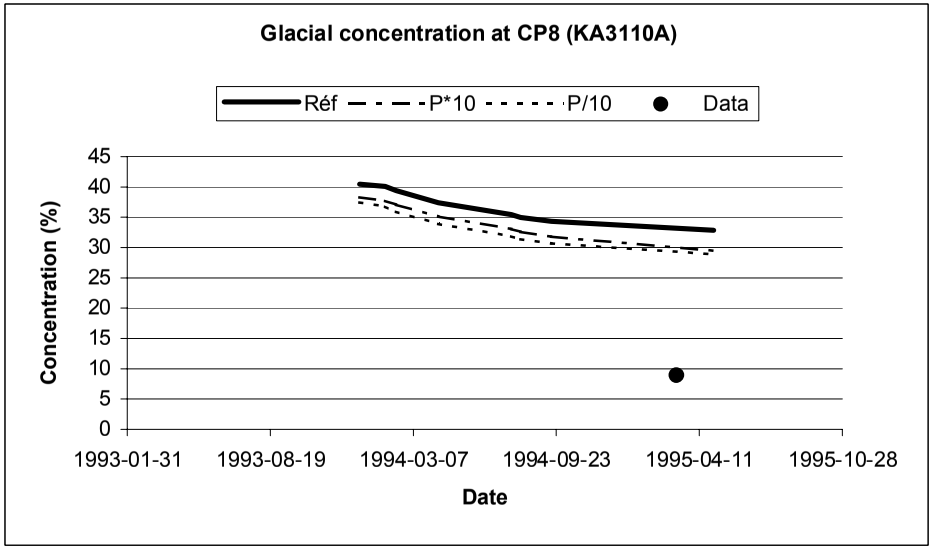

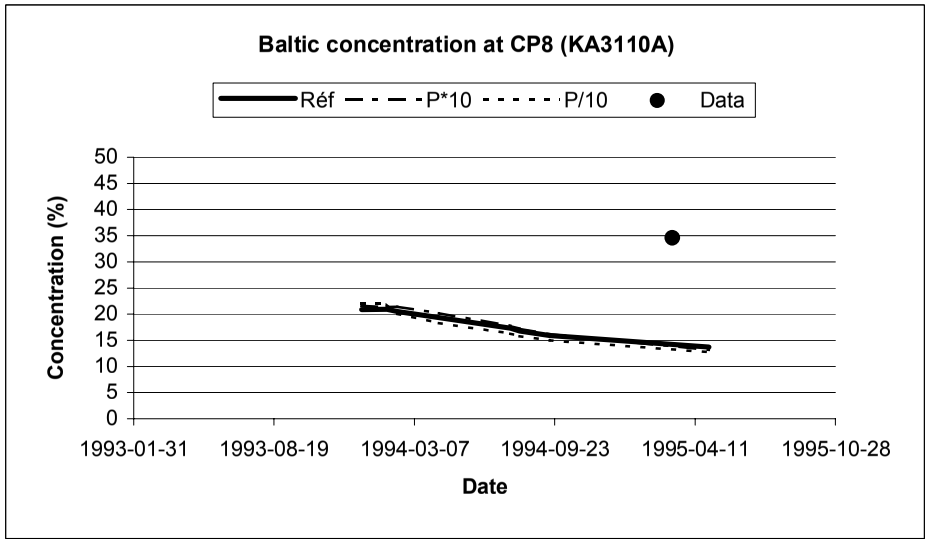

Figure 42 : role of kinematic porosity at CP11

Sensitivity analysis on Pc for NE-2, NNW-7 and NE-4

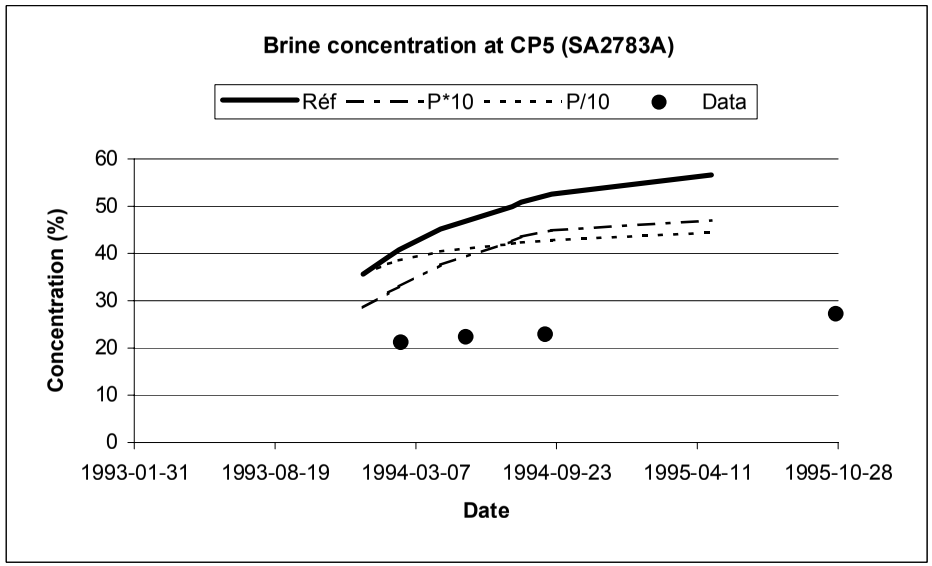

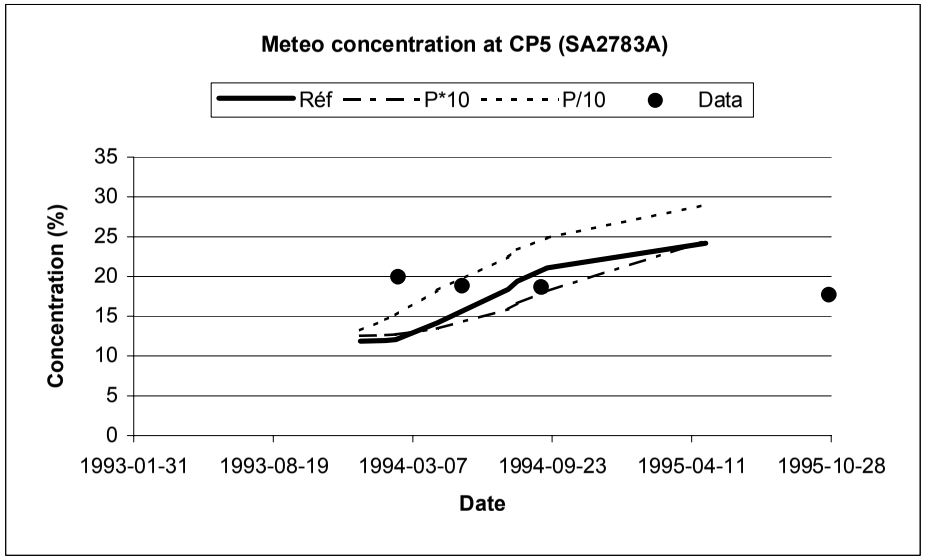

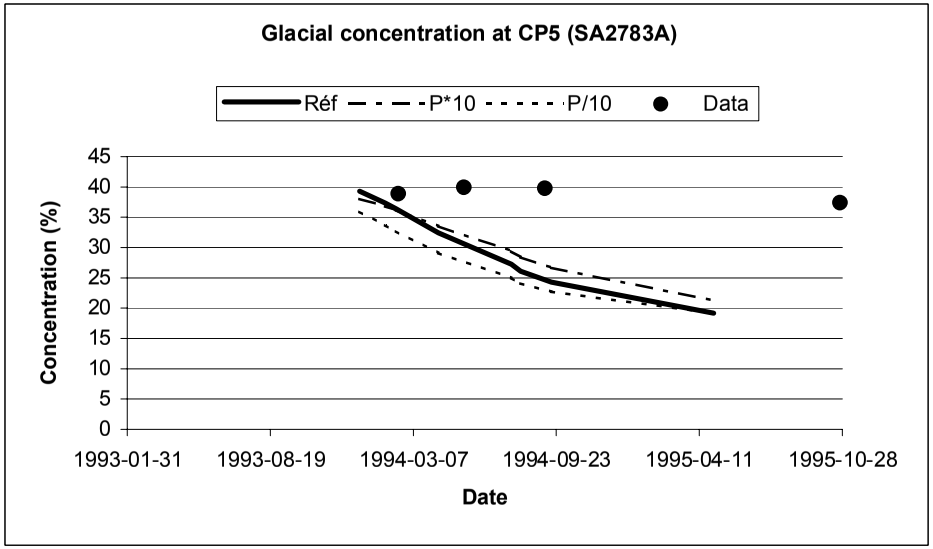

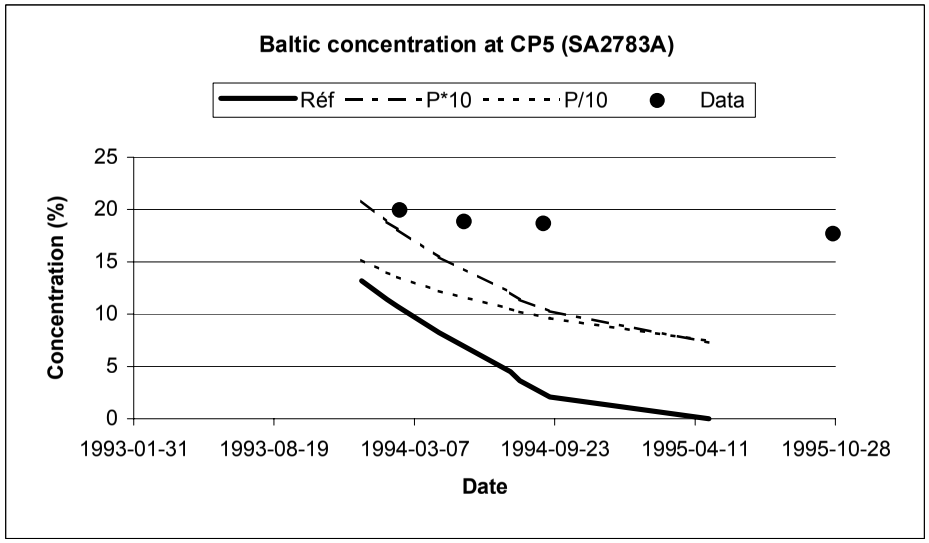

Figure 43 : role of kinematic porosity at CP5

Sensitivity analysis on Ss

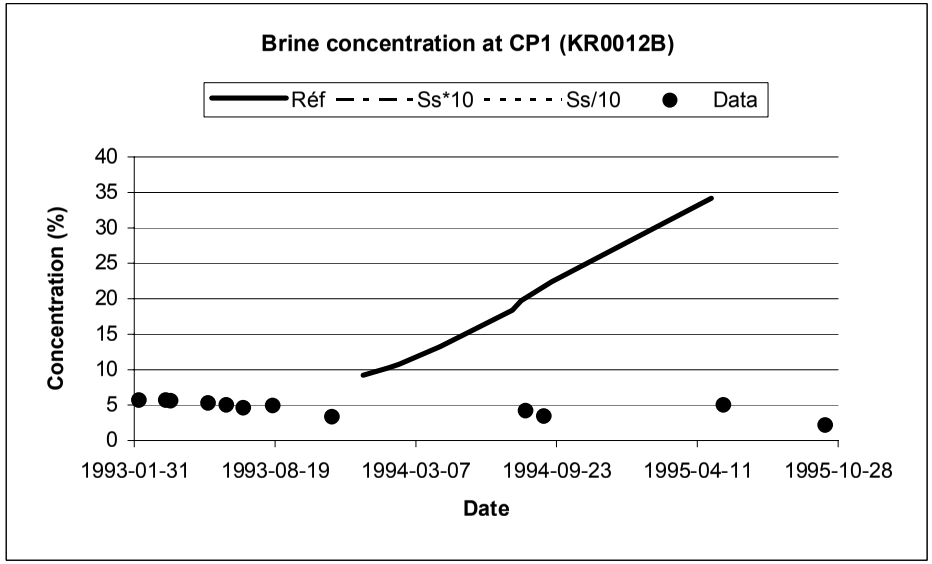

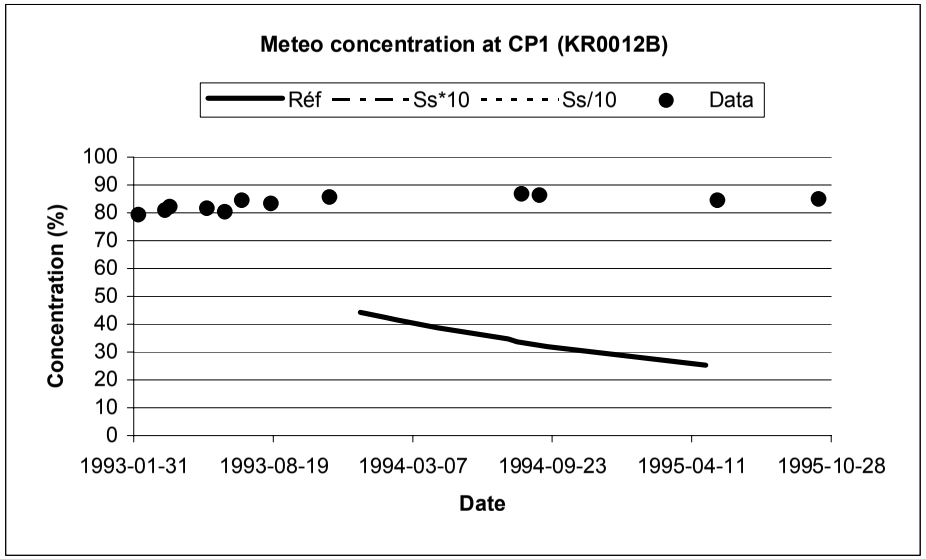

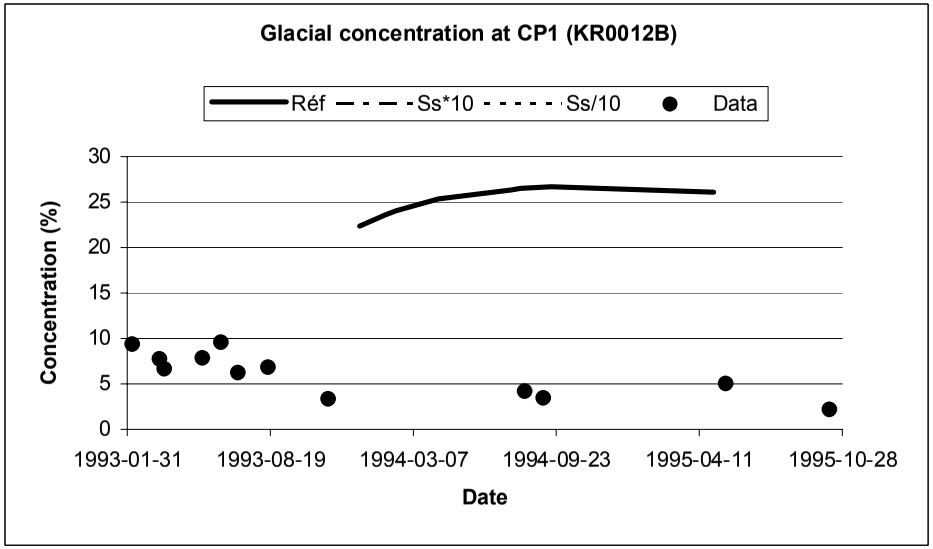

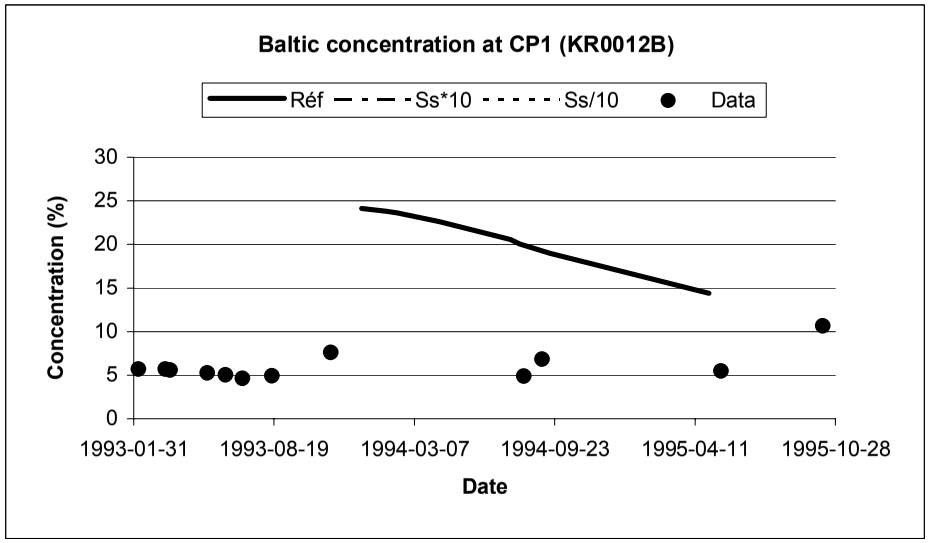

Figure 44 : role of Specific Storage at CP1

Sensitivity analysis on Ss

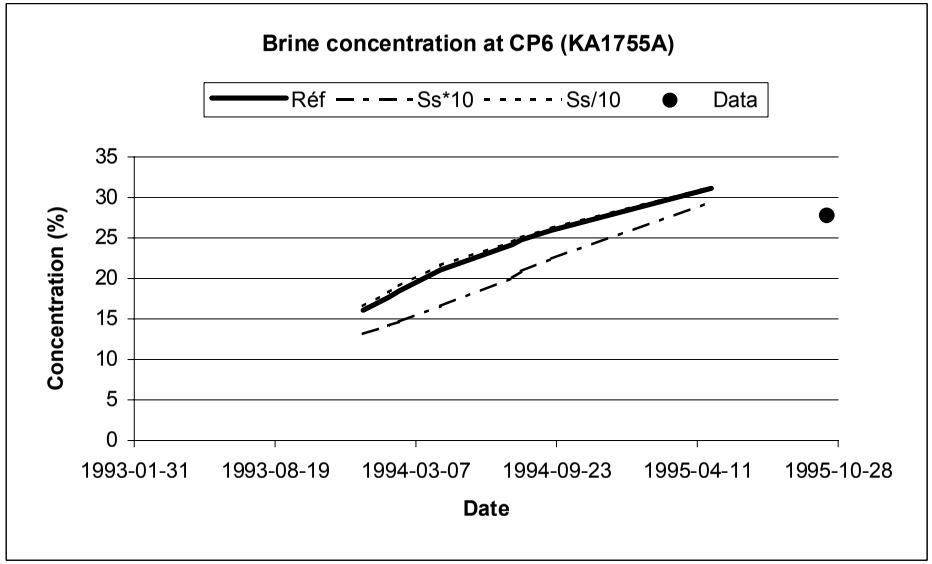

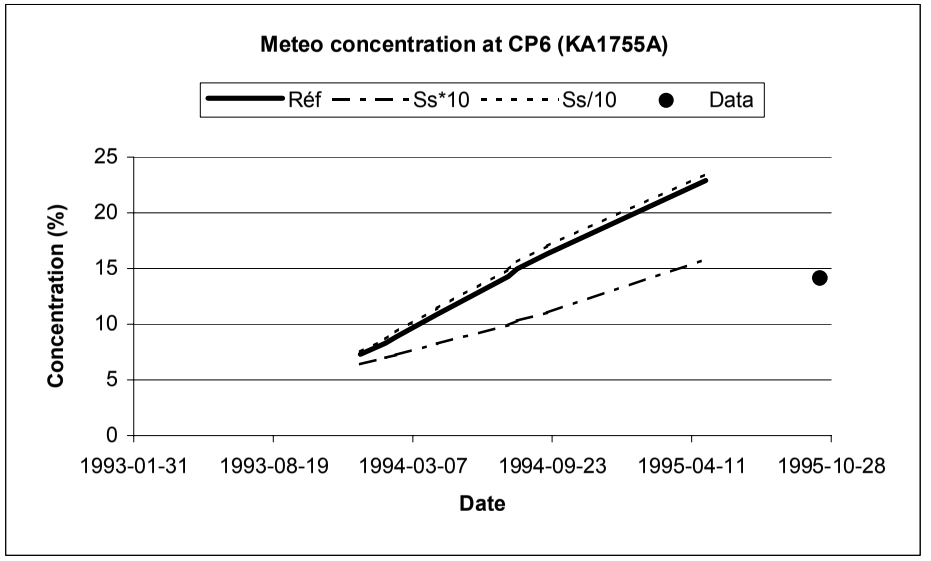

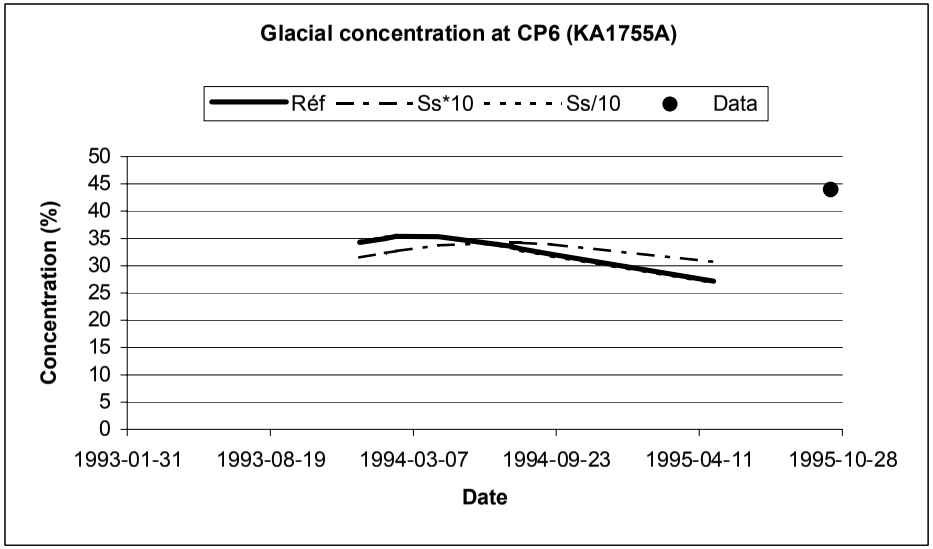

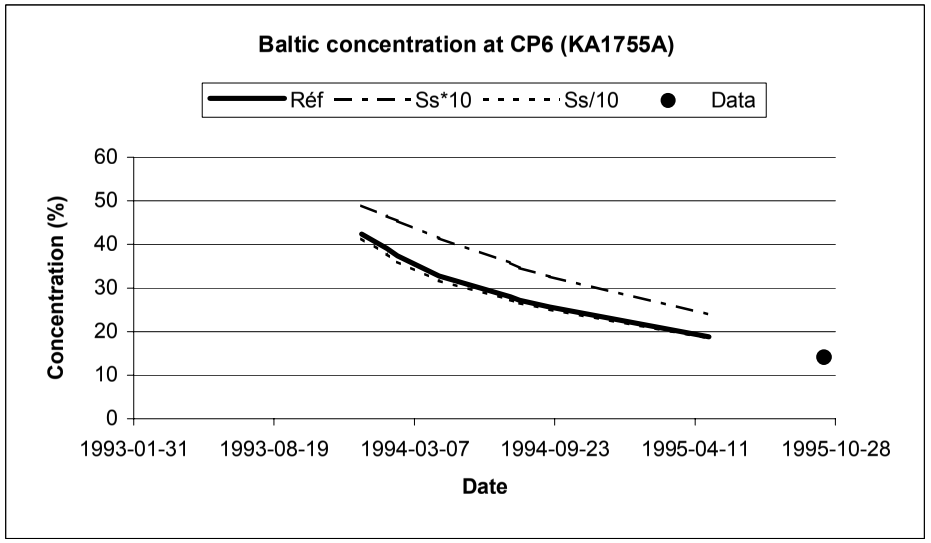

Figure 45 : role of Specific Storage at CP6

Sensitivity analysis on Ss

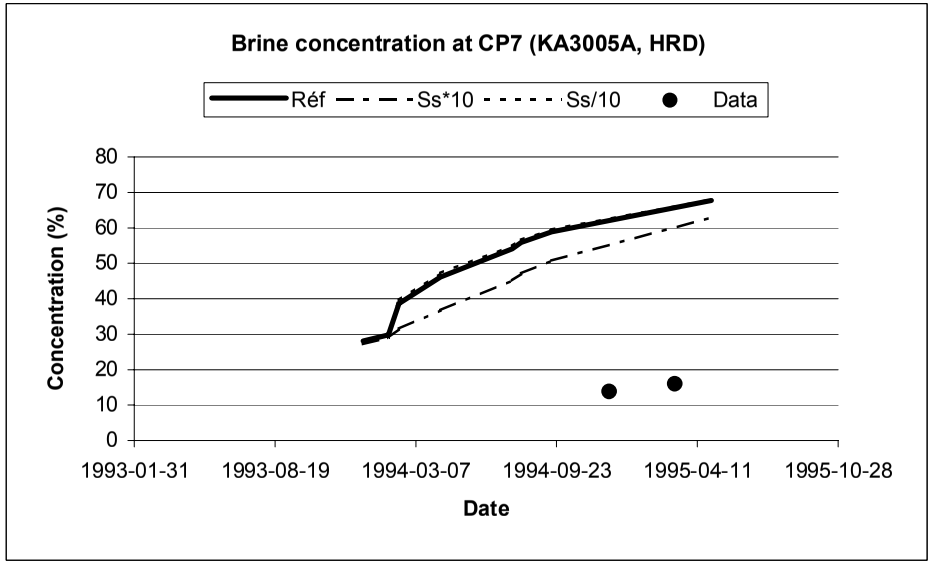

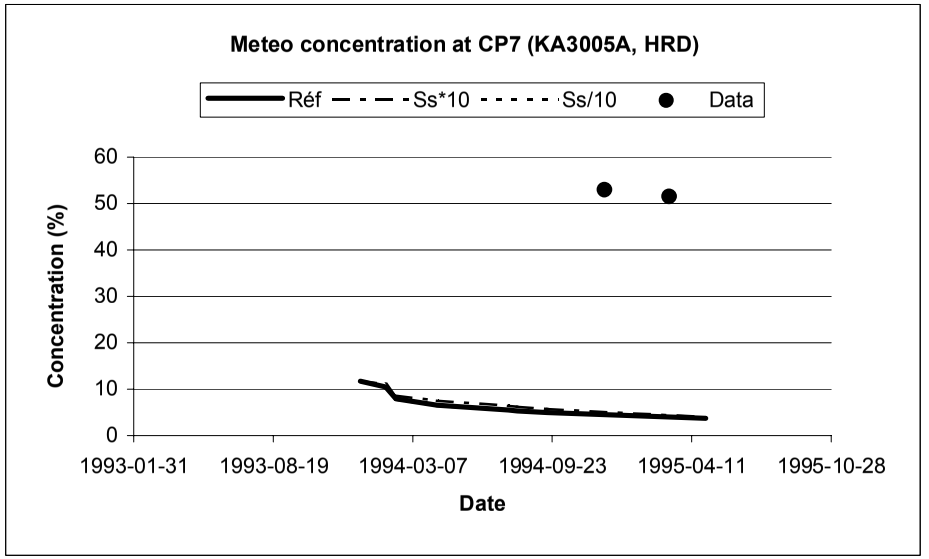

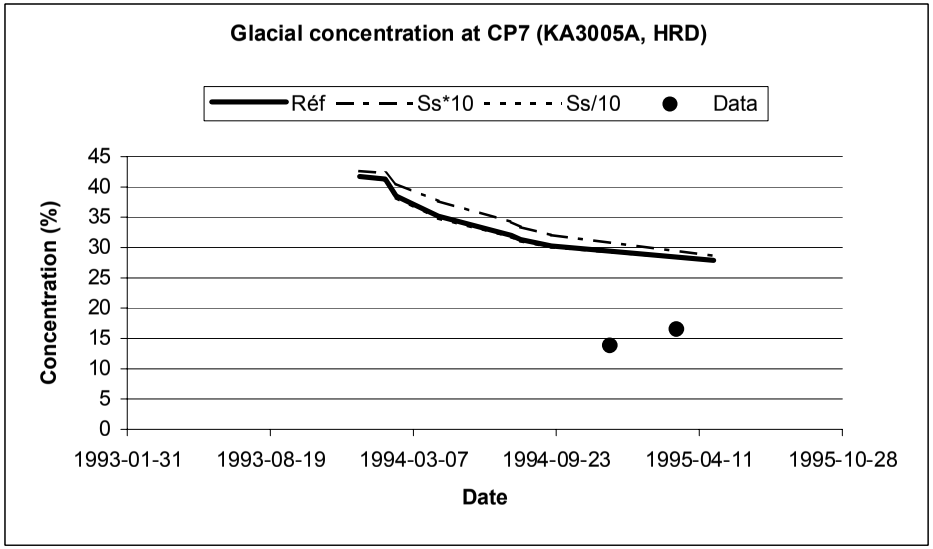

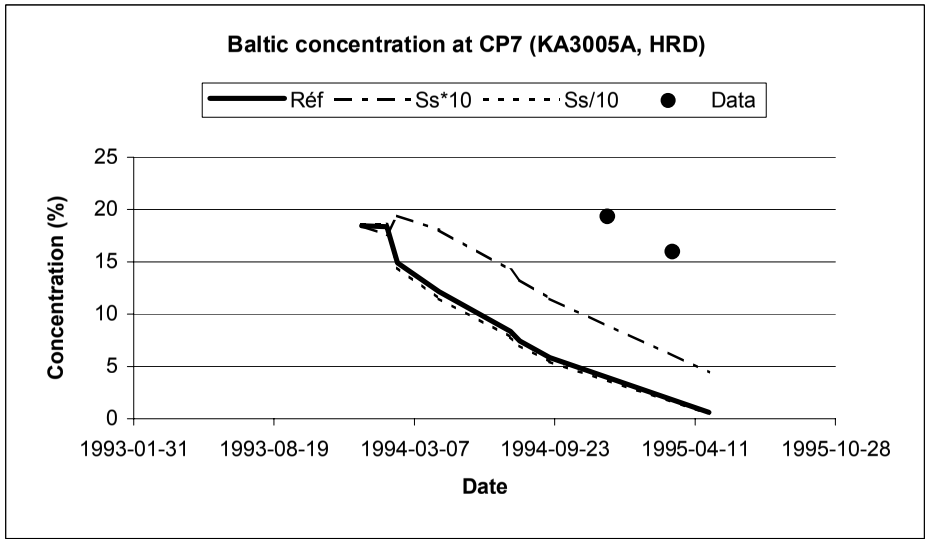

Figure 46 : role of Specific Storage at CP7

Sensitivity analysis on Dispersivity

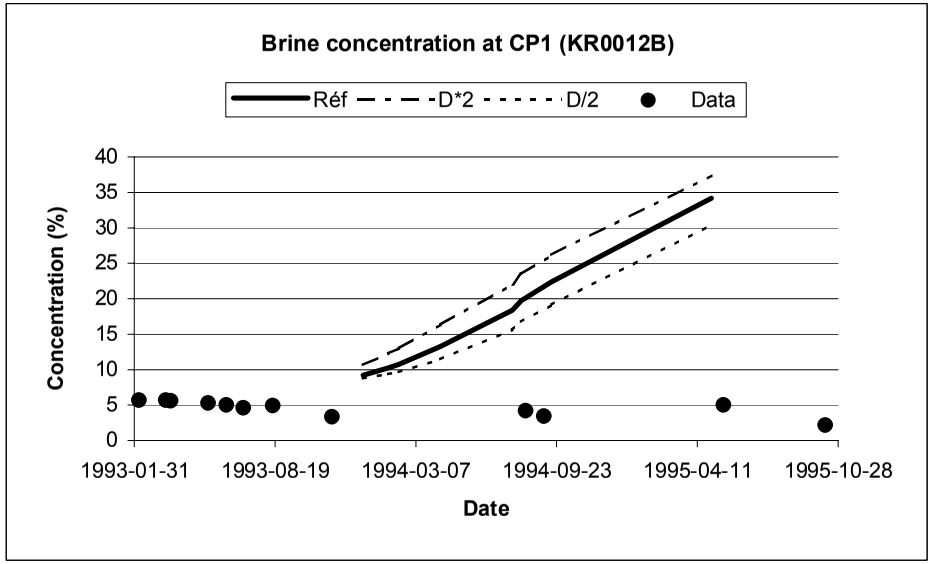

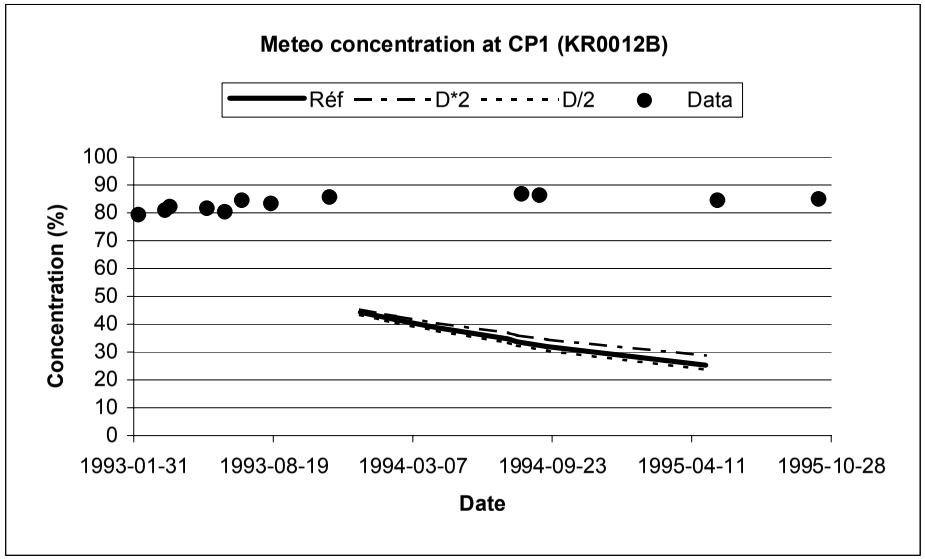

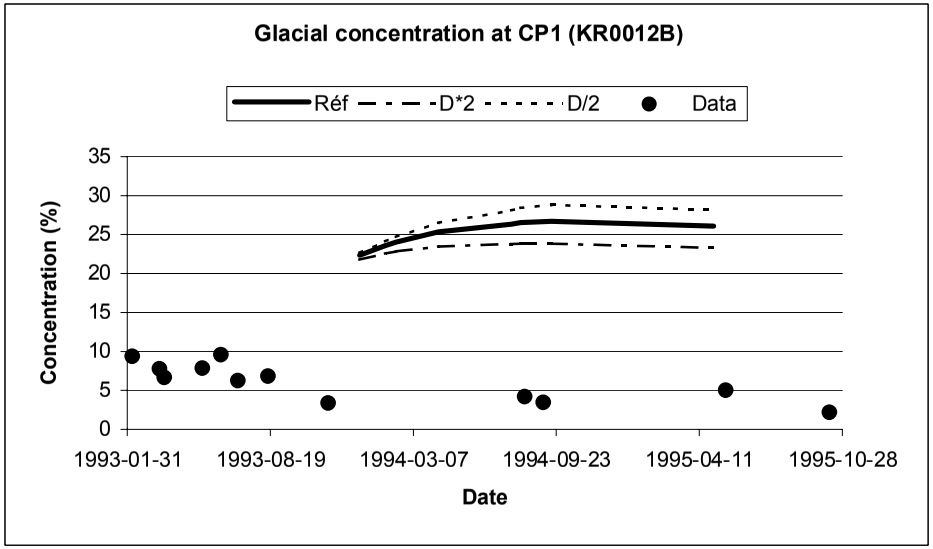

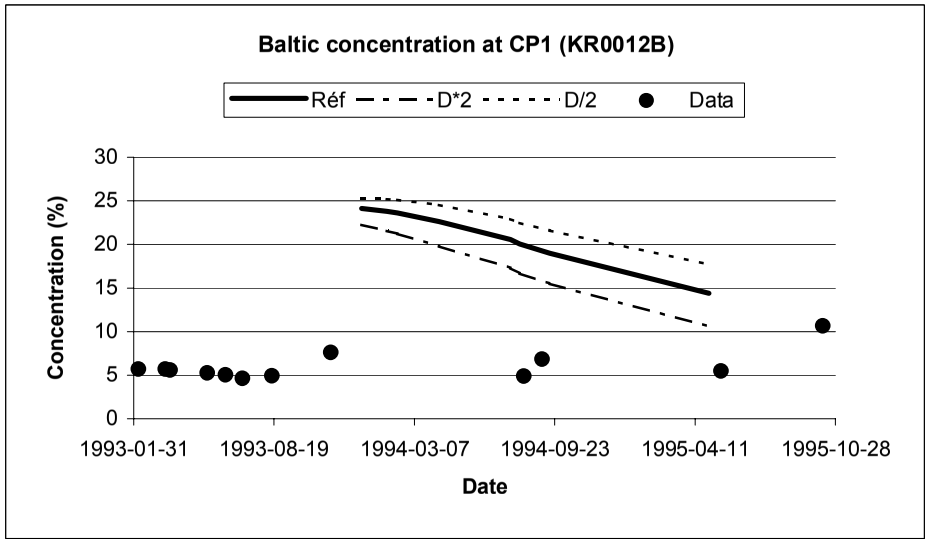

Figure 47 : role of Dispersivity at CP1

Sensitivity analysis on Dispersivity

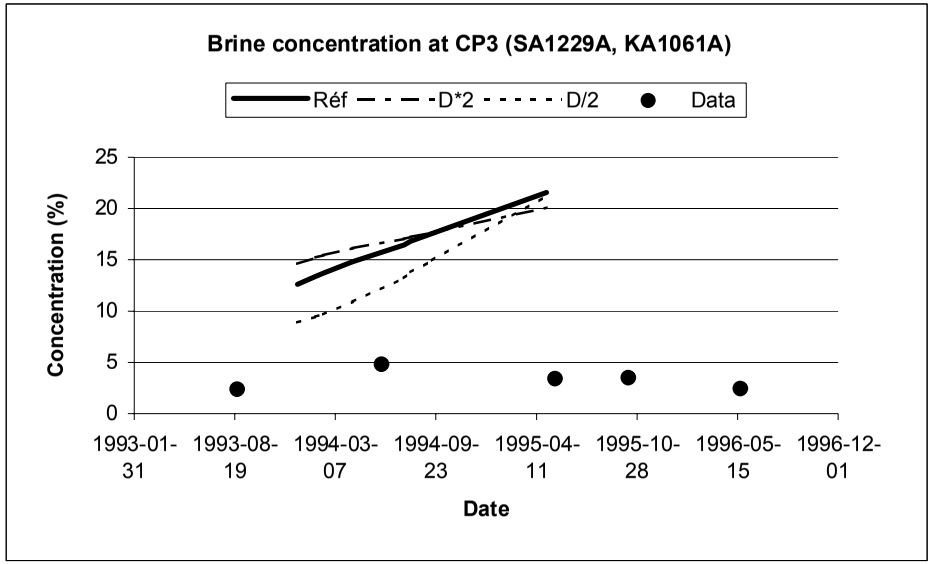

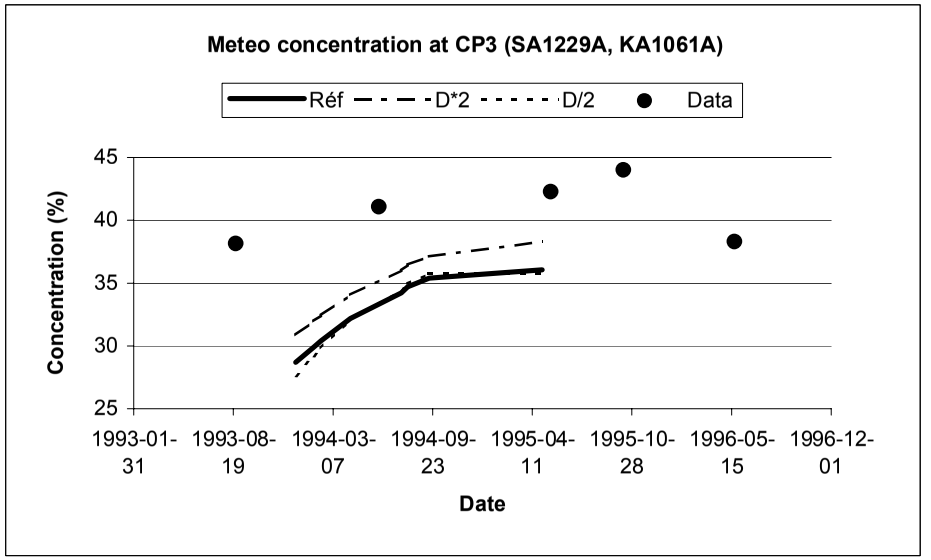

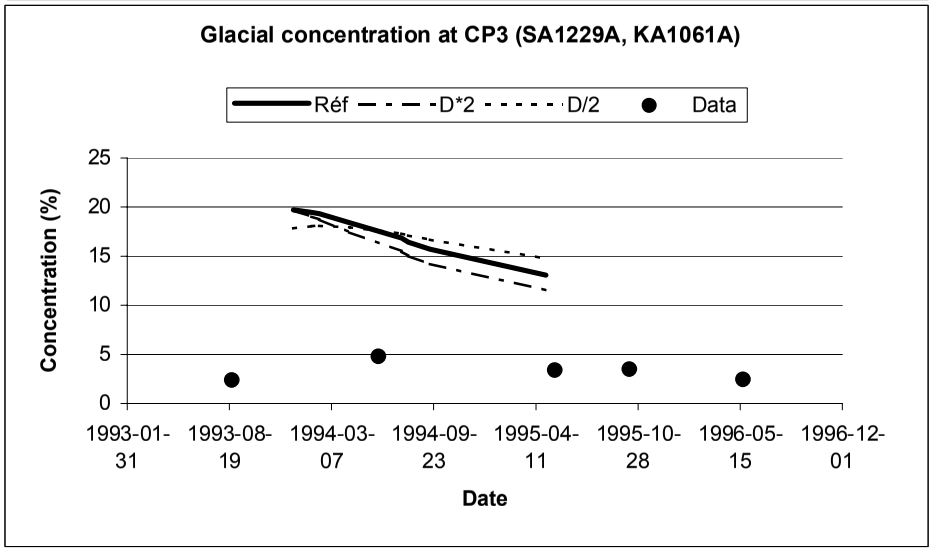

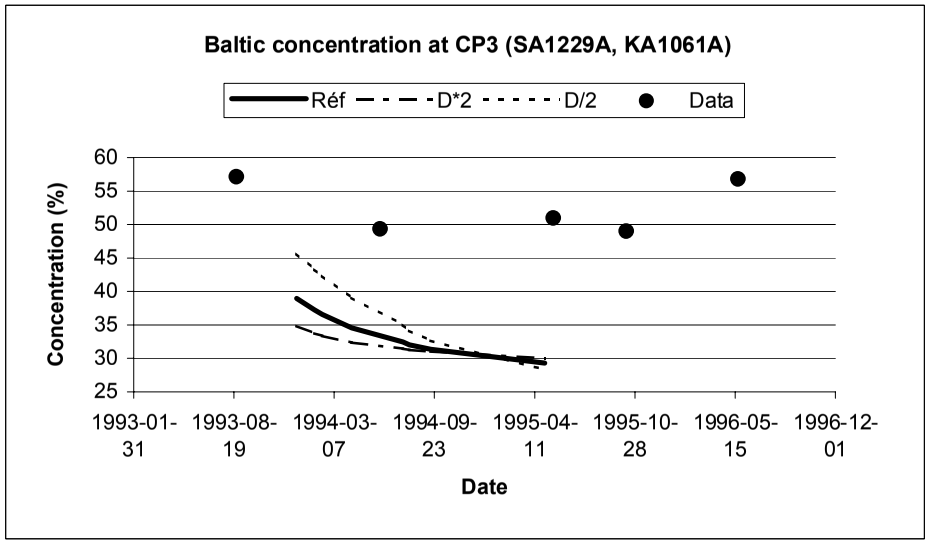

Figure 48 : role of Dispersivity at CP3

Sensitivity analysis on Dispersivity

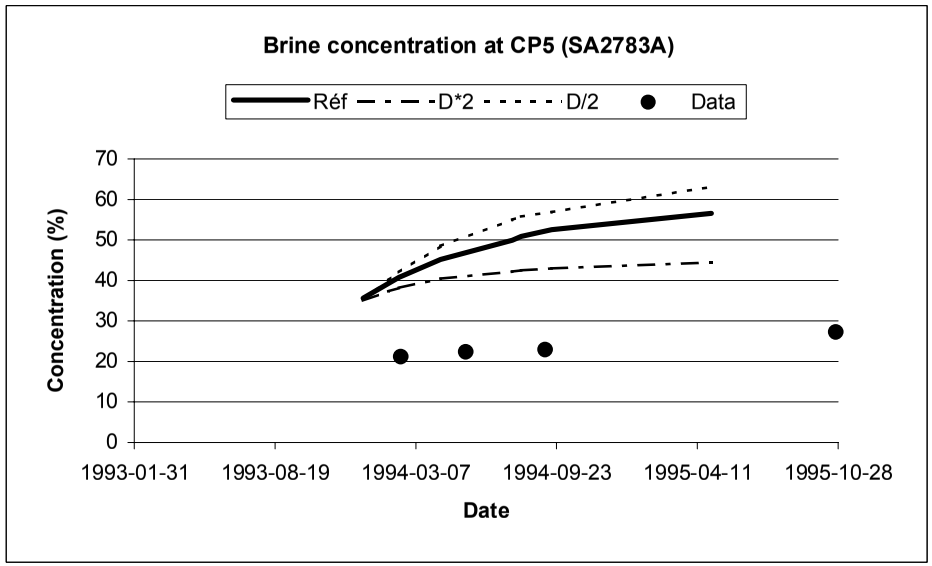

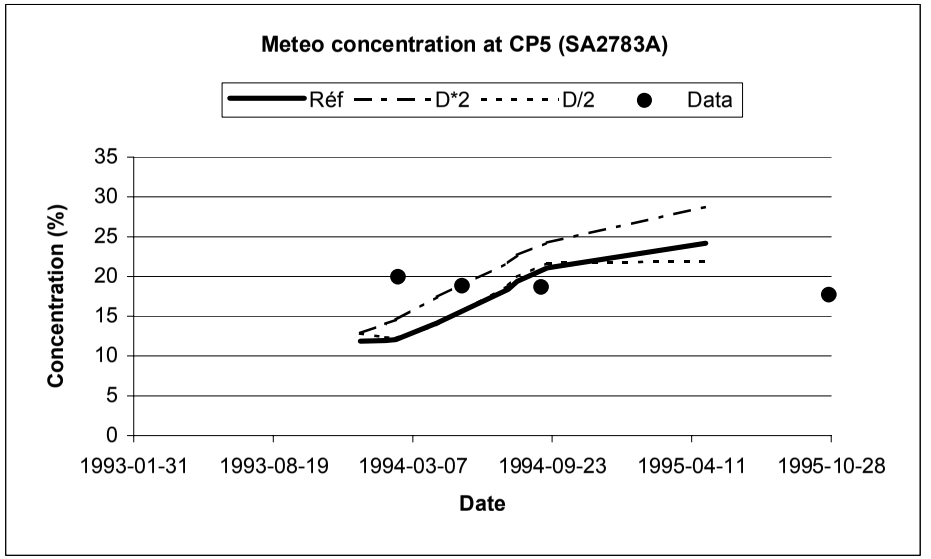

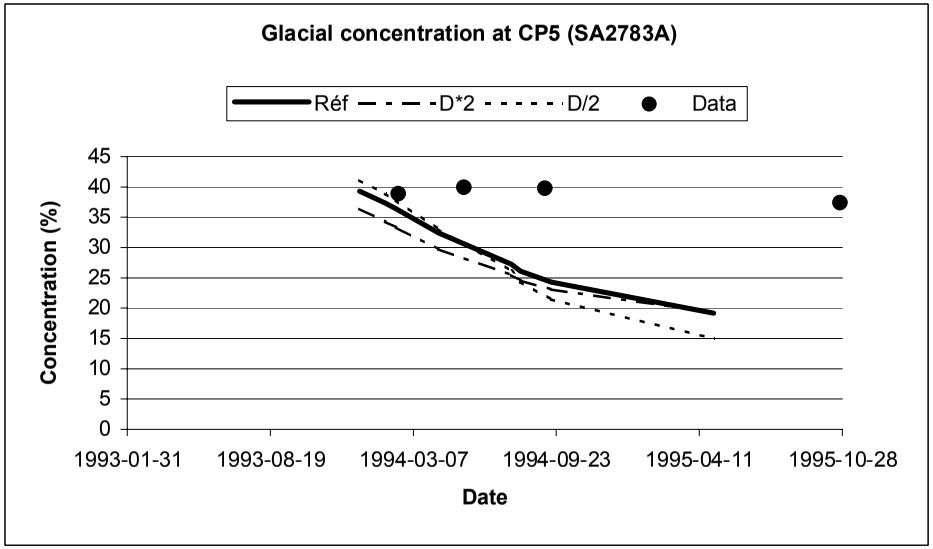

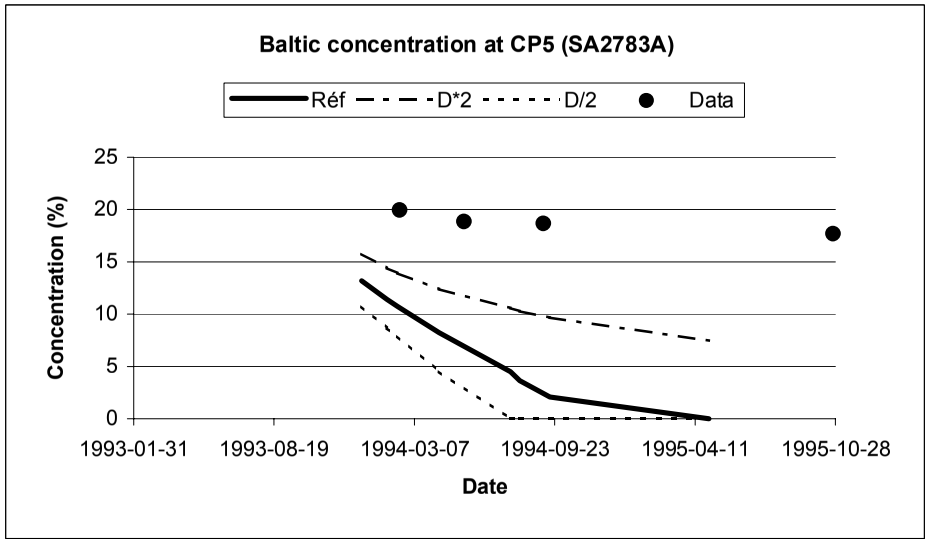

Figure 49 : role of Dispersivity at CP5

Sensitivity analysis on Dispersivity

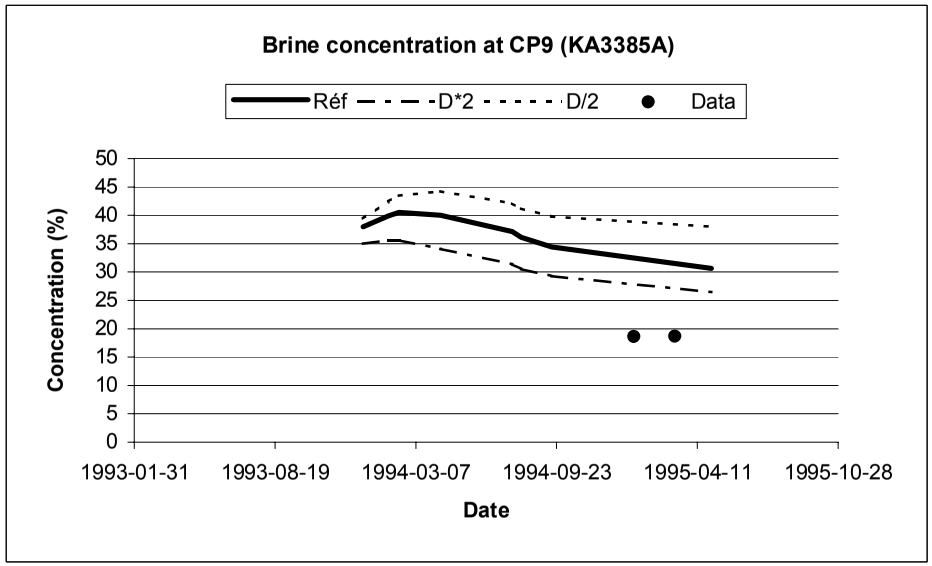

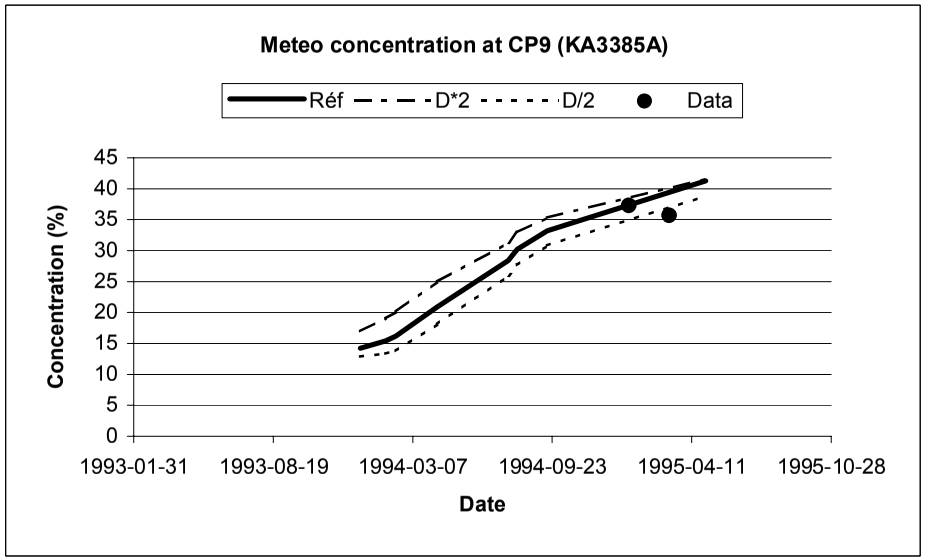

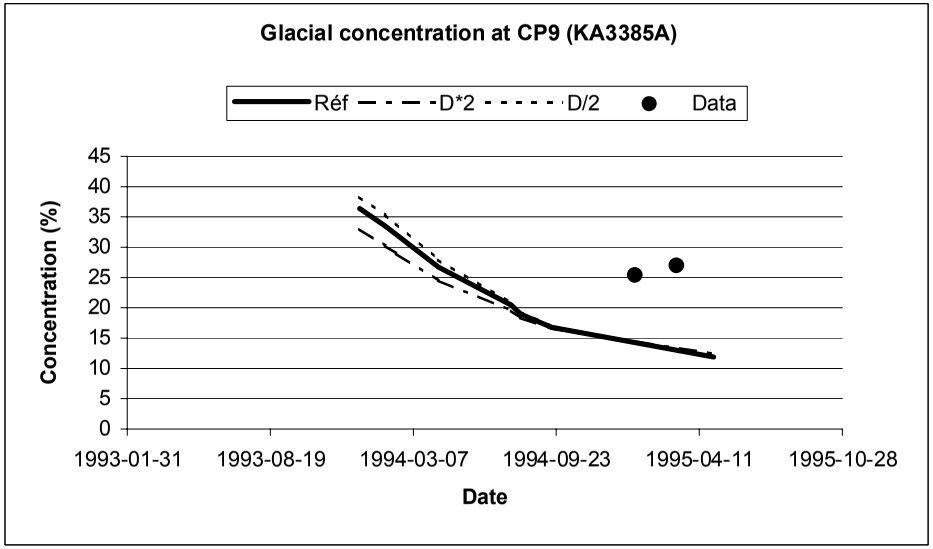

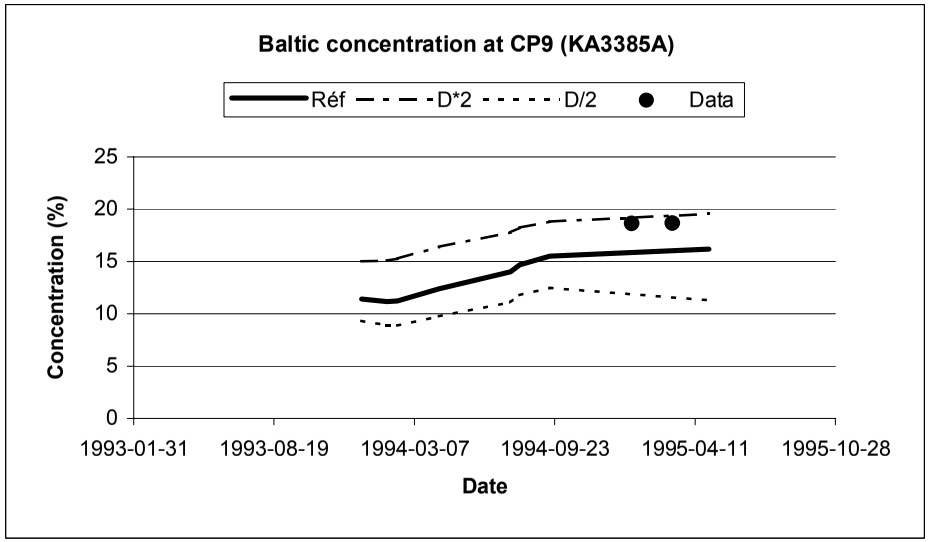

Figure 50 : role of Dispersivity at CP9

optimised results using hydraulic and concentration data

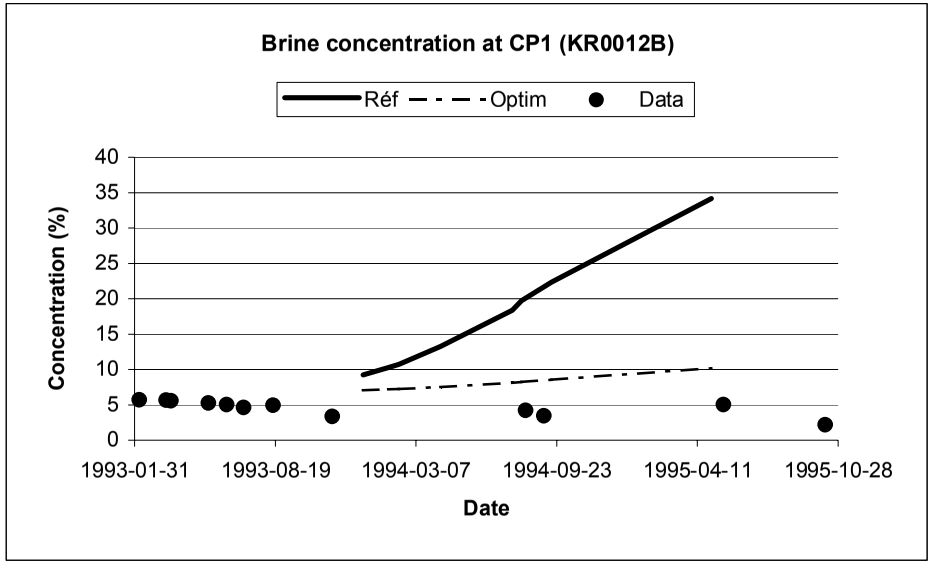

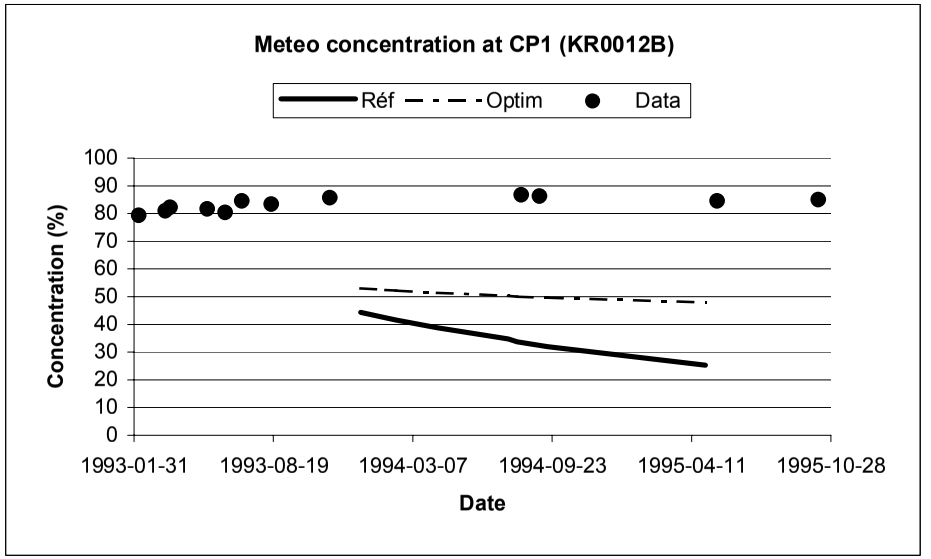

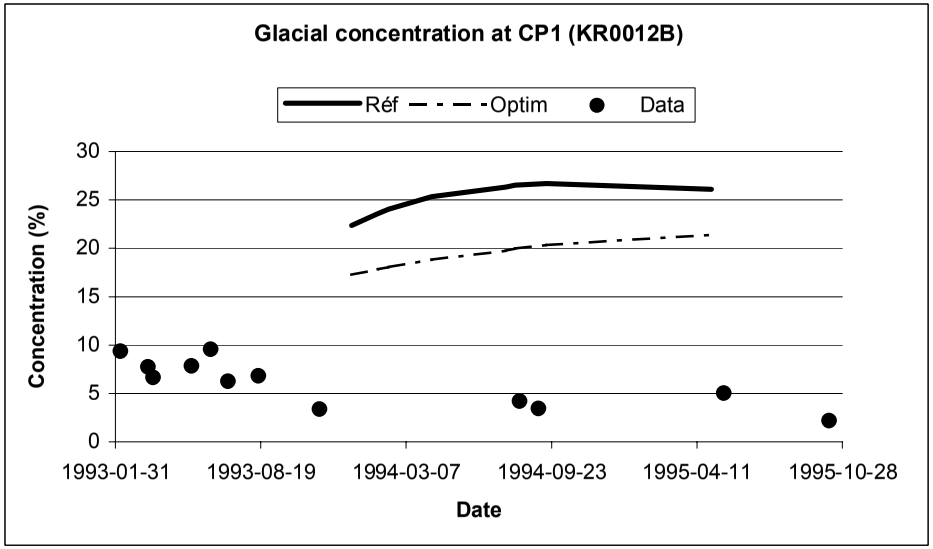

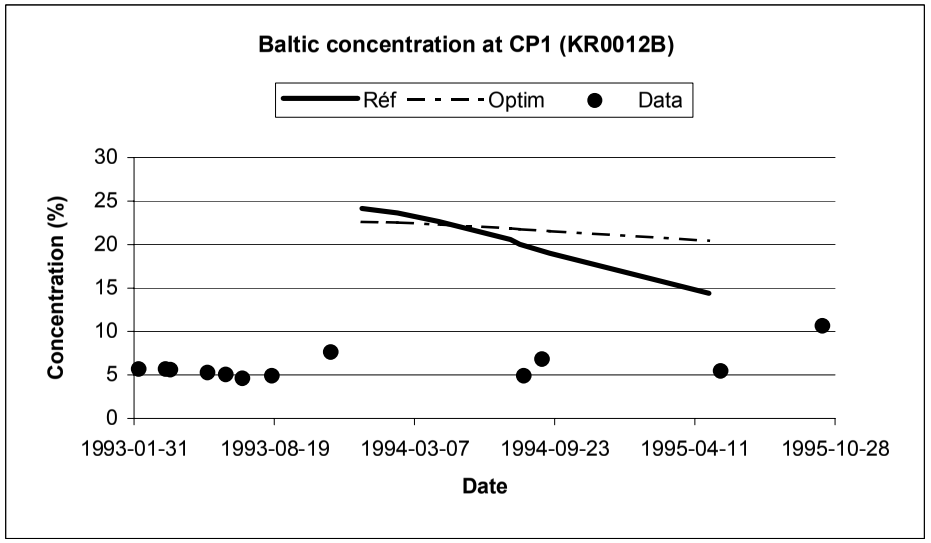

Figure 51 : Best results at CP1

optimised results using hydraulic and concentration data

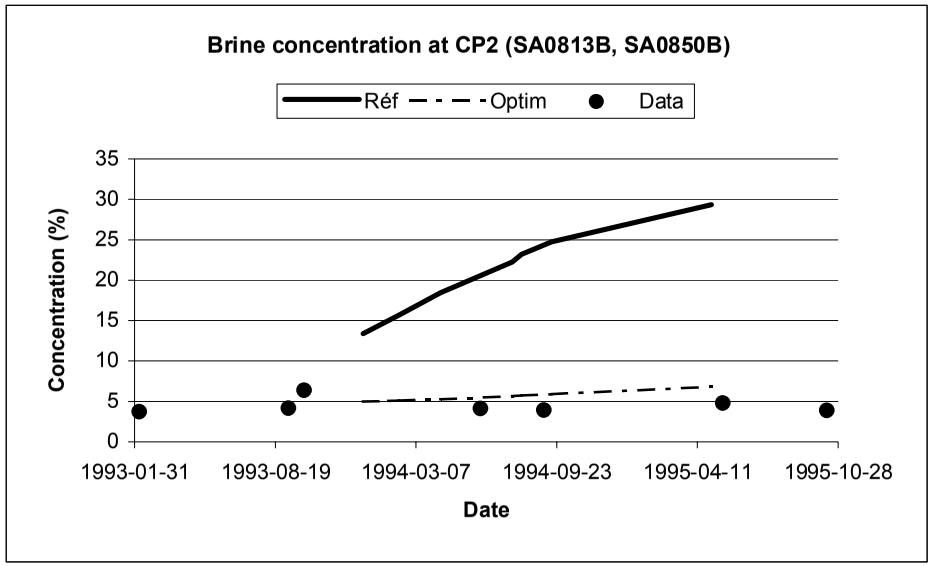

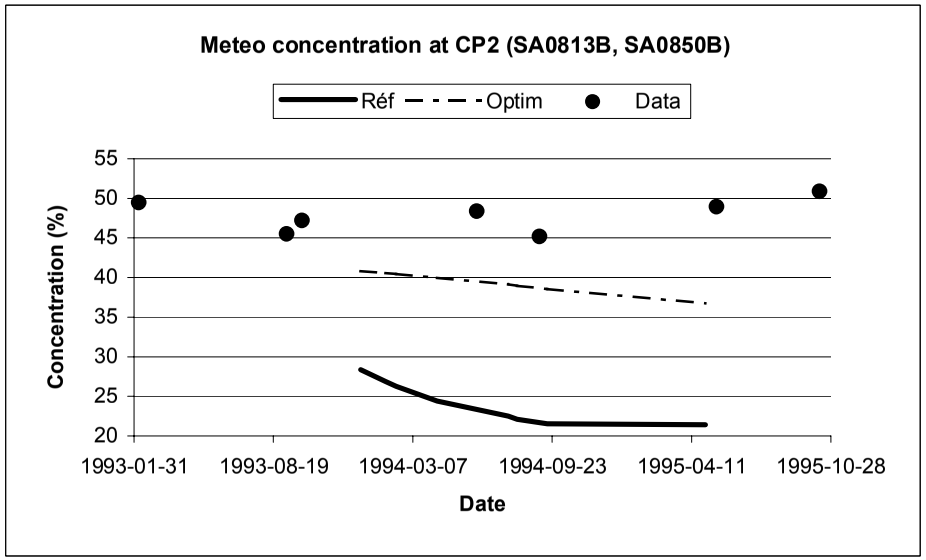

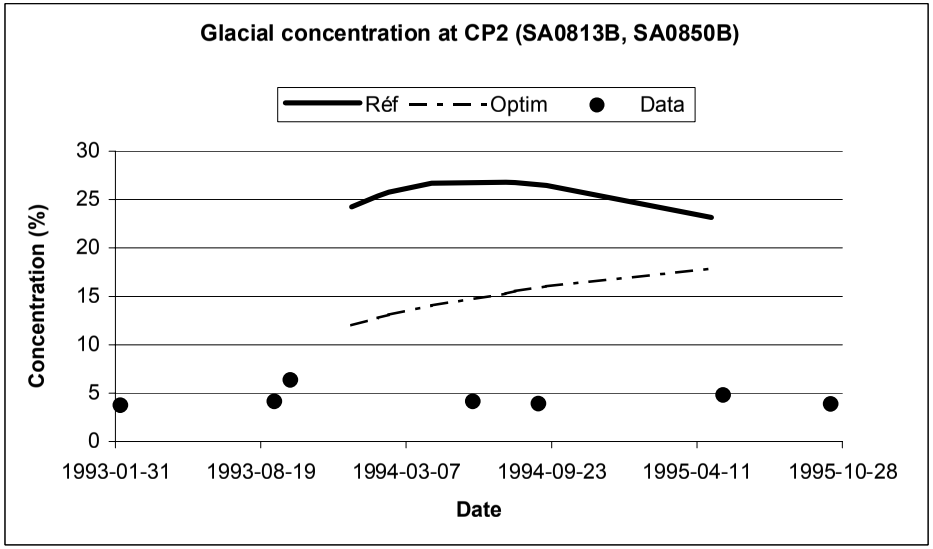

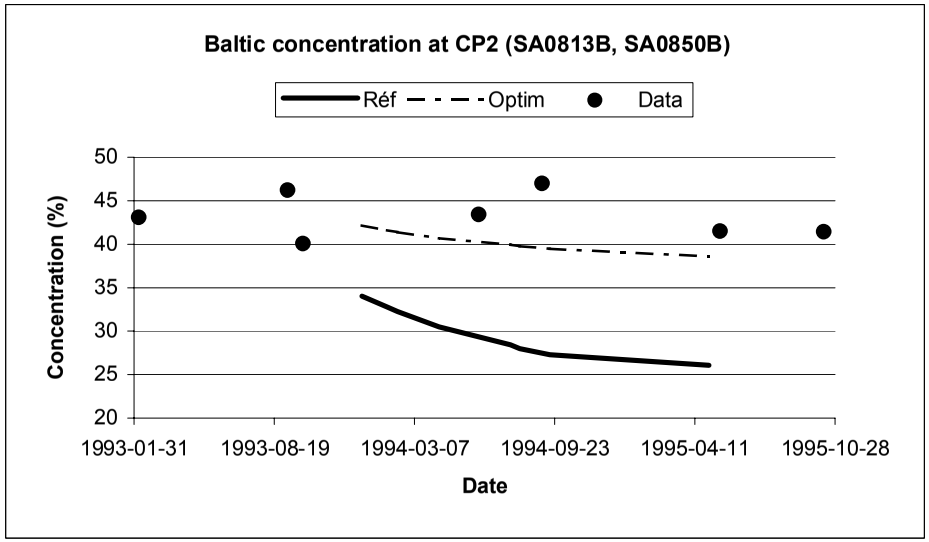

Figure 52 : Best results at CP2

optimised results using hydraulic and concentration data

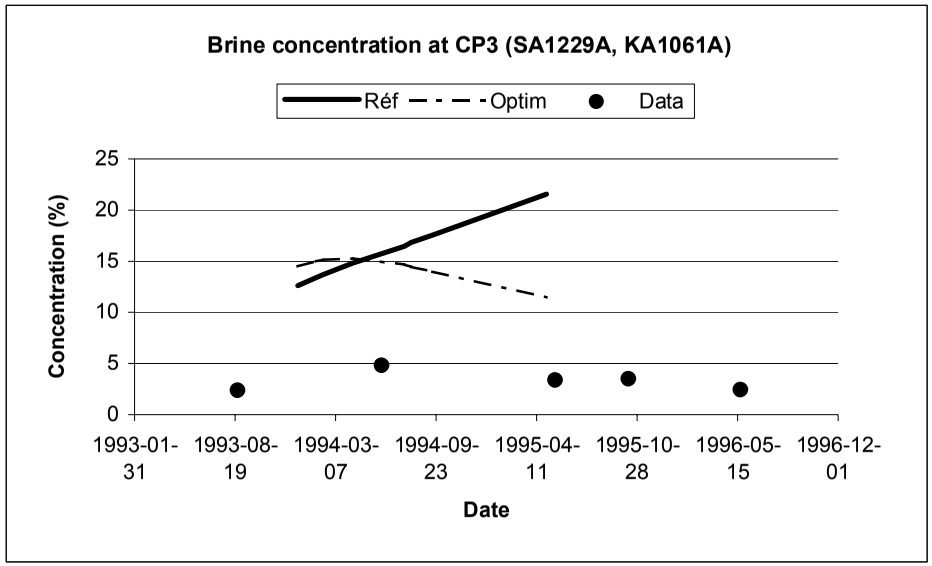

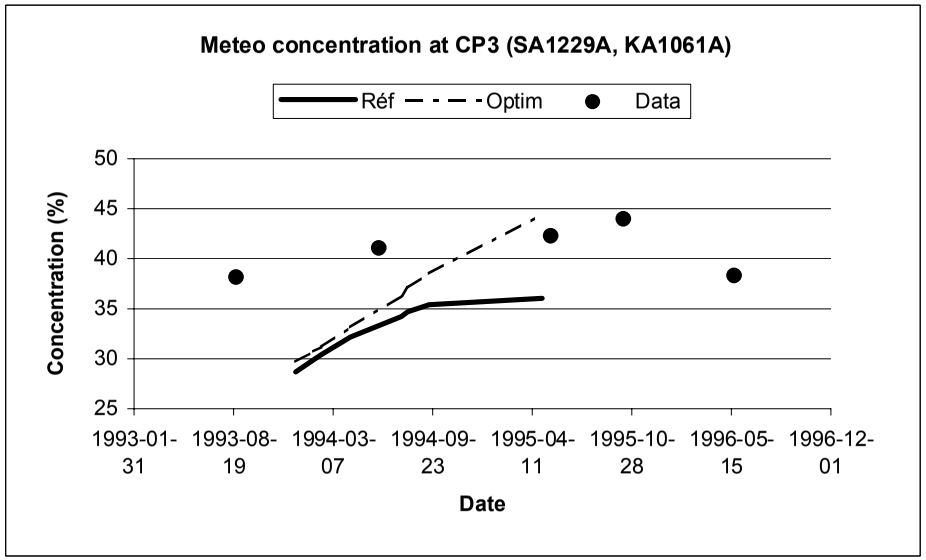

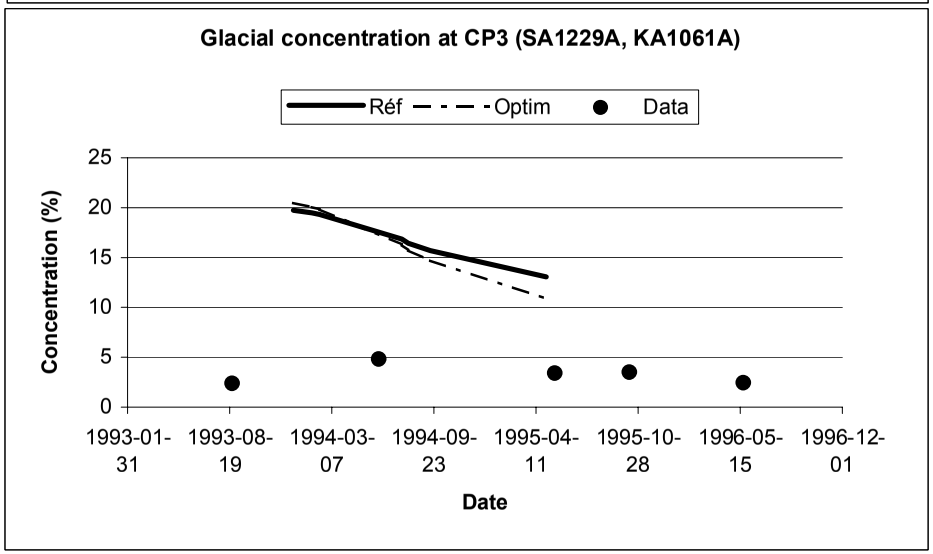

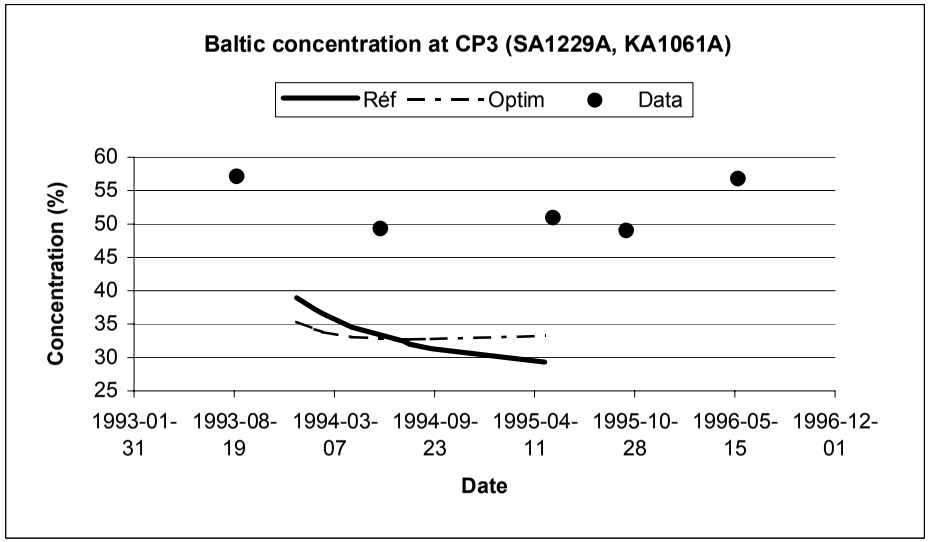

Figure 53 : Best results at CP3-1

optimised results using hydraulic and concentration data

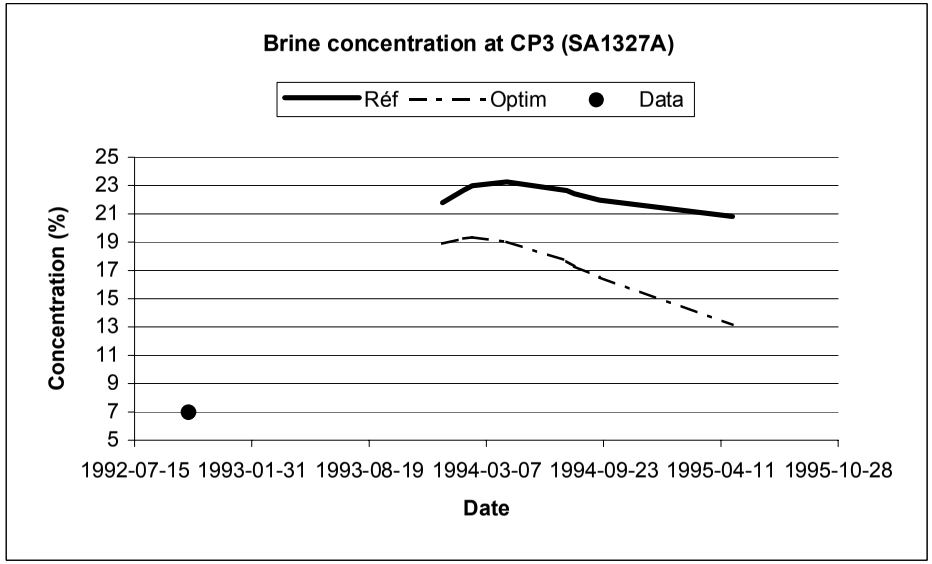

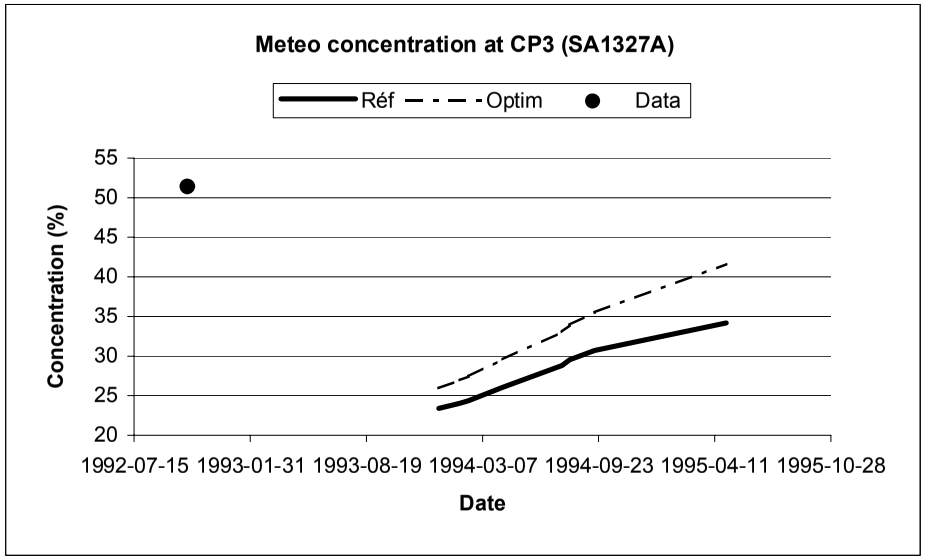

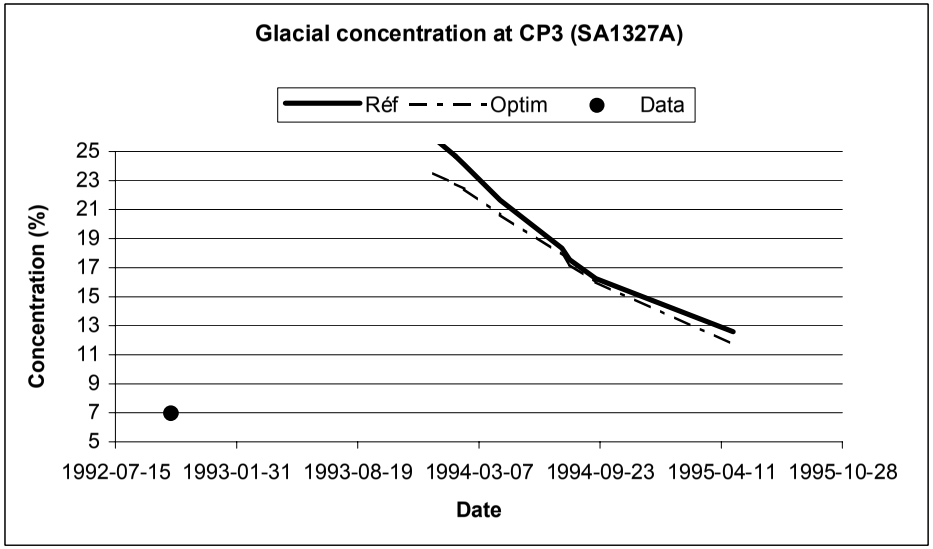

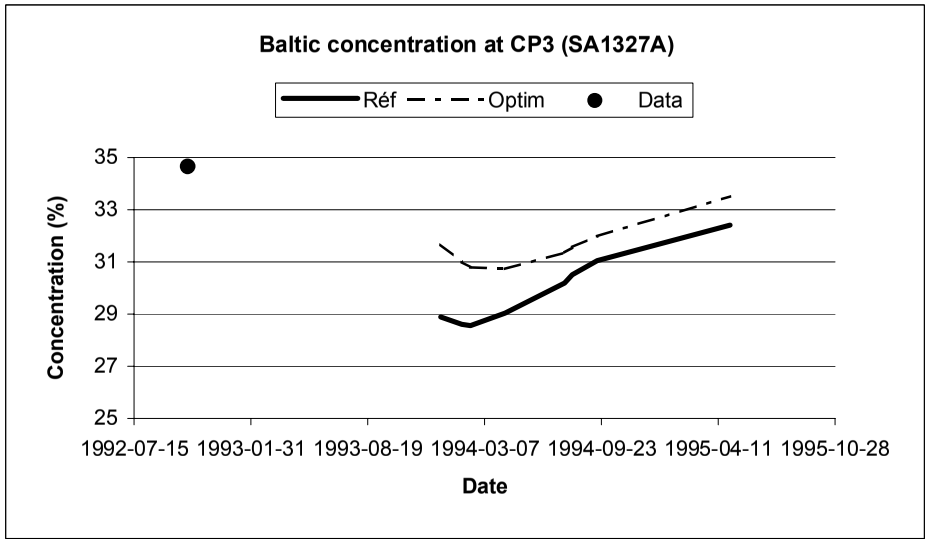

Figure 54 : Best results at CP3-2

Optimised results using hydraulic and concentration data

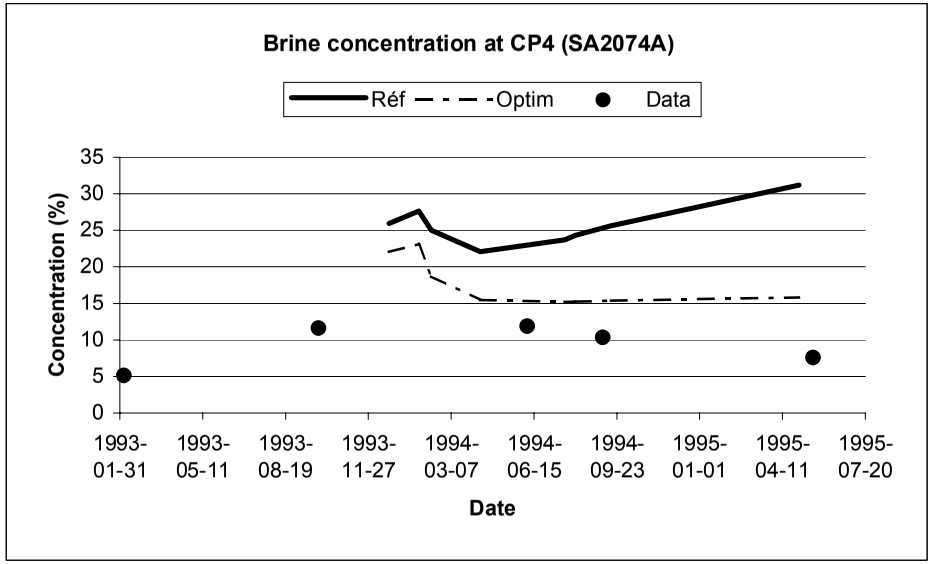

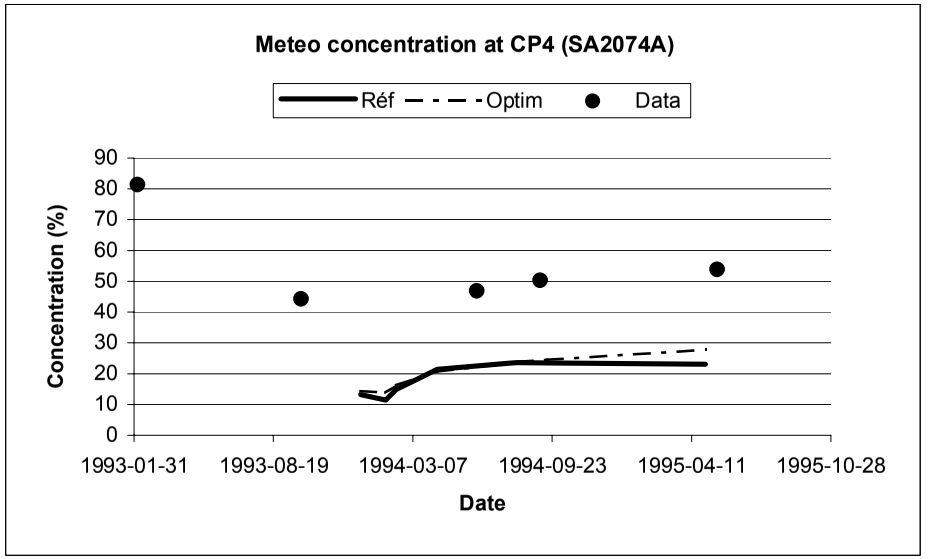

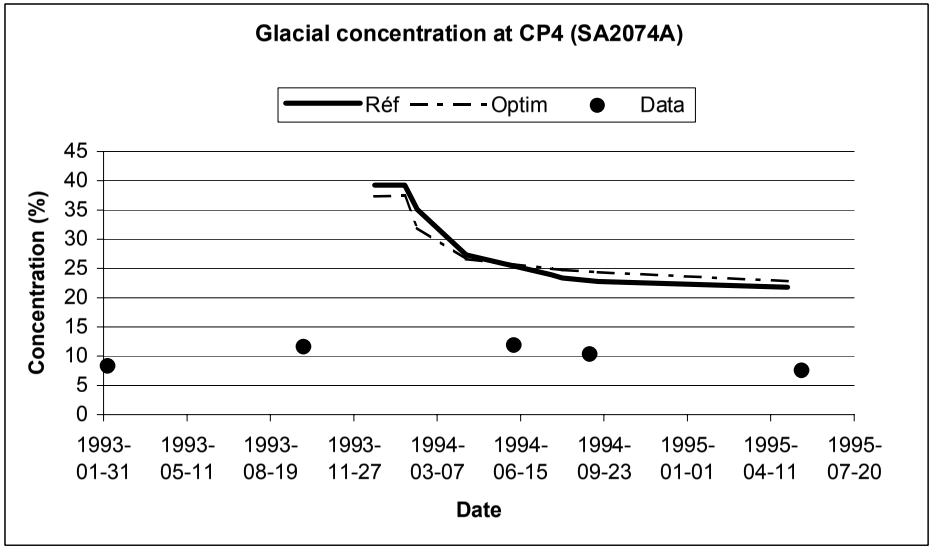

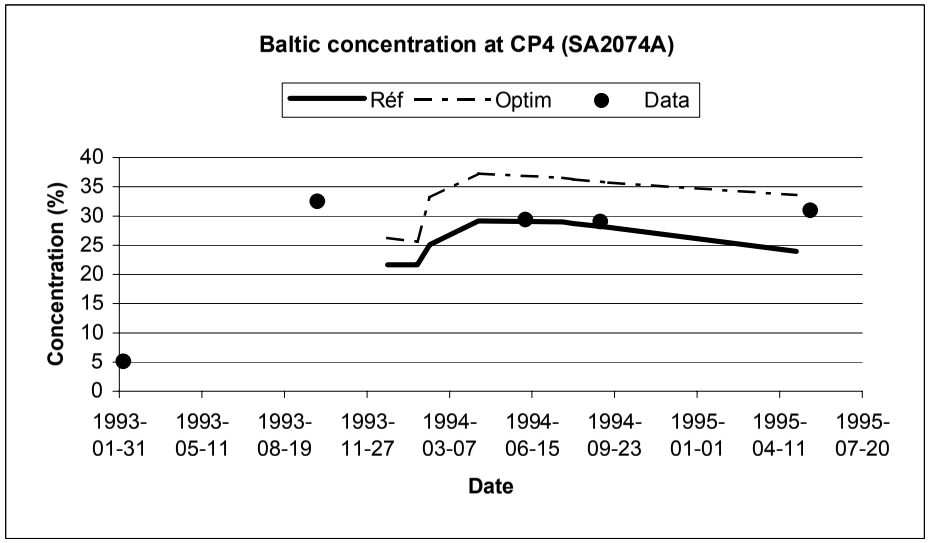

Figure 55 : Best results at CP4

optimised results using hydraulic and concentration data

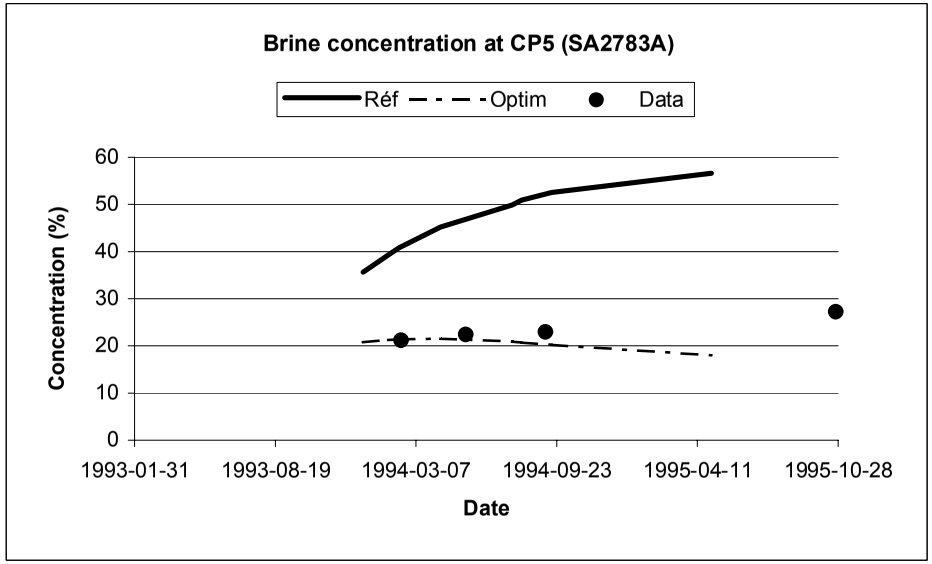

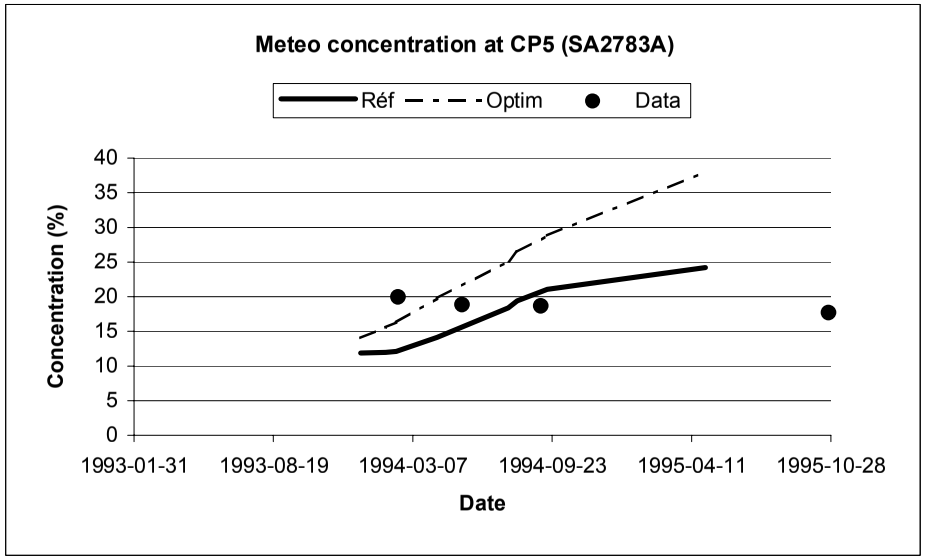

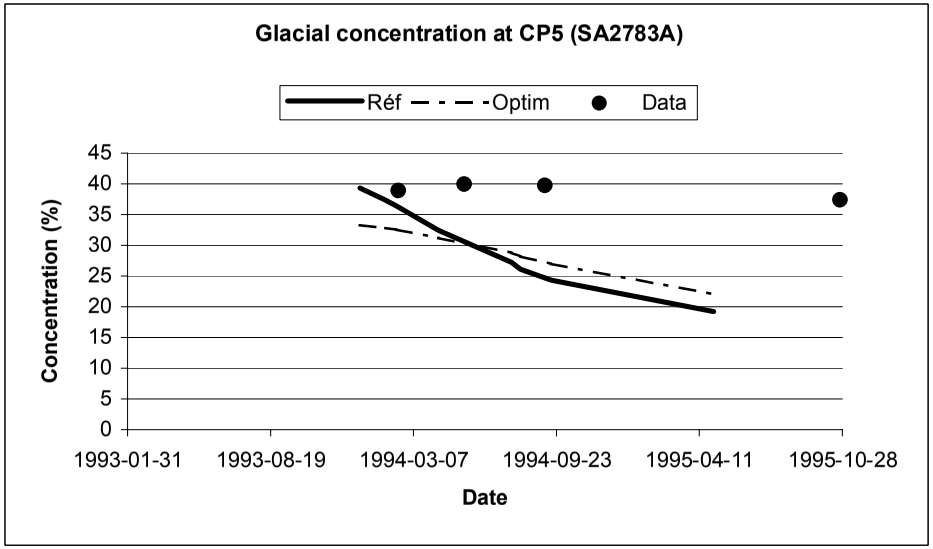

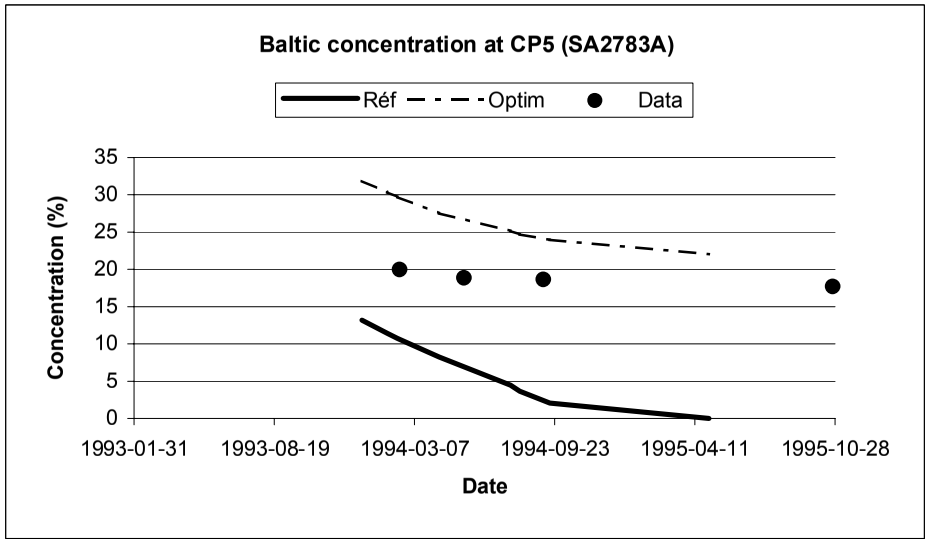

Figure 56 : Best results at CP5

Optimised results using hydraulic and concentration data

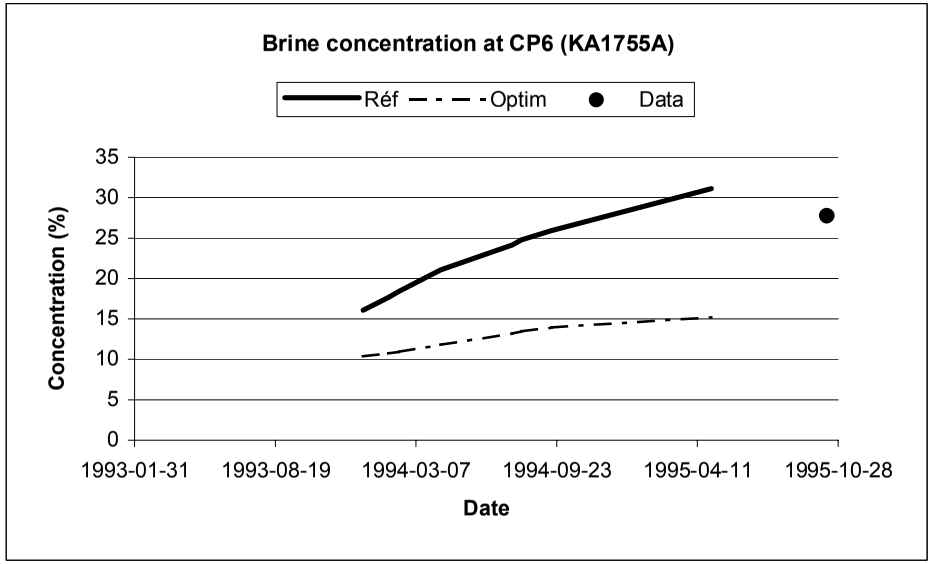

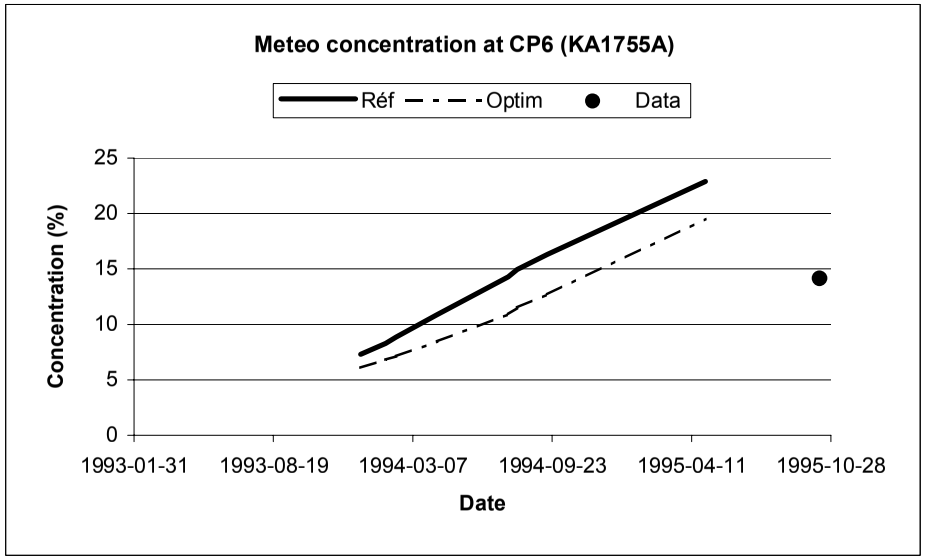

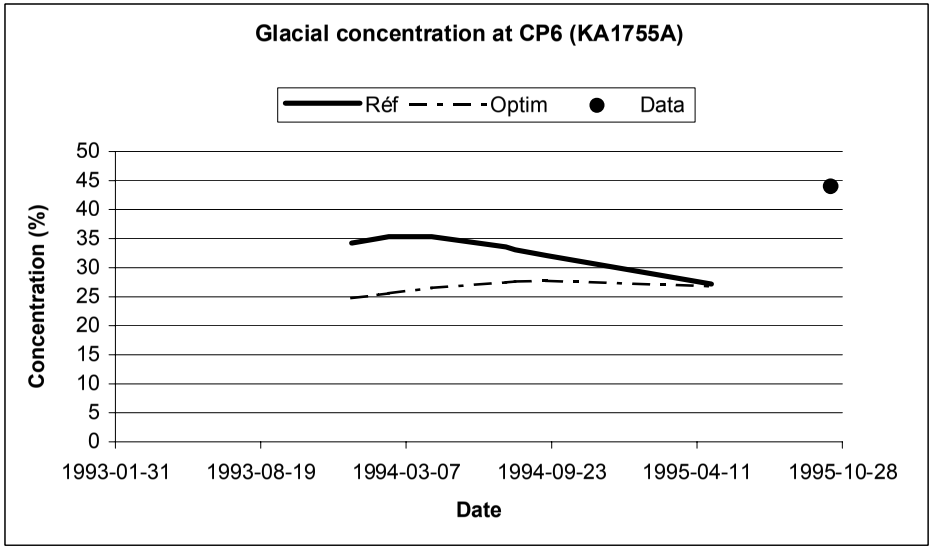

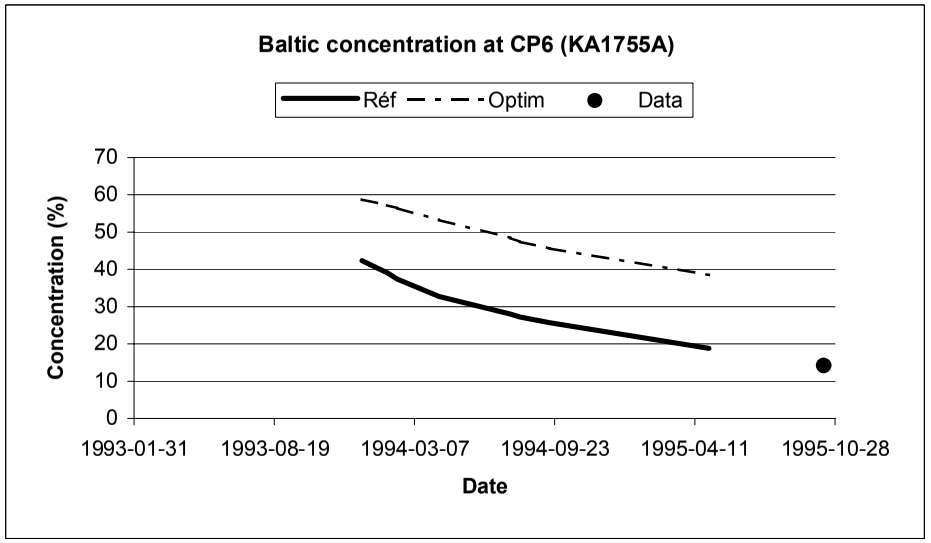

Figure 57 : Best results at CP6

Optimised results using hydraulic and concentration data

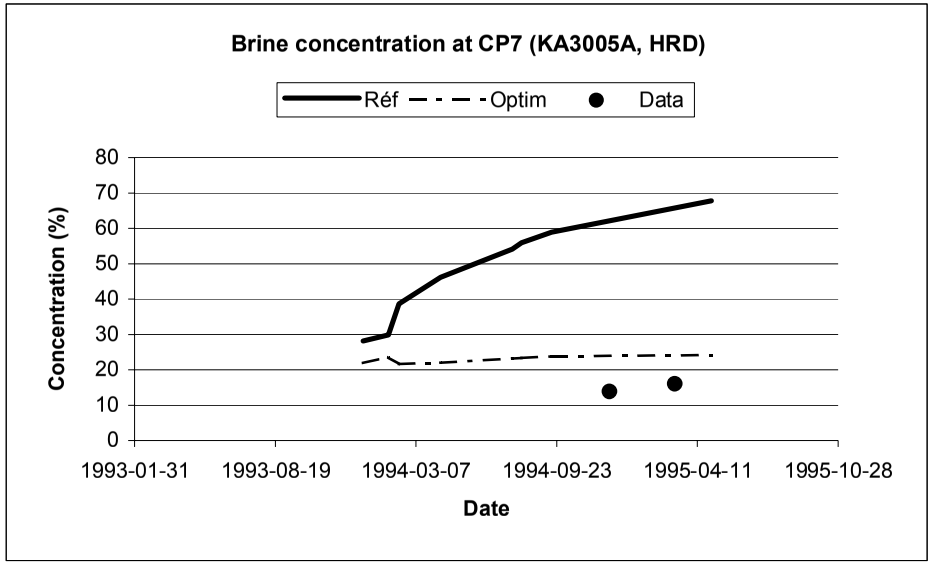

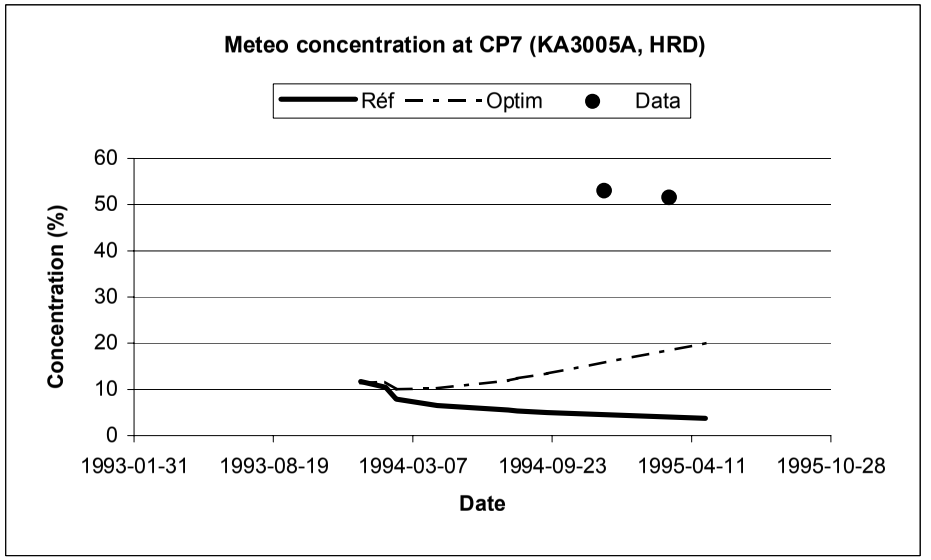

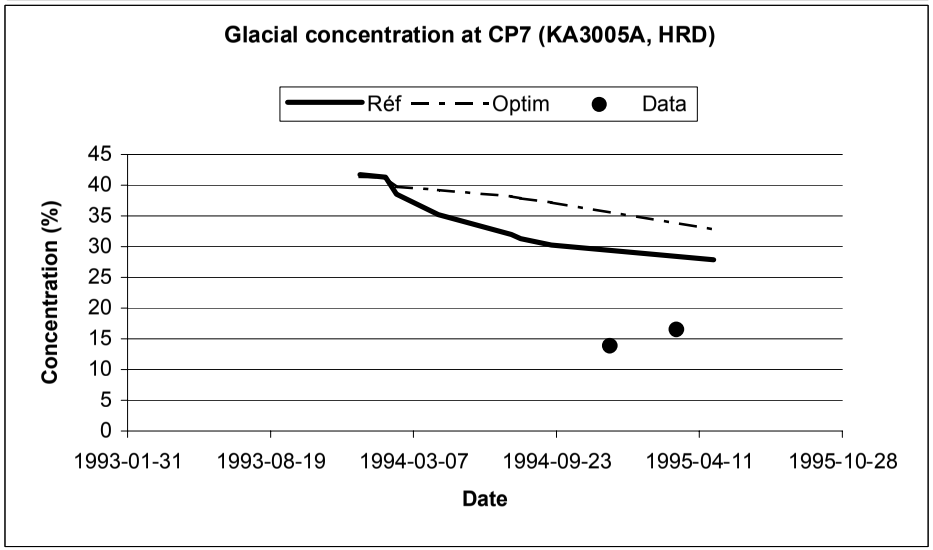

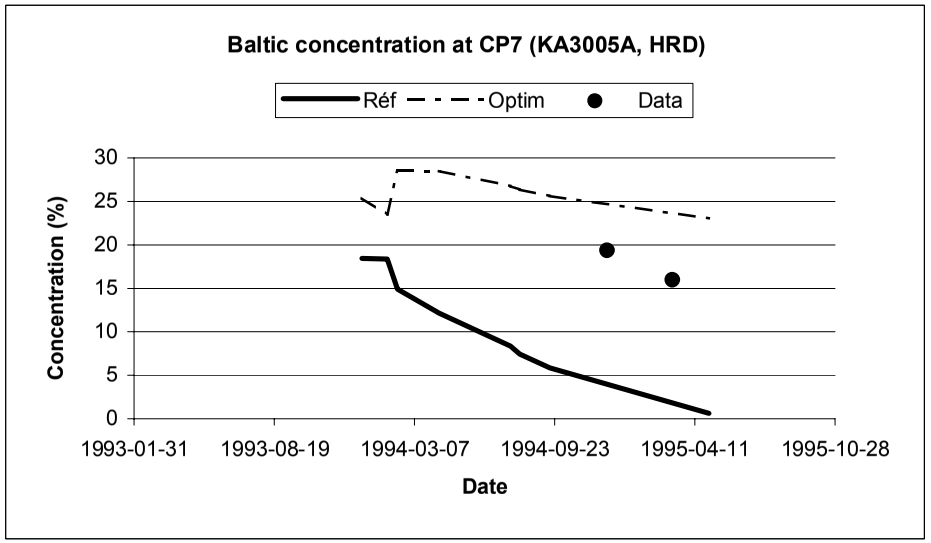

Figure 58 : Best results at CP7

Optimised results using hydraulic and concentration data

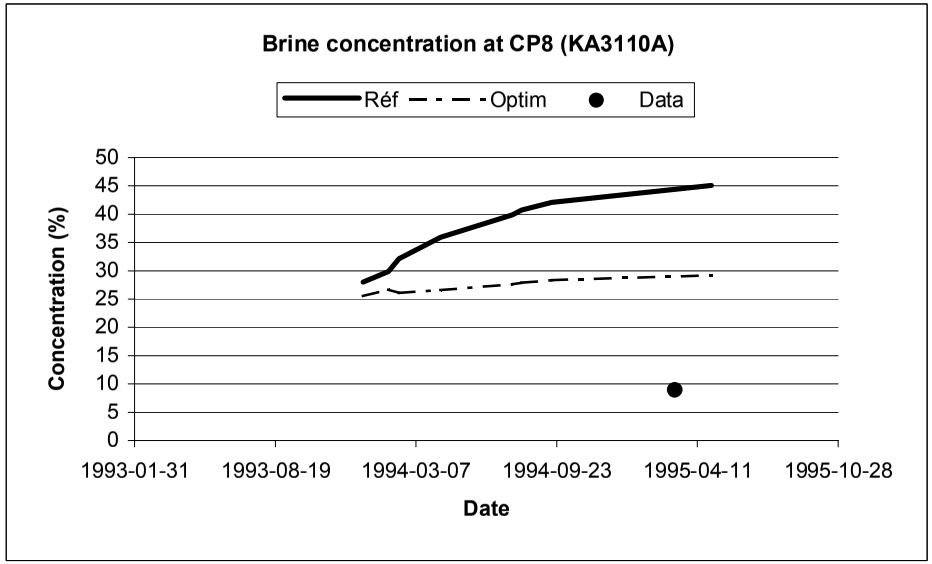

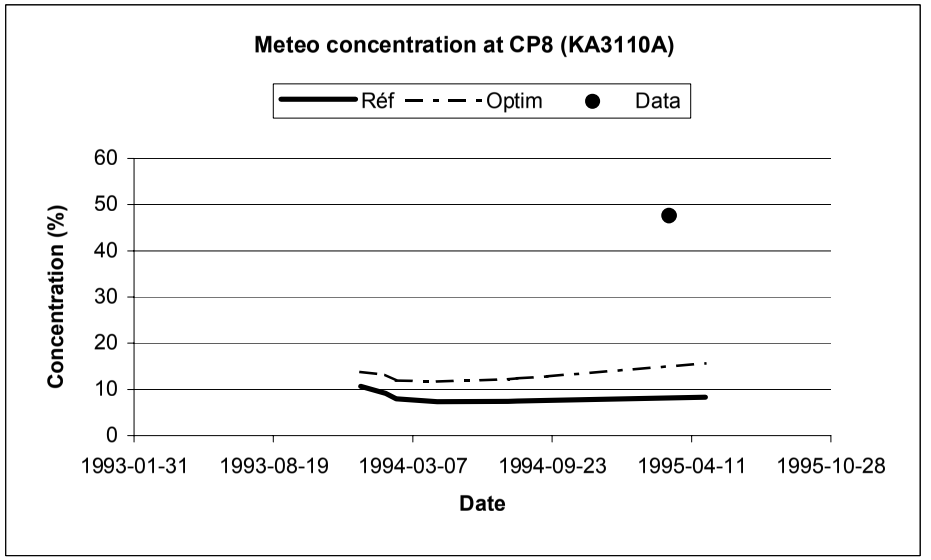

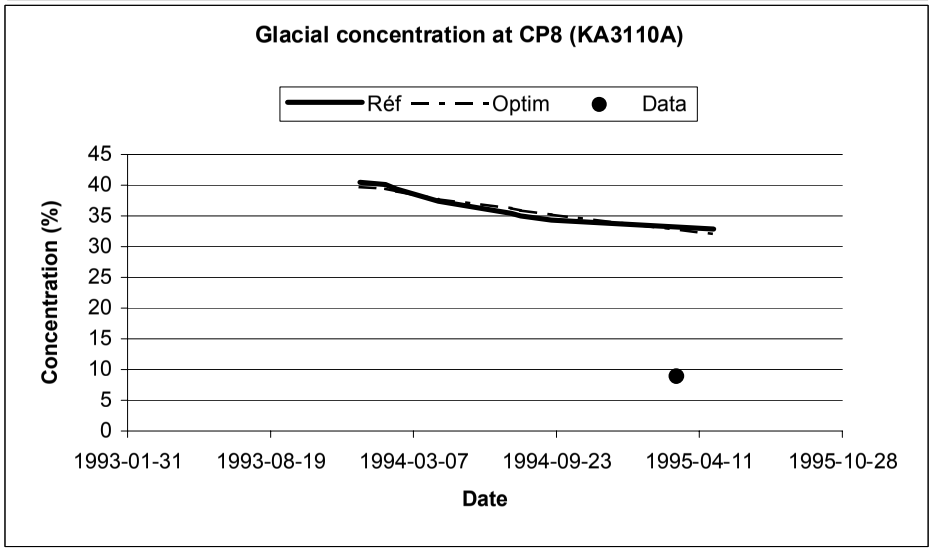

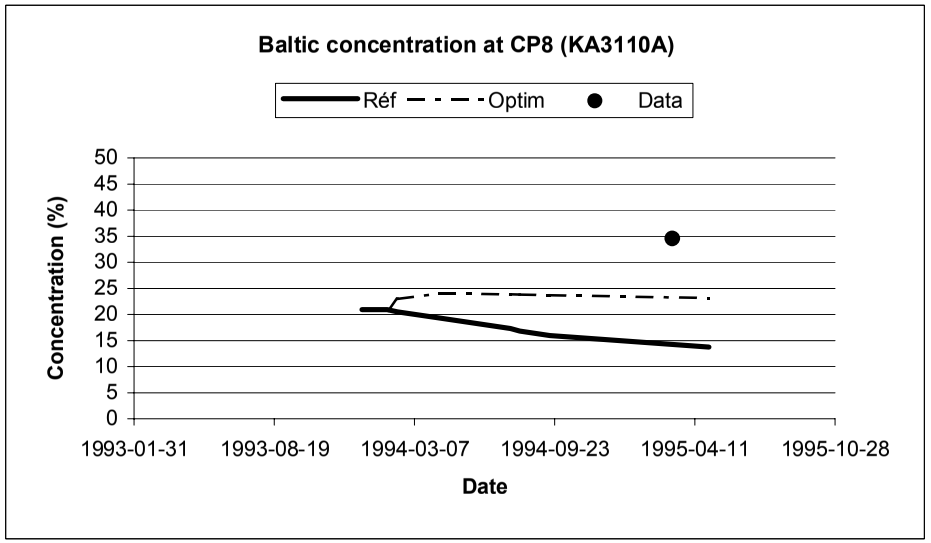

Figure 59 : Best results at CP8

Optimised results using hydraulic and concentration data

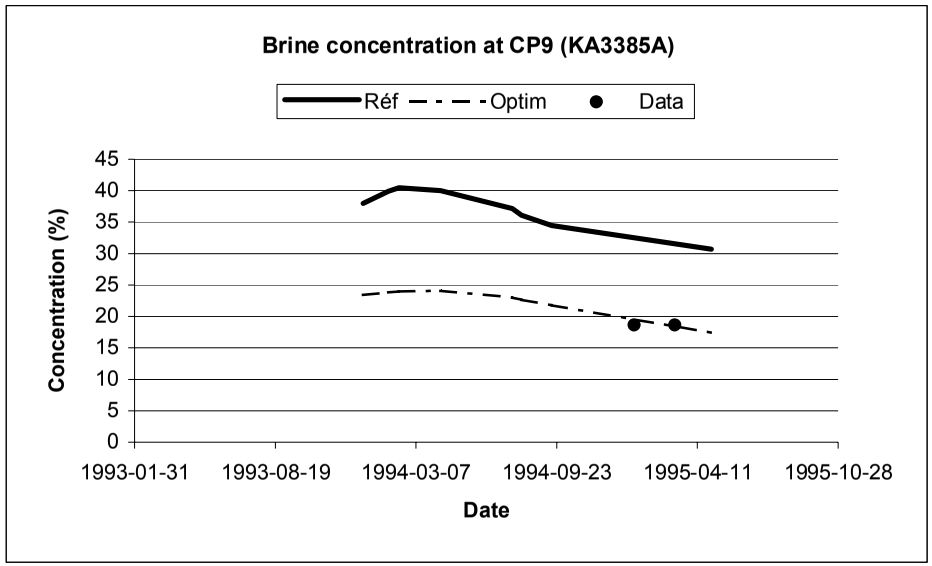

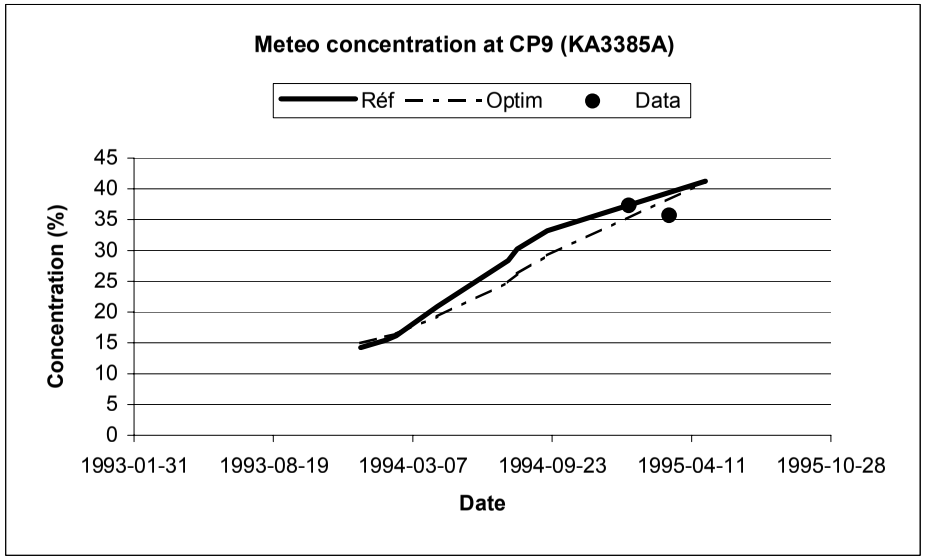

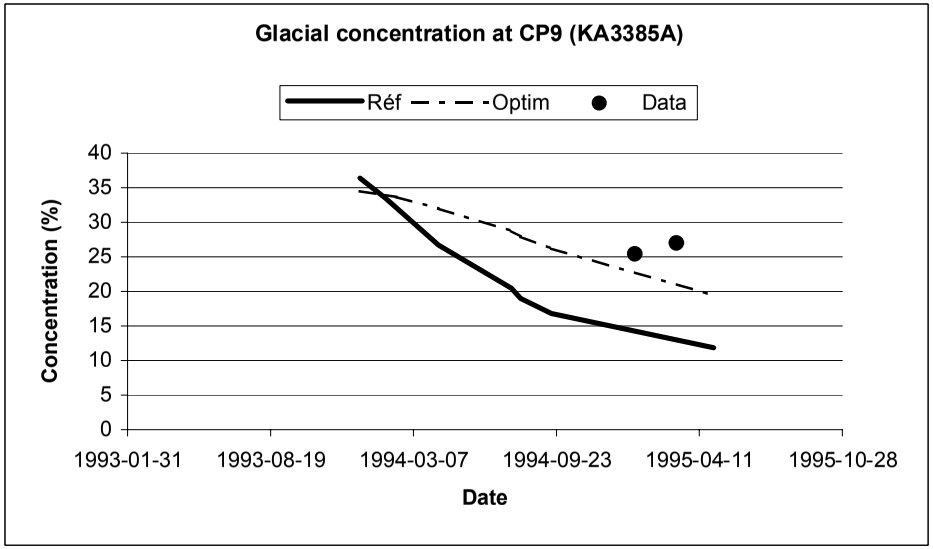

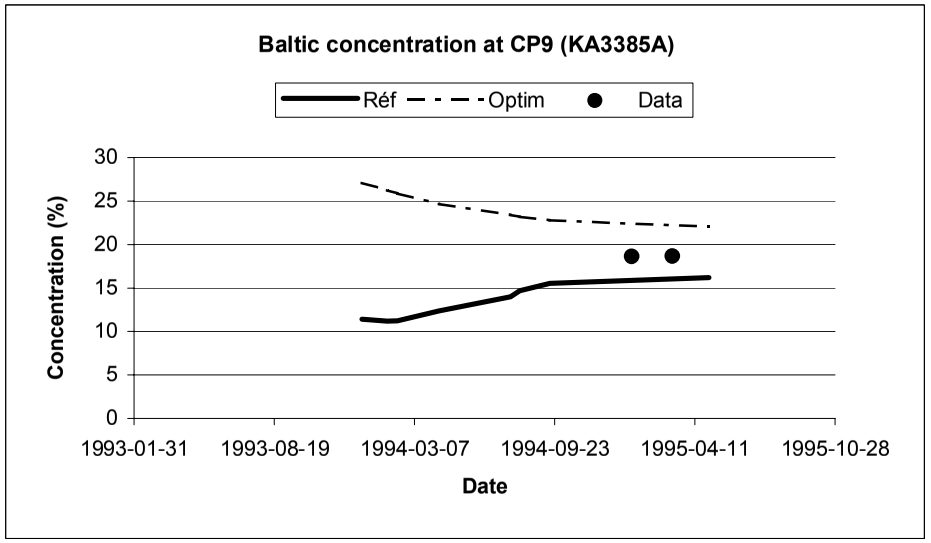

Figure 60 : Best results at CP9

optimised results using hydraulic and concentration data

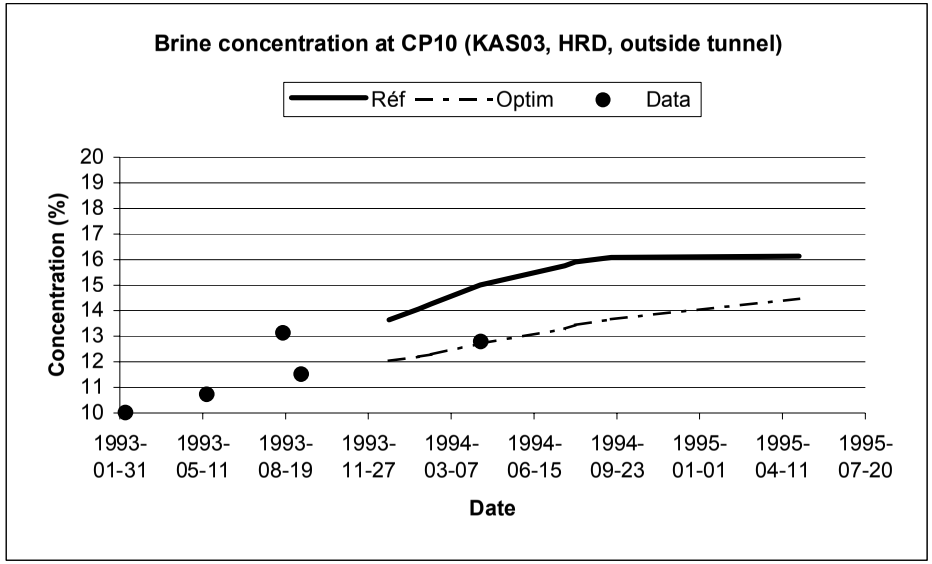

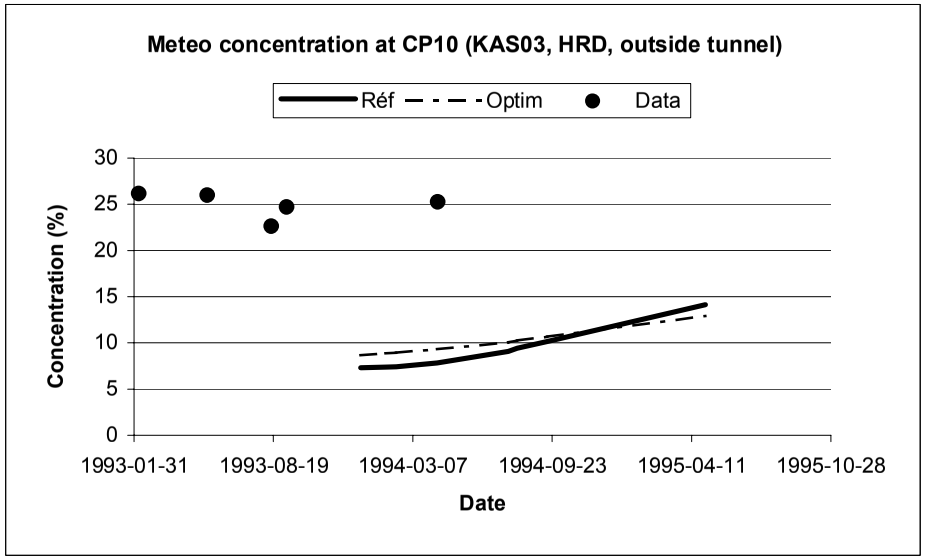

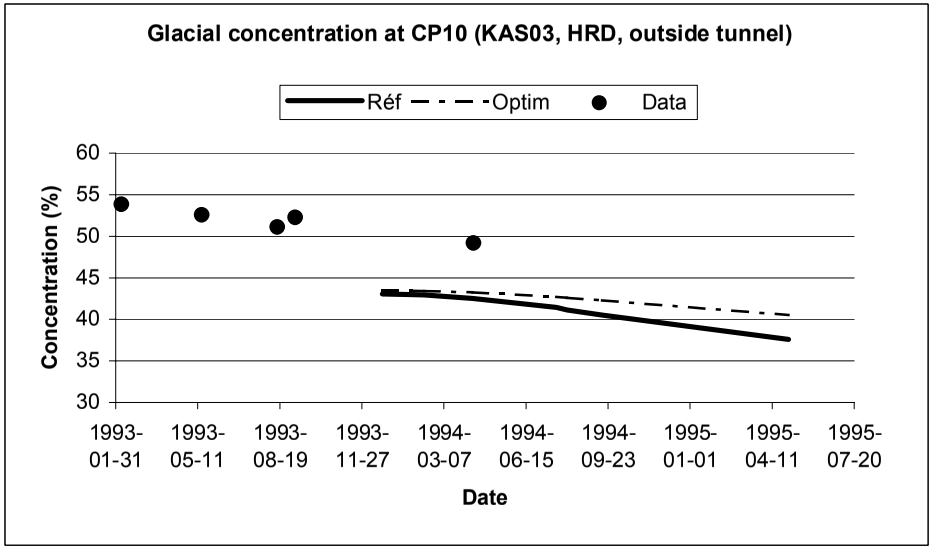

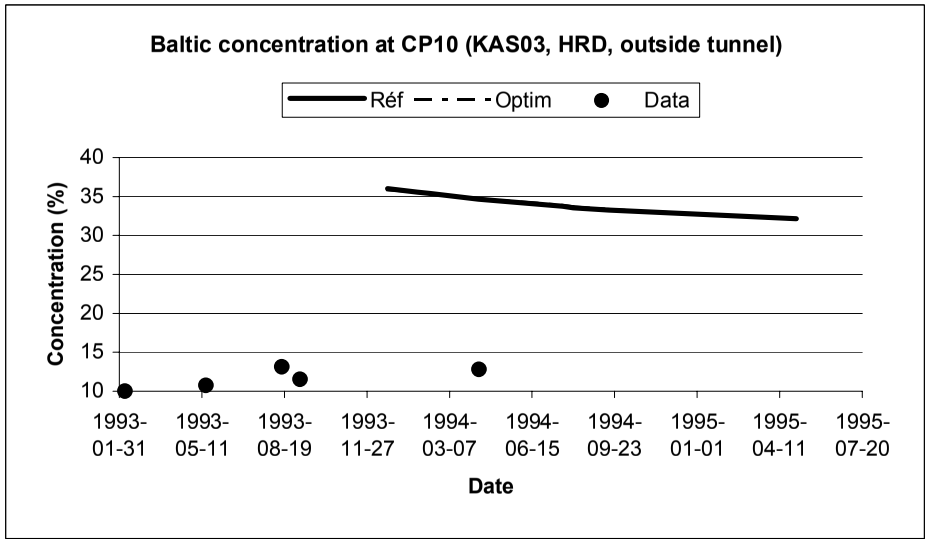

Figure 61 : Best results at CP10

Optimised results using hydraulic and concentration data

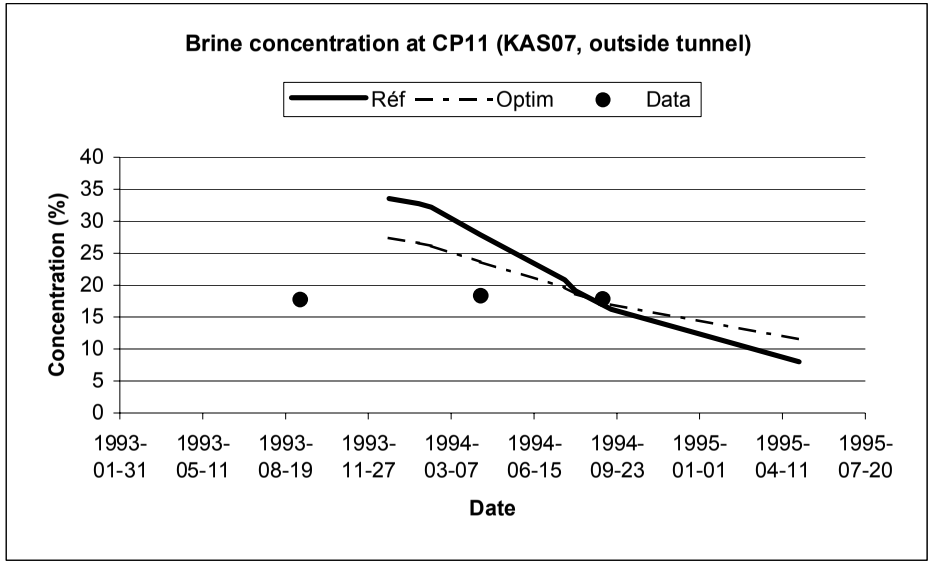

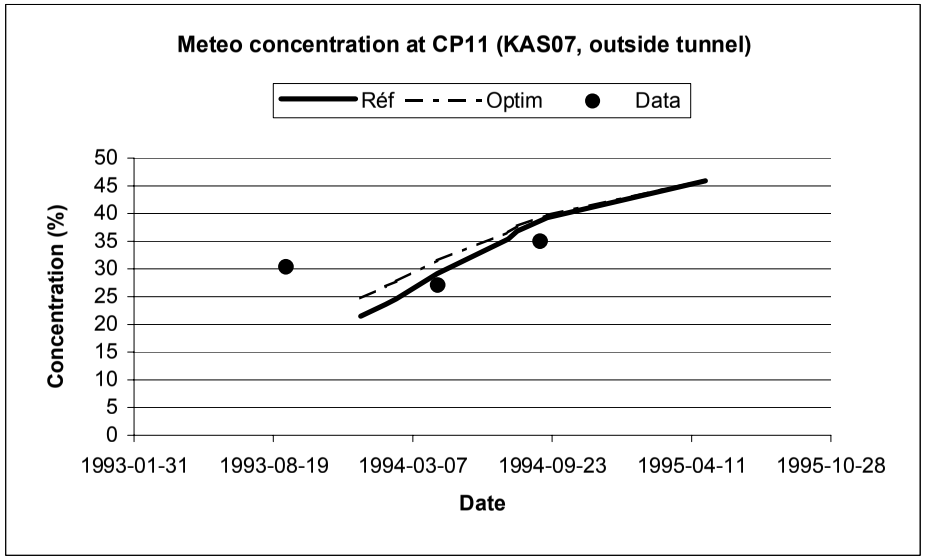

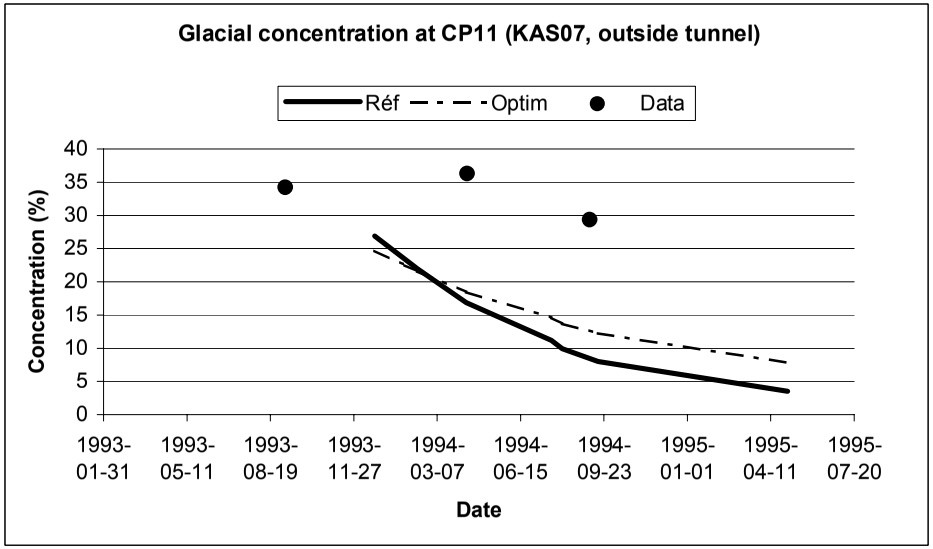

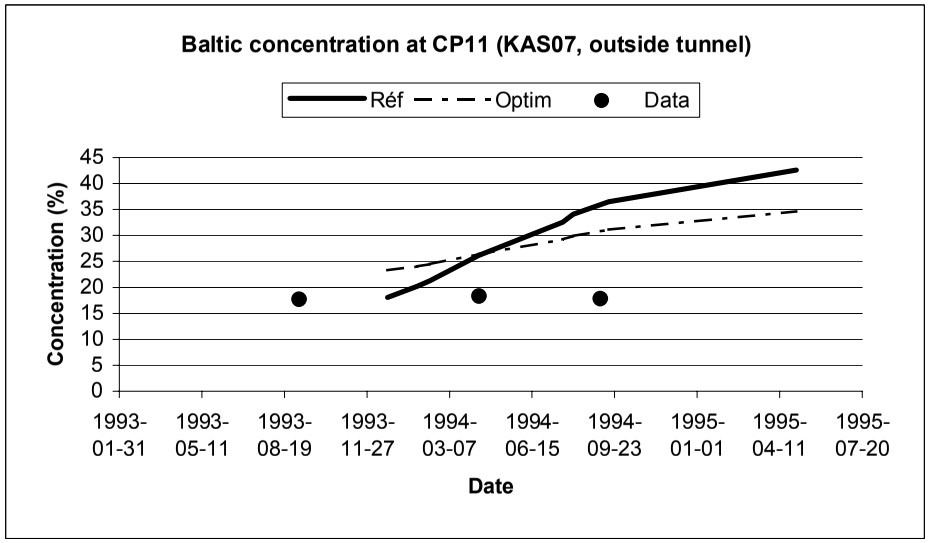

Figure 62 : Best results at CP11

APPENDIX 2, Table 3

Table 3 : Percentage of error in concentration at the 11 Control points for 2 different dates (ANTEA)

		Control Points													
		CP1 KR0012B		CP2 SA0813B, SA0850B		CP3 SA1229A, KA1061A		CP3 SA1327A		CP4 SA2074A		CP5 SA2783A		CP6 KA1755A	
		1993-12-22	1995-05-01	*1993-12-22*	1995-05-01	*1993-12-22*	1995-05-01	*1993-12-22*	1995-05-01	*1993-12-22*	1995-05-01	*1993-12-22*	1995-05-01	*1993-12-22*	1995-05-01
Permeability *10	Brine	*4*	28	4	4	*8*	16			*16*	44	*8*	28		
	Glacial	*16*	20	16	0	*16*	8			*24*	14	*0*	14		
	Meteo	*40*	58	8	18	*10*	4			*30*	34	*8*	2		
	Baltic	*18*	8	2	12	*12*	20			*12*	22	*0*	16		
Permeability /10	Brine	*4*	28	6	16	*8*	16			*14*	16	*14*	30		
	Glacial	*16*	20	16	16	*14*	8			*26*	12	*0*	16		
	Meteo	*40*	58	16	20	*10*	4			*30*	36	*6*	2		
	Baltic	*18*	8	6	12	*12*	20			*10*	8	*6*	16		
Head Boundary (= 0 MASL)	Brine	*0*	4	8	20	*8*	6			*12*	10	*10*	16		
	Glacial	*12*	18	18	16	*14*	6			*26*	8	*4*	28		
	Meteo	*34*	42	18	22	*10*	2			*28*	16	*2*	48		
	Baltic	*20*	18	8	14	*12*	16			*10*	0	*6*	4		
Head Boundary (=init)	Brine	*4*	32	8	22	*10*	16			*14*	26	*10*	0		
	Glacial	*16*	18	18	14	*14*	6			*24*	12	*4*	20		
	Meteo	*38*	56	18	22	*8*	2			*30*	22	*0*	28		
	Baltic	*16*	4	8	14	*18*	20			*8*	16	*4*	6		
kinematic Porosity *10	Brine	*4*	32	8	24	*10*	16			*12*	26	*6*	16		
	Glacial	*16*	18	18	16	*16*	8			*24*	14	*0*	14		
	Meteo	*38*	56	18	24	*8*	4			*30*	26	*6*	6		
	Baltic	*16*	4	8	14	*16*	20			*6*	14	*0*	8		
kinematic Porosity /10	Brine	*4*	32	10	20	*10*	16			*14*	28	*14*	14		
	Glacial	*16*	18	18	14	*14*	6			*24*	12	*2*	16		
	Meteo	*38*	56	18	20	*8*	2			*30*	26	*6*	12		
	Baltic	*16*	4	8	14	*16*	18			*8*	14	*4*	8		
Specific Storage *10	Brine	*4*	28	6	26	*8*	16			*12*	18	*8*	32		
	Glacial	*16*	20	18	20	*16*	8			*26*	12	*2*	14		
	Meteo	*40*	58	16	26	*10*	6			*30*	28	*8*	0		
	Baltic	*18*	8	8	18	*12*	20			*8*	4	*0*	16		
Specific Storage /10	Brine	*4*	28	8	24	*8*	16			*12*	22	*14*	26		
	Glacial	*16*	20	18	16	*14*	8			*26*	12	*0*	16		
	Meteo	*40*	58	18	24	*10*	4			*30*	28	*6*	6		
	Baltic	*18*	8	8	16	*12*	20			*10*	6	*6*	16		
Dispersivity *2	Brine	*4*	32	8	22	*10*	16			*14*	28	*12*	14		
	Glacial	*16*	18	18	14	*14*	6			*24*	12	*2*	16		
	Meteo	*38*	56	18	22	*8*	2			*30*	26	*6*	10		
	Baltic	*16*	4	8	14	*16*	18			*8*	14	*4*	8		
Dispersivity /2	Brine	*2*	24	6	24	*4*	16			*12*	12	*14*	34		
	Glacial	*16*	22	18	20	*12*	10			*28*	10	*2*	22		
	Meteo	*40*	60	16	26	*12*	6			*30*	28	*6*	4		
	Baltic	*20*	12	8	18	*6*	20			*10*	4	*8*	16		
Reference (first run)	Brine	*4*	28	8	24	*8*	16			*12*	22	*14*	26		
	Glacial	*16*	20	18	18	*14*	8			*26*	12	*0*	16		
	Meteo	*40*	58	18	24	*10*	4			*30*	28	*8*	6		
	Baltic	*18*	8	8	16	*12*	20			*10*	6	*6*	16		
Optimased Parameters values	**Brine**	***2***	**4**	**0**	**0**	***10***	**6**			***10***	**6**	***0***	**10**		
	Glacial	***12***	**16**	**6**	**12**	***16***	**6**			***24***	**14**	***4***	**14**		
	Meteo	***30***	**36**	**6**	**10**	***10***	**2**			***28***	**24**	***4***	**20**		
	Baltic	***16***	**14**	**0**	**4**	***16***	**16**			***4***	**2**	***10***	**4**		

Table 3 : Percentage of error in concentration at the 11 Control points for 2 different dates (ANTEA)

		Control Points					
		CP7	CP8	CP9	CP10	CP11	
		KA3005A	KA3110A	KA3385A	KAS03	KAS07	MEAN
		1993-12-22 1995-05-01	*1993-12-22* 1995-05-01	*1993-12-22* 1995-05-01	*1993-12-22* 1995-05-01	*1993-12-22* 1995-05-01	CP1-CP11
Permeability *10	Brine	50	34	2	*0*	*14*	17
	Glacial	8	24	16	*6*	*6*	13
	Meteo	44	40	10	*18*	*6*	22
	Baltic	16	18	0	*24*	*0*	12
Permeability /10	Brine	44	40	12	*0*	*16*	18
	Glacial	12	22	14	*6*	*8*	14
	Meteo	46	40	4	*16*	*6*	22
	Baltic	10	20	2	*22*	*0*	11
Head Boundary (= 0 MASL)	Brine	4	26	12	*2*	*14*	10
	Glacial	0	22	22	*6*	*10*	14
	Meteo	4	34	36	*16*	*2*	21
	Baltic	0	14	0	*20*	*0*	9
Head Boundary (=init)	Brine	32	34	2	*2*	*10*	15
	Glacial	6	18	16	*6*	*10*	13
	Meteo	26	30	24	*16*	*0*	21
	Baltic	10	22	4	*22*	*2*	12
kinematic Porosity *10	Brine	40	36	10	*0*	*10*	17
	Glacial	10	20	12	*6*	*6*	13
	Meteo	40	36	2	*16*	*6*	21
	Baltic	10	20	0	*24*	*2*	11
kinematic Porosity /10	Brine	40	36	6	*2*	*8*	17
	Glacial	8	18	14	*6*	*10*	13
	Meteo	38	36	6	*16*	*4*	21
	Baltic	12	20	0	*22*	*4*	11
Specific Storage *10	Brine	44	36	18	*0*	*16*	18
	Glacial	12	22	12	*6*	*4*	14
	Meteo	46	38	0	*18*	*8*	22
	Baltic	10	20	4	*24*	*2*	11
Specific Storage /10	Brine	48	36	10	*0*	*14*	18
	Glacial	10	22	14	*6*	*8*	14
	Meteo	46	38	6	*16*	*6*	22
	Baltic	14	20	2	*22*	*0*	12
Dispersivity *2	Brine	40	36	6	*0*	*8*	17
	Glacial	8	18	14	*6*	*10*	13
	Meteo	38	36	6	*16*	*4*	21
	Baltic	12	20	0	*22*	*4*	11
Dispersivity /2	Brine	34	34	18	*0*	*18*	17
	Glacial	10	26	14	*6*	*6*	15
	Meteo	40	40	2	*16*	*8*	22
	Baltic	4	20	6	*22*	*2*	12
Reference (first run)	Brine	48	36	10	*0*	*14*	18
	Glacial	10	22	14	*6*	*8*	14
	Meteo	46	38	6	*16*	*6*	23
	Baltic	14	20	2	*22*	*0*	12
Optimased Parameters values	**Brine**	**6**	**20**	**0**	***0***	***8***	**5**
	Glacial	**16**	**22**	**6**	***6***	***10***	**12**
	Meteo	**30**	**32**	**6**	***16***	***4***	**17**
	Baltic	**6**	**10**	**2**	***22***	***4***	**9**

APPENDIX 3, Questionnaire

RESPONSES TO MODELLING QUESTIONNAIRE FOR TASK 5

worked December 1999, ANTEA

Table 1 Description of model for water flow calculations

TOPIC	Example	Our Model
Type of model	Stochastic continuum model	Double porosity model : explicit 3D representation of matrix and fractures
Process description	Darcy´s flow including density driven flow. (Transport equation for salinity is used for calculation of the density)	Darcy's equation
Geometric framework and parameters	Model size: 1.8x1.8x1 km^3 . Deterministic features: All deterministic features provided in the data set. Rock outside the deterministic features modelled as stochastic continuum.	Model size : size of the M3 model : 3.750x 2.520x1.500 km^3 Local fractures : Most of the deterministic local features, only EW-7 and NNW-3 are not represented. Regional fractures : SFZ-03, SFZ-04, SFZ-05, SFZ-07 (continuation of EW-1), SFZ-11, SFZ-12 (continuation of NE-1), SFZ-14 Rock Mass Domain : deterministic. Two domains : SRD-4 is modelled independently
Material properties and hydrological properties	Deterministic features: Transmissivity (T), Storativity(S) Rock outside deterministic features: Hydraulic conductivity(K), Specific storage (Ss)	Fractures : Conductivity (K), specific storage (Ss) Rock mass domain : Conductivity (K), specific storage (Ss)
Spatial assignment method	Deterministic features: Constant within each feature (T,S). No changes due to calibration. Rock outside deterministic features: (K,Ss) lognormal distribution with correlation length xx. Mean, standard deviation and correlation based on calibration of the model	Fractures : constant properties within each features (T, Ss, Ne). Change of K for some features (SFZ-05, NE-2, NNW-7, NE-3, NNW-4, NE-4) du to calibration procedure. Rock Mass domain : constant properties within each zone (SRD-4, rest). No change
Boundary conditions	Surface: Constant flux. Sea: Constant head Vertical-North: Fixed pressure based on vertical salinity distribution. Vertical-East: Fixed pressure based on vertical salinity distribution. Vertical-South: Fixed pressure based on vertical salinity distribution. Vertical-West: Fixed pressure based on vertical salinity distribution. Bottom: No flux. Linear change by time based regional simulations for undisturbed conditions and with Äspö tunnel present.	Earth (island + continent) : constant flux. Change du to calibration. Sea + lake : constant head. Other external boundaries : Based on Swenson regional model. Tunnel and shaft : time varying fluxes.
Numerical tool	PHOENICS	TAFFETAS

Numerical method	Finite volume method	Mixte Hybrid Finite Element
Output parameters	Head, flow and salinity field.	Head, Flow

Table 2 Description of model for tracer transport calculations

TOPIC	EXAMPLE	Our model
Type of model	Stochastic continuum model	Double porosity model : explicit 3D representation of matrix and fractures
Process description	Advection and diffusion, spreading due to spatially variable velocity and molecular diffusion.	Advection
Geometric framework and parameters	Model size: 1.8x1.8x1 km^3 . Deterministic features: All deterministic features provided in the data set. Rock outside the deterministic features modelled as stochastic continuum.	Model size : size of the M3 model : 3.750x 2620x1500 km^3 Local fractures : Most of the deterministic local features, only EW-7 and NNW-3 are not represented. Regional fractures : SFZ-03, SFZ-04, SFZ-05, SFZ-07 (continuation of EW-1), SFZ-11, SFZ-12 (continuation of NE-1), SFZ-14 Rock Mass Domain : deterministic. Two domains : SRD-4 is modelled independently
Material properties	Flow porosity (ne)	Cinematic porosity (ne)
Spatial assignment method	ne based on hydraulic conductivity value (TR 97-06) for each cell in model, including deterministic features and rock outside these features.	Ne based on hydraulic conductivity (TR 97-06) for each fracture, SRD4 and rock mass domain
Boundary conditions	Mixing ratios for endmembers as provided as initial conditions in data sets.	Island and continent : 100% Meteoric water Sea : 100% Baltic water Other boundaries : Mixing ratios for endmembers based on M3 calculations
Numerical tool	PHOENICS	TAFFETAS
Numerical method	Particle tracking method or tracking components by solving the advection/diffusion equation for each component	Mixte Hybrid Finite Element
Output parameters	Breakthrough curves	Concentration fields, breakthrough curves

Table 3 Description of model for chemical reactions calculations

TOPIC	EXAMPLE	Our model
Type of model	xxx	
Process description	Mixing. Reactions: Xx, Yy,Zz,Dd…..	Mixing : this is no chemical reactions. We performed only advection transport of the four endmemders. The model is already described in Table 1 and Table 2.
Geometric framework and parameters	Modelling reactions within one fracture zone, NE-1.	
Reaction parameters	Xx: a=ff, b=gg,… Yy: c=. Zz: d=...	
Spatial distribution of reactions assumed	Xx: seafloor sediments Yz: Bedrock below sea, superficial Dd: Bedrock ground surface, superficial Yz: Bedrock below sea, at depth Zz: Bedrock ground surface, at depth Yy, Zz: near tunnel	
Boundary/initial conditions for the reactions	Xx: aaa… Yy: bbb…	
Numerical tool	Phreeque	
Numerical method	xx	
Output parameters	xx	

Table 4a Summary of data usage

Data del. No	Data	Importance of data (see notes)	Comment
1	Hydrochemical data 1	-	I only used mixing ratios calculated by M3
1a	Surface bore holes- undisturbed conditions, Äspö-Laxemar	-	
1b	Surface bore holes- disturbed conditions (by tunnel excavation), Äspö	-	
1c	Surface bore holes- undisturbed conditions, Ävrö	-	
1d	Surface bore holes- sampled during drilling, Äspö	-	
1e	Data related to the Redox experiment	-	
1f	Tunnel and tunnel bore holes- disturbed conditions	-	
2	Hydogeological data 1	**M**	
2a1	Annual mean air temperature	-	
2a2	Annual mean precipitation	X	
2a3	Annual mean evapotranspiration	X	
2b1	Tunnel front position by time	**M**	
2b2	Shaft position by time	**M**	
2c1	Geometry of main tunnel	**M**	
2c2	Geometry of shafts	**M**	
2d	Hydrochemistry at weirs (Cloride, pH, Electrical conductivity, period: July 1993- Aug 1993)	-	
2e	Geometry of the deterministic large hydraulic features (Most of them are fracture zones)	**M**	

Table 4b Summary of data usage

Data del. No	Data	Importance of data (see notes)	Comment
3	Hydrogeological data 2	**P**	
3a	Monthly mean flow rates measured at weirs. Tunnel section 0-2900m, period May 1991 – January 1994	**P**	
3b	Piezometric levels for period June 1st 1991 – May 21st 1993. Values with 30 days interval (Task 3 data set)	-	It is an important data base, but I had no time to use it
3c	Salinity levels in bore hole sections for period -Sept 1993. (Task 3 data set)	-	
3d	Undisturbed piezometric levels	-	It is an important data base, but I had no time to use it
3e	Co-ordinates for bore hole sections	m	
3f	Piezometric levels for period July 1st 1990 – January 24st 1994. Daily values.	-	A daily time step is to small to be usefull in a site scale analysis aver several years
4	Hydochemical data 2	**P**	I used directly the voxels generated by M3, all the other data were neglected in data set 7

4a	Chemical components, mixing proportions and deviations for all bore hole sections used in the M3 calculations	-	
4b	Bore holes with time series, > 3 samples (part of 4a)	-	
4c	Bore holes sections interpreted to intersect deterministic large hydraulic features (Most of them are fracture zones) (part of 4a)	-	
4d	Chemical components, mixing proportions and deviations. Grid data based on interpolation. Undisturbed conditions	-	Use of data set 7
4e	Chemical components, mixing proportions and deviations. Grid data based on interpolation. Disturbed conditions (by tunnel excavation)	-	Use of data set 7
4f	Boundary and initial conditions. Chemical components, mixing proportions and deviations (1989). Grid data for vertical boundaries based on interpolation. Undisturbed conditions	-	
4g	Boundary conditions after tunnel construction (1996) Chemical components, mixing proportions and deviations. Grid data for vertical boundaries based on interpolation. Disturbed conditions (by tunnel excavation)	-	

Table 4c Summary of data usage

Data del. No	Data	Importance of data (see notes)	Comment
5	Geographic data 1	m	
5a	Äspö coast line	m	I needed cast lines for continent an all the island surrounding ASPO as well
5b	Topography of Äspö and the nearby surroundings	-	Could have been interesting, but no time to use it
6	Hydro tests and tracer tests	-	Interesting but no time to use it
6a	Large scale interference tests (19 tests)	-	Interesting but no time to use it
6b	Long time pump and tracer test, LPT2	-	Interesting but no time to use it
7	Hydrochemical data 3, update of data delivery 4 based on new endmembers. Recommended to be used instead of 4.	**P**	
7a	Chemical components, mixing proportions and deviations for all bore hole sections used in the M3 calculations	**P**	
7b	Bore holes with time series, > 3 samples (part of 7a)	-	
7c	Bore holes sections interpreted to intersect deterministic large hydraulic features (Most of them are fracture	-	

	zones) (part of 7a)		
7d	Chemical components, mixing proportions and deviations. Grid data based on interpolation. Undisturbed conditions	**P**	
7e	Chemical components, mixing proportions and deviations. Grid data based on interpolation. Disturbed conditions (by tunnel excavation)	**P**	
7f	Boundary and initial conditions. Chemical components, mixing proportions and deviations (1989). Grid data for vertical boundaries based on interpolation. Undisturbed conditions	-	Determined from 7d and 7e
7g	Boundary conditions after tunnel construction (1996) Chemical components, mixing proportions and deviations. Grid data for vertical boundaries based on interpolation. Disturbed conditions (by tunnel excavation)	-	Determined from 7d and 7e

Table 4d Summary of data usage

Data del. No	Data	Importance of data (see notes)	Comment
8	Performance measures and reporting 1		
8a	Performance measures		
8b	Suggested control points. 6 points in tunnel section 0-2900m and 3 point in tunnel section 2900-3600m.	-	Use of data set 13
8c	Suggested flowchart for illustration of modelling		
9	Hydrogeological data 3	p	
9a	Monthly mean flow rates measured at weirs. Tunnel section 0-2900m, period: May 1991- Dec 1996.	p	
10	Geographic data 2		
10a	Topography of Äspö and the nearby surroundings (larger area than 5b)	m	Could be interesting but no time to use it
10b	Co-ordinates for wetlands	-	
10c	Co-ordinates for lakes	-	
10d	Co-ordinates for catchments	-	
10e	Co-ordinates for streams	-	
10f	Co-ordinate transformation Äspö system- RAK	m	
11	Boundary and initial conditions	**P**	
11a	Pressure before tunnel construction, from the regional SKB model (TR 97-09)	**P**	
11b	Salinity before tunnel construction, from the regional SKB model (TR 97-09)	-	
11c	Pressure after tunnel construction, from the regional SKB model (TR 97-	**P**	

	09)		
11d	Salinity after tunnel construction, from the regional SKB model (TR 97-09)	-	

Table 4e Summary of data usage

Data del. No	Data	Importance of data (see notes)	Comment
12	Performance measures and reporting 2		
12a	Suggested control points. 6 points in tunnel section 0-2900m and 3 point in tunnel section 2900-3600m (same as 8b) and 2 outside the tunnel.	-	Use of data set 13
13	Transport parameters compiled	-	Interesting but no time …
13a	LPT2 tracer tests	-	
13b	Tracer test during passage of fracture zone NE-1	-	
13c	Redox tracer tests	-	
13d	TRUE-1 tracer tests	-	
14	Hydrochemical data 4		
14a	Groundwater reactions to consider within TASK5 modelling (Description of how M3 calculates the contribution of reactions and identifying dominating reactions based on the M3 calculations.	x	
15	Co-ordinates for the test sections defining the control points	**M**	
16	Co-ordinates for bore holes drilled from the tunnel	x	

Table 4f Summary of data usage

Data del. No	Data	Importance of data (see notes)	Comment
17	Hydogeological data - prediction period	-	
17a	Hydrochemistry at weirs (Cloride, pH, Electrical conductivity, period: July 1993- Dec 1995)	-	
17b	Piezometric levels for period July 1st 1990 – Dec 1996. Daily values.	-	
18	Hydochemical data - prediction period.	-	
18a	Chemical components, mixing proportions and deviations for all bore hole sections used in the M3 calculations. Data for tunnel section 2900-3600m.	-	
18b	Bore holes with time series, > 3 samples (part of 18a)	-	
18c	Bore holes sections interpreted to intersect deterministic large hydraulic features (Most of them are fracture zones) (part of 18a)	-	
	Other data (part of data to Task 1, 3 and 4)	-	
	Fracture orientation, fracture spacing and trace length – tunnel data	-	
	Fracture orientation, fracture spacing– mapping of cores	-	
	Fracture orientation, fracture spacing and trace length – mapping of outcrops	-	

P = data of great importance for quantitative estimation of model parameters
p = data of less importance for quantitative estimation of model parameters
M = data of great importance used qualitatively for setting up model
m = data of less importance used qualitatively for setting up model
X = data useful as general background information
- = data not used